

NASA CR-175043  
GARRETT 21-5705

# DILUTION JET MIXING PROGRAM SUPPLEMENTARY REPORT

by

R. SRINIVASAN  
C. WHITE

Garrett Turbine Engine Company  
A Division of The Garrett Corporation

March 1986

Prepared for

National Aeronautics and Space Administration  
NASA-Lewis Research Center

Contract NAS3-22110

## TABLE OF CONTENTS

	<u>Page</u>
1.0 SUMMARY	1
2.0 INTRODUCTION	3
3.0 DESCRIPTION OF TEST RIG, INSTRUMENTATION, AND DATA REDUCTION	5
4.0 RESULTS OF NUMERICAL CALCULATIONS	11
5.0 VELOCITY TRAJECTORY CORRELATIONS	15
6.0 RESULTS OF VELOCITY MEASUREMENTS	19
7.0 CONCLUSIONS	23
LIST OF SYMBOLS	25
REFERENCES	218

## LIST OF ILLUSTRATIONS

<u>Figure</u>	<u>Title</u>	<u>Page</u>
1	Dilution Jet Mixing Rig Schematic	27
2	Schematics of Test Sections Used in the Program $H_0 = 10.16 \text{ cm}$	28
3	Schematic of Orifice Plate Configurations	29
4	Total Pressure, Thermocouple, and Static Pressure Rake	30
5	Predicted Temperature Distributions for Test Case 1 - Table 1	31
6	Comparison Between Predicted and Measured Temperature Distributions for Test Case 1 - Table 1	32
7	Predicted Velocity Distributions for Test Case 1 - Table 1	33
8	Comparison Between Predicted and Measured Velocity Distributions for Test Case 1 - Table 1	34
9	Predicted Temperature Distributions for Test Case 2 - Table 1	35
10	Comparison Between Predicted and Measured Temperature Distributions for Test Case 2 - Table 1	36
11	Predicted Velocity Distributions for Test Case 2 - Table 1	37
12	Comparison Between Predicted and Measured Velocity Distributions for Test Case 2 - Table 1	38
13	Predicted Temperature Distributions for Test Case 3 - Table 1	39
14	Comparison Between Predicted and Measured Temperature Distributions for Test Case 3 - Table 1	40
15	Predicted Velocity Distributions for Test Case 3 - Table 1	41
16	Comparison Between Predicted and Measured Velocity Distributions for Test Case 3 - Table 1	42

LIST OF ILLUSTRATIONS (Contd)

<u>Figure</u>	<u>Title</u>	<u>Page</u>
17	Predicted Temperature Distributions for Test Case 4 - Table 1	43
18	Comparison Between Predicted and Measured Temperature Distributions for Test Case 4 - Table 1	44
19	Predicted Velocity Distributions for Test Case 4 - Table 1	45
20	Comparison Between Predicted and Measured Velocity Distributions for Test Case 4 - Table 1	46
21	Predicted Temperature Distributions for Test Case 5 - Table 1	47
22	Comparison Between Predicted and Measured Temperature Distributions for Test Case 5 - Table 1	48
23	Predicted Velocity Distributions for Test Case 5 - Table 1	49
24	Comparison Between Predicted and Measured Velocity Distributions for Test Case 5 - Table 1	50
25	Predicted Temperature Distributions for Test Case 6 - Table 1	51
26	Comparison Between Predicted and Measured Temperature Distributions for Test Case 6 - Table 1	52
27	Predicted Velocity Distributions for Test Case 6 - Table 1	53
28	Comparison Between Predicted and Measured Velocity Distributions for Test Case 6 - Table 1	54
29	Predicted Temperature Distributions for Test Case 7 - Table 1	55
30	Comparison Between Predicted and Measured Temperature Distributions for Test Case 7 - Table 1	56
31	Predicted Velocity Distributions for Test Case 7 - Table 1	57

LIST OF ILLUSTRATIONS (Contd)

<u>Figure</u>	<u>Title</u>	<u>Page</u>
32	Comparison Between Predicted and Measured Velocity Distributions for Test Case 7 - Table 1	58
33	Predicted Temperature Distributions for Test Case 8 - Table 1	59
34	Comparison Between Predicted and Measured Temperature Distributions for Test Case 8 - Table 1	60
35	Predicted Velocity Distributions for Test Case 8 - Table 1	61
36	Comparison Between Predicted and Measured Velocity Distributions for Test Case 8 - Table 1	62
37	Predicted Temperature Distributions for Test Case 9 - Table 1	63
38	Comparison Between Predicted and Measured Temperature Distributions for Test Case 9 - Table 1	64
39	Predicted Velocity Distributions for Test Case 9 - Table 1	65
40	Comparison Between Predicted and Measured Velocity Distributions for Test Case 9 - Table 1	66
41	Predicted Temperature Distributions for Test Case 10 - Table 1	67
42	Comparison Between Predicted and Measured Temperature Distributions for Test Case 10 - Table 1	68
43	Predicted Velocity Distributions for Test Case 10 - Table 1	69
44	Comparison Between Predicted and Measured Velocity Distributions for Test Case 10 - Table 1	70

LIST OF ILLUSTRATIONS (Contd)

<u>Figure</u>	<u>Title</u>	<u>Page</u>
45	Predicted Temperature Distributions for Test Case 11 - Table 1	71
46	Comparison Between Predicted and Measured Temperature Distributions for Test Case 11 - Table 1	72
47	Predicted Velocity Distributions for Test Case 11 - Table 1	73
48	Comparison Between Predicted and Measured Velocity Distributions for Test Case 11 - Table 1	74
49	Predicted Temperature Distributions for Test Case 12 - Table 1	75
50	Comparison Between Predicted and Measured Temperature Distributions for Test Case 12 - Table 1	76
51	Predicted Velocity Distributions for Test Case 12 - Table 1	77
52	Comparison Between Predicted and Measured Velocity Distributions for Test Case 12 - Table 1	78
53	Predicted Temperature Distributions for Test No. 13 - Table 2	79
54	Comparison Between Predicted and Measured Temperature Distributions for Test No. 13 - Table 2	80
55	Predicted Velocity Distributions for Test No. 13 - Table 2	81
56	Comparison Between Predicted and Measured Velocity Distributions for Test No. 13 - Table 2	82
57	Predicted Temperature Distributions for Test No. 14 - Table 2	83
58	Comparison Between Predicted and Measured Temperature Distributions for Test No. 14 - Table 2	84
59	Predicted Velocity Distributions for Test No. 14 - Table 2	85

LIST OF ILLUSTRATIONS (Contd)

<u>Figure</u>	<u>Title</u>	<u>Page</u>
60	Comparison Between Predicted and Measured Velocity Distributions for Test No. 14 - Table 2	86
61	Predicted Temperature Distributions for Test No. 15 - Table 2	87
62	Comparison Between Predicted and Measured Temperature Distributions for Test No. 15 - Table 2	88
63	Predicted Velocity Distributions for Test No. 15 - Table 2	89
64	Comparison Between Predicted and Measured Velocity Distributions for Test No. 15 - Table 2	90
65	Predicted Temperature Distributions for Test No. 16 - Table 2	91
66	Comparison Between Predicted and Measured Temperature Distributions for Test No. 16 - Table 2	92
67	Predicted Velocity Distributions for Test No. 16 - Table 2	93
68	Comparison Between Predicted and Measured Velocity Distributions for Test No. 16 - Table 2	94
69	Predicted Temperature Distributions for Test No. 17 - Table 2	95
70	Comparison Between Predicted and Measured Temperature Distributions for Test No. 17 - Table 2	96
71	Predicted Velocity Distributions for Test No. 17 - Table 2	97
72	Comparison Between Predicted and Measured Velocity Distributions for Test No. 17 - Table 2	98
73	Predicted Temperature Distributions for Test No. 18 - Table 2	99
74	Comparison Between Predicted and Measured Temperature Distributions for Test No. 18 - Table 2	100

LIST OF ILLUSTRATIONS (Contd)

<u>Figure</u>	<u>Title</u>	<u>Page</u>
75	Predicted Velocity Distributions for Test No. 18 - Table 2	101
76	Comparison Between Predicted and Measured Velocity Distributions for Test No. 18 - Table 2	102
77	Comparison Between Predicted and Measured Velocity Trajectories For S/D = 2 and H <sub>0</sub> /D = 4	103
78	Comparison Between Predicted and Measured Velocity Trajectories Including Effects of Mainstream Profiles and Flow Area Convergence at Intermediate J for Orifice Plate 01/02/04	104
79	Comparison of Predicted and Measured Velocity Trajectories for Different Jet Diameters, S/H = 0.5	105
80	Predicted and Measured Velocity Trajectories for Non-Uniform Mainstream Profile and Flow Area Convergence, S/D = 4, H <sub>0</sub> /D = 8	106
81	Predicted and Measured Velocity Trajectories for Different Convergence and Jet Injection Angles, S/D = 4, H <sub>0</sub> /D = 8	107
82	Predicted and Measured Velocity Trajectories for S/D = 4, H <sub>0</sub> /D = 4	108
83	Predicted and Measured Velocity Trajectories for a Straight Duct for S/D = 2, H <sub>0</sub> /D = 8	109
84	Predicted and Measured Velocity Trajectories in Convergent Duct with Non-Uniform Mainstream Profile, S/D = 4, H <sub>0</sub> /D = 8 (Test Section V)	110
85	Predicted and Measured Velocity Trajectories for Opposed Jets, S/D = 2, H <sub>0</sub> /D = 8	111
86	Predicted and Measured Velocity Trajectories for Opposed Jets, S/D = 4, H <sub>0</sub> /D = 8	112
87	Predicted and Measured Velocity Trajectories for Opposed Jets With Non-Uniform Mainstream Profile	113

LIST OF ILLUSTRATIONS (Contd)

<u>Figure</u>	<u>Title</u>	<u>Page</u>
88	Predicted and Measured Velocity Trajectories with Unequal Momentum Flux Ratios, Flow Area Convergence, for Opposed Jets; S/D = 2, H <sub>0</sub> /D = 8	114
89	Predicted and Measured Velocity Trajectories for Opposed Jets in Convergent Ducts, S/D = 4, H <sub>0</sub> /D = 8	115
90	Predicted and Measured Velocity Trajectories for Opposed Jets with S/D = 4, H <sub>0</sub> /D = 8	116
91	Comparison Between Predicted and Measured Velocity Trajectories For Opposed In-line Jets with H <sub>0</sub> /D = 4 in a Straight Duct	117
92	Predicted and Measured Velocity Trajectories with Opposed Jets in Convergent Ducts, S/D = 2, H <sub>0</sub> /D = 4	118
93	Predicted and Measured Velocity Trajectories for 2-D Slots	119
94	Predicted and Measured Velocity Trajectories for the Remaining Test Cases in Phase II	120
95	Predicted and Measured Velocity Trajectories for Streamlined and Bluff Slots (Equivalent Size and Spacing to Orifice Plate 01/02/04)	121
96	Predicted and Measured Velocity Trajectories for Double Row of Jets (Plate M-3 and M-5)	122
97	Comparison of Predicted and Measured Velocity Trajectories for Plate 01/02/04, Plate M-4, and Equivalent Single Row of Jet Configurations	123
98	Predicted and Measured Velocity Trajectories for Double Row of Jets with Unequal Momentum Flux Ratios	124
99	Comparisons of Predicted and Measured Velocity Trajectories for 45-degree Slot and Equivalent Circular Holes	125
100	Measured Velocity Distributions for Test No. 1 of DJM Phase I Testing	127

LIST OF ILLUSTRATIONS (Contd)

<u>Figure</u>	<u>Title</u>	<u>Page</u>
101	Measured Velocity Distributions for Test No. 2 of DJM Phase I Testing	128
102	Measured Velocity Distributions for Test No. 3 of DJM Phase I Testing	129
103	Measured Velocity Distributions for Test No. 4 of DJM Phase I Testing	130
104	Measured Velocity Distributions for Test No. 5 of DJM Phase I Testing	131
105	Measured Velocity Distributions for Test No. 6 of DJM Phase I Testing	132
106	Measured Velocity Distributions for Test No. 7 of DJM Phase I Testing	133
107	Measured Velocity Distributions for Test No. 8 of DJM Phase I Testing	134
108	Measured Velocity Distributions for Test No. 9 of DJM Phase I Testing	135
109	Measured Velocity Distributions for Test No. 10 of DJM Phase I Testing	136
110	Measured Velocity Distributions for Test No. 11 of DJM Phase I Testing	137
111	Measured Velocity Distributions for Test No. 12 of DJM Phase I Testing	138
112	Measured Velocity Distributions for Test No. 13 of DJM Phase I Testing	139
113	Measured Velocity Distributions for Test No. 14 of DJM Phase I Testing	140
114	Measured Velocity Distributions for Test No. 15 of DJM Phase I Testing	141
115	Measured Velocity Distributions for Test No. 16 of DJM Phase I Testing	142

LIST OF ILLUSTRATIONS (Contd)

<u>Figure</u>	<u>Title</u>	<u>Page</u>
116	Measured Velocity Distributions for Test No. 17 of DJM Phase I Testing	143
117	Measured Velocity Distributions for Test No. 18 of DJM Phase I Testing	144
118	Measured Velocity Distributions for Test No. 23 of DJM Phase I Testing	145
119	Measured Velocity Distributions for Test No. 24 of DJM Phase I Testing	146
120	Measured Velocity Distributions for Test No. 25 of DJM Phase I Testing	147
121	Measured Velocity Distributions for Test No. 26 of DJM Phase I Testing	148
122	Measured Velocity Distributions for Test No. 27 of DJM Phase I Testing	149
123	Measured Velocity Distributions for Test No. 28 of DJM Phase I Testing	150
124	Measured Velocity Distributions for Test No. 29 of DJM Phase I Testing	151
125	Measured Velocity Distributions for Test No. 30 of DJM Phase I Testing	152
126	Measured Velocity Distributions for Test No. 31 of DJM Phase I Testing	153
127	Measured Velocity Distributions for Test No. 32 of DJM Phase I Testing	154
128	Measured Velocity Distributions for Test No. 33 of DJM Phase I Testing	155
129	Measured Velocity Distributions for Test No. 34 of DJM Phase I Testing	156
130	Measured Velocity Distributions for Test No. 3 of DJM Phase II Testing	157
131	Measured Velocity Distributions for Test No. 4 of DJM Phase II Testing	158

LIST OF ILLUSTRATIONS (Contd)

<u>Figure</u>	<u>Title</u>	<u>Page</u>
132	Measured Velocity Distributions for Test No. 5 of DJM Phase II Testing	159
133	Measured Velocity Distributions for Test No. 6 of DJM Phase II Testing	160
134	Measured Velocity Distributions for Test No. 12 of DJM Phase II Testing	161
135	Measured Velocity Distributions for Test No. 13 of DJM Phase II Testing	162
136	Measured Velocity Distributions for Test No. 14 of DJM Phase II Testing	163
137	Measured Velocity Distributions for Test No. 15 of DJM Phase II Testing	164
138	Measured Velocity Distributions for Test No. 16 of DJM Phase II Testing	165
139	Measured Velocity Distributions for Test No. 17 of DJM Phase II Testing	166
140	Measured Velocity Distributions for Test No. 18 of DJM Phase II Testing	167
141	Measured Velocity Distributions for Test No. 19 of DJM Phase II Testing	168
142	Measured Velocity Distributions for Test No. 20 of DJM Phase II Testing	169
143	Measured Velocity Distributions for Test No. 21 of DJM Phase II Testing	170
144	Measured Velocity Distributions for Test No. 22 of DJM Phase II Testing	171
145	Measured Velocity Distributions for Test No. 23 of DJM Phase II Testing	172
146	Measured Velocity Distributions for Test No. 24 of DJM Phase II Testing	173

LIST OF ILLUSTRATIONS (Contd)

<u>Figure</u>	<u>Title</u>	<u>Page</u>
147	Measured Velocity Distributions for Test No. 25 of DJM Phase II Testing	174
148	Measured Velocity Distributions for Test No. 26 of DJM Phase II Testing	175
149	Measured Velocity Distributions for Test No. 35 of DJM Phase II Testing	176
150	Measured Velocity Distributions for Test No. 36 of DJM Phase II Testing	177
151	Measured Velocity Distributions for Test No. 37 of DJM Phase II Testing	178
152	Measured Velocity Distributions for Test No. 38 of DJM Phase II Testing	179
153	Measured Velocity Distributions for Test No. 39 of DJM Phase II Testing	180
154	Measured Velocity Distributions for Test No. 40 of DJM Phase II Testing	181
155	Measured Velocity Distributions for Test No. 41 of DJM Phase II Testing	182
156	Measured Velocity Distributions for Test No. 42 of DJM Phase II Testing	183
157	Measured Velocity Distributions for Test No. 45A of DJM Phase II Testing	184
158	Measured Velocity Distributions for Test No. 45B of DJM Phase II Testing	185
159	Measured Velocity Distributions for Test No. 45C of DJM Phase II Testing	186
160	Measured Velocity Distributions for Test No. 49 of DJM Phase II Testing	187
161	Measured Velocity Distributions for Test No. 50 of DJM Phase II Testing	188

LIST OF ILLUSTRATIONS (Contd)

<u>Figure</u>	<u>Title</u>	<u>Page</u>
162	Measured Velocity Distributions for Test No. 1 of DJM Phase III Testing	189
163	Measured Velocity Distributions for Test No. 2 of DJM Phase III Testing	190
164	Measured Velocity Distributions for Test No. 3 of DJM Phase III Testing	191
165	Measured Velocity Distributions for Test No. 4 of DJM Phase III Testing	192
166	Measured Velocity Distributions for Test No. 5 of DJM Phase III Testing	193
167	Measured Velocity Distributions for Test No. 6 of DJM Phase III Testing	194
168	Measured Velocity Distributions for Test No. 7 of DJM Phase III Testing	195
169	Measured Velocity Distributions for Test No. 8 of DJM Phase III Testing	196
170	Measured Velocity Distributions for Test No. 9 of DJM Phase III Testing	197
171	Measured Velocity Distributions for Test No. 10 of DJM Phase III Testing	198
172	Measured Velocity Distributions for Test No. 11 of DJM Phase III Testing	199
173	Measured Velocity Distributions for Test No. 12 of DJM Phase III Testing	200
174	Measured Velocity Distributions for Test No. 13 of DJM Phase III Testing	201
175	Measured Velocity Distributions for Test No. 14 of DJM Phase III Testing	202
176	Measured Velocity Distributions for Test No. 15 of DJM Phase III Testing	203

LIST OF ILLUSTRATIONS (Contd)

<u>Figure</u>	<u>Title</u>	<u>Page</u>
177	Measured Velocity Distributions for Test No. 16 of DJM Phase III Testing	204
178	Measured Velocity Distributions for Test No. 17 of DJM Phase III Testing	205
179	Measured Velocity Distributions for Test No. 18 of DJM Phase III Testing	206
180	Measured Velocity Distributions for Test No. 19 of DJM Phase III Testing	207
181	Measured Velocity Distributions for Test No. 20 of DJM Phase III Testing	208
182	Measured Velocity Distributions for Test No. 21 of DJM Phase III Testing	209
183	Measured Velocity Distributions for Test No. 22 of DJM Phase III Testing	210

LIST OF TABLES

<u>Table</u>	<u>Title</u>	<u>Page</u>
1	Test Cases of 3-D Calculations Performed in Host Aerothermal Modeling Program	12
2	Test Cases of 3-D Calculations Performed in the NASA Dilution Jet Mixing Program	13
3	Configurations and Flow Conditions for Phase I, Series 1 Tests	211
4	Configurations and Flow Conditions for Phase I, Series 2 Tests	211
5	Configurations and Flow Conditions for Phase I, Series 3 Tests	212
6	Configurations and Flow Conditions for Phase I, Series 4 Tests	212
7	Configurations and Flow Conditions for Phase II, Series 5 Tests	213
8	Configurations and Flow Conditions for Phase II, Series 6 Tests	213
9	Configurations and Flow Conditions for Phase II, Series 7 Tests	214
10	Configurations and Flow Conditions for Phase II, Series 8 Tests	215
11	Configurations and Flow Conditions for Phase III, Series 9 Tests	217
12	Configurations and Flow Conditions for Phase III, Series 10 Tests	217



## 1.0 SUMMARY

In this report, velocity and temperature distributions predicted by a 3-D numerical model are presented and compared with measurements taken during the Dilution Jet Mixing program (Contract NAS3-22110). In addition, empirical correlations for the jet velocity trajectory developed in this program are presented. For all of the configurations tested in the Dilution Jet Mixing program (Phases I through III), measurements of both temperature and velocity distributions were made at several axial stations. The measured temperature distributions were reported in the three previous reports. The measured velocity distributions for all test cases performed in this program are presented in this report in the form of contour and oblique plots. The velocity distributions show characteristics similar to those observed in temperature distributions.



## 2.0 INTRODUCTION

Advanced aircraft propulsion gas turbine engines for civil and military applications require increased thrust or horsepower per unit airflow. The increased power density often results in higher average combustor discharge temperature with attendant reduction of the available dilution air. Effective use must be made of the available dilution air to tailor the combustor discharge temperature distribution.

The combustor discharge temperature quality is influenced by nearly all aspects of the combustor design and in particular by the dilution zone. To tailor the combustor discharge temperature pattern, the discharge temperature distribution must be characterized in terms of the dilution zone geometric and flow parameters. Such characterization requires an improved understanding of the dilution jet mixing processes.

The present program has been undertaken to acquire a data base of dilution jet mixing characteristics, to develop empirical jet mixing correlations and to validate combustor analytical design models.

The main objectives of the NASA Dilution Jet Mixing Program are to quantify the effects of the following on the jet mixing characteristics with a confined cross-flow:

- o Orifice geometry, momentum flux ratio, and density ratio
- o Nonuniform mainstream temperature and velocity profiles upstream of dilution orifices
- o Cold versus hot jet injection

- o Cross-stream flow area convergence (accelerating cross-stream) as encountered in practical dilution-zone geometries.
- o 2-D slots versus circular orifices
- o Discrete noncircular orifices
- o Single-sided versus opposed (in-line and staggered) jets
- o Single row versus double row of jets

Besides generating a data base, a limited number of 3-D numerical computations were made for several dilution jet configurations. The comparison between the numerical predictions and the test data are presented in Section 4.

As a part of the program, an empirical model describing the jet mixing characteristics was developed. The model results for temperature field are reported in References 1 through 3. The empirical model also predicts the jet velocity trajectory for all the configurations tested in the program. A description of the empirical model for velocity trajectory and the comparison between data and model results are provided in Section 5.

The temperature measurements obtained in this program are reported in References 1 through 3. This report contains all the velocity data obtained in the NASA Dilution Jet Mixing Program under Contract NAS3-22110.

### 3.0 DESCRIPTION OF TEST RIG, INSTRUMENTATION, AND DATA REDUCTION

#### 3.1 Test Rig

A schematic layout of the jet mixing test rig is presented in Figure 1. The mainstream airflow is ducted from the test cell main air supply through a 15.24-cm internal diameter pipe. A transition section connects the inlet pipe to a rectangular cross section of constant width (30.48 cm) and adjustable height.

A perforated plate with 25 holes of 1.43-cm diameter provides a relatively uniform airstream at the profile generator plenum. The profile generator duct incorporates an adjustable bottom wall to match the test section inlet height, which can vary from 10.16 cm to 15.24 cm.

A separate air supply enables the profile generator to provide the desired radial profile of temperature and velocity upstream of the jet-injection plane.

A third air supply allows the dilution injection orifices to vary jet velocity and density. A number of interchangeable dilution orifice plates and test section geometries are used to study confined jet mixing with the mainstream. To minimize the rig thermal losses, the rig walls are insulated with a 2.54-cm thick layer of Kaolite insulation.

Detailed descriptions of the profile generator, test sections, and dilution orifice plates are provided in References 1 through 3. The test sections used in this program are shown in Figure 2, and the orifice plate configurations employed are illustrated in Figure 3.

The rig instrumentation includes a number of wall static pressure taps and flow thermocouples, in addition to a traversing Pt/Ps/T rake.

### 3.2 Instrumentation

The dilution jet mixing characteristics were determined by measuring temperature and pressure distributions within the test section at different axial stations. A traversing probe (Figure 4) is used for this purpose.

The probe consists of a 20-element thermocouple rake with 20 total-pressure sensors on one side and 20 static-pressure rakes on the other side. The nominal transverse spacing between the thermocouple rake and the total pressure rake is 0.508 cm. The spacing between the thermocouple and the static pressure elements is 0.508 cm.

The height of the probe between the top and the bottom elements is 9.35 cm. The first element is located 0.405 cm from the top wall of the constant-height test section (Test Section I). All the elements are equally spaced in the vertical direction, providing a nominal spacing of 0.492 cm.

The total-pressure sensor elements are made of Inconel tubes with an outside diameter of 0.16 cm and a wall thickness of 0.023 cm. The internal conical design of the tube at the inlet provides a  $\pm 15$  degree flow insensitivity angle. The static pressure tubes, similar to the total pressure sensors, are dead-ended with four bleeding holes of 0.03-cm diameter 90 degrees apart and 0.7 cm from the tip. The total temperature sensors are type K thermocouple wires with insulated junctions encased in 0.10-cm inside diameter tubes, supported by 0.21-cm inside diameter enveloping tubes. The insulated junction tubes exposed to the air stream are 0.76-cm long. The sensing elements have a straight length of 1.52 cm or more

before the first bend to the probe core, where all tubes are inserted in a rectangular probe shield,  $4.32 \times 0.67$  cm.

The probe is mounted on a traversing system that allows travel in three directions. This system allows for a 30.48-cm traverse in the X-direction (mainstream flow direction) and 22.86 cm in the radial (Y) and transverse (Z) directions with an accuracy of  $\pm 0.015$  percent. The flow field mapping in the Z direction is made at several planes starting at  $Z/S = -0.5$  at intervals of 0.1. The measurements in the X-direction were made at axial planes between  $X/H_0 = 0.25$  and  $X/H_0 = 2.0$ .

The temperature and pressure values from the test rig instrumentation are recorded on magnetic tape through a central computerized data acquisition system. An on-line data display system provides real-time information on selected raw data for monitoring the flow conditions. The raw data from the magnetic tape is used for detail data reduction, analysis, and correlation.

### 3.3 Data Reduction

The pressure recordings from the probe rake were used to compute the velocity  $V(X,Y,Z)$  at the point  $(X,Y,Z)$ . An interpolation scheme was used to compute pressure ( $P_s$ ) values at the point where probe thermocouples are located. From these total and static pressures, a nondimensionalized velocity,  $V(X,Y,Z)/V_j$ , was computed.  $V(X,Y,Z)$  is obtained from

$$V(X,Y,Z) = \left\{ 2 [P_t(X,Y,Z) - P_s(X,Y,Z)] / \rho(X,Y,Z) \right\}^{1/2}$$

The jet velocity,  $V_j$ , is calculated from

$$V_j = 4 \dot{m}_j / (\rho_j N \pi D^2 C_D)$$

where  $D$  is the orifice diameter,  $N$  is the number of orifices,  $\rho_j$  is the jet density ( $P_j/RT_j$ ), and  $C_D$  is the orifice discharge coefficient.

The orifice discharge coefficients were determined by measuring the pressure drop across the orifice plate (without cross flow) for a range of mass flow rates. The discharge coefficient,  $C_D$ , was obtained from the relation

$$\frac{\Delta P}{P} = 1.99 \left[ \frac{\dot{w}_c}{AC_D} \right]^2$$

where,  $\dot{w}_c$  is the corrected flow rate in  $\text{lbm/sec}$  and  $A$  is the geometric area of the orifices in square inches.

$$\text{Note: } \dot{w}_c = \dot{w}_a \frac{\sqrt{\beta}}{\delta}, \text{ where } \beta = \frac{T(^\circ R)}{518.67}, \text{ and } \delta = \frac{P(\text{psi})}{14.696}$$

The velocity vector in the vicinity of the jet injection plane is predominantly in the radial direction. In such regions, the velocity values obtained from the rake probe are not expected to be accurate.

An important parameter relevant to the jet description is the jet momentum flux ratio,  $J$ , defined as

$$J = \rho_j V_j^2 / (\rho_m V_m^2)$$

where

$\rho_j$  = Jet density

$\rho_m$  = Mainstream density =  $P_m/(RT_m)$

$V_j$  or  $V_{JET}$  = Jet velocity at the orifice Vena Contracta

$V_m$  or  $V_{MAIN}$  = Mainstream Velocity =  $\dot{m}_m / (\rho_m A_m)$

$A_m$  = Effective mainstream flow area.

$\dot{m}_m$  = Mainstream flow rate

Other flow parameters of interest are:

Mass flux ratio (blowing rate), M or BLORAT =  $\rho_j V_j / \rho_m V_m$

Temperature ratio, TRATIO =  $T_j / T_m$

Density ratio, DENRATIO =  $\rho_j / \rho_m$

Velocity ratio =  $V_j / V_m$ .

The geometric parameters of importance associated with the orifice configuration are:  $S/D_j$  and  $H_0/D_j$ , where  $D_j$  is the effective jet diameter defined by

$$D_j = D \left( C_D \right)^{0.5}$$

The quantities described in this section define the geometric and flow conditions of each test and are reported along with the reduced data.

The average mainstream velocity,  $V_m$  and the average jet velocity,  $V_j$ , are mass weighted average values for the test. They represent the correct momentum flux for the mainstream and the jet, respectively.



#### 4.0 RESULTS OF NUMERICAL CALCULATIONS

The empirical correlations developed in this program and other existing empirical models describing the jet mixing characteristics are applicable only within the scope of the experiments from which these models are generated. Many practical combustion systems have geometries that are not investigated in these experiments. The jet mixing behavior in such systems can be predicted by 3-D numerical calculations. In the Host Aerothermal Modeling Program Phase I (Contract NAS3-23523), 3-D numerical calculations were performed for 10 dilution jet mixing test cases. The predicted temperature distributions are reported in Reference 4.

The 3-D calculations performed in that program include the test configurations shown in Table 1. The predicted temperature and velocity distributions by the 3-D model for these cases are presented in Figures 5 through 52 in the form of oblique and contour plots. The velocity distributions show the same characteristics as the predicted temperature distributions.

The 3-D model underestimates the mixing of the velocity field. Decreasing the number of finite-difference grids tends to increase the mixing, which demonstrates that the solution is grid dependent and that the numerical diffusion effects are significant. The jet velocity penetration (corresponding to maximum velocity point) and the acceleration of the cross flow around the jet are correctly predicted by the model; but the magnitudes of the predicted velocity are only within 20 percent of the measured values.

As a part of the Phase III Dilution Jet Mixing Program, similar 3-D numerical calculations were made for six dilution jet configurations shown in Table 2.

The predicted temperature and velocity distributions for these six cases are presented in Figures 53 through 76. These figures

TABLE 1. SAMPLE CASES OF 3-D CALCULATIONS PERFORMED IN  
HOST AEROTHERMAL MODELING PROGRAM

Case No.	Orifice Configuration	Number of Nodes	Orifice Dia (cm)	S/D	H <sub>0</sub> /D	J	DJM Test Case No.	
							Phase	Test No.
1	Single-Sided	35x33x17	1.27	2.0	8.0	22.32	I	5
2	Single-Sided	27x26x8	1.27	2.0	8.0	22.32	I	5
3	Single-Sided	35x33x17	1.27	2.0	8.0	92.63	I	6
4	Single-Sided	27x26x8	1.27	2.0	8.0	92.63	I	6
5	Single-Sided	35x33x17	1.80	2.83	5.66	25.48	II	50
6	Single-Sided	32x29x21	1.80	2.83	5.66	25.48	II	50
7	Single-Sided	45x23x19	2.54	2.0	4.0	18.59	I	2
8	Single-Sided	40x23x21	2.54	4.0	4.0	23.51	I	4
9	Single-Sided	40x23x21	2.54	4.0	4.0	5.31	I	3
10	Top Cold Profile	45x23x19	2.54	2.0	4.0	31.79	I	13
11	Opposed In-Line	35x33x17	1.27	2.0	8.0	24.94	II	2
12	Opposed Staggered	22x27x33	2.54	4.0	4.0	26.41	II	28

TABLE 2. SAMPLE CASES OF 3-D CALCULATIONS PERFORMED IN  
THE NASA DILUTION JET MIXING PROGRAM

Case No.	Orifice Configuration	Number of Nodes	Orifice Dia (cm)	S/D	H <sub>0</sub> /D	J	DJM Test Case No.	
							Phase	Test No.
13	Single-Sided	36x29x19	1.27	4.0	8.0	28.37	I	7
14	In-Line, 2 Rows	41x23x21	1.80 1.80	2.83 2.83	5.66 5.66	26.27 26.85	III	6
15	Single-Sided Conv. Duct	42x28x17	2.54	2.0	4.0	26.36	I	26
16	45-Deg. Slot	45x23x19	2.54	2.0	4.0	27.13	III	19
17	Offset, 2 Rows	41x23x21	1.80 1.27	2.83 2.00	5.66 8.00	26.79 26.63	III	11
18	Single-Sided	45x23x19	2.54	2.00	4.00	26.24	III	22

show the contour and oblique plots of nondimensionalized temperature and velocity distributions, along with their vertical profiles along the jet centerplane. The following general conclusions are made from these figures:

- o The jet velocity penetration is farther than the temperature penetration.
- o The 3-D model underestimates the mixing of velocity and temperature fields, especially in the transverse direction.
- o The predicted centerplane velocity profiles are in good agreement with the data. The centerplane velocity profiles are more accurately predicted by the 3-D model than the temperature profiles.
- o For 45-degree slots, the 3-D numerical model correctly predicts the transverse shift of the centerplane profiles, as well as the rotation of the theta contours. The rotation of theta contours is not predicted by the Garrett empirical model for angled slots.
- o The 3-D model predictions are in qualitative agreement with the data. Improvements in the numerics and turbulence models are needed to accurately correlate with the measurements.

## 5.0 VELOCITY TRAJECTORY CORRELATIONS

The interaction of dilution jets injected normally into a confined cross flow is highly complex and three-dimensional in nature. Accurate characterization of this interaction requires multidimensional models. Such models are currently in development and are not yet validated. Furthermore, the multidimensional models are not currently cost effective for making hardware changes in the combustor to meet the combustor exit profile requirements. In order to aid the combustor design efforts, GTEC developed empirical models for characterizing the dilution jet mixing in confined cross flows, by using the data obtained in this program. The empirical model is based upon the correlations reported in Reference 5. The GTEC correlations are applicable to the following configurations:

- o Single sided and opposed jets
- o Single row as well as multiple rows of jets
- o Circular and noncircular jets
- o 2-D slots and discrete angled slots.
- o Nonuniform cross flow temperature and velocity profiles
- o Flow area convergence.

Descriptions of the empirical model and its results were reported in References 1 through 3. In these references, only the temperature field was presented. In addition to correlating the temperature field, the empirical model also estimates velocity trajectory.

The expression for jet velocity trajectory developed in the GTEC empirical model is based upon the following form proposed by Walker and Eberhardt (Reference 6):

$$Y_v/D_j = 0.549 J^{0.12} (S/D_j)^{0.23} (H_0/D_j)^{0.57} (X/D_j)^{0.18} \quad (1)$$

where,

$y_v$  is the jet velocity penetration

$D_j$  is the effective jet diameter

$S$  is the orifice spacing

$H_0$  is the channel height at jet injection plane

$J$  is the momentum flux ratio.

Preliminary comparison between data and this expression indicated poor agreement between the two. Based upon the data obtained in this Dilution Jet Mixing Program, the following expression was developed at GTEC for correlating the jet velocity trajectory:

$$\left(\frac{y_v}{D_j}\right) = a_o J^{0.12} \left(\frac{S}{D_j}\right)^{0.23} \left(\frac{H_0}{D_j}\right)^{0.57} \left(\frac{x}{D_j}\right)^\alpha \quad (2)$$

where,

$$a_o = 0.765 \left[1 + \frac{dH}{dx}\right]^{0.35} \quad (3)$$

$$\alpha = 0.12 \left[1 + \frac{dH}{dx}\right]^{1.25} \quad (4)$$

and  $\frac{dH}{dx}$  is a measure of the rate of area change.

For a straight duct

$(dH/dx = 0)$   $a_o = 0.765$  and  $\alpha = 0.12$ .

Note the difference between equations (1) and (2), namely, larger value of empirical constant  $a_o$  and slower decay in the stream-wise direction. Both these equations give the same jet trajectory for  $X/D_j = 250$ .

The results obtained from equation (2) and their comparison with test data are presented in Figures 77 through 99. In these figures, the locations of measured jet trajectories are shown by symbols, and predictions are shown by solid lines. For opposed and double rows of holes, the trajectories corresponding to the bottom injections or aft row of jets, whichever is applicable, are shown by the broken lines. In these figures, the data points were obtained by interpolating between the measured values. It is important to note that the velocity measurements were made using a probe rake. Such measurements are not expected to be accurate close to the jet injection plane. Consequently, the velocity trajectory data in those regions are not accurate. The following general conclusions are made by comparing the trajectories obtained from the empirical model with the test data:

- The empirical model correctly predicts, within measurement accuracy, the trajectories for  $S/D = 2$  and underestimates it for  $S/D = 4$ .
- The model underestimates jet velocity trajectories for tests using convergent ducts.
- For opposed jets, the empirical model accurately predicts the jet penetrations for in-line arrangements; the agreement between data and model results are poor for staggered configurations.
- The empirical model underestimates the jet penetrations for 2-D slots when equation (2) is used with  $S/D_j=1$  and  $H_0/D_j$  is replaced by  $H_0/w$ , where  $w$  is the slot width.
- Jet velocity trajectories for bluff slots and 45-degree slots are accurately predicted by the model, while those

for streamlined slots are underestimated. For these discrete slots, the  $D_j$  values employed in equation (2) correspond to those of equivalent area circular holes.

- o For double rows of jets, the model accurately estimates jet penetrations for in-line arrangement and underestimates them for staggered and offset configurations. For multiple rows of jets, the lead row jet penetrations correlate well with the measurements.
- o The empirical model for velocity trajectory must be evaluated against more accurate data on trajectory.

## 6.0 RESULTS OF VELOCITY MEASUREMENTS

In References 1 through 3, the measured temperature distributions were presented for all test cases performed in Phases I through III. The test configurations and flow conditions for these tests are presented in Tables 3 through 12. In all these test cases, total and static pressure measurements were made in addition to obtaining thermocouple data, as described in paragraph 4.1. From the total and static pressure data, the axial velocity component is computed in the form described in paragraph 4.2. The measurements obtained from the rake probe are not reliable in some regions, especially in regions close to the injection plane where the velocity vectors are not aligned with the total pressure elements. In these regions, the measured rake probe static pressures show higher values than the corresponding total pressure data. The velocity values in such situations are set equal to zero. The measured velocity distributions are presented in nondimensional form as  $(U - V_{\text{main}})/V_{\text{jet}}$ .

Evaluation of the test data showed that for some of the test cases, the accuracy of velocity data was very poor. For these test cases, the velocity data will not be presented:

- o Phase I - Tests 19 through 22 and 35 through 38.
- o Phase II - Tests 1, 2, 7, 8, 9, 10, 11, 27 through 34, 43, and 44, 46, 47, 48 and 51.

For the remaining test cases performed in Phases I through III, the nondimensionalized velocity distributions are presented in the form of contour plots and oblique plots. These results are shown in Figures 100 through 183. The following conclusions are drawn from the velocity data:

- o The jet velocity penetration (location of maximum velocity) is farther than the jet temperature penetration. However, when the jet penetration is close to the opposite wall, the jet velocity and temperature centerlines are close to each other.
- o The rate at which laterally two-dimensional profiles are obtained for velocity is faster than the rate for temperature distributions.
- o The jet-to-mainstream density ratio,  $\rho_j/\rho_m$ , has at best a second order influence on the velocity distributions for a given momentum flux ratio.
- o The influence of nonuniform mainstream velocity profile on the velocity distribution is significant; but the superposition scheme applicable to temperature distributions may not be applicable to velocity distributions (Figures 112-117 and 135-140).
- o Flow area convergence enhances jet mixing. Velocity distributions in an asymmetrically convergent duct with jet injection from the flat wall (Figures 122-125) are very similar to those in an equivalent symmetrically convergent duct (Figures 118-121) at the same momentum flux ratio. For an asymmetrically convergent duct with jet injection from the slant wall, the velocity gradients in the vertical direction (Figures 126-129) are steeper than those with flat wall injection or symmetrical convergence. The jet spreading rates in the transverse direction are faster for slant wall jets than the other two configurations.
- o Opposed jets injected into an asymmetrically convergent duct produce velocity distributions (Figures 149-156) similar to those in a symmetrically convergent duct

(Figures 141-148) beyond  $X/H_0 = 0.5$ . In the regions closer to the injection plane, the jets from the slant wall show deeper penetration than those from the flat wall.

- Orifice plates having the same  $S/H_0$  ratio produce similar velocity distributions at the same momentum flux ratios.
- The velocity distributions produced by streamlined slots are similar to those of equivalent area circular holes with the same  $S/H_0$  and momentum flux ratio in regions beyond  $X/H_0 = 1$ . In the regions closer to the jet injection plane, the velocity profiles for streamlined slots show smaller vertical gradients compared to equivalent area circular holes.
- The bluff slots have smaller jet velocity penetration compared to streamlined slots or equivalent area circular holes, but the velocity distributions are more two-dimensional in nature. The bluff slots produce larger vertical velocity gradients compared to equivalent area circular holes.
- Double rows of in-line jets with  $S/D = 2.83$ ,  $H_0/D = 5.66$  (Plate M-3, Figure 3) produce velocity distributions very similar to those of single row of jets with the same spacing and diameter at the same momentum flux ratio. The velocity profiles for these two orifices are similar, while the magnitudes are different. Plate M-3 produces smaller velocity gradients in the vertical direction than the equivalent area circular holes (Plate 01/02/04) at the same momentum flux ratio.
- The configuration with a double row of dissimilar holes (Plate M-5, Figure 3) produces steeper velocity gradients

in the vertical direction compared to Plate M-3. These gradients are still smaller compared to those produced by a single row of jet of equivalent area.

- o In orifice Plate M-5, increasing the flows in the downstream row of jets increases the velocity gradients in the vertical direction.
- o Plate M-6 (with leading row of holes having  $S/D = 2$  and  $H_0/D = 8$ ) produces velocity profiles very similar to those of orifice plate 01/02/08 (single row with  $S/D = 2$  and  $H_0/D = 8$ ) (See Figure 3 for orifice configurations.).
- o The 45-degree slot generates a skewed vortex field, which shifts the velocity centerplanes in the direction of slot. In addition, the vortex field rotates the velocity contours about the axis of the slot.

## 7.0 CONCLUSIONS

The NASA Dilution Jet Mixing program under Contract NAS3-2210, was directed toward characterizing mixing processes of jets injected into a confined cross flow. Measurements of temperature and velocity were made for several orifice shapes and configurations. The velocity distributions for these test cases are presented in this report. In addition, empirical correlations were developed to quantify the jet velocity trajectory. Comparison between the data and the empirical model shows agreement within the accuracy of measurements for most of the jet configurations studied.

As a part of the program, 3-D numerical calculations were performed for several different orifice configurations. The 3-D model underestimates the mixing of velocity and temperature fields. Advanced numerics and turbulence models are needed to improve the accuracy of 3-D model predictions.



## LIST OF SYMBOLS

A	Test section cross-sectional area at survey plane
AR	Aspect Ratio (frontal width/streamwide length)
C <sub>D</sub>	Orifice discharge coefficient
D	Geometric orifice diameter
D <sub>j</sub>	Effective orifice diameter
H <sub>0</sub>	Duct height at the jet injection plane
J	Momentum flux ratio $\rho_j V_j^2 / \rho_m V_m^2$
P <sub>t</sub>	Stagnation pressure
P <sub>s</sub>	Static pressure
S	Orifice spacing
T	Temperature
V	Velocity
X	x direction, parallel to duct axis
Y	y direction, parallel to orifice centerline (radial direction)
Y <sub>V</sub>	Centerplane velocity trajectory
Z	z direction, normal to duct axis (transverse direction)

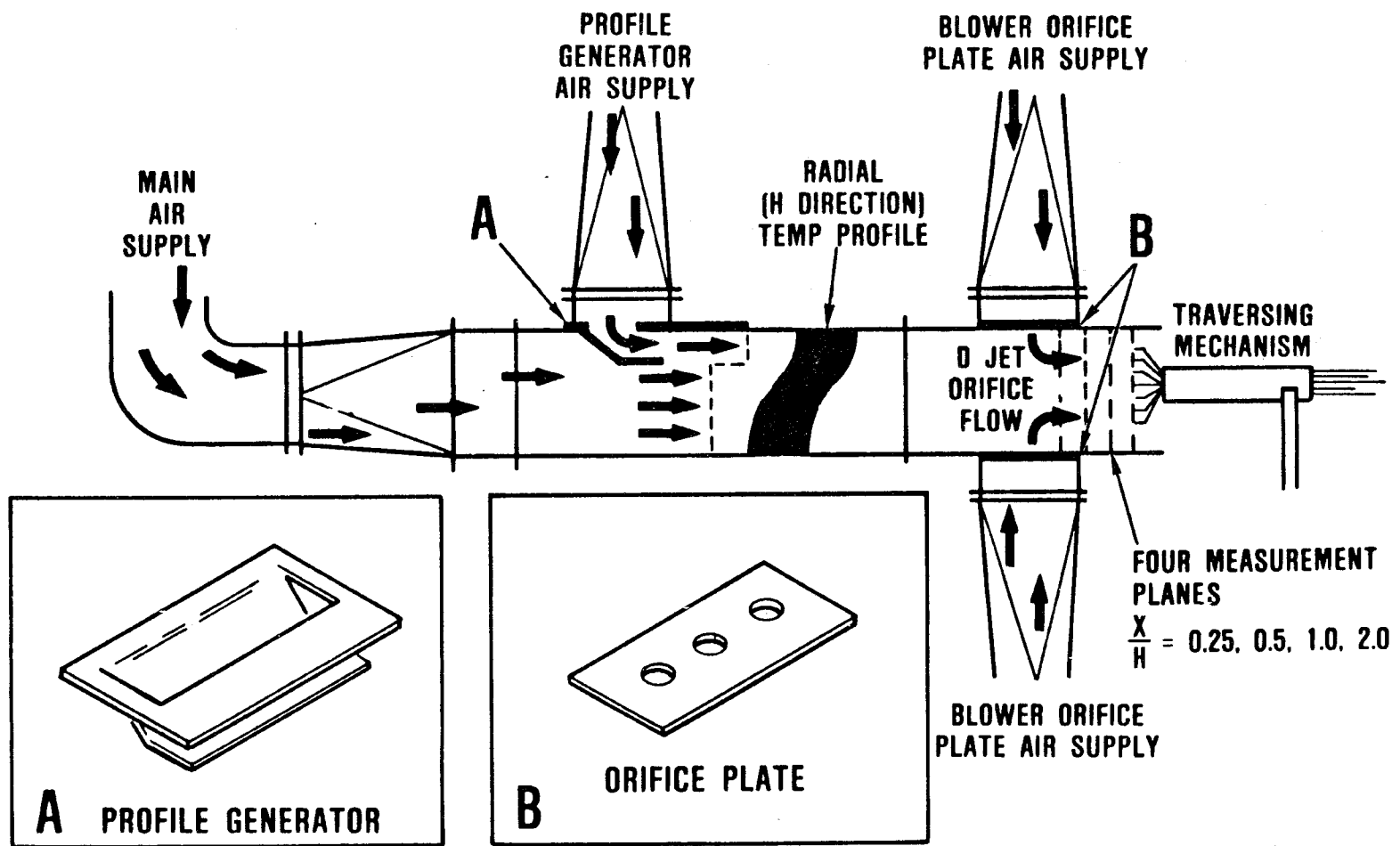
### Greek

$\theta$	Temperature difference ratio
$\rho$	Density

### Subscripts

av	Average
EB	Equilibrium value
j	Jet property
max	Maximum
m	Cross-flow property, average value
F	First or lead row jet conditions
B	Back or aft row jet conditions





23-SVG1657-2

Figure 1. Dilution Jet Mixing Rig Schematic.

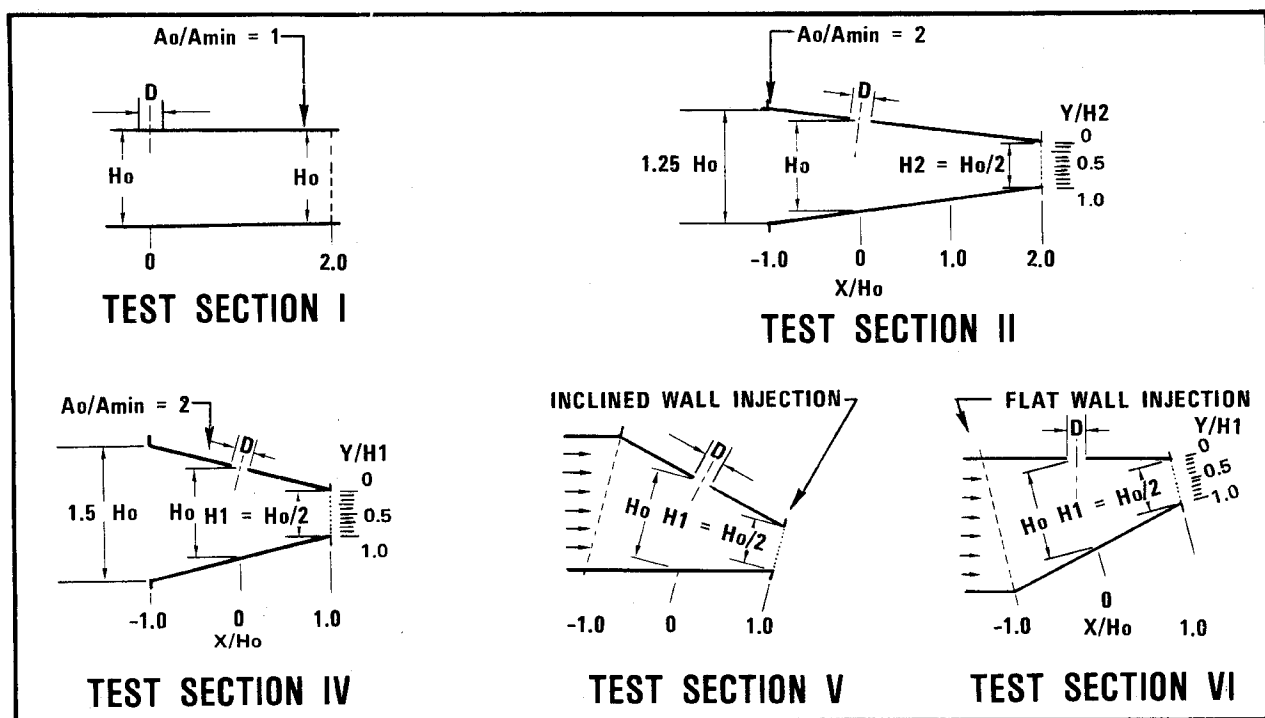
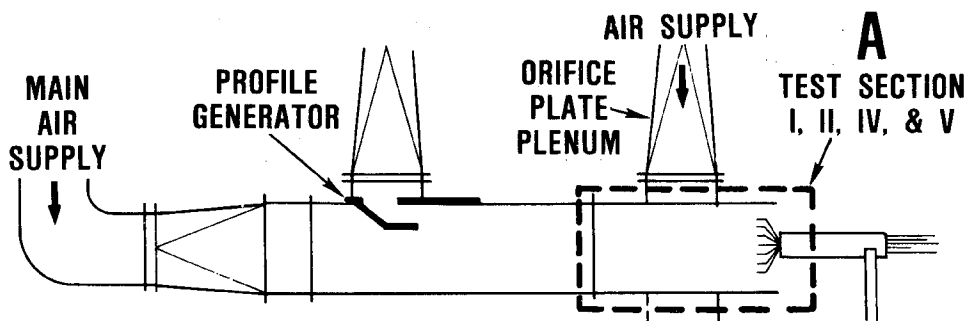
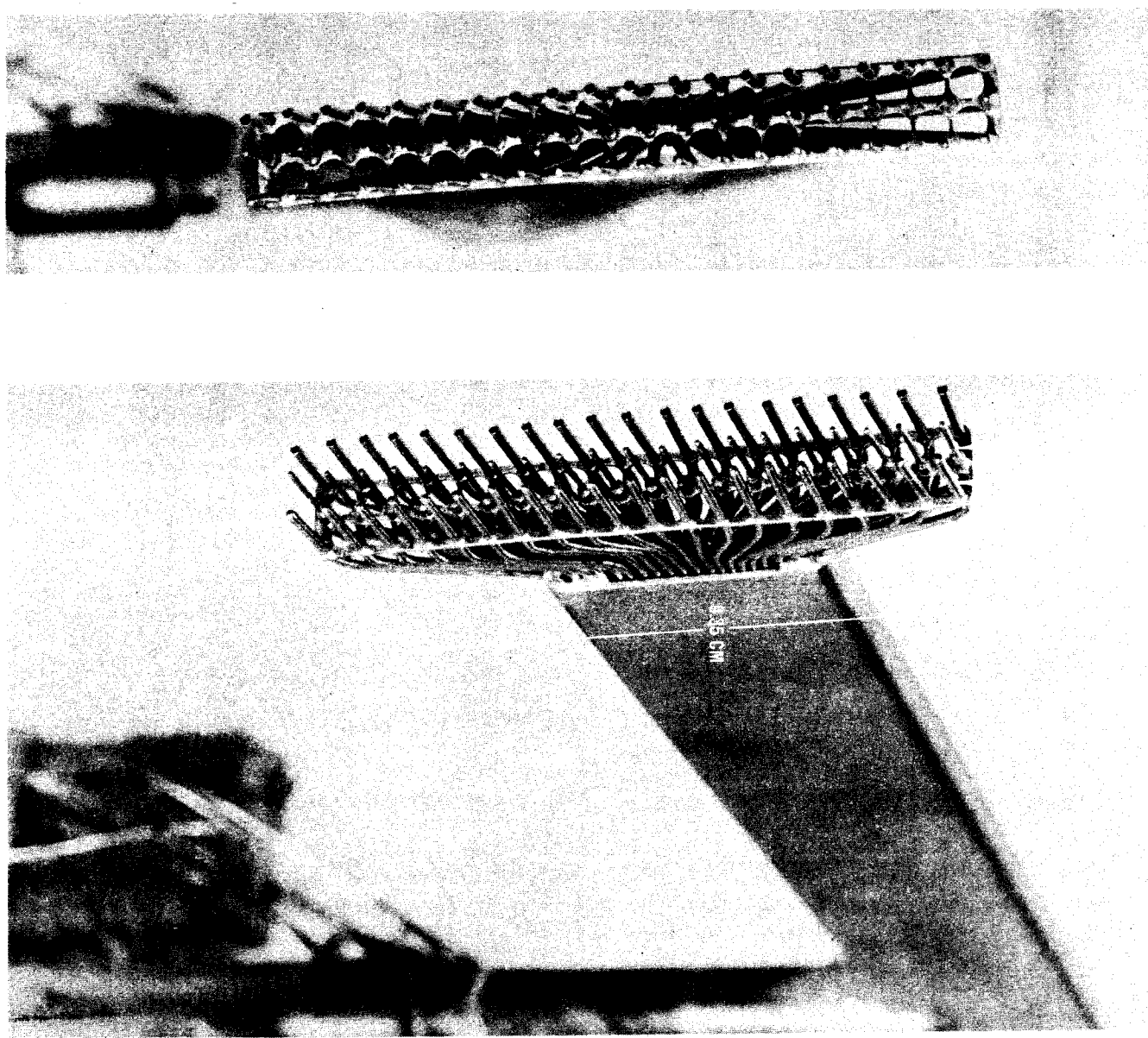


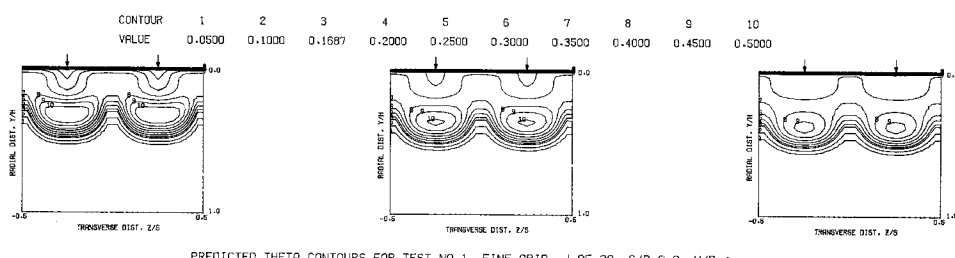
Figure 2. Schematics of Test Sections Used in the Program  $H_0=10.16$  cm.

<u>CONFIGURATION</u>	<u>SYMBOL</u>	<u>ORIFICE DIAMETER (CM)</u>	<u>S/D</u>	<u>H<sub>0</sub>/D</u>
○○○○○    $\leftarrow \infty \rightarrow$	01/02/04	2.54	2	4
○    $\leftarrow \infty \rightarrow$    ○	01/04/04	2.54	4	4
○○○○○○○○○○○○○○    $\leftarrow \infty \rightarrow$	01/02/08	1.27	2	8
○○○○○○○○○○    $\leftarrow \infty \rightarrow$	01/04/08	1.27	4	8
○○○○○○○○○○    $\leftarrow \infty \rightarrow$	01/03/06	1.80	2.83	5.66
□    $\leftarrow \infty \rightarrow$    □   □	SQUARE	2.25	4	4
—   —   —	WIDE SLOT	1.024	1	9.92
—   —   —	NARROW SLOT	0.5144	1	19.75
○○○○○    $\leftarrow \infty \rightarrow$	STREAMLINED SLOT	2.54	2	4
○○○○○    $\leftarrow \infty \rightarrow$	BLUFF SLOT	2.54	2	4
○○○○○    $\leftarrow \infty \rightarrow$    ○○○○○	PLATE M-3	1.80 1.80	2.83 2.83	5.66 5.66
○    $\leftarrow \infty \rightarrow$    ○   ○	PLATE M-4	2.54 2.54	4 4	4 4
○○○○○○○○○○○○○○    $\leftarrow \infty \rightarrow$	PLATE M-5	1.80 1.27	2.83 2.0	5.66 8.0
○○○○○○○○○○○○○○    $\leftarrow \infty \rightarrow$	PLATE M-6	1.27 1.83	2.0 2.83	8.0 5.66
○○○○○○○○○○○○○○    $\leftarrow \infty \rightarrow$	PLATE M-7	2.54	2	4

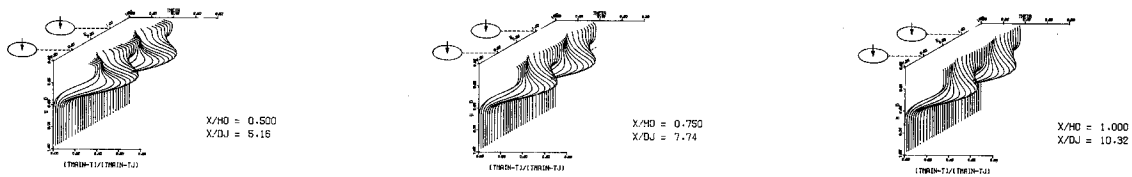
Figure 3. Orifice Plate Configurations.

Figure 4. Total Pressure, Thermocouple, and Static Pressure Rake.



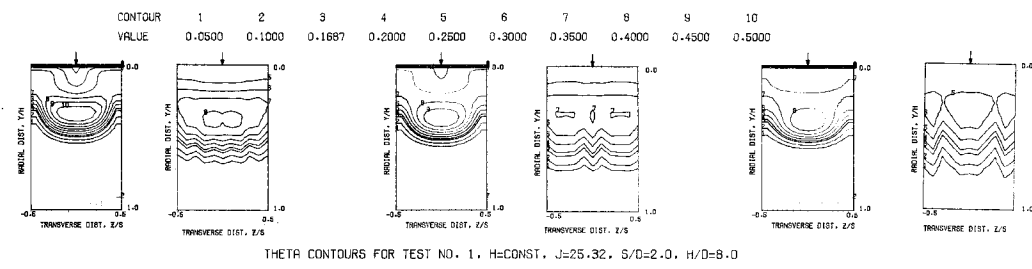


PREDICTED THETA CONTOURS FOR TEST NO.1, FINE GRID, J=25.32, S/D=2.0, H/D=8.0

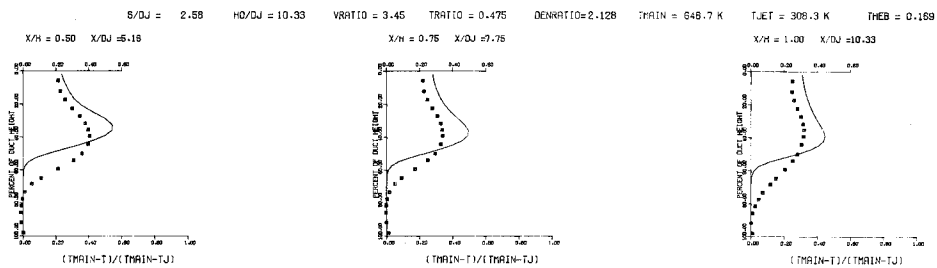


PREDICTED THETA DISTRIBUTIONS FOR TEST NO. 1, FINE GRID, J=25.32, S/D=2.0, H/D=8.0

Figure 5. Predicted Temperature Distributions for Test Case 1 - Table 1.



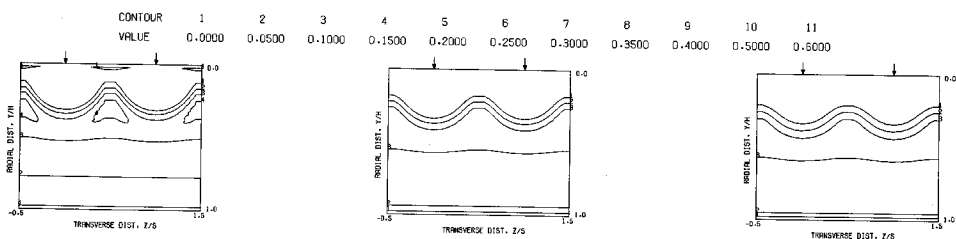
THETA CONTOURS FOR TEST NO. 1,  $H=CONST.$ ,  $J=25.32$ ,  $S/D=2.0$ ,  $H/D=8.0$



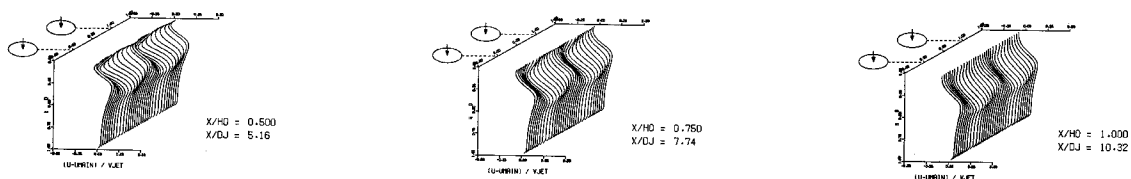
COMPARISON BETWEEN DATA AND PREDICTIONS FOR TEST NO. 1, STRAIGHT DUCT,  $T_M = CONST.$

$J = 25.32, S/D = 2.00, H/D = 8.00$

Figure 6. Comparison Between Predicted and Measured Temperature Distributions for Test Case 1 - Table 1.

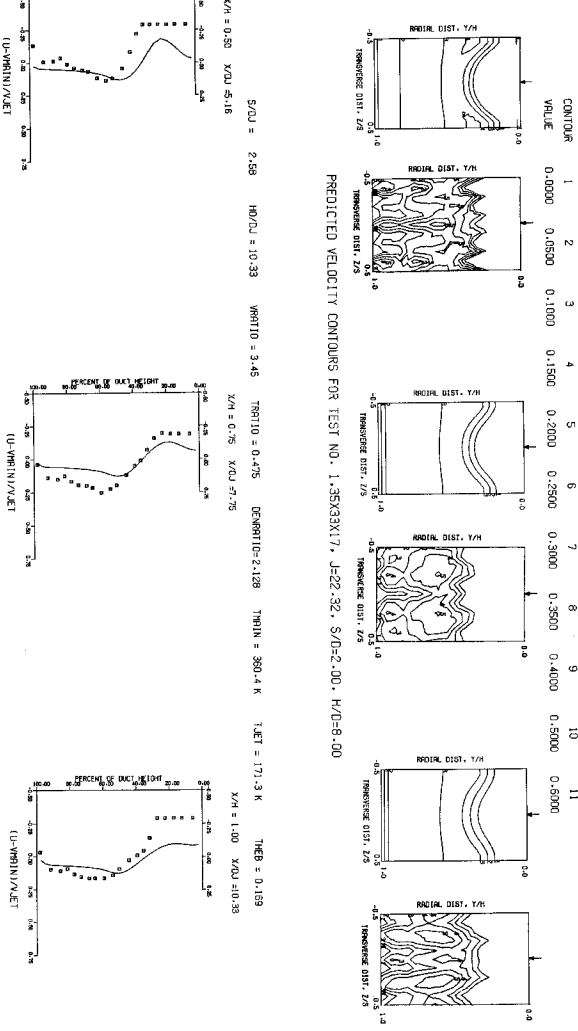


PREDICTED VELOCITY CONTOURS FOR TEST NO. 1.35X33X17, J=22.32, S/D=2.00, H/D=8.00



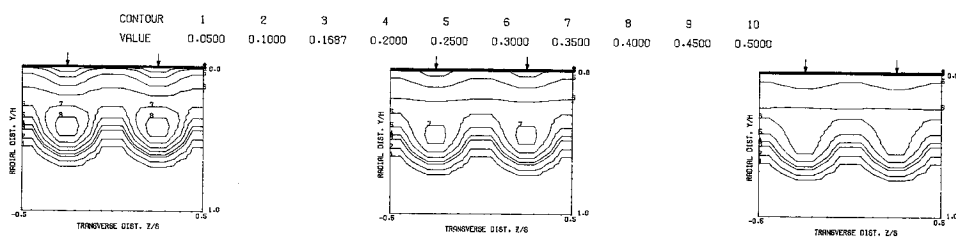
PREDICTED VELOCITY DISTRIBUTIONS FOR TEST NO. 1.35X33X17, J=22.32, S/D=2.00, H/D=8.00

Figure 7. Predicted Velocity Distributions for Test Case 1 - Table 1.

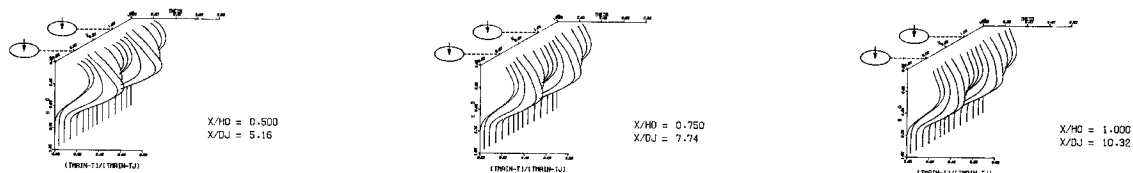


COMPARISON BETWEEN DATA AND PREDICTIONS FOR TEST 1: 1-35X33X17, SINGLE SIDED ROW OF JETS, J = 22.32, S/D = 2.00, H/D = 8.00

Figure 8. Comparison Between Predicted and Measured Velocity Distributions for Test Case 1 - Table 1.

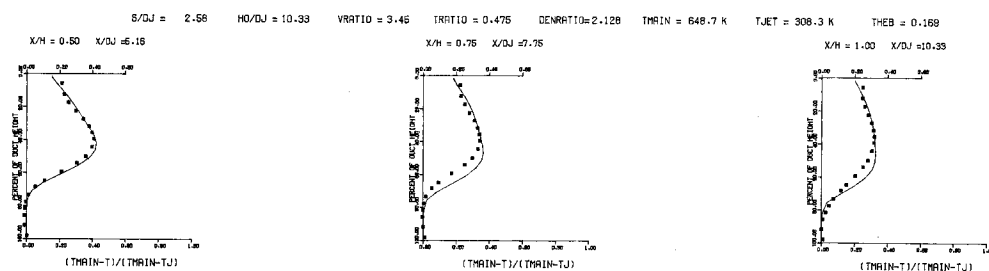
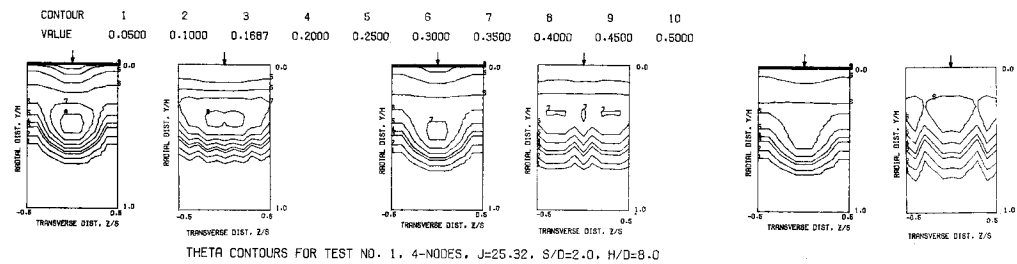


PREDICTED THETA CONTOURS FOR TEST NO. 1.4-NODE JET.  $J=25.32$ ,  $S/D=2.0$ ,  $H/D=8.0$



PREDICTED THETA DISTRIBUTIONS FOR TEST NO. 1.4-NODE JET.  $J=25.32$ ,  $S/D=2.0$ ,  $H/D=8.0$

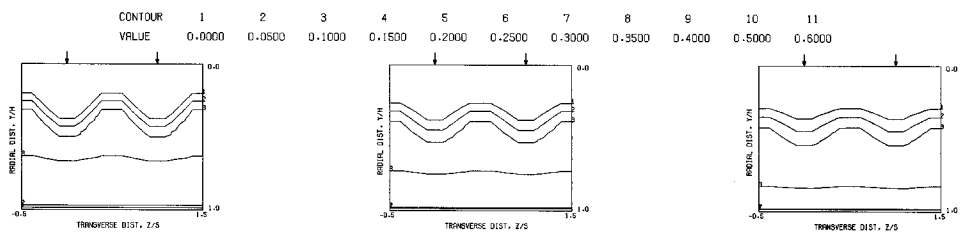
Figure 9. Predicted Temperature Distributions for Test Case 2 - Table 1.



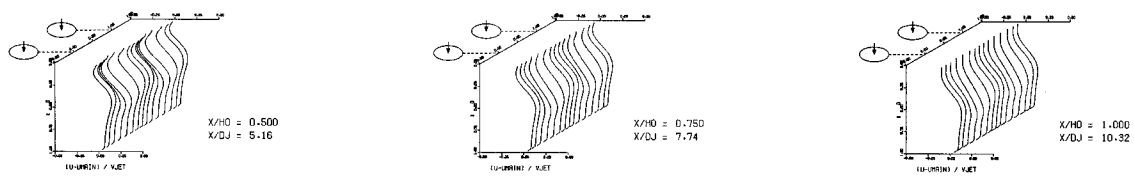
COMPARISON BETWEEN DATA AND PREDICTIONS FOR TEST NO. 1, STRAIGHT DUCT, 4-NODE JET,

$J = 25.32, S/D = 2.00, H/D = 0.00$

Figure 10. Comparison Between Predicted and Measured Temperature Distributions for Test Case 2 - Table 1.

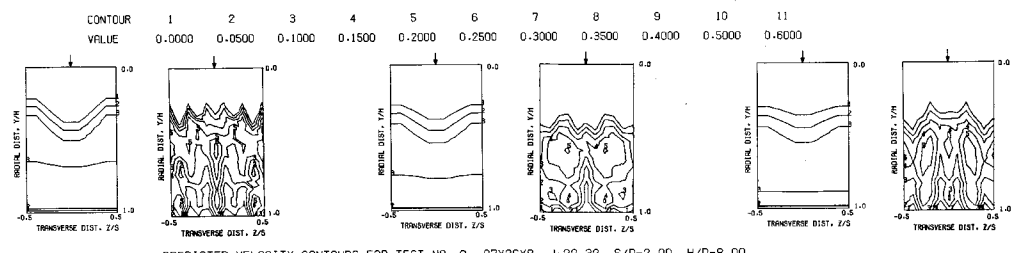


PREDICTED VELOCITY CONTOURS FOR TEST NO. 2, 27X26X8, J=22.32, S/D=2.00, H/D=8.00

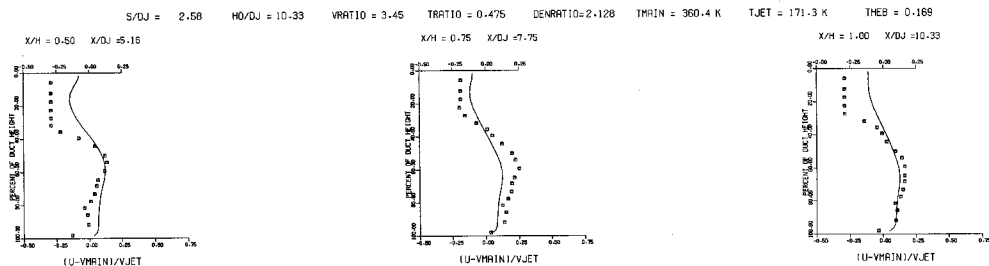


PREDICTED VELOCITY DISTRIBUTIONS FOR TEST NO. 2, 27X26X8, J=22.32, S/D=2.00, H/D=8.00

Figure 11. Predicted Velocity Distributions for Test Case 2 - Table 1.

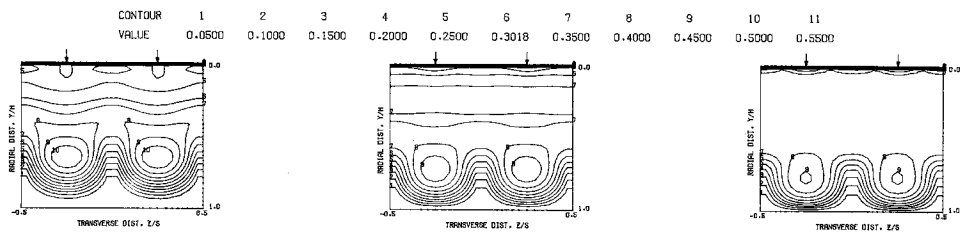


PREDICTED VELOCITY CONTOURS FOR TEST NO. 2. 27X25XB, J=22.32, S/D=2.00, H/D=8.00

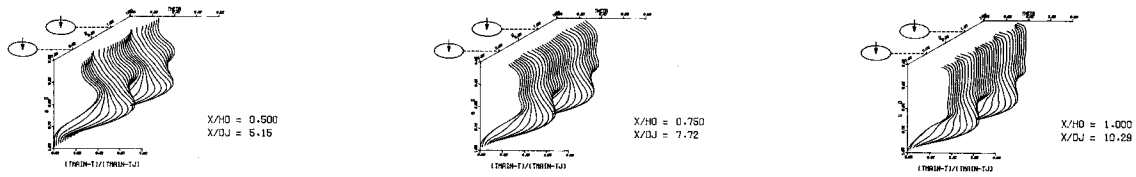


COMPARISON BETWEEN DATA AND PREDICTIONS FOR TEST 2. 27X25XB, SINGLE SIDED ROW OF JETS, J = 22.32, S/D = 2.00, H/D = 8.00

Figure 12. Comparison Between Predicted and Measured Velocity Distributions for Test Case 2 - Table 1.

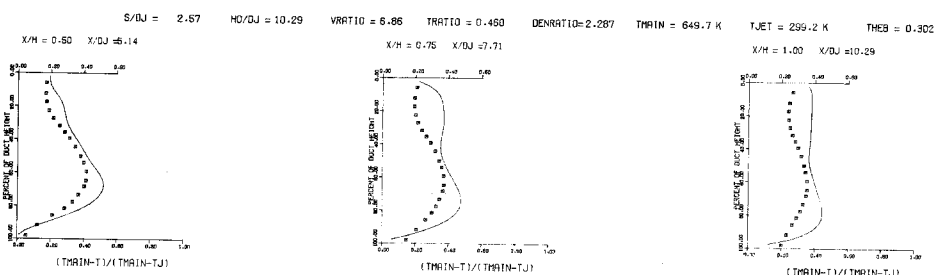
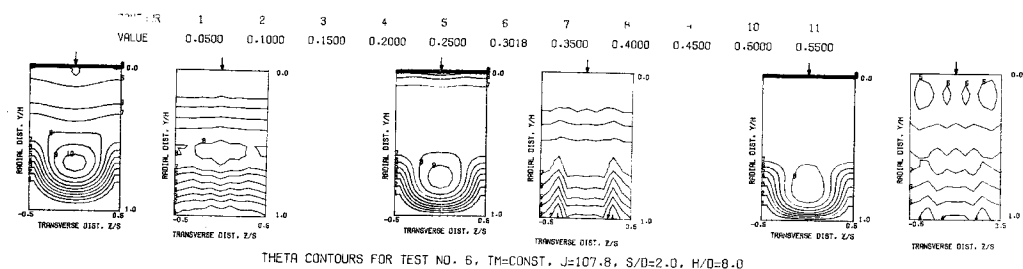


PREDICTED THETA CONTOURS FOR TEST NO. 6, FINE GRID,  $J=107.8$ ,  $S/D=2.0$ ,  $H/D=8.0$



PREDICTED THETA DISTRIBUTIONS FOR TEST NO. 6, FINE GRID,  $J=107.8$ ,  $S/D=2.0$ ,  $H/D=8.0$

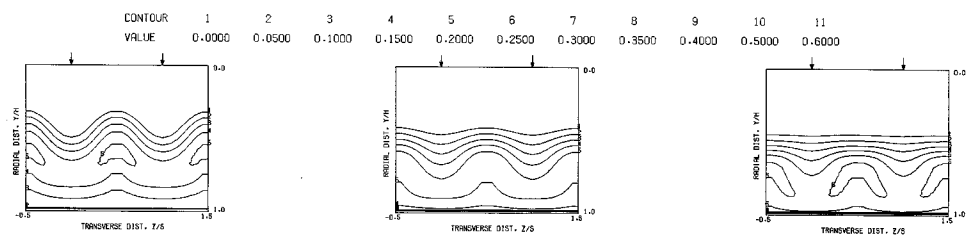
Figure 13. Predicted Temperature Distributions for Test Case 3 - Table 1.



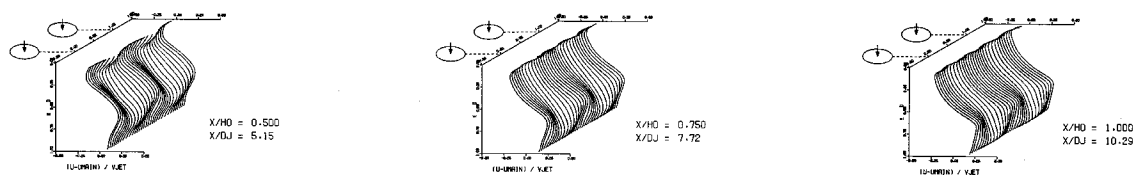
COMPARISON BETWEEN DATA AND PREDICTIONS FOR TEST NO. 6, TEST SECTION I, TMIN=CONST.

J = 107.78 , S/D = 2.00 , H/D = 8.00

Figure 14. Comparison Between Predicted and Measured Temperature Distributions for Test Case 3 - Table 1.

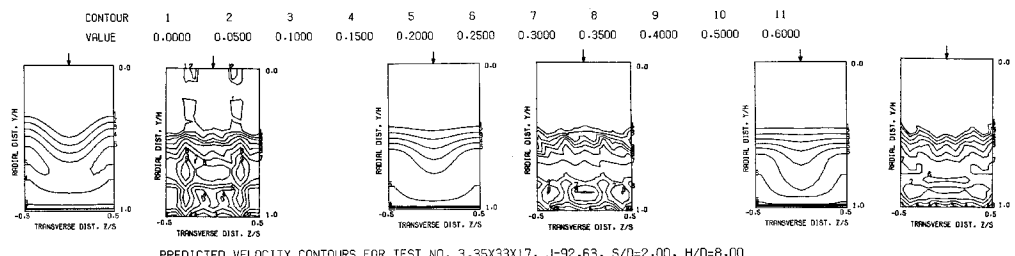


PREDICTED VELOCITY CONTOURS FOR TEST NO. 3.35X33X17, J=92.63, S/D=2.00, H/D=8.00

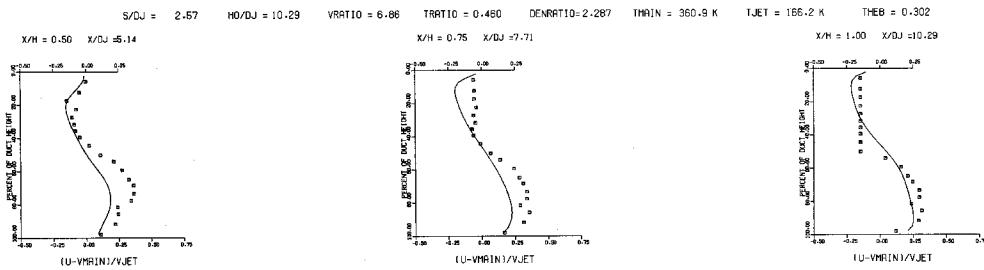


PREDICTED VELOCITY DISTRIBUTIONS FOR TEST NO. 3.35X33X17, J=92.63, S/D=2.00, H/D=8.00

Figure 15. Predicted Velocity Distributions for Test Case 3 - Table 1.

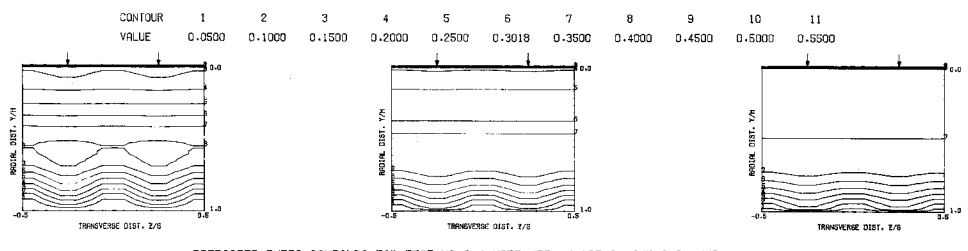


PREDICTED VELOCITY CONTOURS FOR TEST NO. 3.35X33X17, J=92.63, S/D=2.00, H/D=8.00

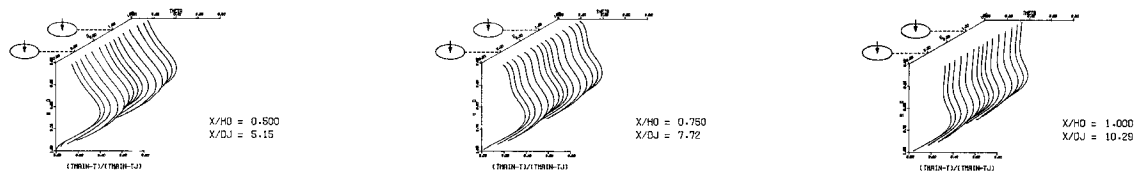


COMPARISON BETWEEN DATA AND PREDICTIONS FOR TEST 3.35X33X17, SINGLE SIDED ROW OF JETS, J = 92.63, S/D = 2.00, H/D = 8.00

Figure 16. Comparison Between Predicted and Measured Velocity Distributions for Test Case 3 - Table 1.

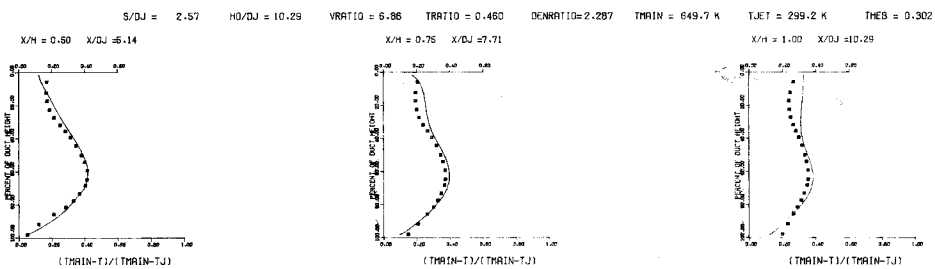
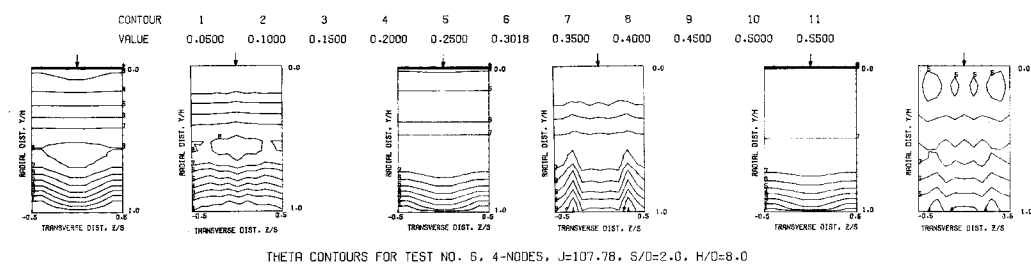


PREDICTED THETA CONTOURS FOR TEST NO. 6.4-NODE JET,  $J=107.8$ ,  $S/D=2.0$ ,  $H/D=8.0$



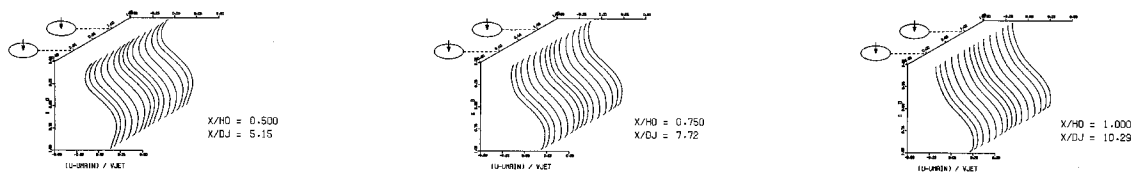
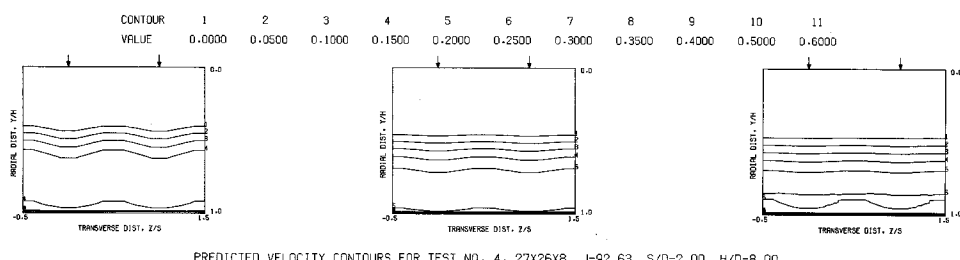
PREDICTED THETA DISTRIBUTIONS FOR TEST NO. 6.4-NODE JET,  $J=107.8$ ,  $S/D=2.0$ ,  $H/D=8.0$

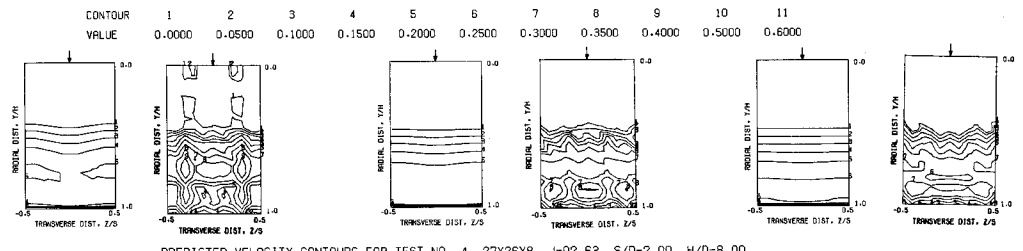
Figure 17. Predicted Temperature Distributions for Test Case 4 - Table 1.



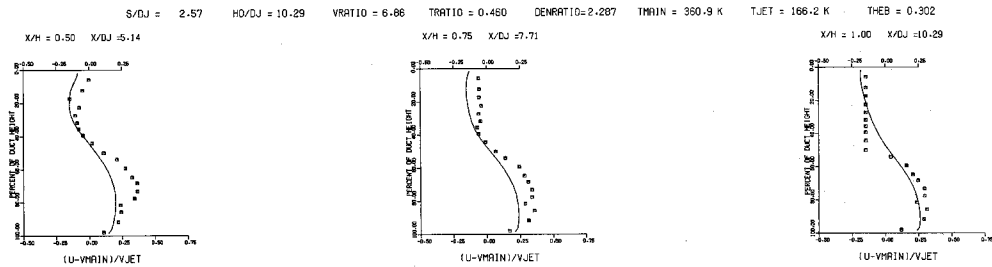
COMPARISON BETWEEN DATA AND PREDICTIONS FOR TEST NO. 6, STRAIGHT DUCT, 4-NODE JET,  $J = 107.78$ ,  $S/D = 2.00$ ,  $H/D = 8.00$

Figure 18. Comparison Between Predicted and Measured Temperature Distributions for Test Case 4 ~ Table 1.



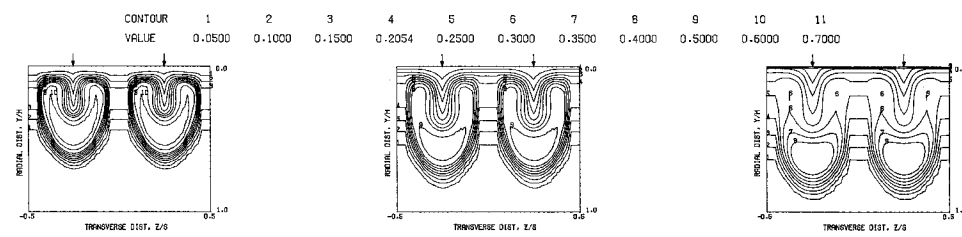


PREDICTED VELOCITY CONTOURS FOR TEST NO. 4, 27X26X8, J=92.63, S/D=2.00, H/D=8.00

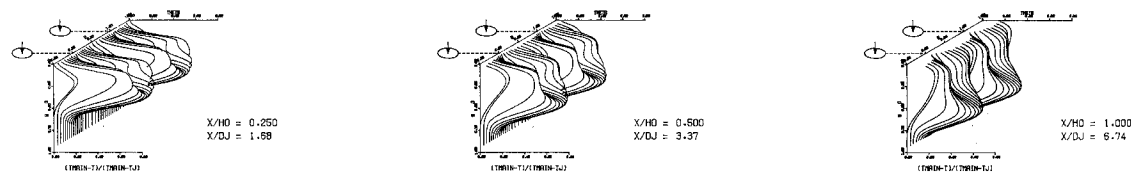


COMPARISON BETWEEN DATA AND PREDICTIONS FOR TEST 4, 27X26X8, SINGLE SIDED ROW OF JETS, J = 92.63, S/D = 2.00, H/D = 8.00

Figure 20. Comparison Between Predicted and Measured Velocity Distributions for Test Case 4 - Table I.

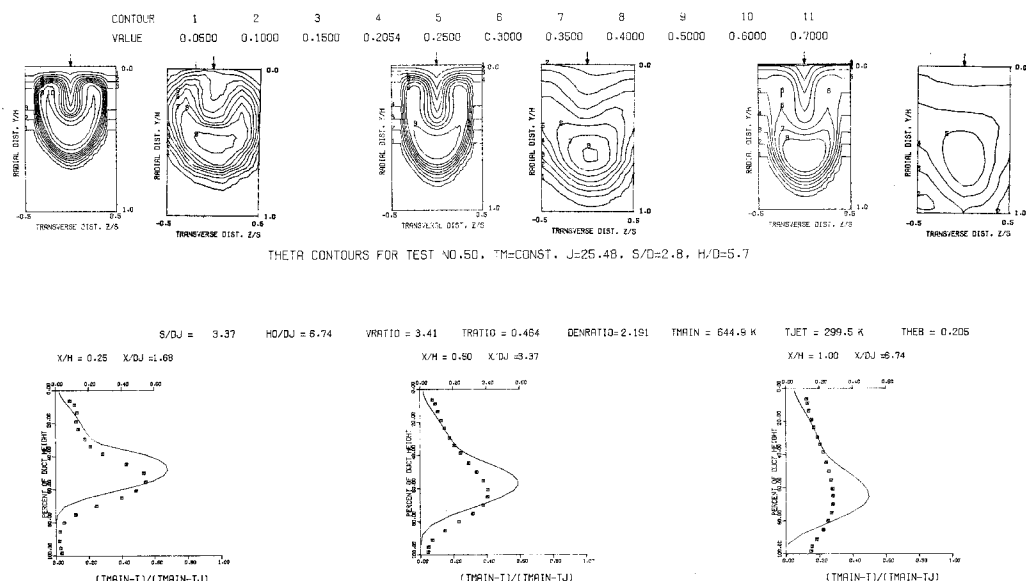


PREDICTED THETA CONTOURS FOR TEST NO. 50. TM=CONST. J=25.48. S/D=2.83. H/D=5.66



PREDICTED THETA DISTRIBUTIONS FOR TEST NO. 50. TM=CONST. J=25.48. S/D=2.83. H/D=5.66

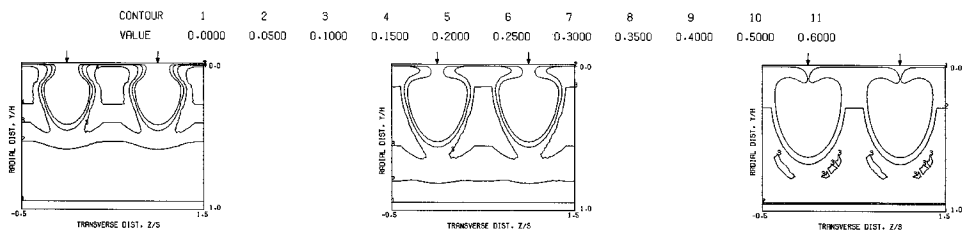
Figure 21. Predicted Temperature Distributions for Test Case 5 - Table 1.



COMPARISON BETWEEN DATA AND PREDICTIONS FOR TEST NO. 50, TEST SECTION I, TM = CONST

J = 25.48 , S/D = 2.83 , H/D = 5.66

Figure 22. Comparison Between Predicted and Measured Temperature Distributions for Test Case 5 - Table I.



PREDICTED VELOCITY CONTOURS FOR TEST NO. 5.35X33X17,  $J=25.48$ ,  $S/D=2.83$ ,  $H/D=5.66$

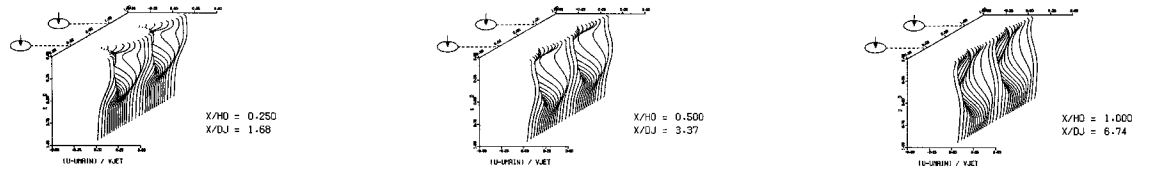
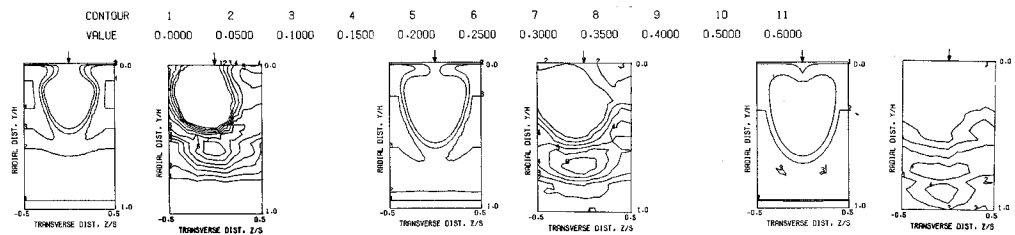
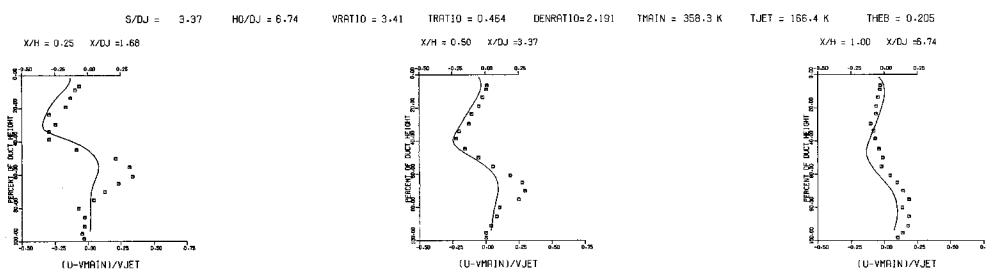


Figure 23. Predicted Velocity Distributions for Test Case 5 -  
Table 1.

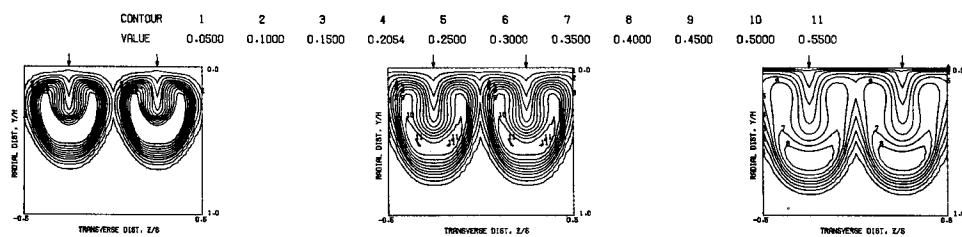


PREDICTED VELOCITY CONTOURS FOR TEST NO. 5.35X33X17, J=25.48, S/D=2.83, H/D=5.66

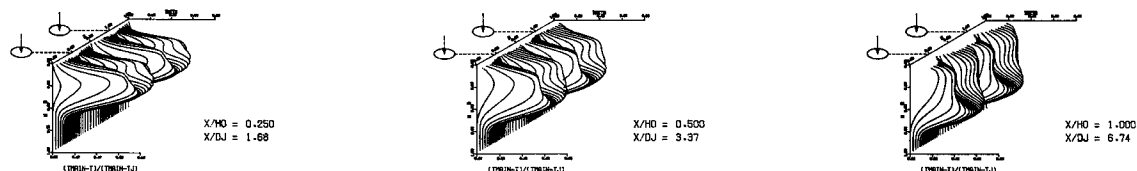


COMPARISON BETWEEN DATA AND PREDICTIONS FOR TEST 5.35X33X17, SINGLE SIDED ROW OF JETS,  $J = 25.48$ ,  $S/D = 2.83$ ,  $H/D = 5.66$

Figure 24. Comparison Between Predicted and Measured Velocity Distributions for Test Case 5 - Table I.

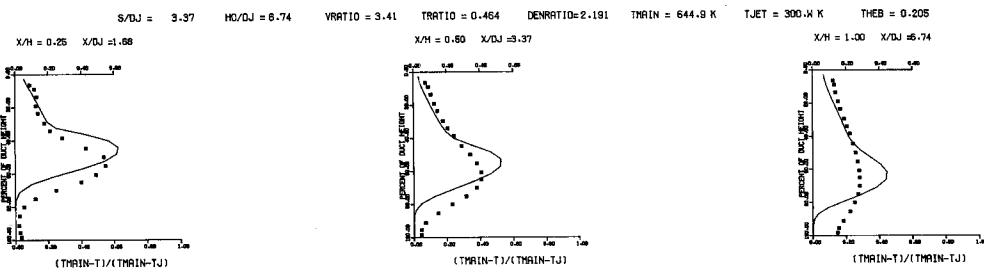
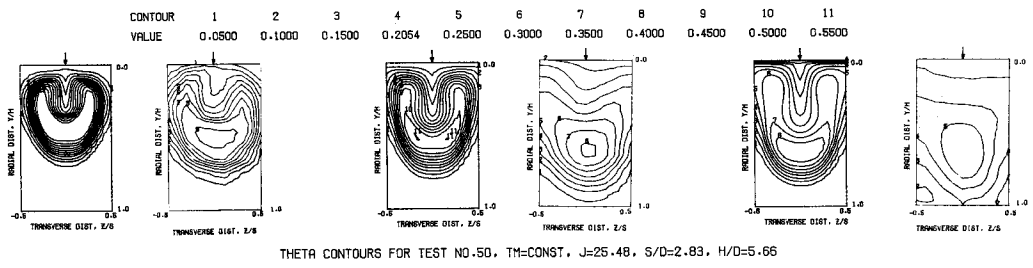


PREDICTED THETA CONTOURS FOR TEST NO. 50, TM=CONST, J=25.48, S/D=2.83, H/D=5.66



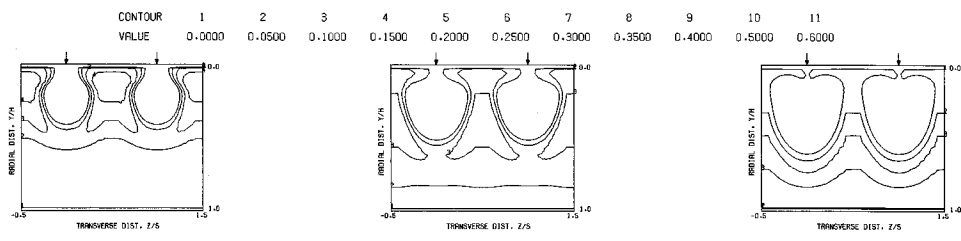
PREDICTED TEMPERATURE DISTRIBUTIONS FOR TEST NO. 50, TM=CONST, J=25.48, S/D=2.83, H/D=5.66

Figure 25. Predicted Temperature Distributions for Test Case 6 - Table 1.

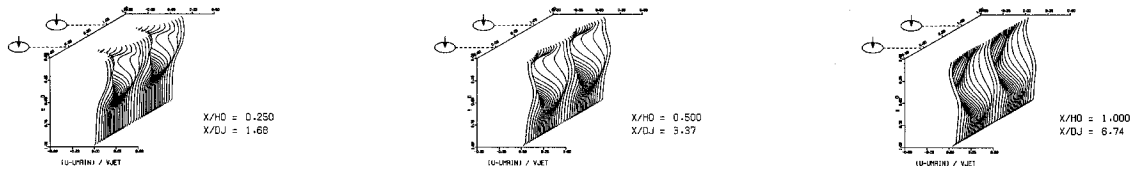


COMPARISON BETWEEN DATA AND PREDICTIONS FOR TEST 50, TM=CONST., TEST SECTION I, J = 25.48, S/D = 2.83, H/D = 5.66

Figure 26. Comparison Between Predicted and Measured Temperature Distributions for Test Case 6 - Table 1.

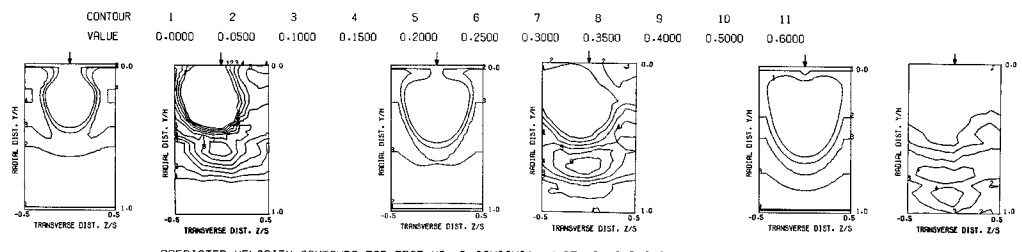


PREDICTED VELOCITY CONTOURS FOR TEST NO. 6.32X29X21, J=25.48, S/D=2.83, H/D=5.66

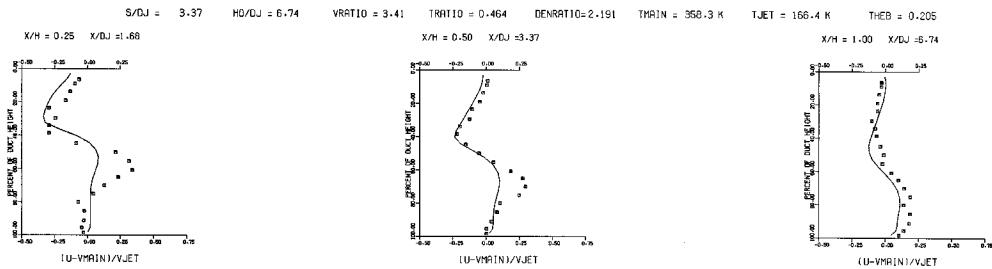


PREDICTED VELOCITY DISTRIBUTIONS FOR TEST NO. 6.32X29X21, J=25.48, S/D=2.83, H/D=5.66

Figure 27. Predicted Velocity Distributions for Test Case 6 - Table 1.

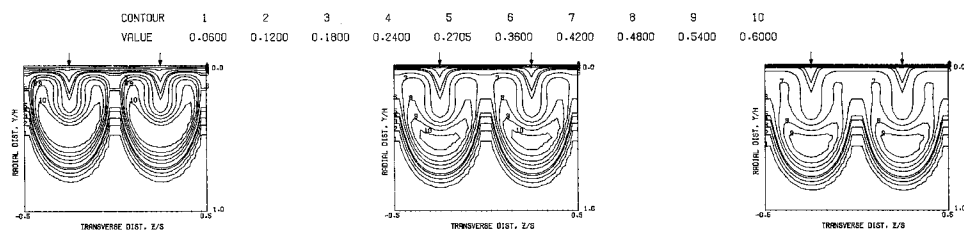


PREDICTED VELOCITY CONTOURS FOR TEST NO. 6.32X29X21, J=25.48, S/D=2.83, H/D=5.66

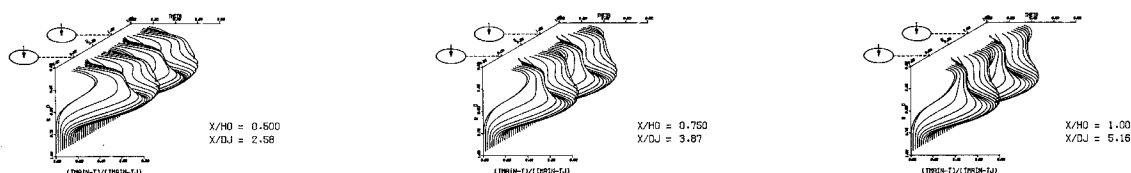


COMPARISON BETWEEN DATA AND PREDICTIONS FOR TEST 6. 32X29X21, SINGLE SIDED ROW OF JETS.  $J = 25.48$ ,  $S/D = 2.83$ ,  $H/D = 5.66$

Figure 28. Comparison Between Predicted and Measured Velocity Distributions for Test Case 6 - Table I.

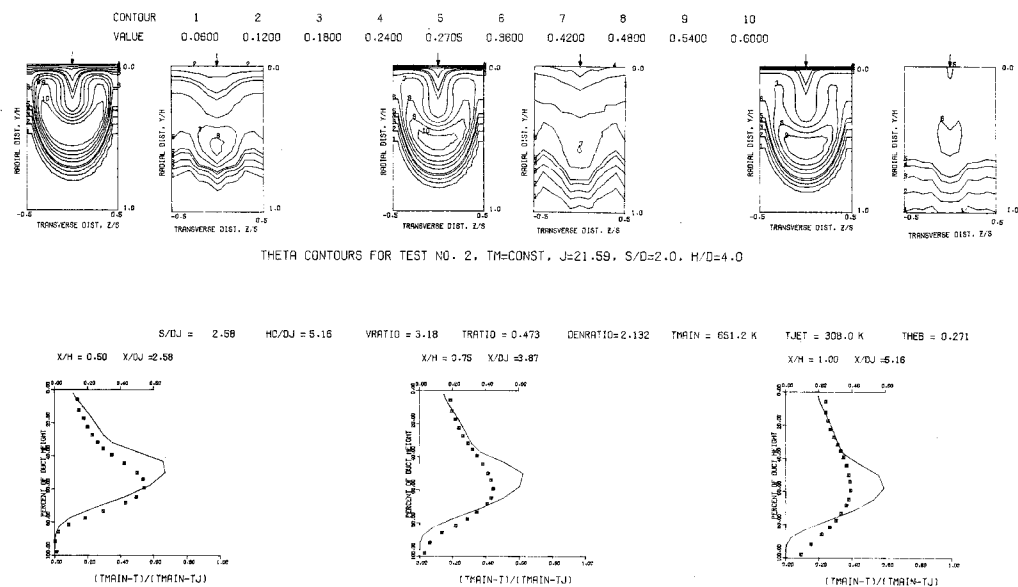


PREDICTED THETA CONTOURS FOR TEST NO. 2, FINE GRID, J=21.59, S/D=2.0, H/D=4.0



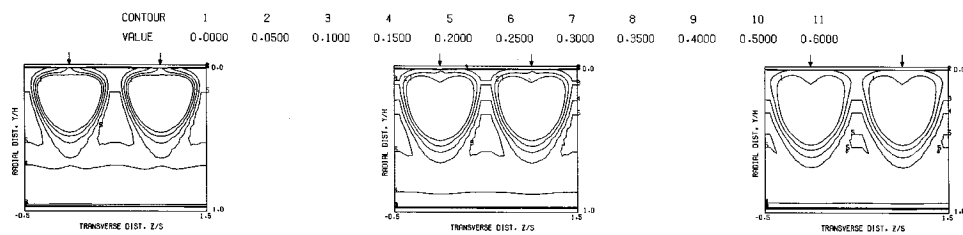
PREDICTED THETA DISTRIBUTIONS FOR TEST NO. 2, FINE GRID, J=21.59, S/D=2.0, H/D=4.0

Figure 29. Predicted Temperature Distributions for Test Case 7 - Table 1.

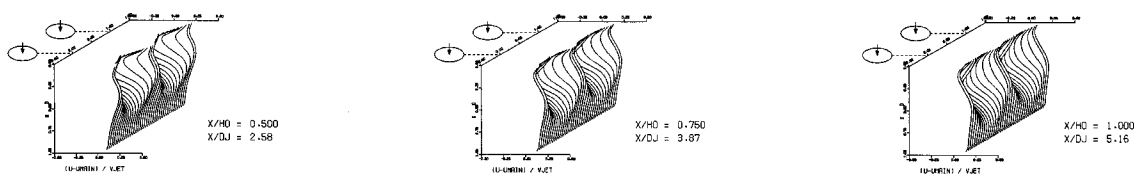


COMPARISON BETWEEN DATA AND PREDICTIONS FOR TEST NO. 02, TEST SECTION 1, TM = CONST., J = 21.59, S/D = 2.00, H/D = 4.00

Figure 30. Comparison Between Predicted and Measured Temperature Distributions for Test Case 7 - Table 1.

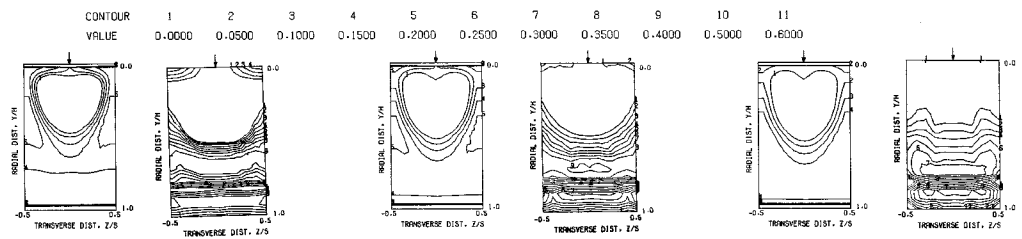


PREDICTED VELOCITY CONTOURS FOR TEST NO. 7, 45X23X19,  $J=18.59$ ,  $S/D=2.00$ ,  $H/D=4.00$

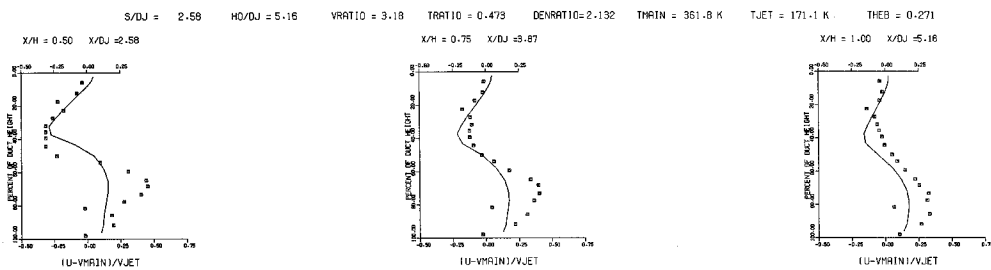


PREDICTED VELOCITY DISTRIBUTIONS FOR TEST NO. 7, 45X23X19,  $J=18.59$ ,  $S/D=2.00$ ,  $H/D=4.00$

Figure 31. Predicted Velocity Distributions for Test Case 7 -  
Table 1.

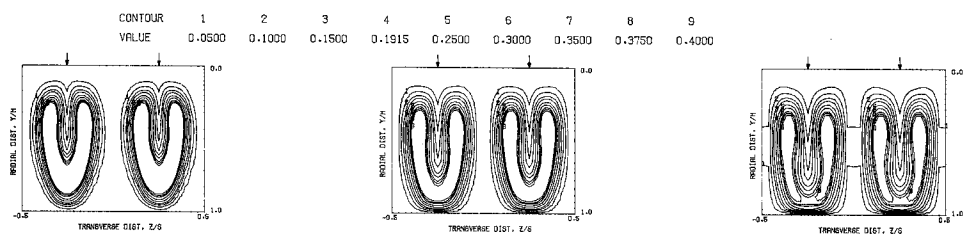


PREDICTED VELOCITY CONTOURS FOR TEST NO. 7.45X23X19, J=18.59, S/D=2.00, H/D=4.00

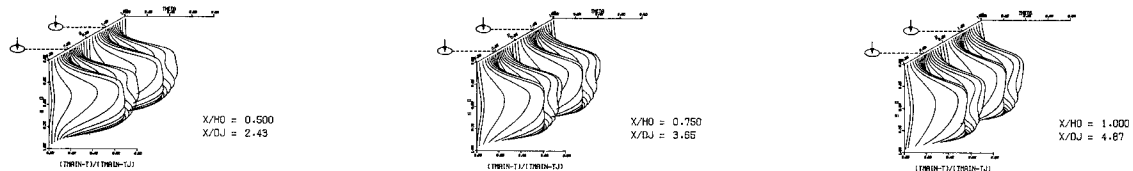


COMPARISON BETWEEN DATA AND PREDICTIONS FOR TEST 7.45X23X19, SINGLE SIDED ROW OF JETS, J = 18.59, S/D = 2.00, H/D = 4.00

Figure 32. Comparison Between Predicted and Measured Velocity Distributions for Test Case 7 - Table 1.

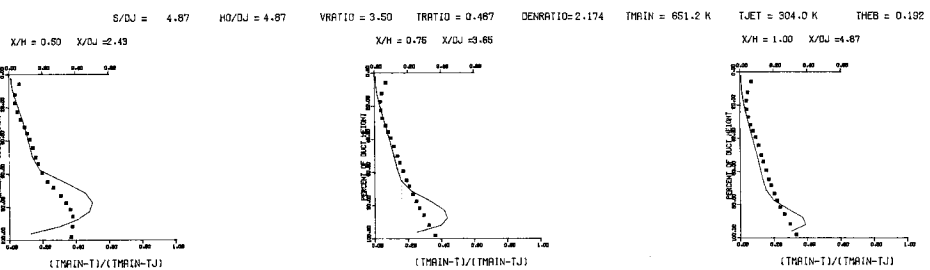
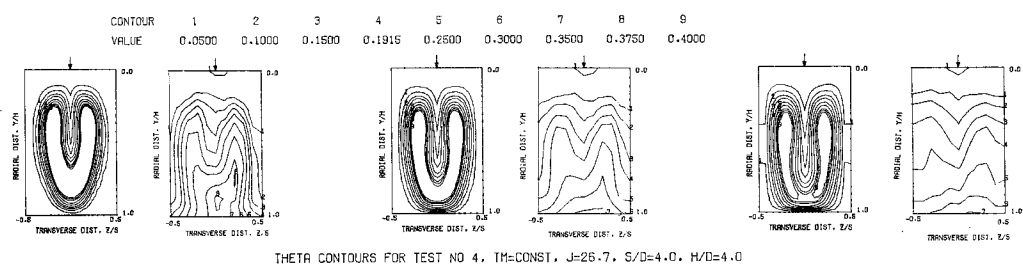


PREDICTED THETA CONTOURS FOR TEST NO.4, FINE GRID, J=26.68, S/D=4.0, H/D=4.0



PREDICTED THETA DISTRIBUTIONS FOR TEST NO. 4, FINE GRID, J=26.68, S/D=4.0, H/D=4.0

Figure 33. Predicted Temperature Distributions for Test Case 8 - Table 1.



COMPARISON BETWEEN DATA AND PREDICTIONS FOR TEST NO. 4, TEST SECTION I, ONE SIDED .    J = 26.68 , S/D = 4.00 , H/D = 4.00

Figure 24. Comparison Between Predicted and Measured Temperature Distributions for Test Case 8 - Table 1.

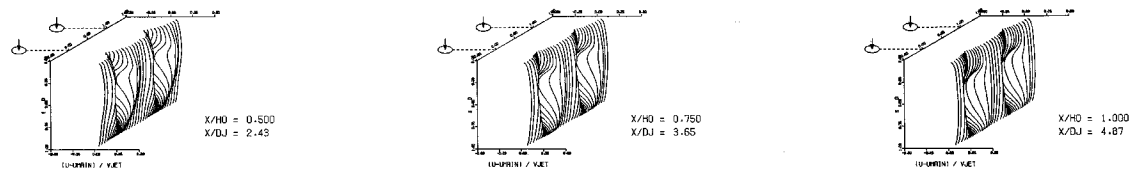
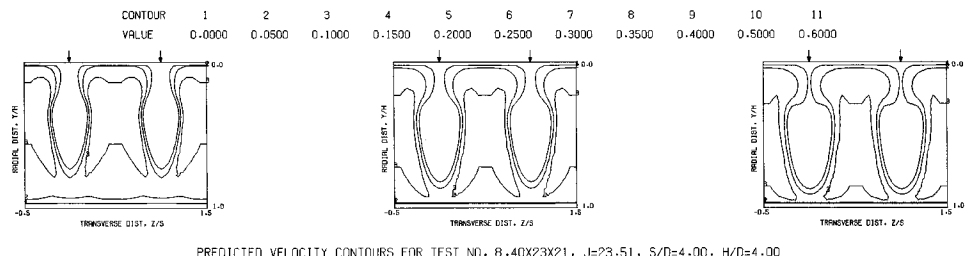


Figure 35. Predicted Velocity Distributions for Test Case 8 - Table 1.

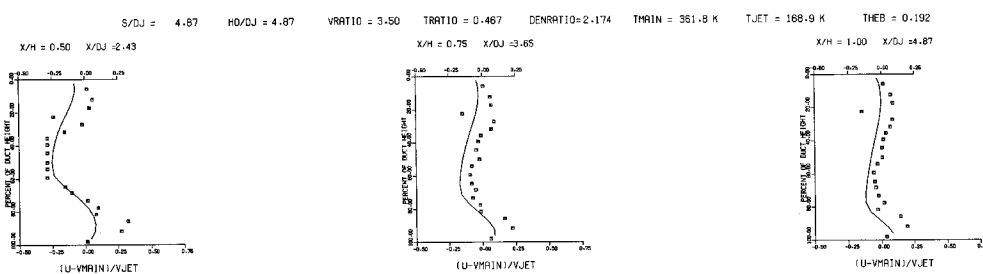
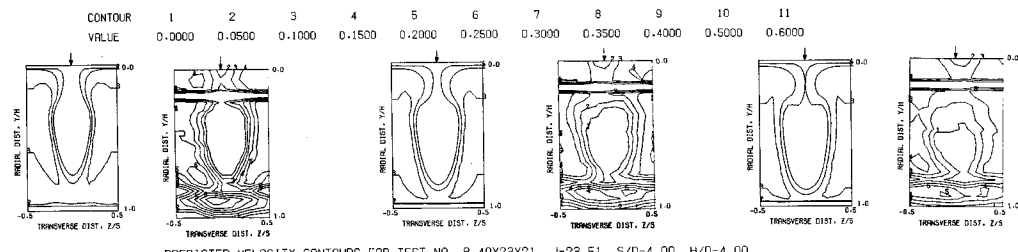
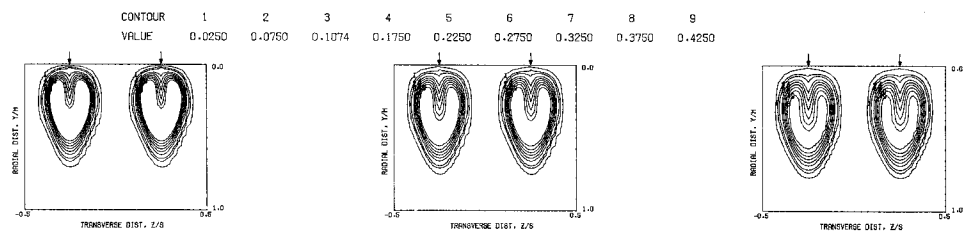
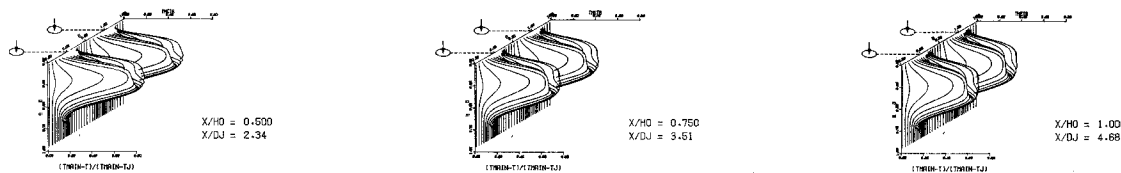


Figure 36. Comparison Between Predicted and Measured Velocity Distributions for Test Case 8 - Table I.

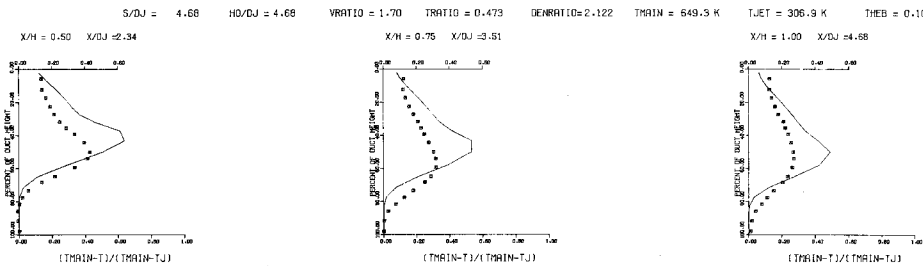
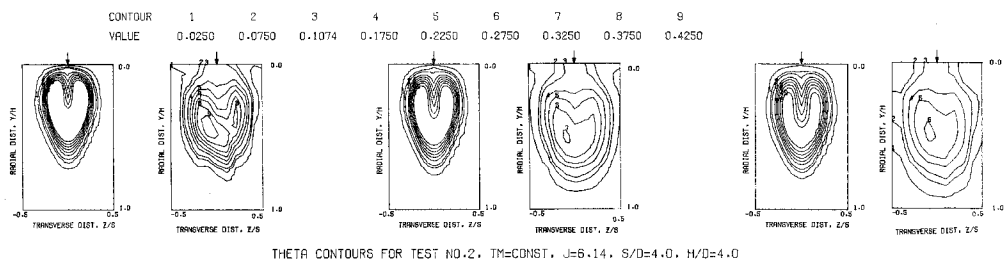


PREDICTED THETA CONTOURS FOR TEST NO. 2, FINE GRID, J=6.14, S/D=4.0, H/D=4.0



PREDICTED THETA DISTRIBUTIONS FOR TEST NO. 2, FINE GRID, J=6.14, S/D=4.0, H/D=4.0

Figure 37. Predicted Temperature Distributions for Test Case 9 - Table 1.



COMPARISON BETWEEN DATA AND PREDICTIONS FOR TEST NO. 2, TEST SECTION I, TM = CONST , J = 6.14 , S/D =4.00 , H/D =4.00

Figure 38. Comparison Between Predicted and Measured Temperature Distributions for Test Case 9 - Table 1.

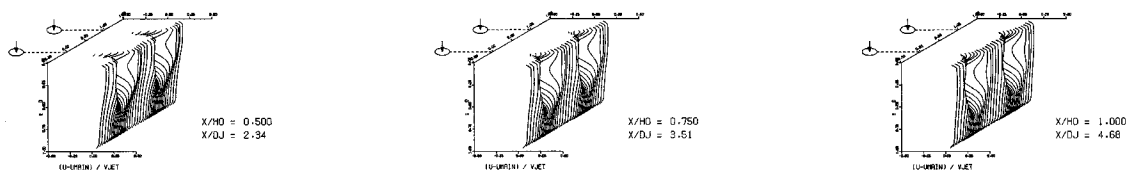
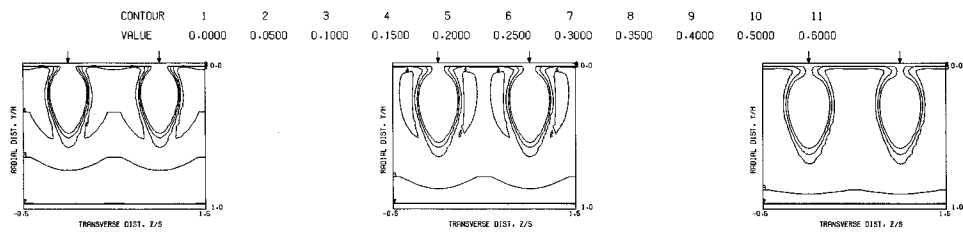
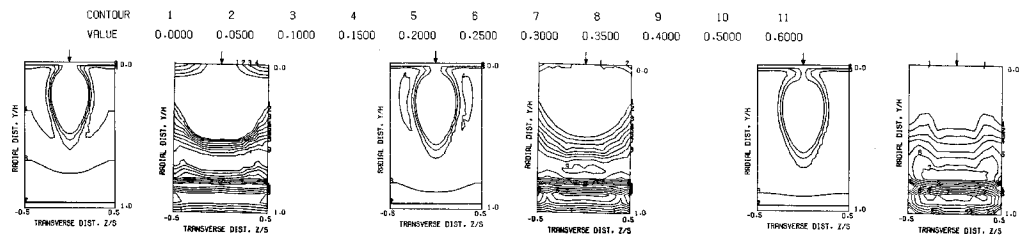
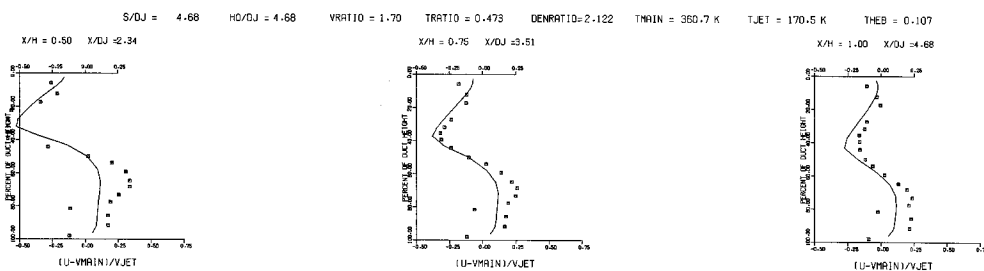


Figure 39. Predicted Velocity Distributions for Test Case 9 - Table 1.

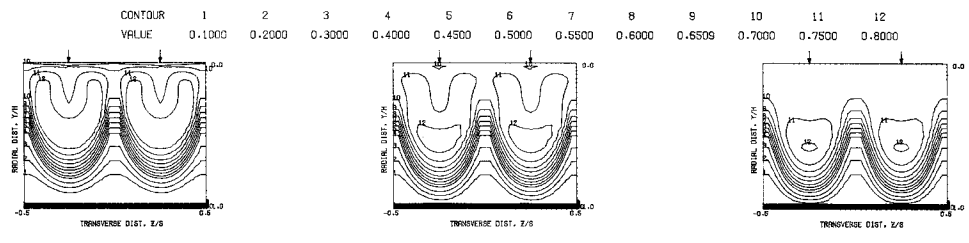


PREDICTED VELOCITY CONTOURS FOR TEST NO. 9, 40X23X21, J=5.31, S/D=4.00, H/D=4.00

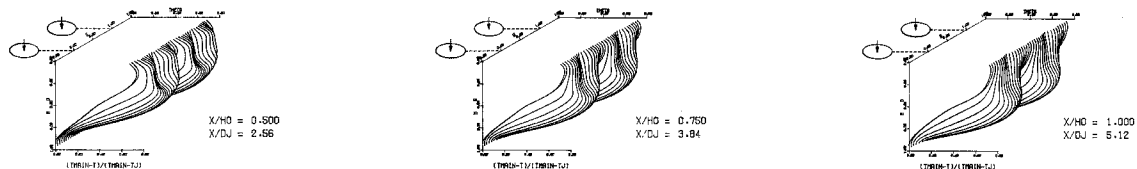


COMPARISON BETWEEN DATA AND PREDICTIONS FOR TEST 9, 40X23X21, SINGLE SIDED ROW OF JETS, J = 5.31 , S/D = 4.00 , H/D = 4.00

Figure 40. Comparison Between Predicted and Measured Velocity Distributions for Test Case 9 - Table 1.



PREDICTED THETA CONTOURS FOR TEST NO.13, TOP COLD,  $J=22.63$ ,  $S/D=2.0$ ,  $H/D=4.0$



PREDICTED THETA DISTRIBUTIONS FOR TEST NO. 13, TOP COLD,  $J=22.63$ ,  $S/D=2.0$ ,  $H/D=4.0$

Figure 41. Predicted Temperature Distributions for Test Case 10 - Table 1.

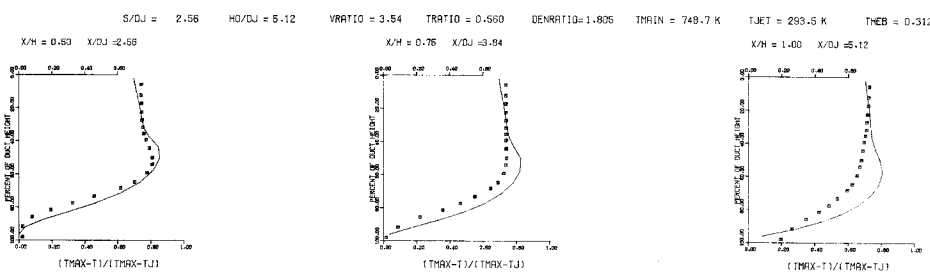
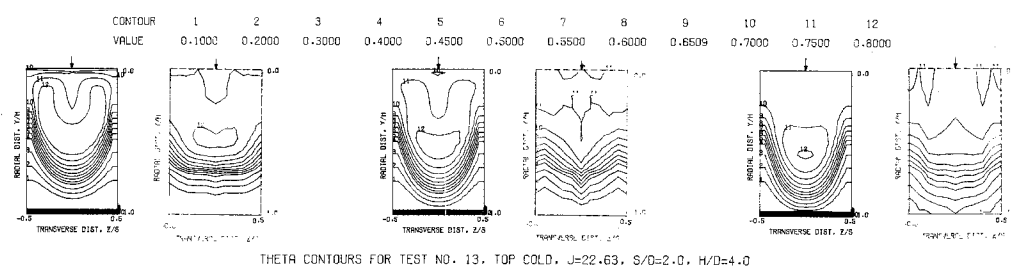
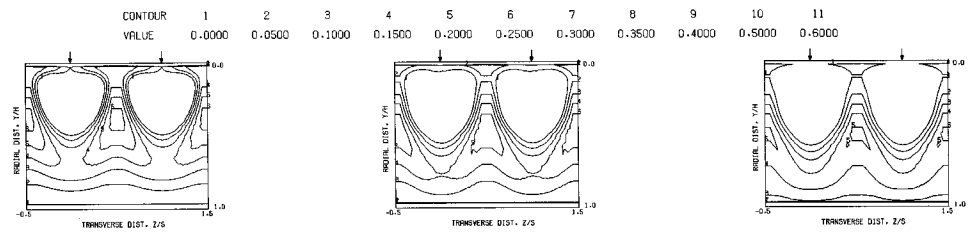
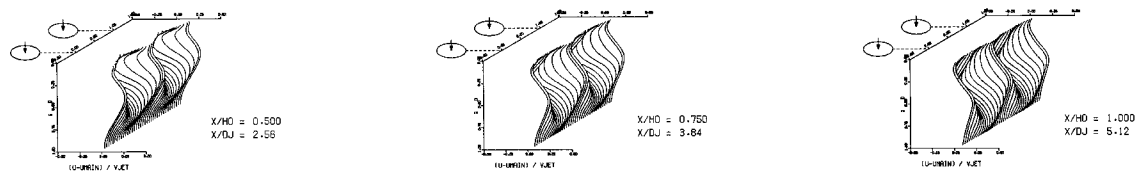


Figure 42. Comparison Between Predicted and Measured Temperature Distributions for Test Case 10 - Table 1.

68

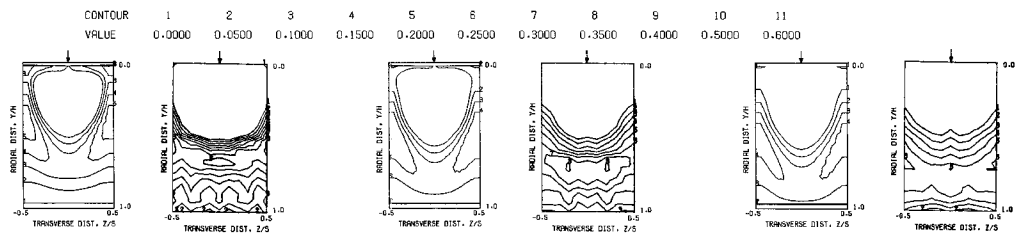


PREDICTED VELOCITY CONTOURS FOR TEST NO. 10. TOP COLD,  $J=31.79$ ,  $S/D=2.00$ ,  $H/D=4.00$

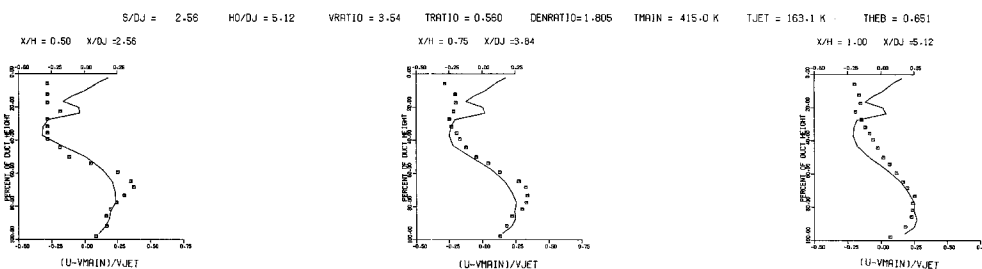


PREDICTED VELOCITY DISTRIBUTIONS FOR TEST NO. 10.45X23X19,  $J=31.79$ ,  $S/D=2.00$ ,  $H/D=4.00$

Figure 43. Predicted Velocity Distributions for Test Case 10 - Table 1.

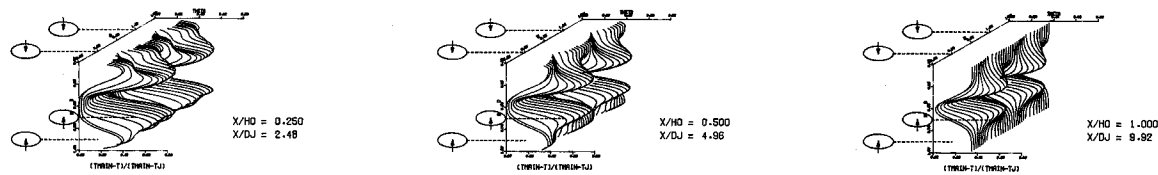
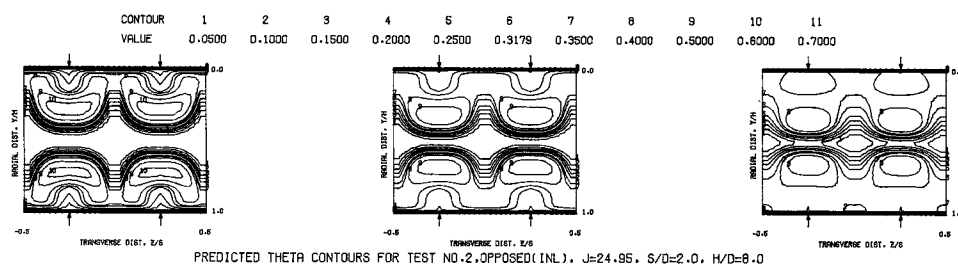


PREDICTED VELOCITY CONTOURS FOR TEST NO.10, TOP COLD,  $J=31.79$ ,  $S/D=2.00$ ,  $H/D=4.00$



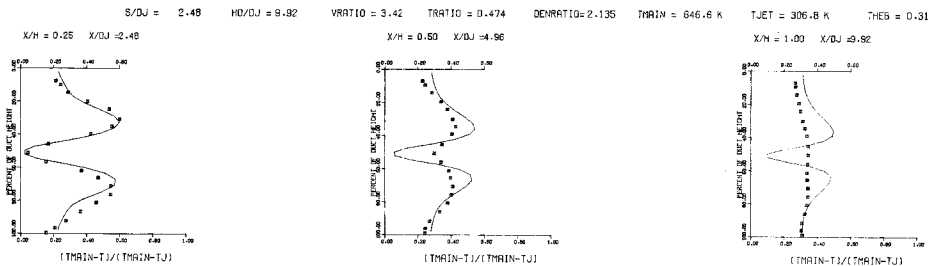
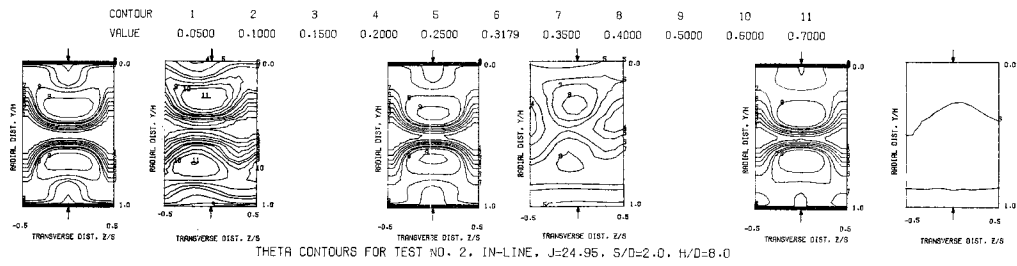
COMPARISON BETWEEN DATA AND PREDICTIONS FOR TEST 10.45X23X19, TOP COLD MAINSTREAM PROFILE,  $J = 31.79$ ,  $S/D = 2.00$ ,  $H/D = 4.00$

Figure 44. Comparison Between Predicted and Measured Velocity Distributions for Test Case 10 - Table 1.



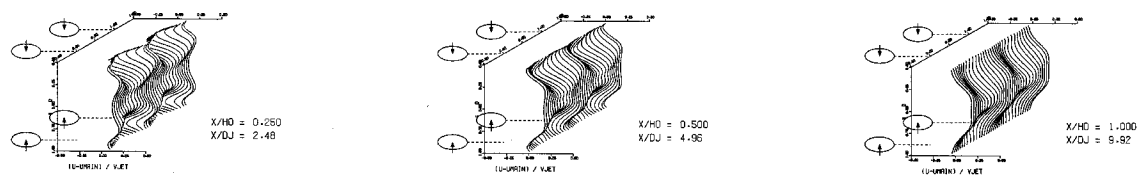
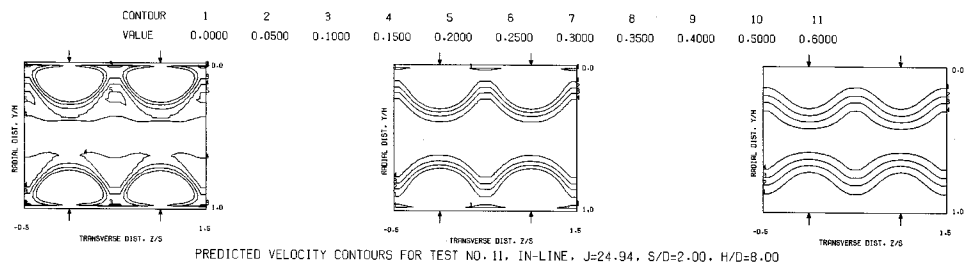
PREDICTED THETA DISTRIBUTIONS FOR TEST NO. 02, IN-LINE,  $J=24.95$ ,  $S/D=2.0$ ,  $H/D=8.0$

Figure 45. Predicted Temperature Distributions for Test Case 11 - Table 1.



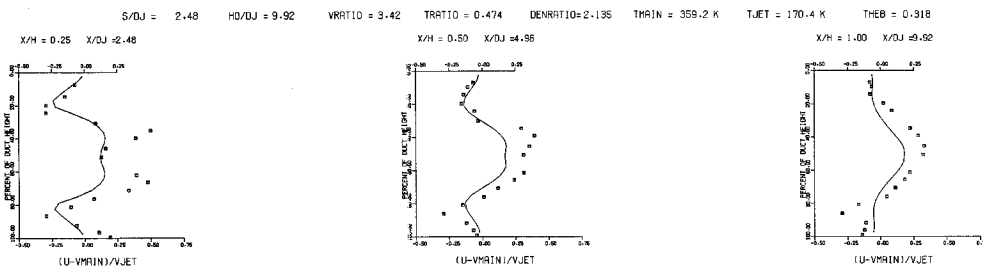
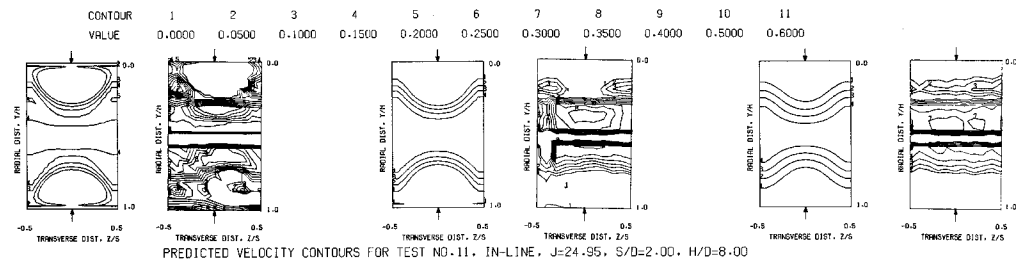
COMPARISON BETWEEN DATA AND PREDICTIONS FOR TEST NO. 2, TEST SECTION I, OPPOSED (INL),  $J = 24.95$ ,  $S/D = 2.00$ ,  $H/D = 8.00$

Figure 46. Comparison Between Predicted and Measured Temperature Distributions for Test Case II - Table 1.



PREDICTED VELOCITY DISTRIBUTIONS FOR TEST NO. II, 35X33X17,  $J=24.94$ ,  $S/D=2.00$ ,  $H/D=8.00$

Figure 47. Predicted Velocity Distribution for Test Case II -  
Table 1.



COMPARISON BETWEEN DATA AND PREDICTIONS FOR TEST 11,35X33X17,OPPOSED IN-LINE ROW OF JETS,J = 24.94 , S/D =2.00 , H/D =8.00

Figure 48. Comparison Between Predicted and Measured Velocity Distributions for Test Case 11 - Table 1.

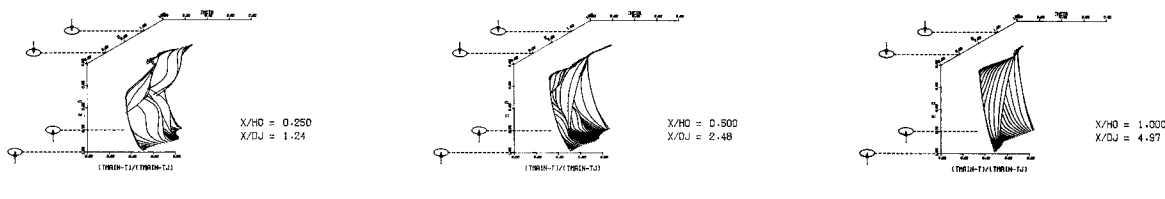
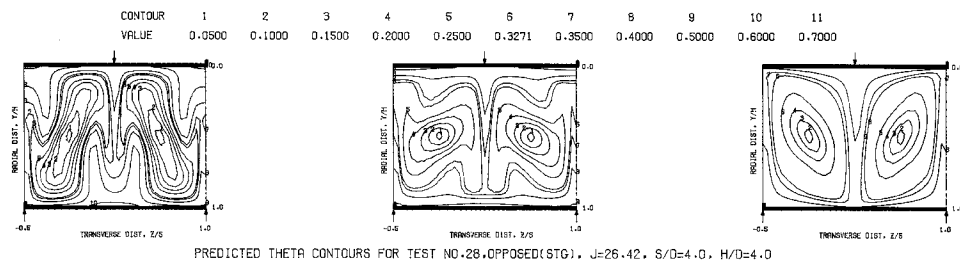
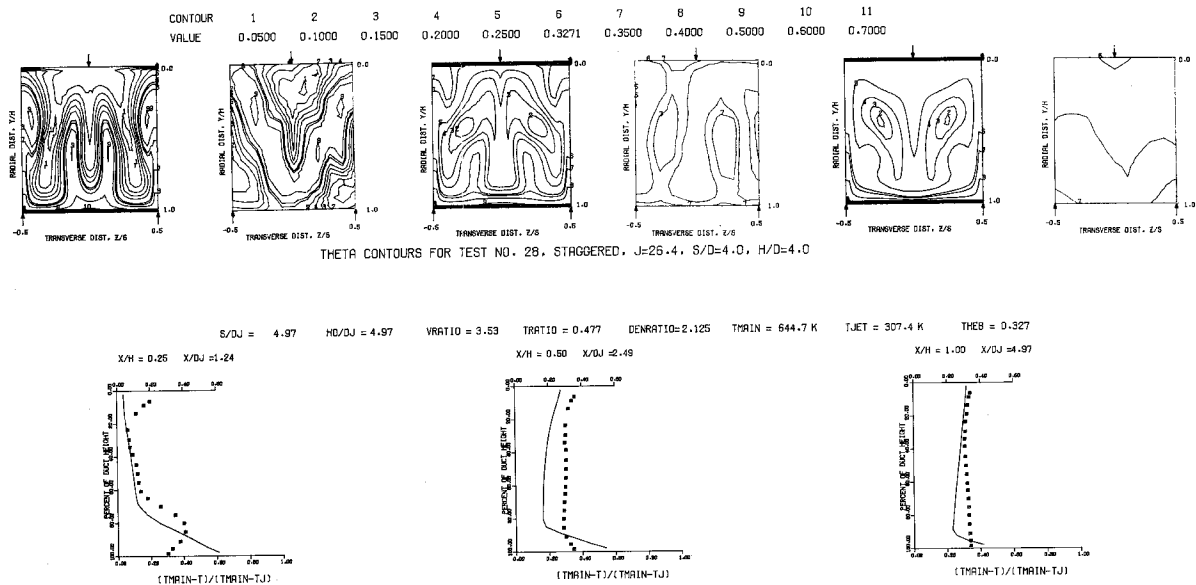


Figure 49. Predicted Temperature Distributions for Test Case 12 - Table 1.



COMPARISON BETWEEN DATA AND PREDICTIONS FOR TEST NO. 28, TEST SECTION I, OPPOSED (STG),  $J = 26.42$ ,  $S/D = 4.00$ ,  $H/D = 4.00$

Figure 50. Comparison Between Predicted and Measured Temperature Distributions for Test Case 12 - Table 1.

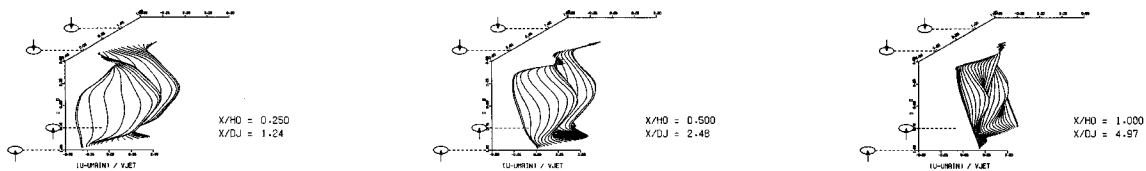
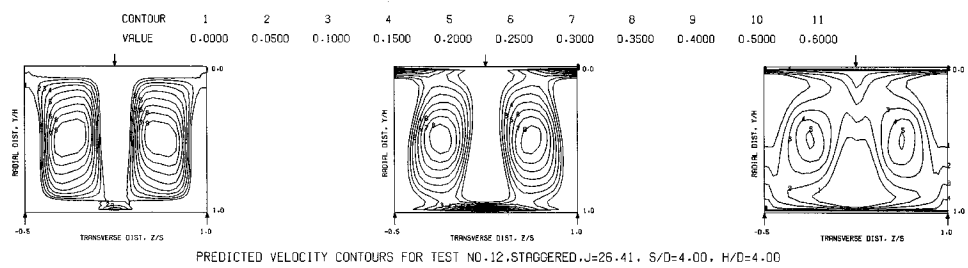
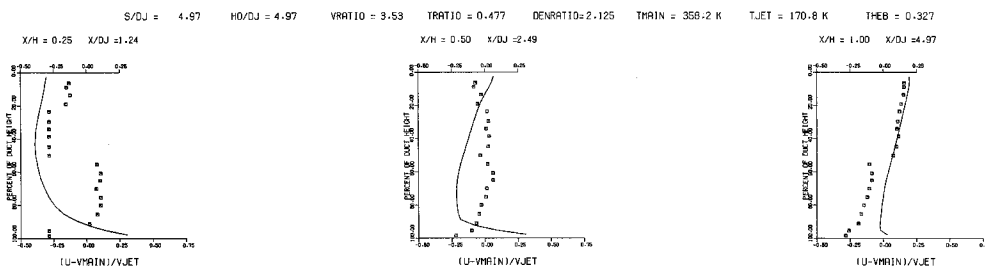
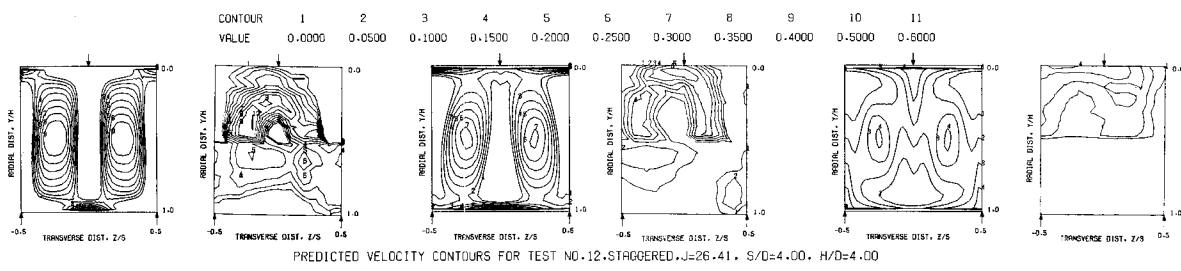
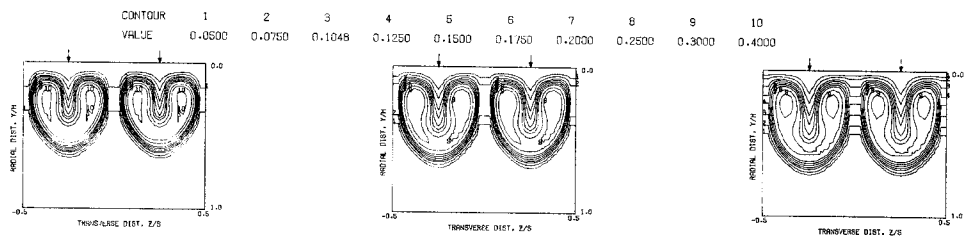


Figure 51. Predicted Velocity Distributions for Test Case 12 - Table 1.

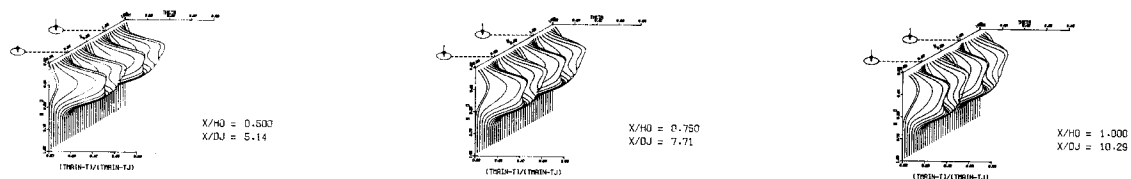


COMPARISON BETWEEN DATA AND PREDICTIONS FOR TEST 12, 22X27X33, OPPOSED STAGGERED JETS, J = 26.41, S/D = 4.00, H/D = 4.00

Figure 52. Comparison Between Predicted and Measured Velocity Distributions for Test Case 12 - Table 1.



PREDICTED THETA CONTOURS FOR TEST NO. 1, TM=CONST., J=26.37, S/D=4.0, H/D=8.0



PREDICTED THETA DISTRIBUTIONS FOR TEST NO. 13, TM=CONST., J=26.37, S/D=4.0, H/D=8.0

Figure 53. Predicted Temperature Distributions for Test No. 13 - Table 2.

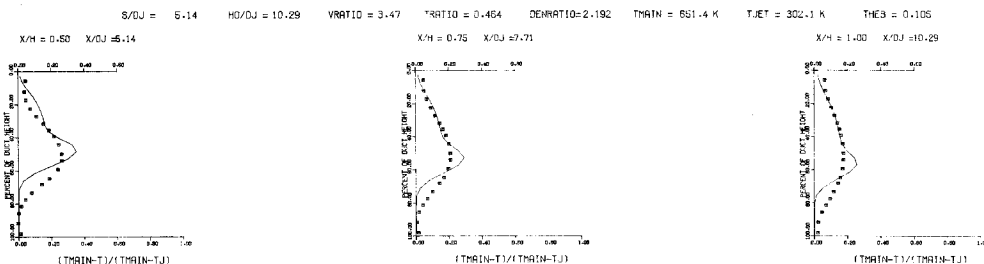
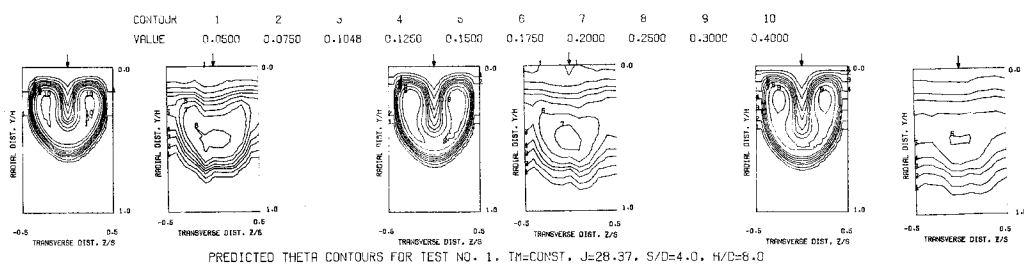


Figure 54. Comparison Between Predicted and Measured Temperature Distributions for Test No. 13 - Table 2.

80

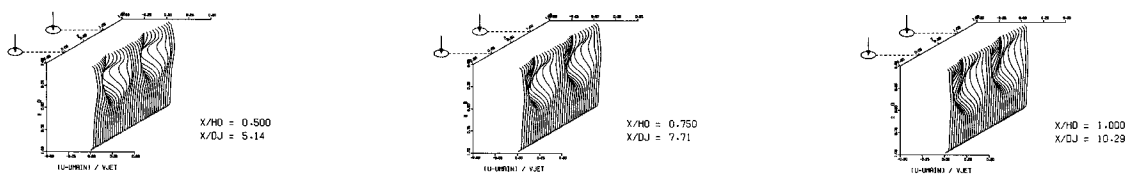
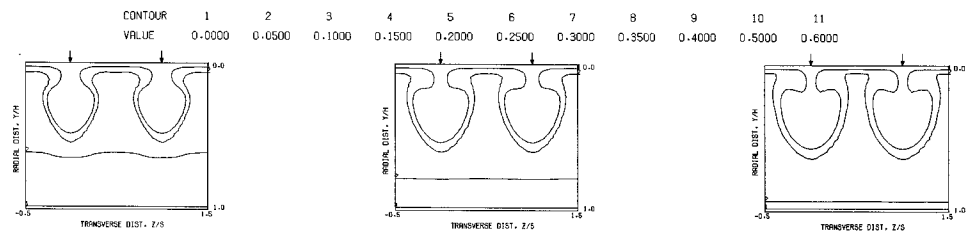
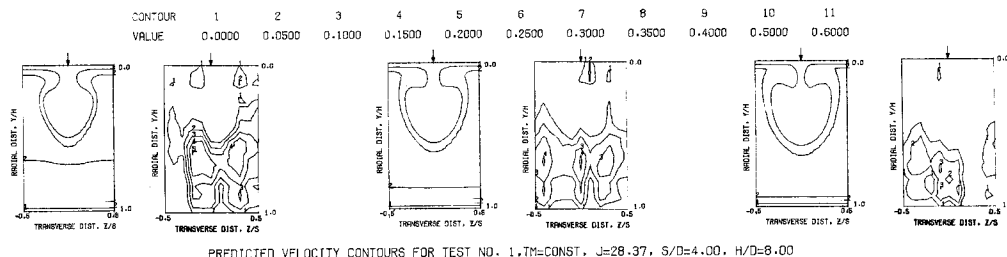
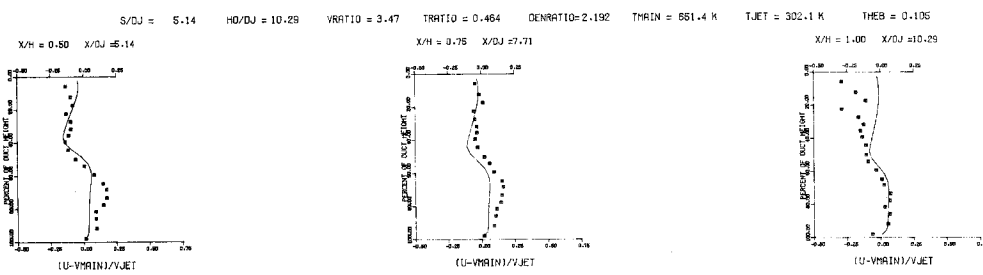


Figure 55. Predicted Velocity Distributions for Test No. 13 ~ Table 2.



PREDICTED VELOCITY CONTOURS FOR TEST NO. 13, TM=CONST., J=28.37, S/D=4.00, H/D=8.00



COMPARISON BETWEEN DATA AND PREDICTIONS FOR TEST 13, TM=CONST., SINGLE SIDED INJECTION  $J = 28.37, S/D = 4.00, H/D = 8.00$

Figure 56. Comparison Between Predicted and Measured Velocity Distributions for Test No. 13 - Table 2.

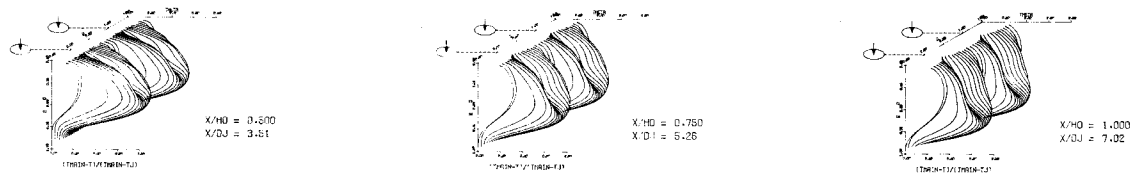
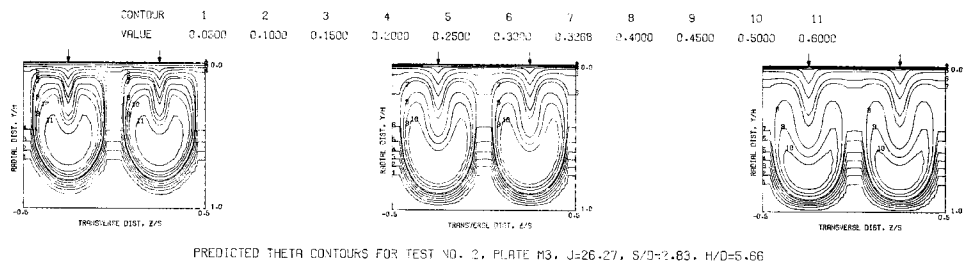
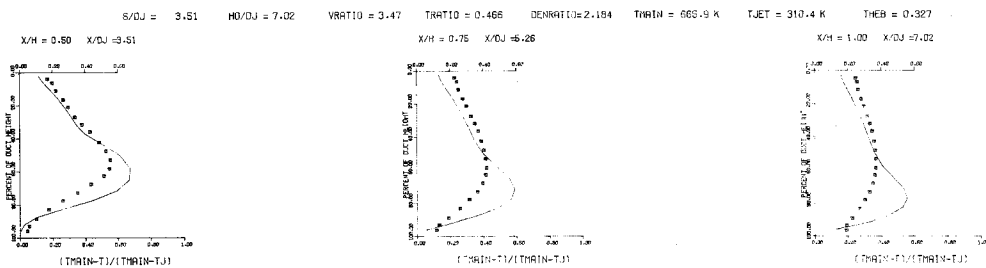
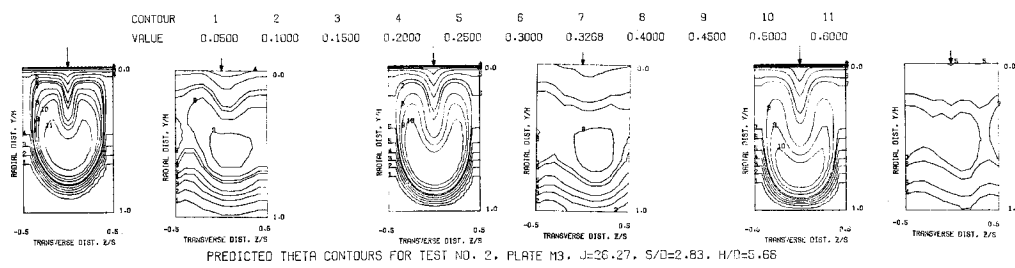
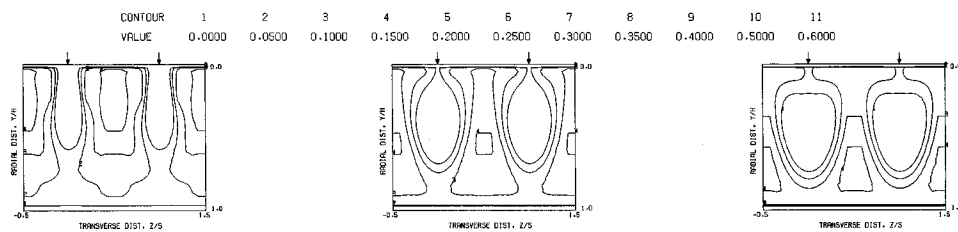


Figure 57. Predicted Temperature Distributions for Test No. 14 - Table 2.

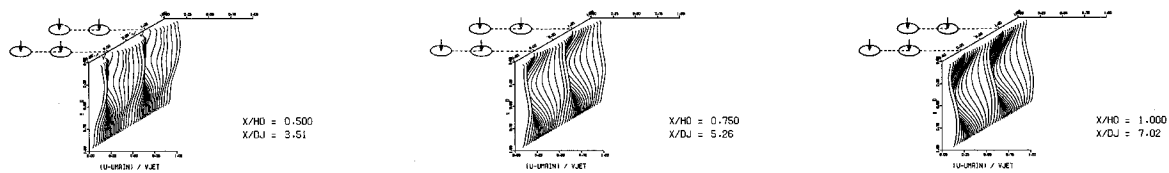


COMPARISON BETWEEN DATA AND PREDICTIONS FOR TEST 14, PLATE M3. AXIAL STAGED INJECTION,  $J = 26.27$ ,  $S/D = 2.83$ ,  $H/D = 5.66$

Figure 58. Comparison Between Predicted and Measured Temperature Distributions for Test No. 14 - Table 2.

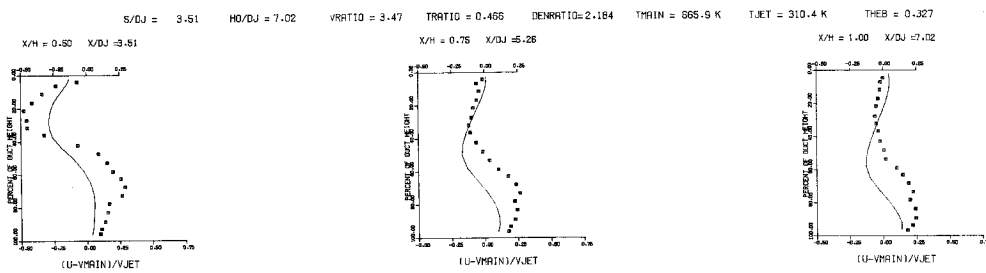
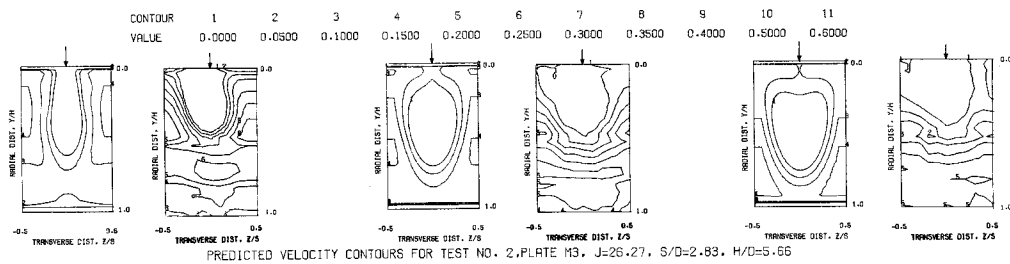


PREDICTED VELOCITY CONTOURS FOR TEST NO. 2.41X23X21. J=26.27, S/D=2.83, H/D=5.66



PREDICTED VELOCITY DISTRIBUTIONS FOR TEST 14-PLATE M3, J=26.27, S/D=2.83, H/D=5.66

Figure 59. Predicted Velocity Distributions for Test No. 14 - Table 2.



COMPARISON BETWEEN DATA AND PREDICTIONS FOR TEST 14-PLATE M3, AXIALLY STAGED INJECTION  $J = 26.27$ ,  $S/D \approx 2.83$ ,  $H/D = 5.66$

Figure 60. Comparison Between Predicted and Measured Velocity Distributions For Test No. 14 - Table 2.

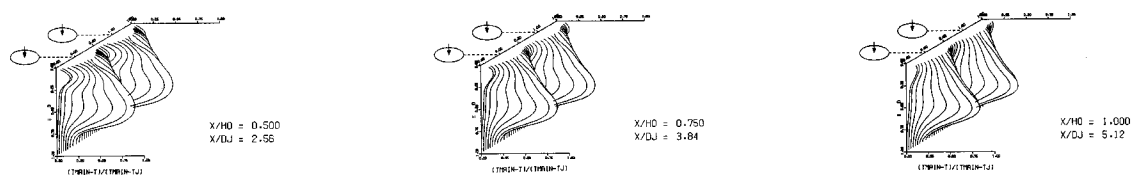
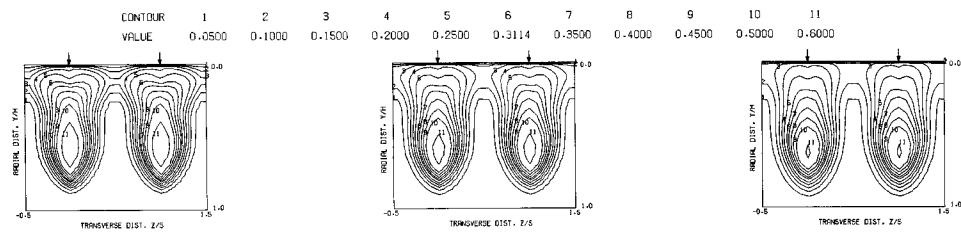
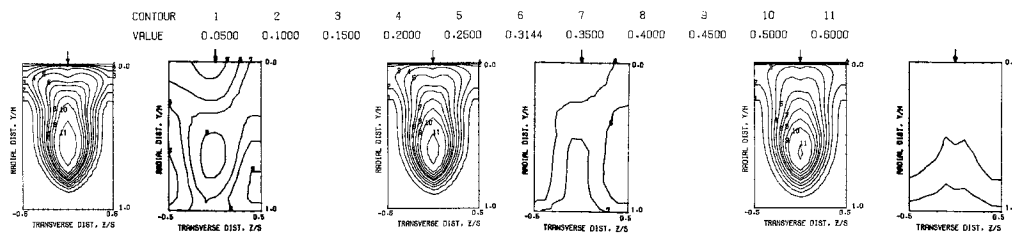
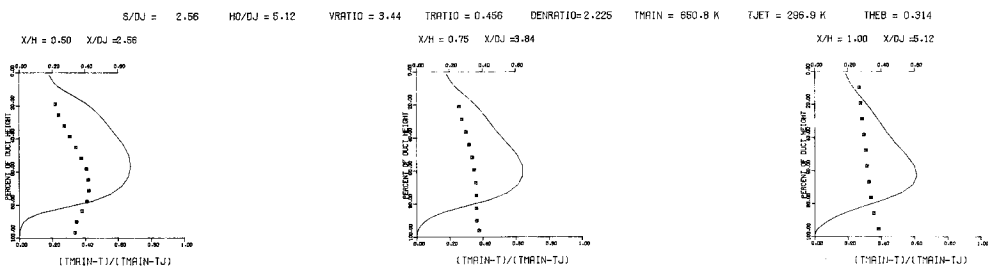


Figure 61. Predicted Temperature Distributions for Test No. 15 - Table 2.

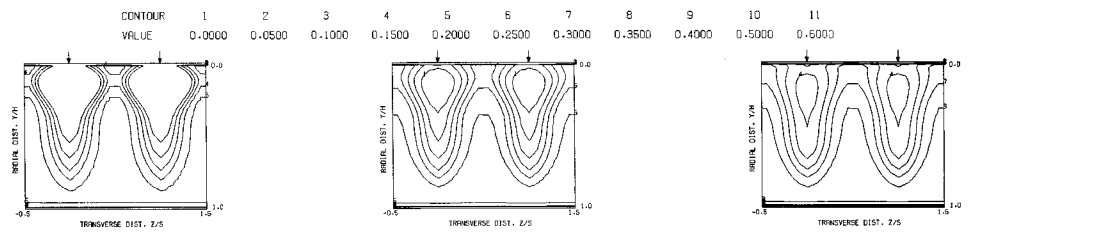


PREDICTED THETA CONTOURS FOR TEST NO. 3, CONV DUCT,  $J=25.36$ ,  $S/D=2.00$ ,  $H/D=4.00$

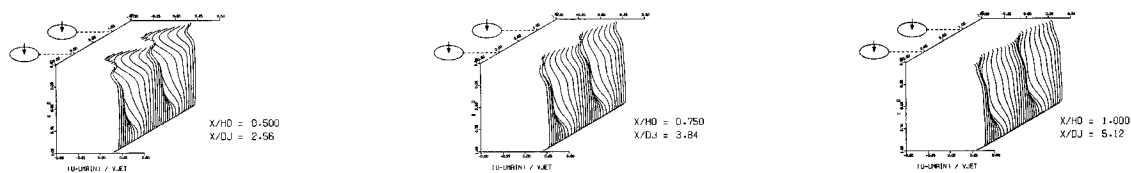


COMPARISON BETWEEN DATA AND PREDICTIONS FOR TEST 13, CONV DUCT, INCLINED WALL INJECTION,  $J = 25.36$ ,  $S/D = 2.00$ ,  $H/D = 4.00$

Figure 62. Comparison Between Predicted and Measured Temperature Distributions for Test No. 13 - Table 2.

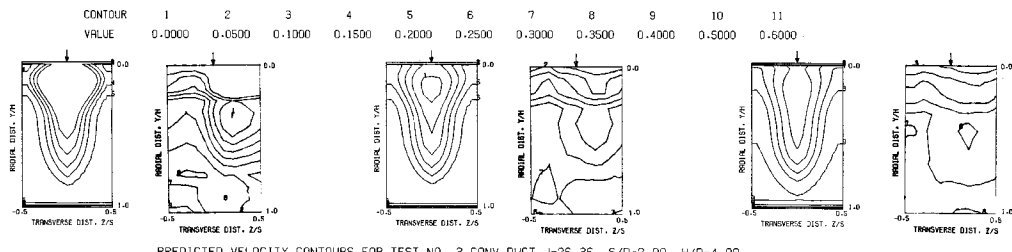


PREDICTED VELOCITY CONTOURS FOR TEST NO. 3, CONV DUCT, J=26.36, S/D=2.00, H/D=4.00

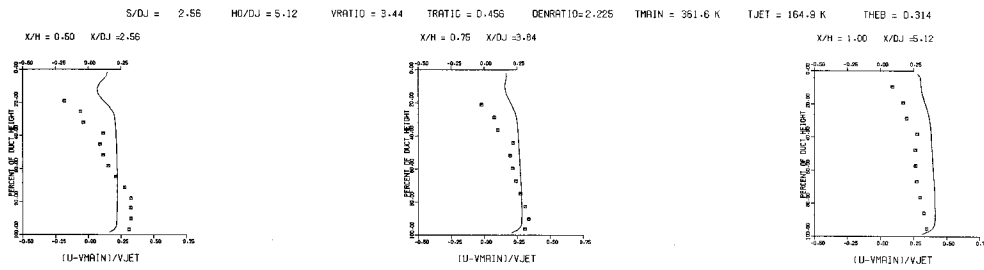


PREDICTED VELOCITY DISTRIBUTIONS FOR TEST NO. 15.42X28X17, J=26.36, S/D=2.00, H/D=4.00

Figure 63. Predicted Velocity Distributions for Test No. 15 - Table 2.



PREDICTED VELOCITY CONTOURS FOR TEST NO. 3.CONV DUCT,J=26.36 , S/D=2.00, H/D=4.00



COMPARISON BETWEEN DATA AND PREDICTIONS FOR TEST 15, 42X28X17, CONV DUCT,SLANT WALL JETS,J = 26.36 , S/D =2.00 , H/D =4.00

Figure 64. Comparison Between Predicted and Measured Velocity Distributions for Test No. 15 - Table 2.

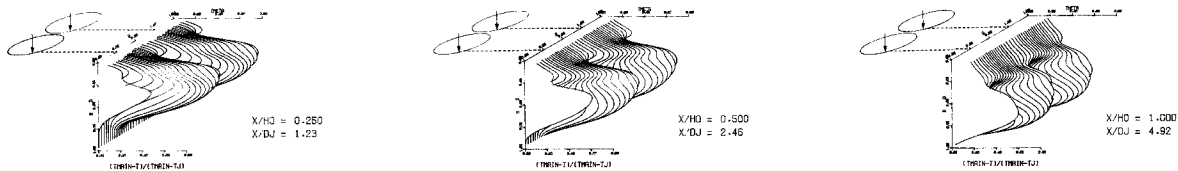
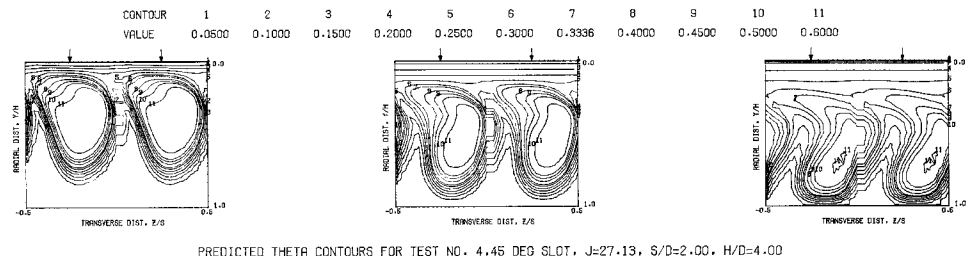
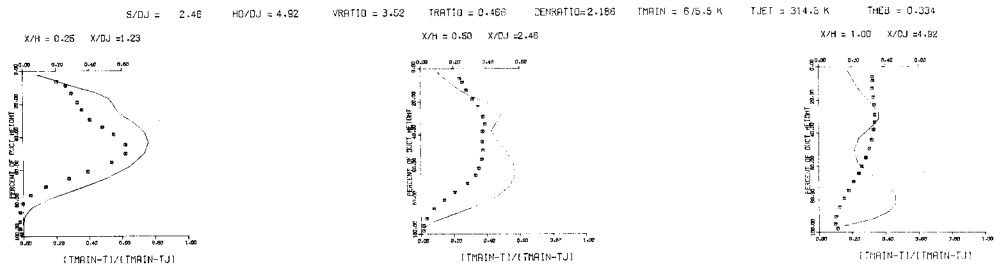
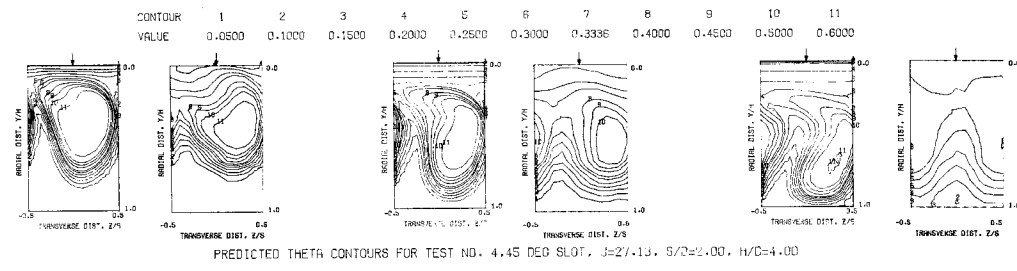
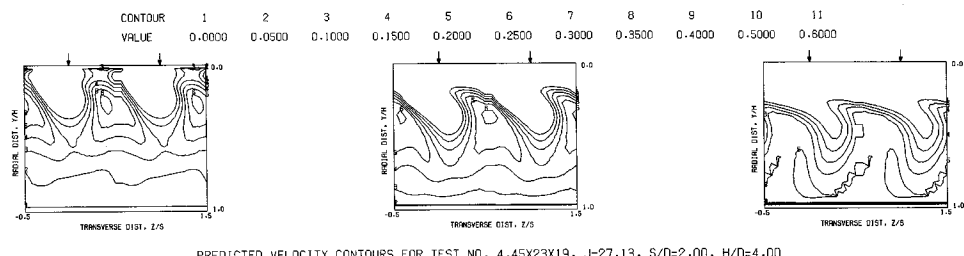


Figure 65. Predicted Temperature Distributions for Test No. 16 - Table 2.

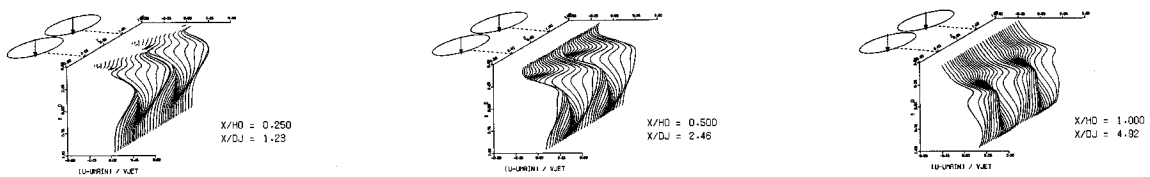


COMPARISON BETWEEN PREDICTED AND MEASURED TEMPERATURE DISTRIBUTIONS FOR TEST 16.45 DEG SLOT, SINGLE SIDED INJECTION     $\beta = 27.13 \rightarrow S/D = 2.00 \rightarrow H/D = 4.00$

Figure 66. Comparison Between Predicted and Measured Temperature Distributions for Test No. 16 - Table 2.

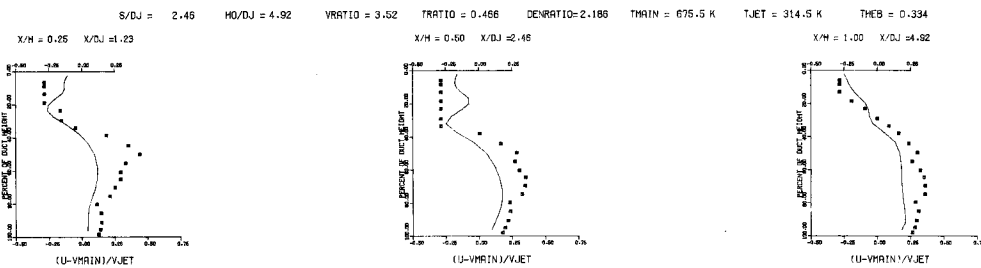
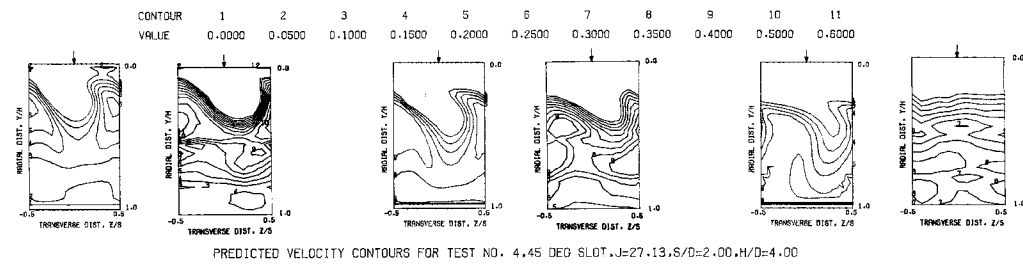


PREDICTED VELOCITY CONTOURS FOR TEST NO. 4.45X23X19, J=27.13, S/D=2.00, H/D=4.00



PREDICTED VELOCITY DISTRIBUTIONS FOR TEST 16, 45 DEGREE SLOT, J=27.13, S/D=2.00

Figure 67. Predicted Velocity Distributions for Test No. 16 - Table 2.



COMPARISON BETWEEN DATA AND PREDICTIONS FOR TEST 16, TM=CONST. 45 DEG SLOT (ONE-SIDED)  $J = 27.13 \quad S/D = 2.00 \quad H/D = 4.00$

Figure 68. Comparison Between Predicted and Measured Velocity Distributions for Test No. 16 - Table 2.

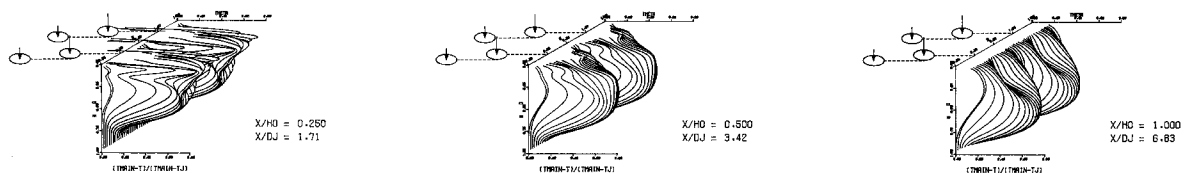
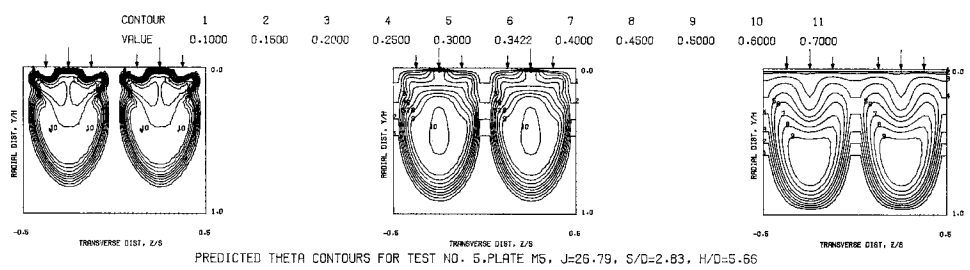
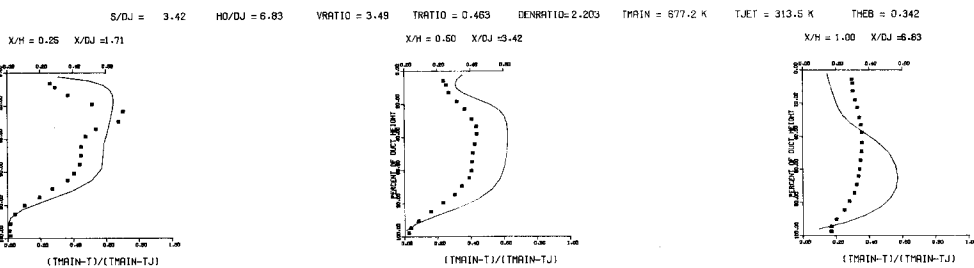
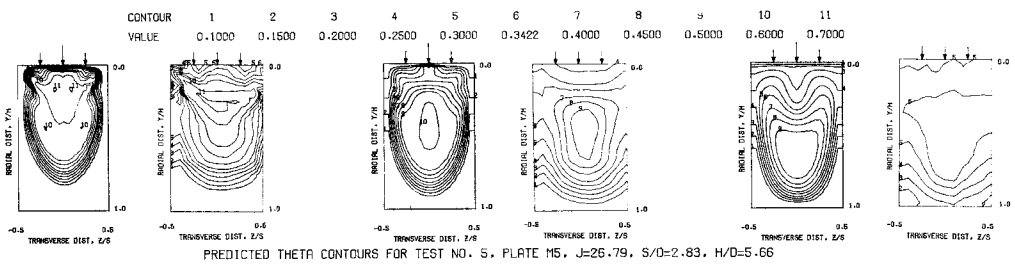


Figure 69. Predicted Temperature Distributions for Test No. 17 - Table 2.



COMPARISON BETWEEN DATA AND PREDICTIONS FOR TEST 17, PLATE MS, AXIAL STAGED INJECTION J = 26.79 , S/D = 2.83 , H/D = 5.66

Figure 70. Comparison Between Predicted and Measured Temperature Distributions for Test No. 17 - Table 2.

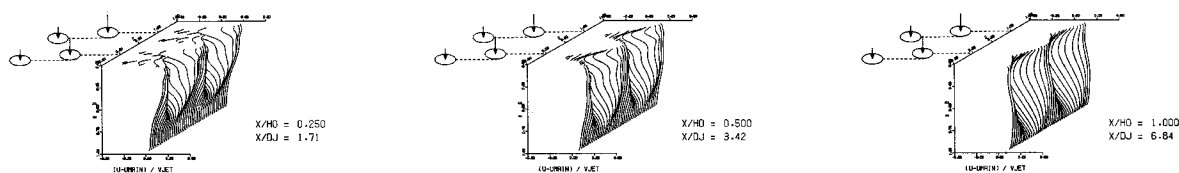
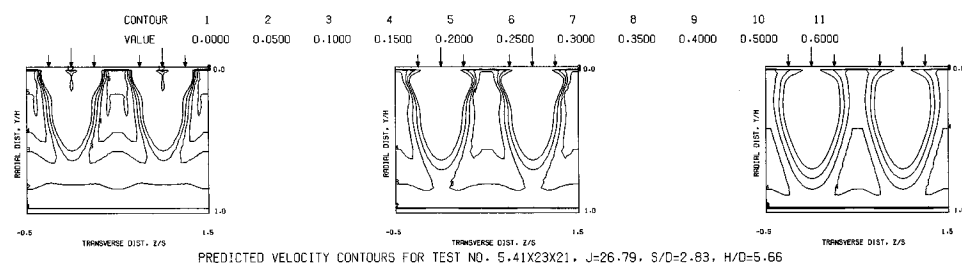
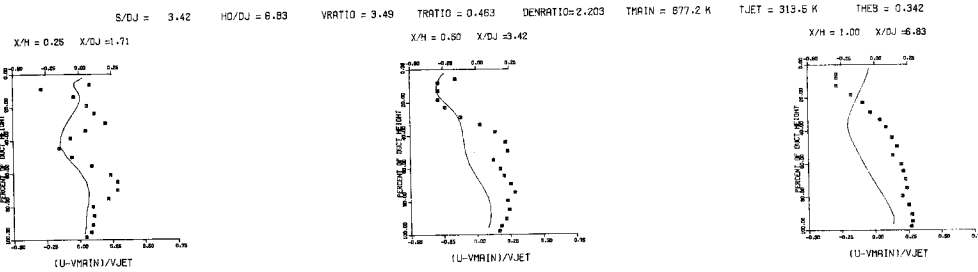
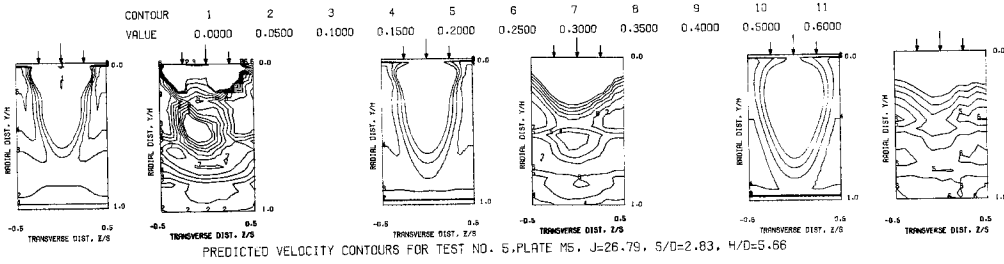
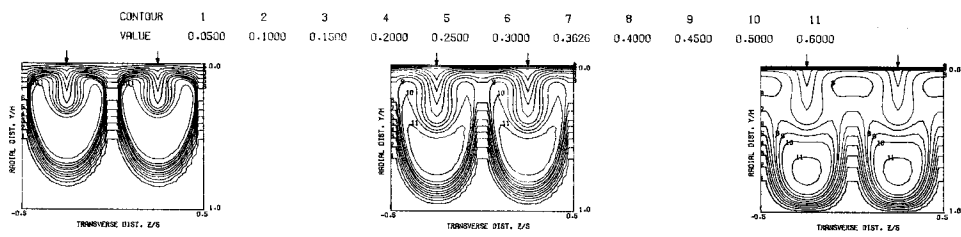


Figure 71. Predicted Velocity Distributions for Test No. 17 - Table 2.

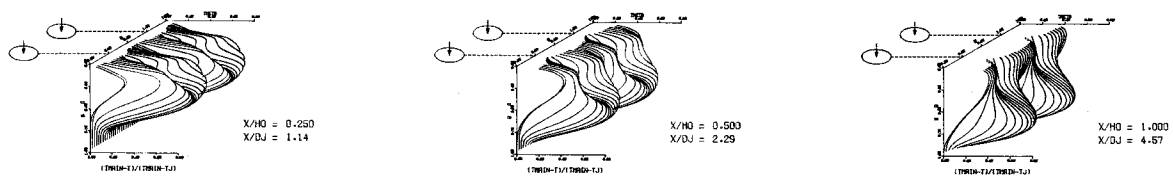


COMPARISON BETWEEN DATA AND PREDICTIONS FOR TEST 17,  $TM=\text{CONST}$ , AXIALLY STAGED INJECTION  $J = 26.79$ ,  $S/D = 2.83$ ,  $H/D = 5.66$

Figure 72. Comparison Between Predicted and Measured Velocity Distributions for Test No. 17 - Table 2.

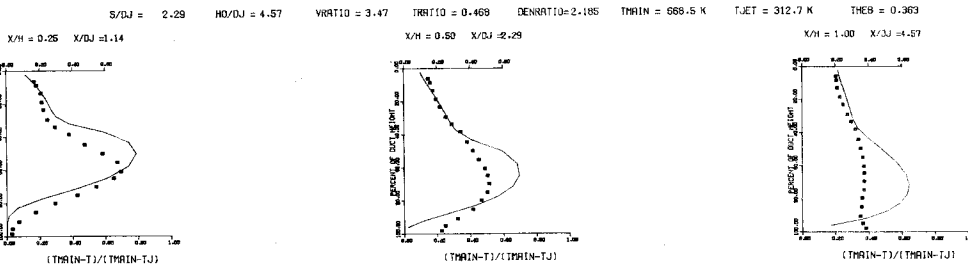
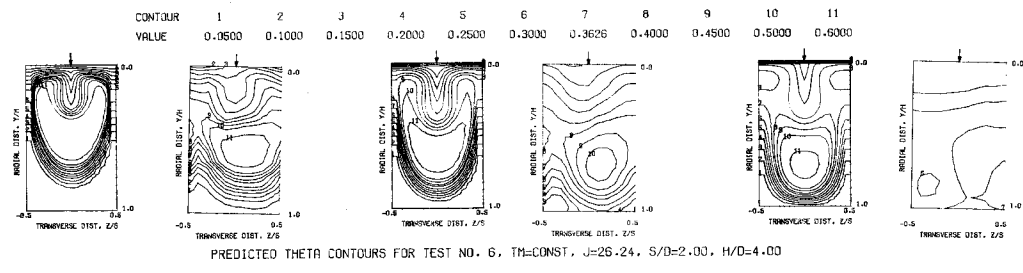


PREDICTED THETA CONTOURS FOR TEST NO. 6, TM=CONST, J=26.24, S/D=2.00, H/D=4.00



PREDICTED THETA DISTRIBUTIONS FOR TEST NO. 18, TM=CONST, J=26.24, S/D=2.00, H/D=4.00

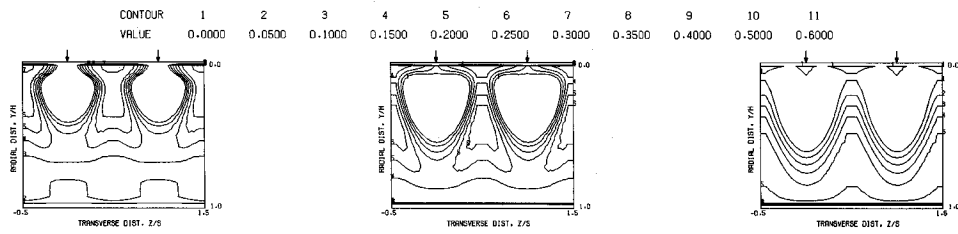
Figure 73. Predicted Temperature Distributions for Test No. 18 - Table 2.



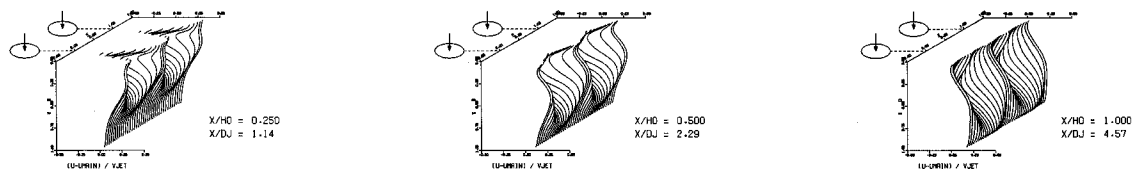
COMPARISON BETWEEN DATA AND PREDICTIONS FOR TEST 18, TM=CONST, SINGLE SIDED INJECTION    J = 26.24    S/D = 2.00    H/D = 4.00

Figure 74. Comparison Between Predicted and Measured Temperature Distributions for Test No. 18 - Table 2.

100

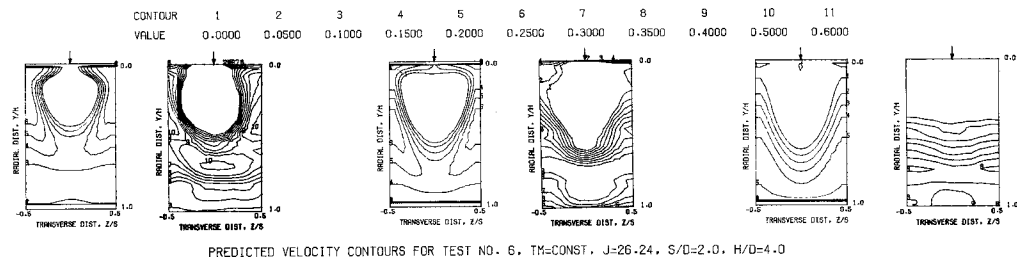


PREDICTED VELOCITY CONTOURS FOR TEST NO. 6.45X23X19, J=26.24, S/D=2.00, H/D=4.00

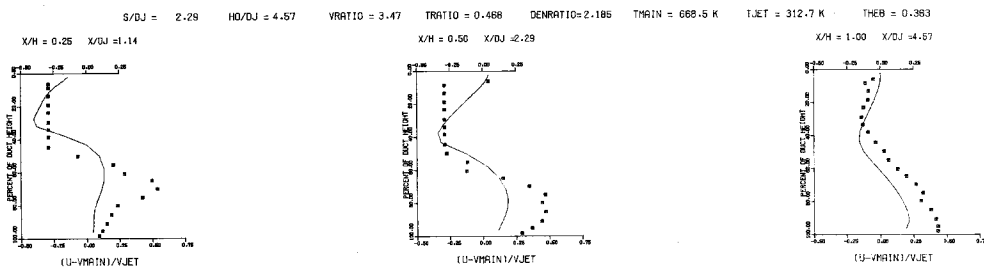


PREDICTED VELOCITY DISTRIBUTIONS FOR TEST 18.45X23X19, J=26.24, S/D=2.00, H/D=4.00

Figure 75. Predicted Velocity Distributions for Test No. 18 - Table 2.



PREDICTED VELOCITY CONTOURS FOR TEST NO. 6. TM=CONST, J=26.24, S/D=2.0, H/D=4.0

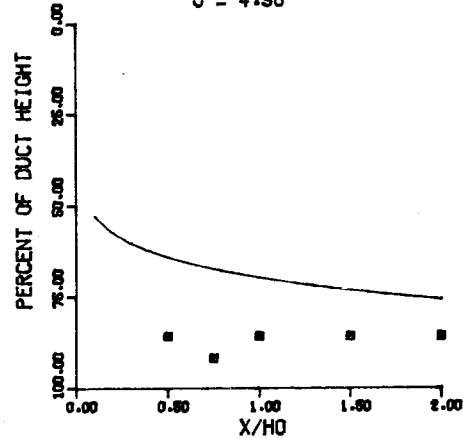


COMPARISON BETWEEN DATA AND PREDICTIONS FOR TEST 18. TM=CONST, SINGLE SIDED INJECTION    $J = 26.24$ ,  $S/D = 2.00$ ,  $H/D = 4.00$

Figure 76. Comparison Between Predicted and Measured Velocity Distributions for Test No. 18 - Table 2.

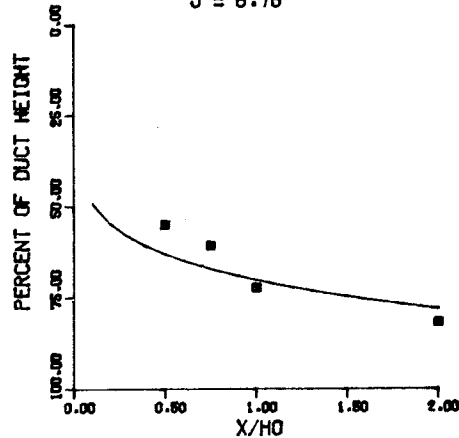
TEST NO 1, ISOTHERMAL T<sub>MAIN</sub>, PHASE I  
ORIFICE PLATE 01/02/04

$$J = 4.98$$



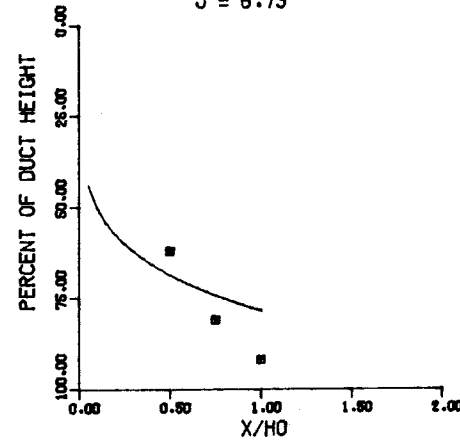
TEST NO 21, CONV DUCT II, PHASE I  
ORIFICE PLATE 01/02/04

$$J = 6.76$$



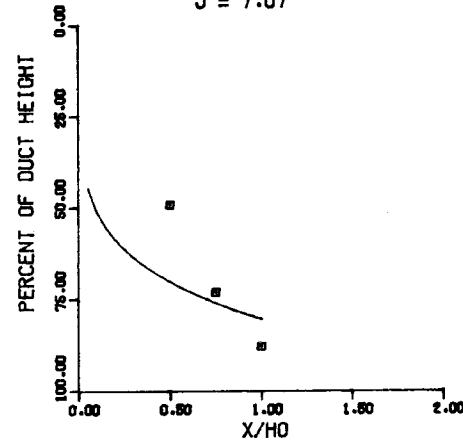
TEST NO 25, CONV DUCT IV, PHASE I  
ORIFICE PLATE 01/02/04

$$J = 6.73$$



TEST NO 29, FLAT WALL JET, PHASE I  
ORIFICE PLATE 01/02/04

$$J = 7.07$$



TEST NO 33, SLANT WALL JET, PHASE I  
ORIFICE PLATE 01/02/04

$$J = 7.04$$

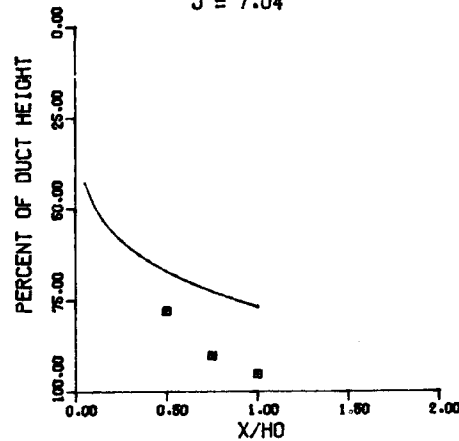
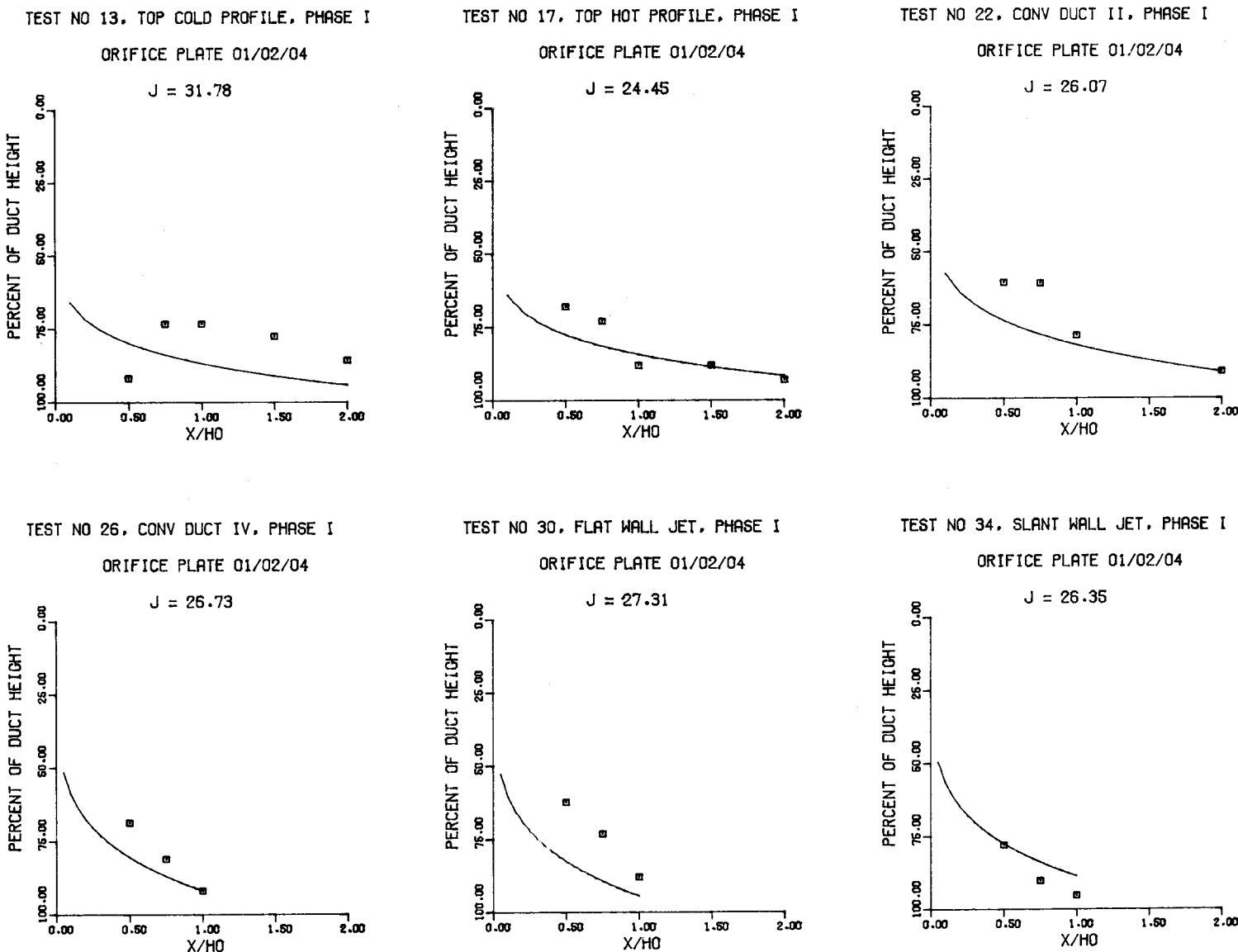


Figure 77. Comparison Between Predicted and Measured Velocity Trajectories  
For S/D = 2 and H<sub>0</sub>/D = 4.



**Figure 78.** Comparison Between Predicted and Measured Velocity Trajectories Including Effects of Mainstream Profiles and Flow Area Convergence at Intermediate  $J$  for Orifice Plate 01/02/04.

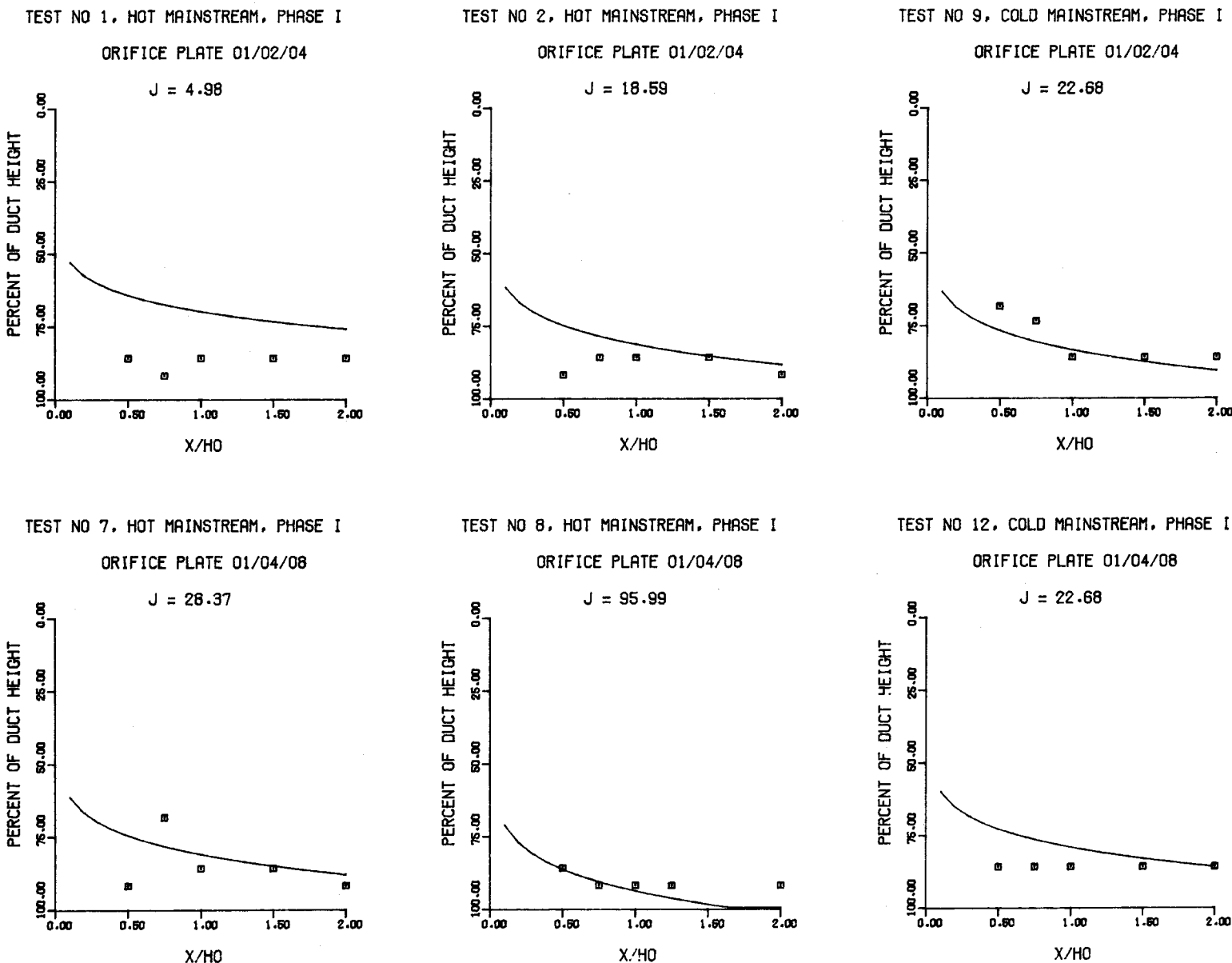


Figure 79. Comparison of Predicted and Measured Velocity Trajectories for Different Jet Diameters,  $S/H = 0.5$ .

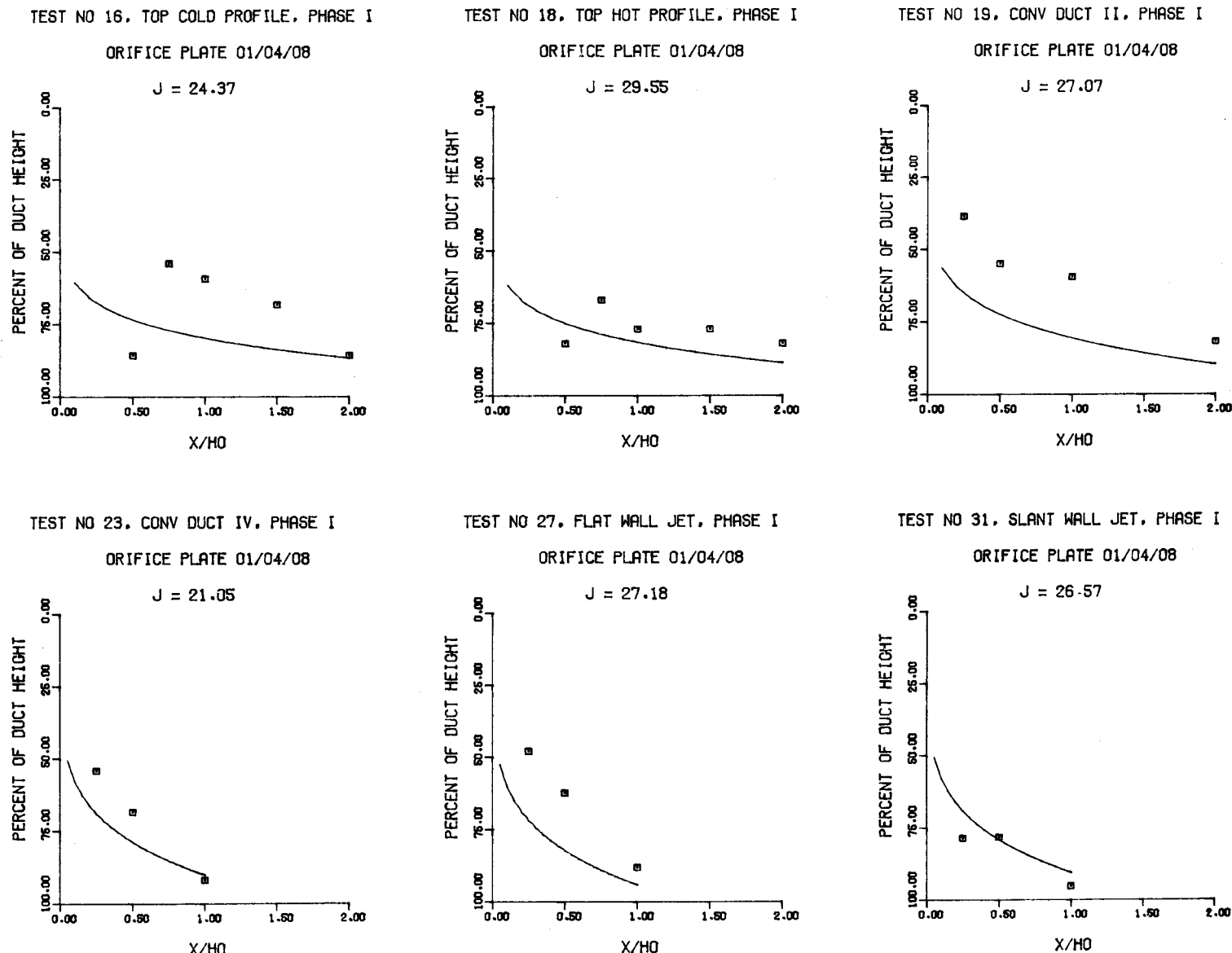
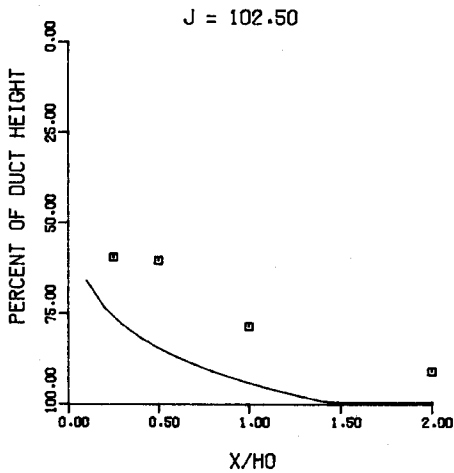
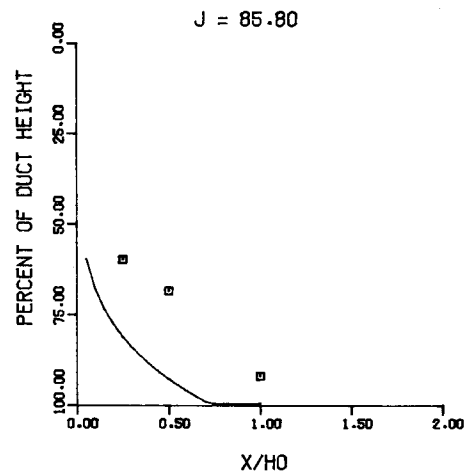


Figure 80. Predicted and Measured Velocity Trajectories for Non-Uniform Mainstream Profile and Flow Area Convergence,  $S/D = 4$ ,  $H_0/D = 8$ .

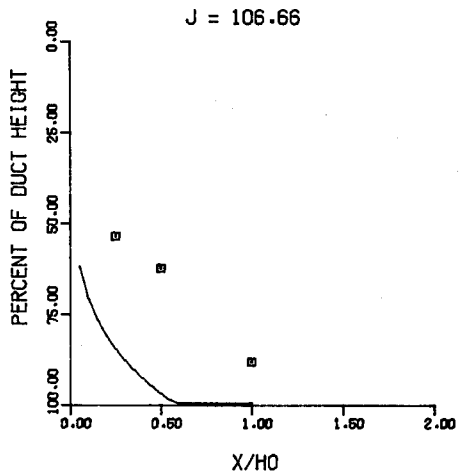
TEST NO 20, CONV DUCT II, PHASE I  
ORIFICE PLATE 01/04/08



TEST NO 24, CONV DUCT IV, PHASE I  
ORIFICE PLATE 01/04/08



TEST NO 28, FLAT WALL JET, PHASE I  
ORIFICE PLATE 01/04/08



TEST NO 32, SLANT WALL JET, PHASE I  
ORIFICE PLATE 01/04/08

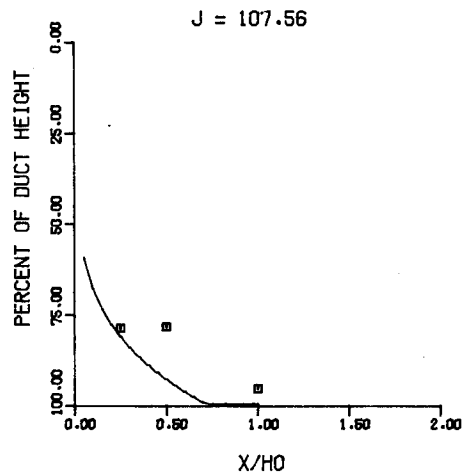
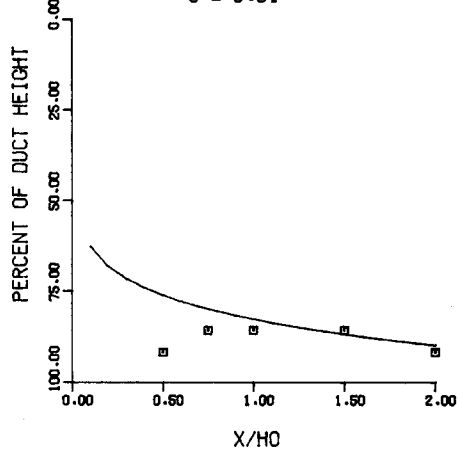


Figure 81. Predicted and Measured Velocity Trajectories for Different Convergence and Jet Injection Angles,  
 $S/D = 4$ ,  $H_0/D = 8$ .

TEST NO 3, HOT MAINSTREAM, PHASE I

ORIFICE PLATE 01/04/04

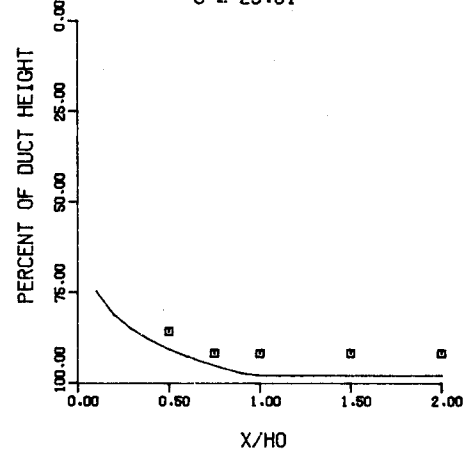
$$J = 5.31$$



TEST NO 4, HOT MAINSTREAM, PHASE I

ORIFICE PLATE 01/04/04

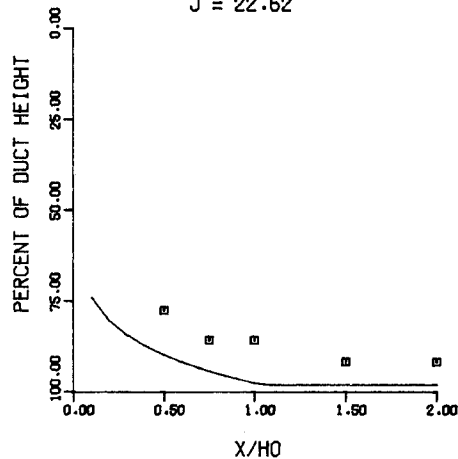
$$J = 23.51$$



TEST NO 10, COLD MAINSTREAM, PHASE I

ORIFICE PLATE 01/04/04

$$J = 22.62$$



TEST NO 18, TOP COLD PROFILE, PHASE I

ORIFICE PLATE 01/04/04

$$J = 6.70$$

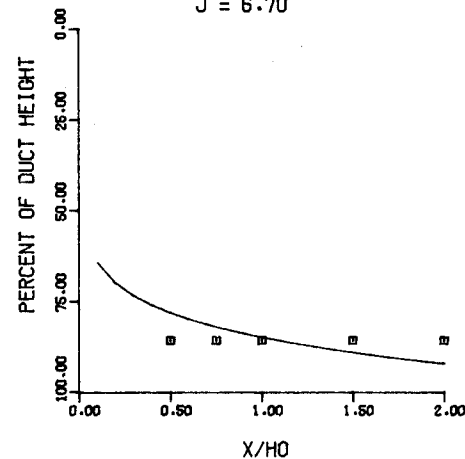
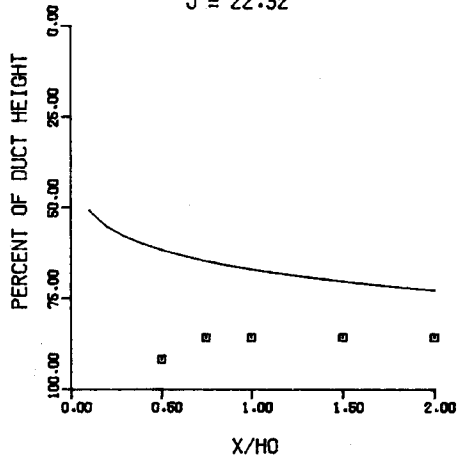


Figure 82. Predicted and Measured Velocity Trajectories in a Straight Duct for  $S/D = 4$ ,  $H_0/D = 4$ .

TEST NO 5, HOT MAINSTREAM, PHASE I

ORIFICE PLATE 01/02/08

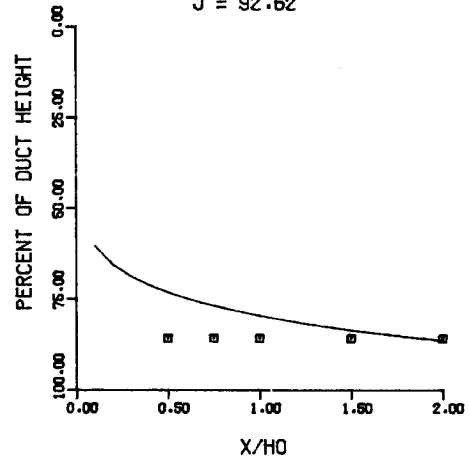
$$J = 22.32$$



TEST NO 6, HOT MAINSTREAM, PHASE I

ORIFICE PLATE 01/02/08

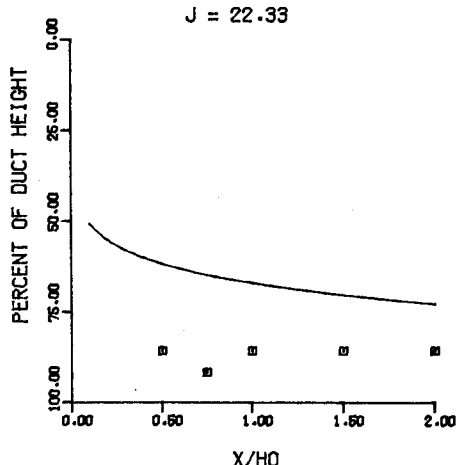
$$J = 92.62$$



TEST NO 11, COLD MAINSTREAM, PHASE I

ORIFICE PLATE 01/02/08

$$J = 22.33$$



TEST NO 15, TOP COLD PROFILE, PHASE I

ORIFICE PLATE 01/02/08

$$J = 99.20$$

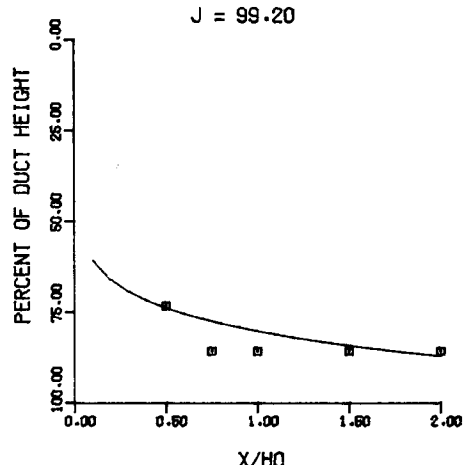
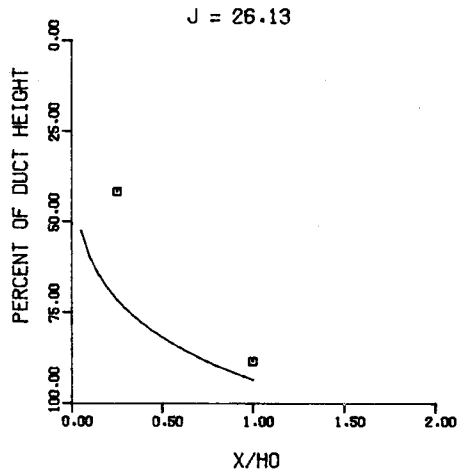
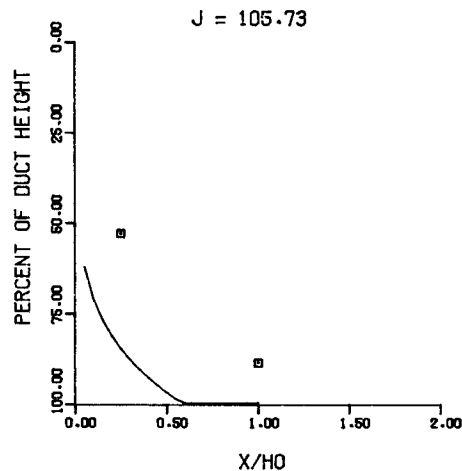


Figure 83. Predicted and Measured Velocity Trajectories in a Straight Duct for  $S/D = 2$ ,  $H_0/D = 8$ .

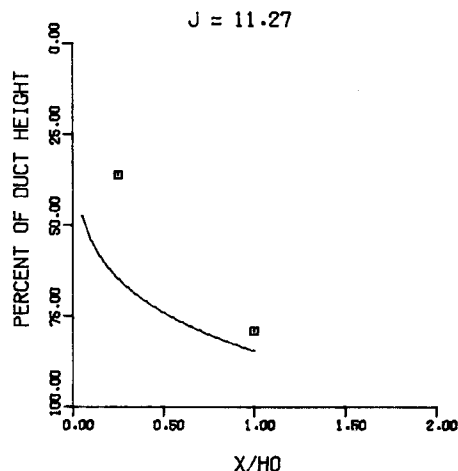
TEST NO 35, TOP COLD PROFILE, T.S. V  
ORIFICE PLATE 01/04/08



TEST NO 36, TOP COLD PROFILE, T.S. V  
ORIFICE PLATE 01/04/08



TEST NO 37, TOP HOT PROFILE, T.S. V  
ORIFICE PLATE 01/04/08



TEST NO 38, TOP HOT PROFILE, T.S. V  
ORIFICE PLATE 01/04/08

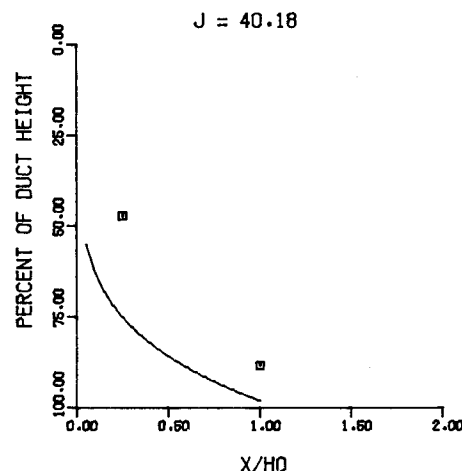
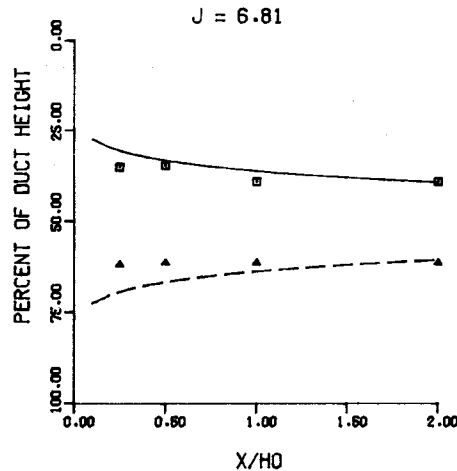
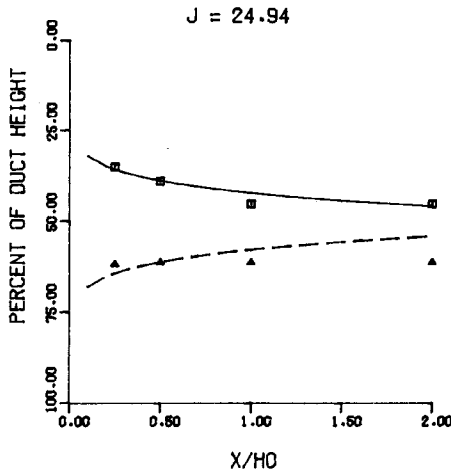


Figure 84. Predicted and Measured Velocity Trajectories in a Symmetrically Convergent Duct with Non-Uniform Mainstream Profile, S/N = 4,  $H_0/D = 8$  (Test Section V).

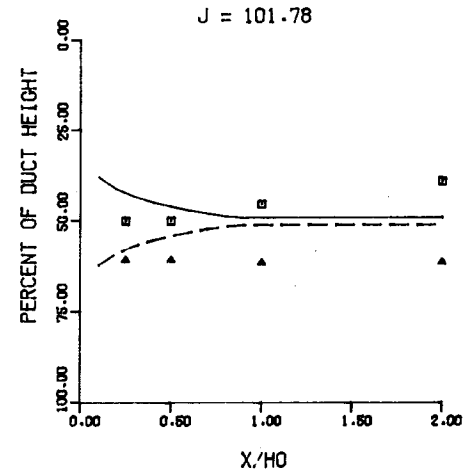
TEST NO 1, OPPOSED JETS, PHASE II  
ORIFICE PLATE 01/02/08 (INL)



TEST NO 2, OPPOSED JETS, PHASE II  
ORIFICE PLATE 01/02/08 (INL)

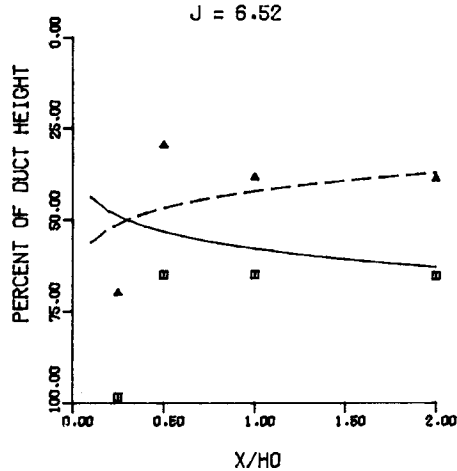


TEST NO 3, OPPOSED JETS, PHASE II  
ORIFICE PLATE 01/02/08 (INL)

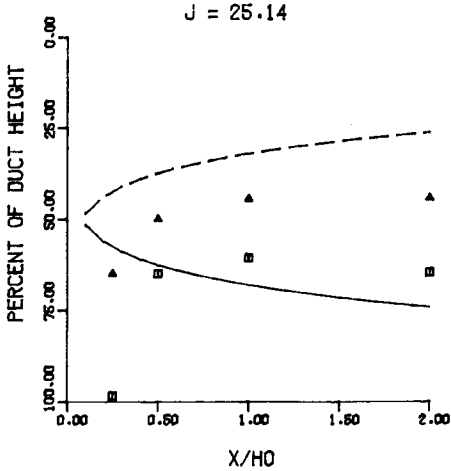


— TOP ROW JET TRAJECTORY      - - - BOTTOM ROW JET TRAJECTORY

TEST NO 4, OPPOSED JETS, PHASE II  
ORIFICE PLATE 01/02/08 (STG)



TEST NO 5, OPPOSED JETS, PHASE II  
ORIFICE PLATE 01/02/08 (STG)



TEST NO 6, OPPOSED JETS, PHASE II  
ORIFICE PLATE 01/02/08 (STG)

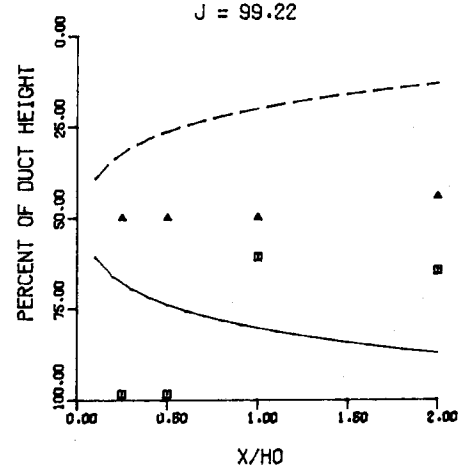


Figure 85. Predicted and Measured Velocity Trajectories for Opposed Jets,  
 $S/D = 2$ ,  $H_0/D = 8$ .

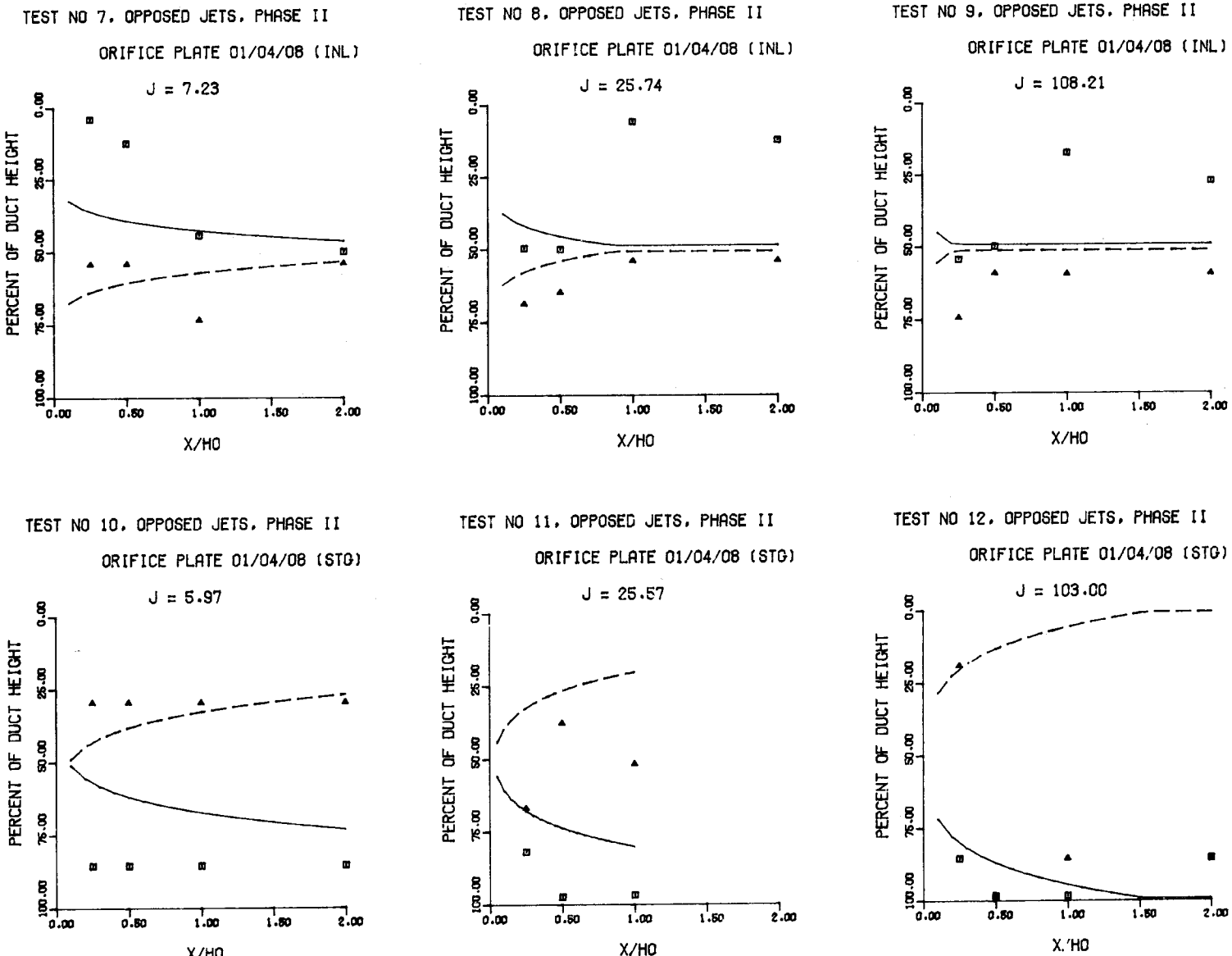
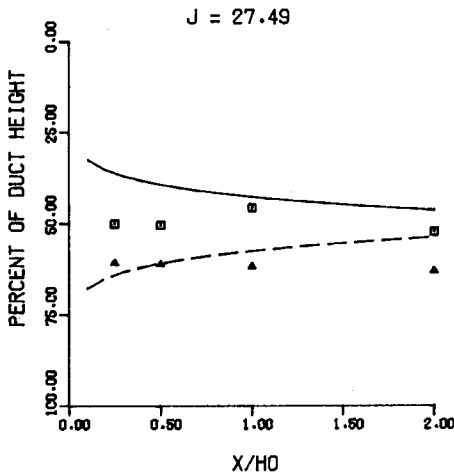
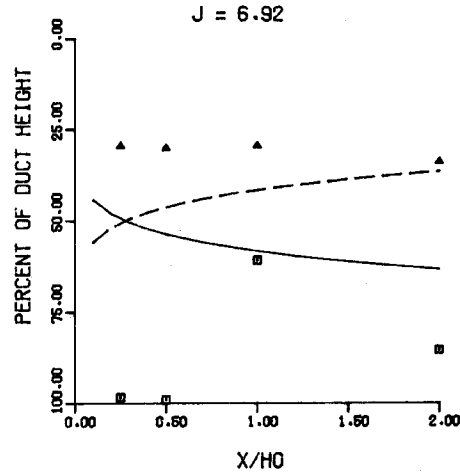


Figure 86. Predicted and Measured Velocity Trajectories for Opposed Jets,  
 $S/D = 4$ ,  $H_0/D = 8$ .

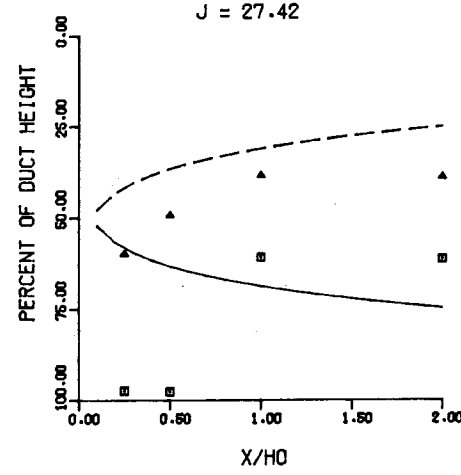
TEST NO 13, TOP COLD PROFILE, PHASE II  
ORIFICE PLATE 01/02/08 (INL)



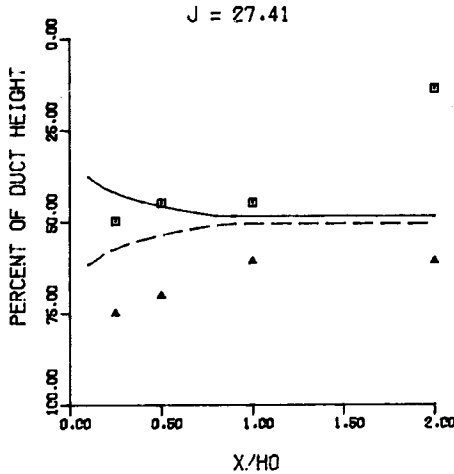
TEST NO 14, TOP COLD PROFILE, PHASE II  
ORIFICE PLATE 01/02/08 (STG)



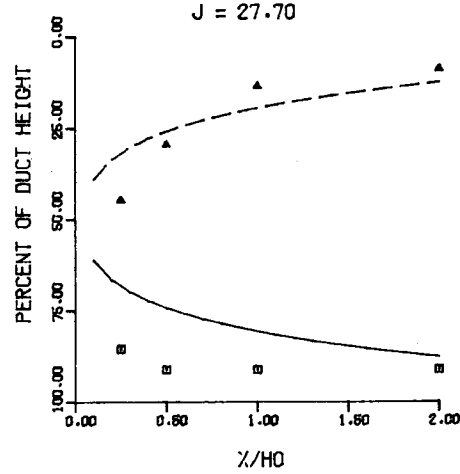
TEST NO 15, TOP COLD PROFILE, PHASE II  
ORIFICE PLATE 01/02/08 (STG)



TEST NO 16, TOP COLD PROFILE, PHASE II  
ORIFICE PLATE 01/04/08 (INL)



TEST NO 17, TOP COLD PROFILE, PHASE II  
ORIFICE PLATE 01/04/08 (STG)



TEST NO 18, TOP COLD PROFILE, PHASE II  
ORIFICE PLATE 01/04/08 (STG)

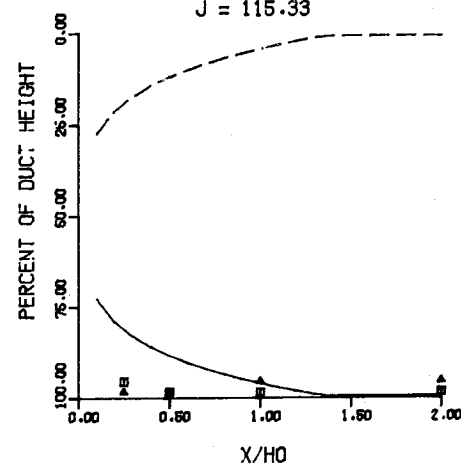
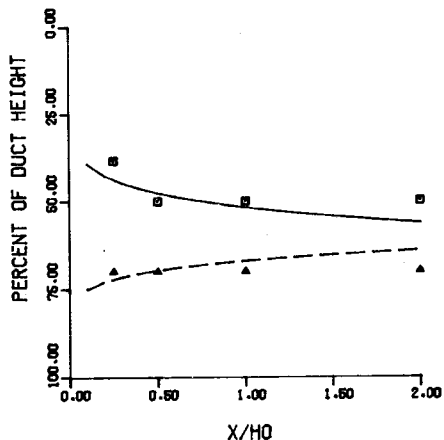
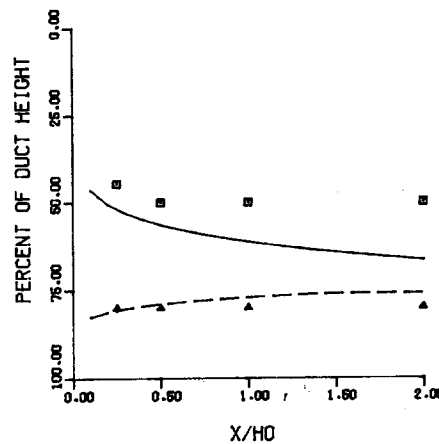


Figure 87. Predicted and Measured Velocity Trajectories for Opposed Jets With Non-Uniform Mainstream Profile.

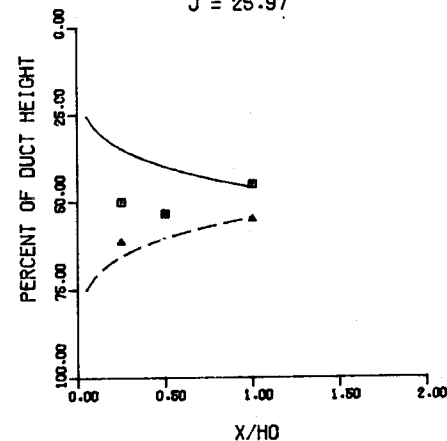
TEST NO 33, JT=40.9, JB=14.7, PHASE II  
ORIFICE PLATE 01/02/08 (INL)



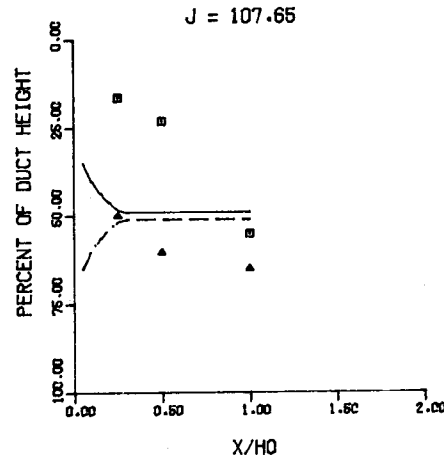
TEST NO 34, JT=58.4, JB=6.5, PHASE II  
ORIFICE PLATE 01/02/08 (INL)



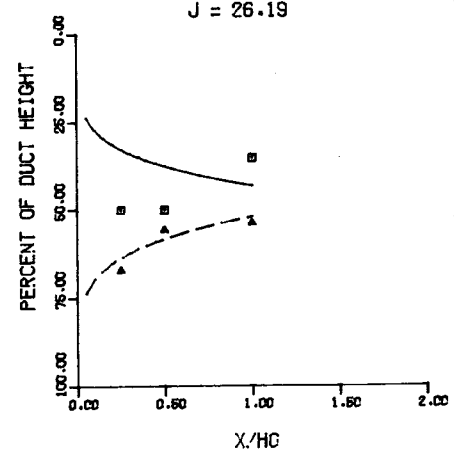
TEST NO 19, SYMMETRIC CONV DUCT-PHASE II  
ORIFICE PLATE 01/02/08 (INL)  
J = 25.97



TEST NO 20, SYMMETRIC CONV DUCT-PHASE II  
ORIFICE PLATE 01/02/08 (INL)



TEST NO 35, ASYMM CONV DUCT, PHASE II  
ORIFICE PLATE 01/02/08 (INL)



TEST NO 36, ASYMM CONV DUCT, PHASE II  
ORIFICE PLATE 01/02/08 (INL)

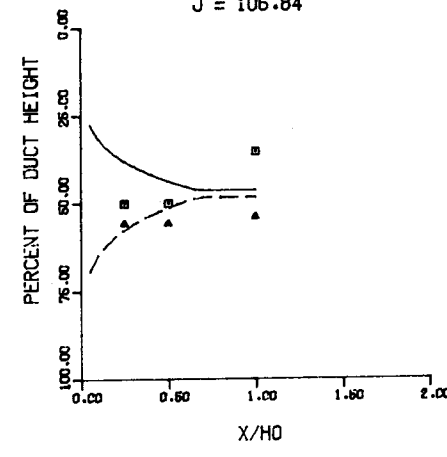
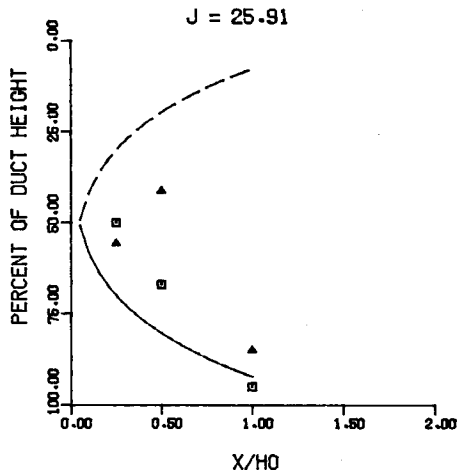
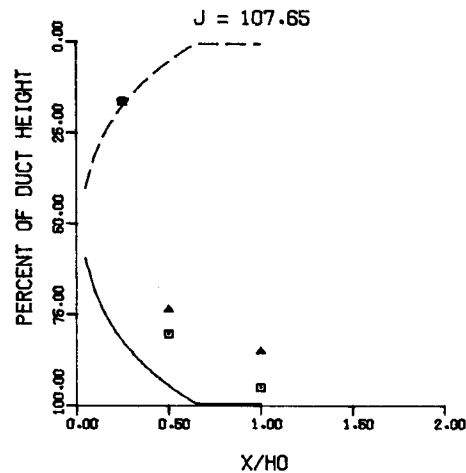


Figure 88. Predicted and Measured Velocity Trajectories with Unequal Momentum Flux Ratios, Flow Area Convergence, for Opposed Jets;  
S/D = 2, H<sub>0</sub>/D = 8.

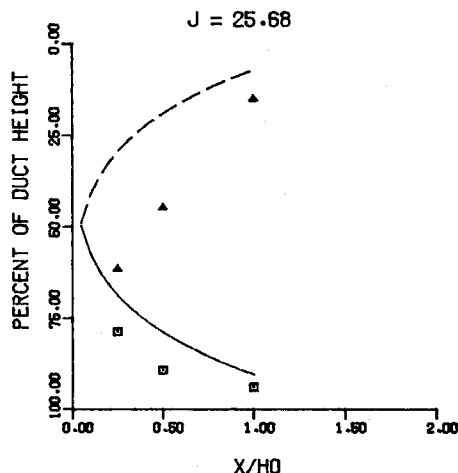
TEST NO 21, SYMM CONV DUCT, PHASE II  
ORIFICE PLATE 01/04/08 (STG)



TEST NO 22, SYMM CONV DUCT, PHASE II  
ORIFICE PLATE 01/04/08 (STG)



TEST NO 37, ASYMM CONV DUCT - PHASE II  
ORIFICE PLATE 01/04/08 (STG)



TEST NO 38, ASYMM CONV DUCT - PHASE II  
ORIFICE PLATE 01/04/08 (STG)

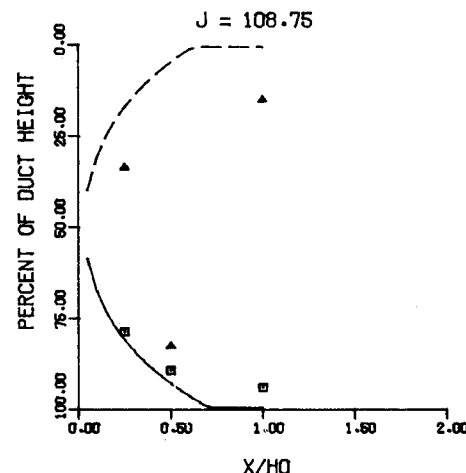


Figure 89. Predicted and Measured Velocity Trajectories for Opposed Jets in Convergent Ducts,  $S/D = 4$ ,  $H_0/D = 8$ .

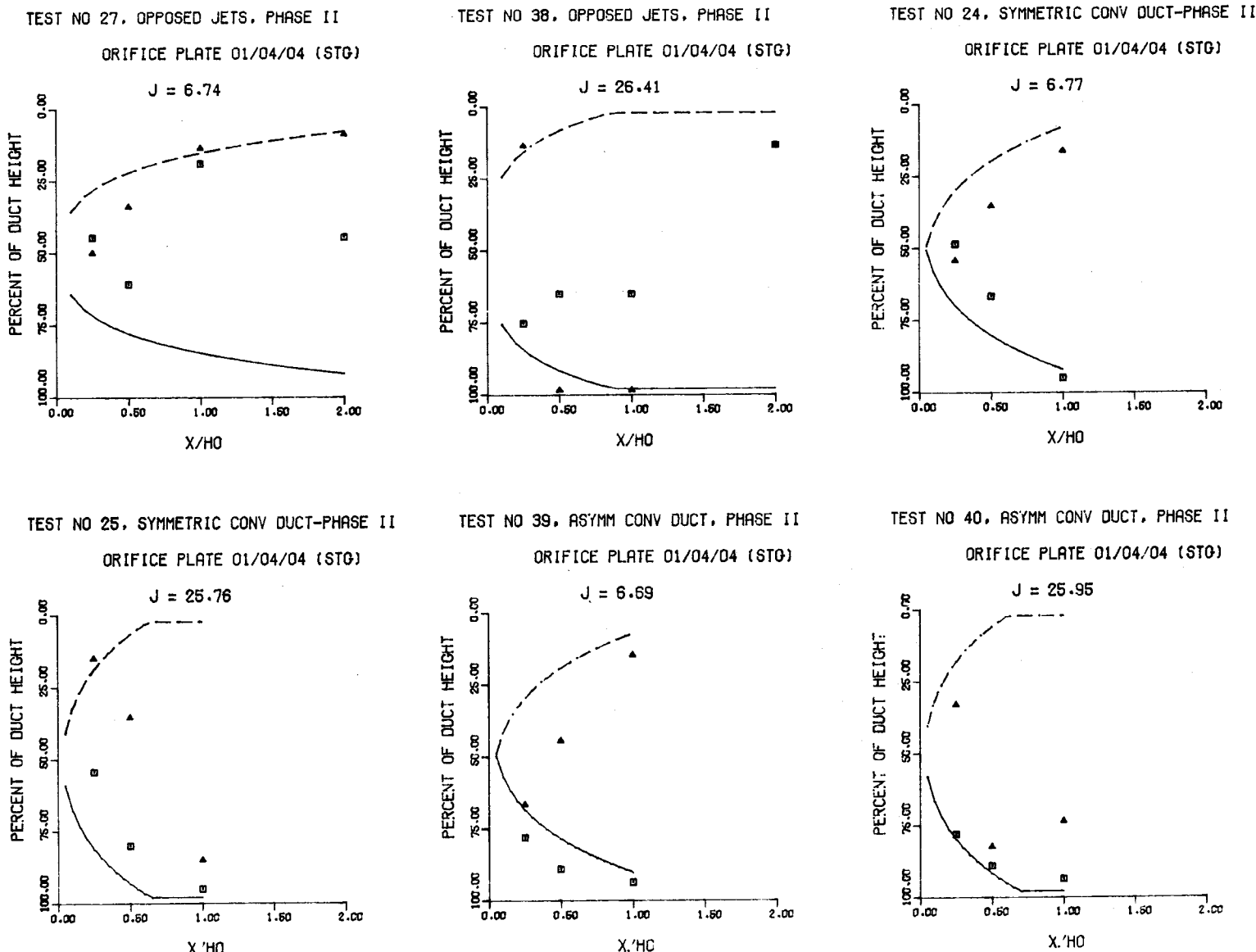
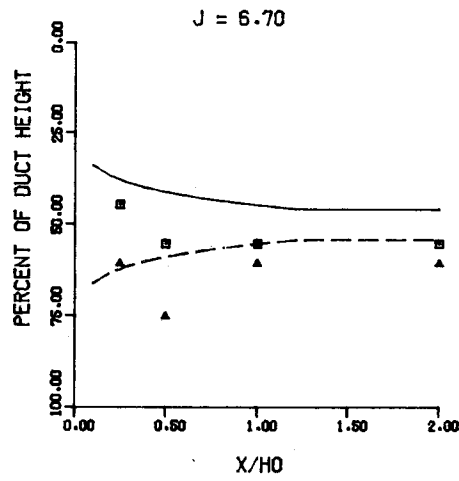
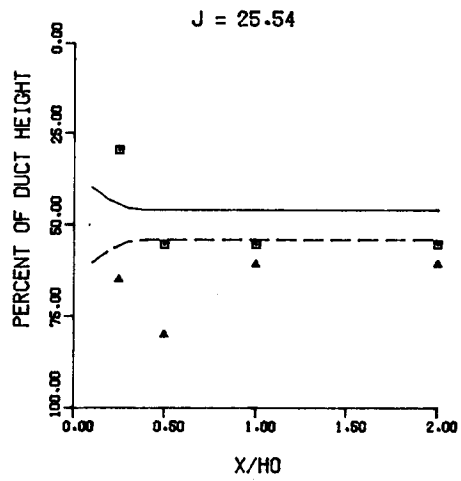


Figure 90. Predicted and Measured Velocity Trajectories for Opposed Jets with  $S/D = 4$ ,  $H_0/D = 8$ .

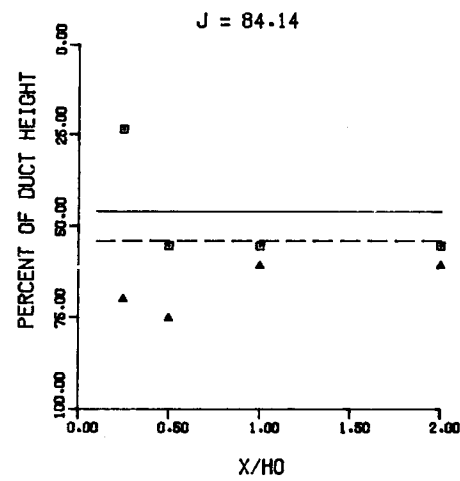
TEST NO 46, OPPOSED JETS, PHASE II  
ORIFICE PLATE 01/02/04 (INL)



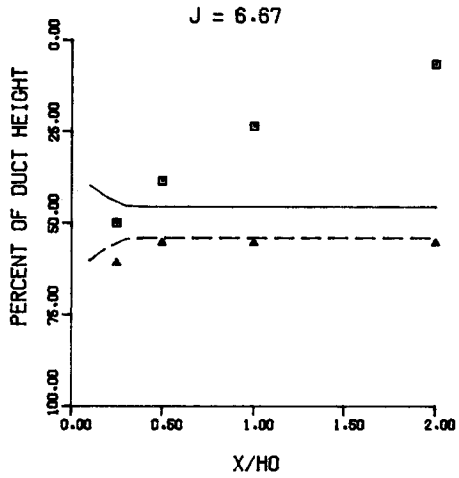
TEST NO 47, OPPOSED JETS, PHASE II  
ORIFICE PLATE 01/02/04 (INL)



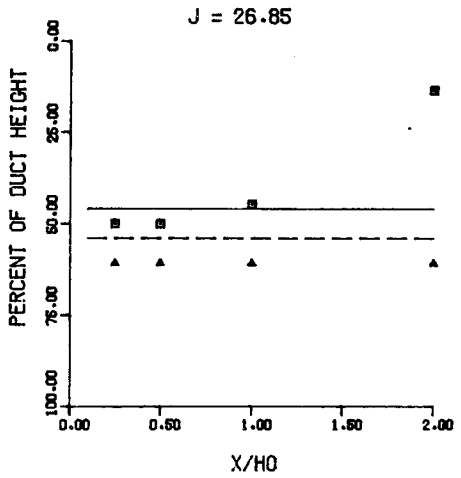
TEST NO 48, OPPOSED JETS - PHASE II  
ORIFICE PLATE 01/02/04 (INL)



TEST NO 51, OPPOSED JETS - PHASE II  
ORIFICE PLATE 01/04/04 (INL)



TEST NO 29, OPPOSED JETS, PHASE II  
ORIFICE PLATE 01/04/04 (INL)



TEST NO 30, OPPOSED JETS, PHASE II  
ORIFICE PLATE 01/04/04 (INL)

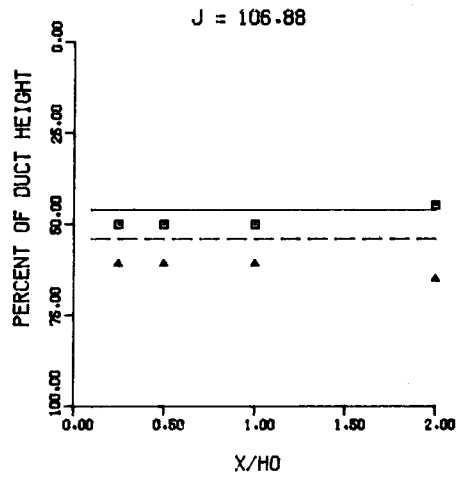
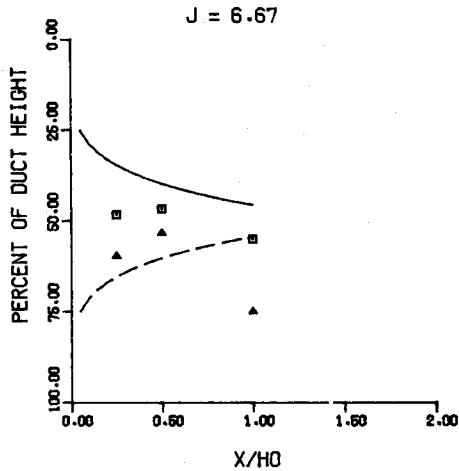
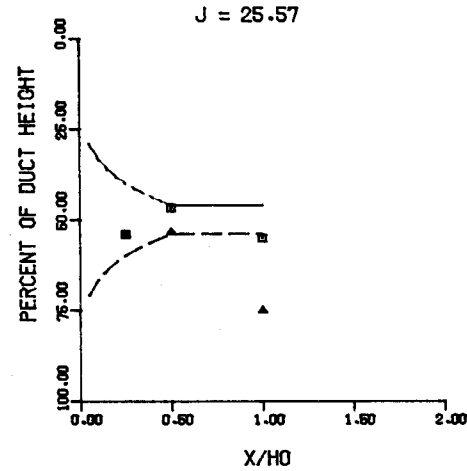


Figure 91. Comparison Between Predicted and Measured Velocity Trajectories  
For Opposed In-line Jets with  $H_0/D = 4$  in a Straight Duct.

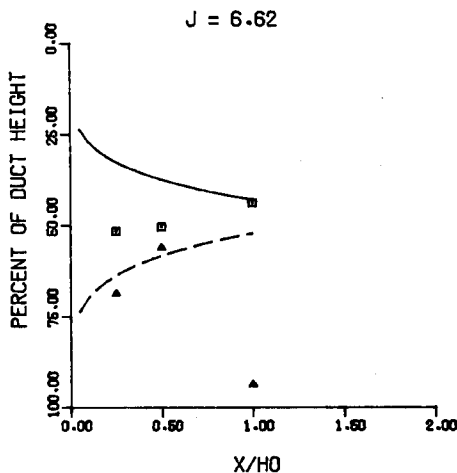
TEST NO 25, SYMM CONV DUCT, PHASE II  
ORIFICE PLATE 01/02/04 (INL)



TEST NO 26, SYMM CONV DUCT, PHASE II  
ORIFICE PLATE 01/02/04 (INL)



TEST NO 41, ASYMM CONV DUCT - PHASE II  
ORIFICE PLATE 01/02/04 (INL)



TEST NO 42, ASYMM CONV DUCT - PHASE II  
ORIFICE PLATE 01/02/04 (INL)

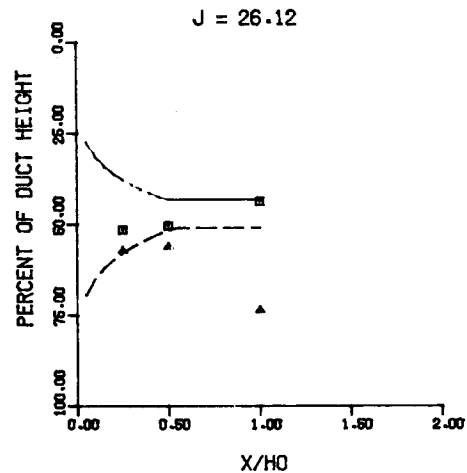
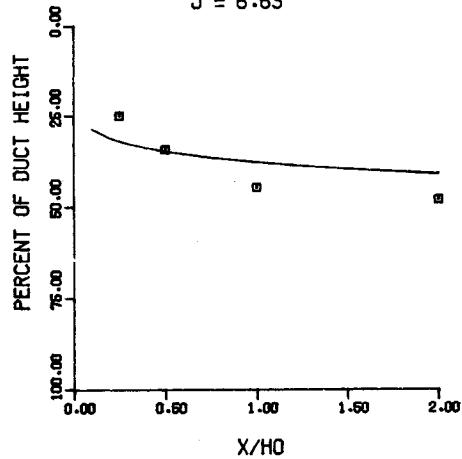


Figure 92. Predicted and Measured Velocity Trajectories with Opposed Jets in Convergent Ducts,  $S/D = 2$ ,  $H_0/D = 4$ .

TEST NO 31A, ONE-SIDED JET, PHASE II

0.5144 CM WIDE SLOT

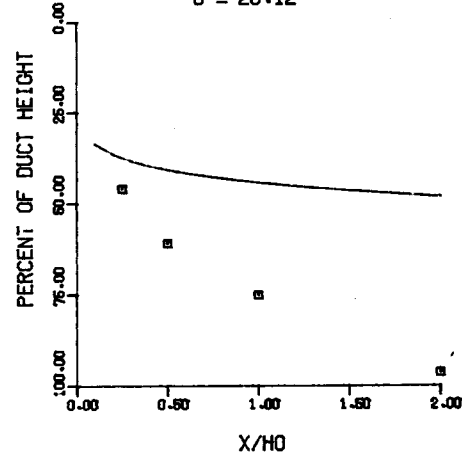
$J = 6.63$



TEST NO 31B, ONE-SIDED JET, PHASE II

0.5144 CM WIDE SLOT

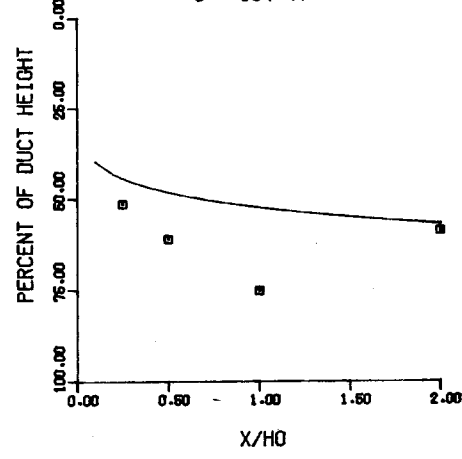
$J = 26.12$



TEST NO 31C, ONE-SIDED JET - PHASE II

0.5144 CM WIDE SLOT

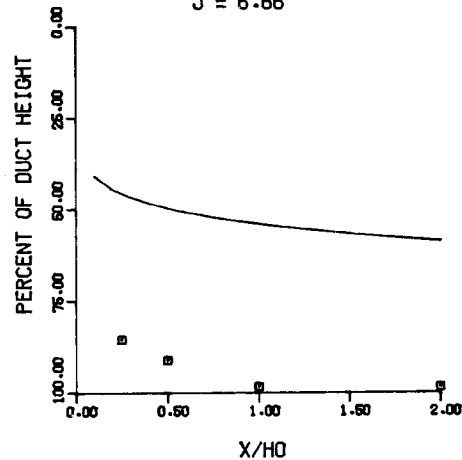
$J = 104.47$



TEST NO 45A, ONE-SIDED JET - PHASE II

1.024 CM WIDE SLOT

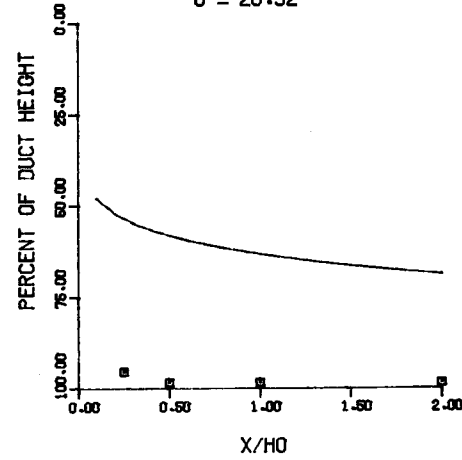
$J = 6.66$



TEST NO 45B, ONE-SIDED JET - PHASE II

1.024 CM WIDE SLOT

$J = 25.32$



TEST NO 45C, ONE-SIDED JET - PHASE II

1.024 CM WIDE SLOT

$J = 78.19$

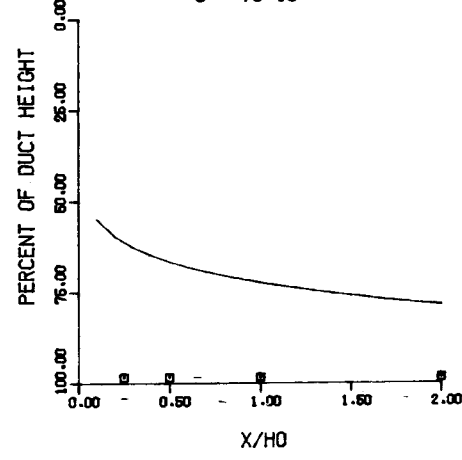
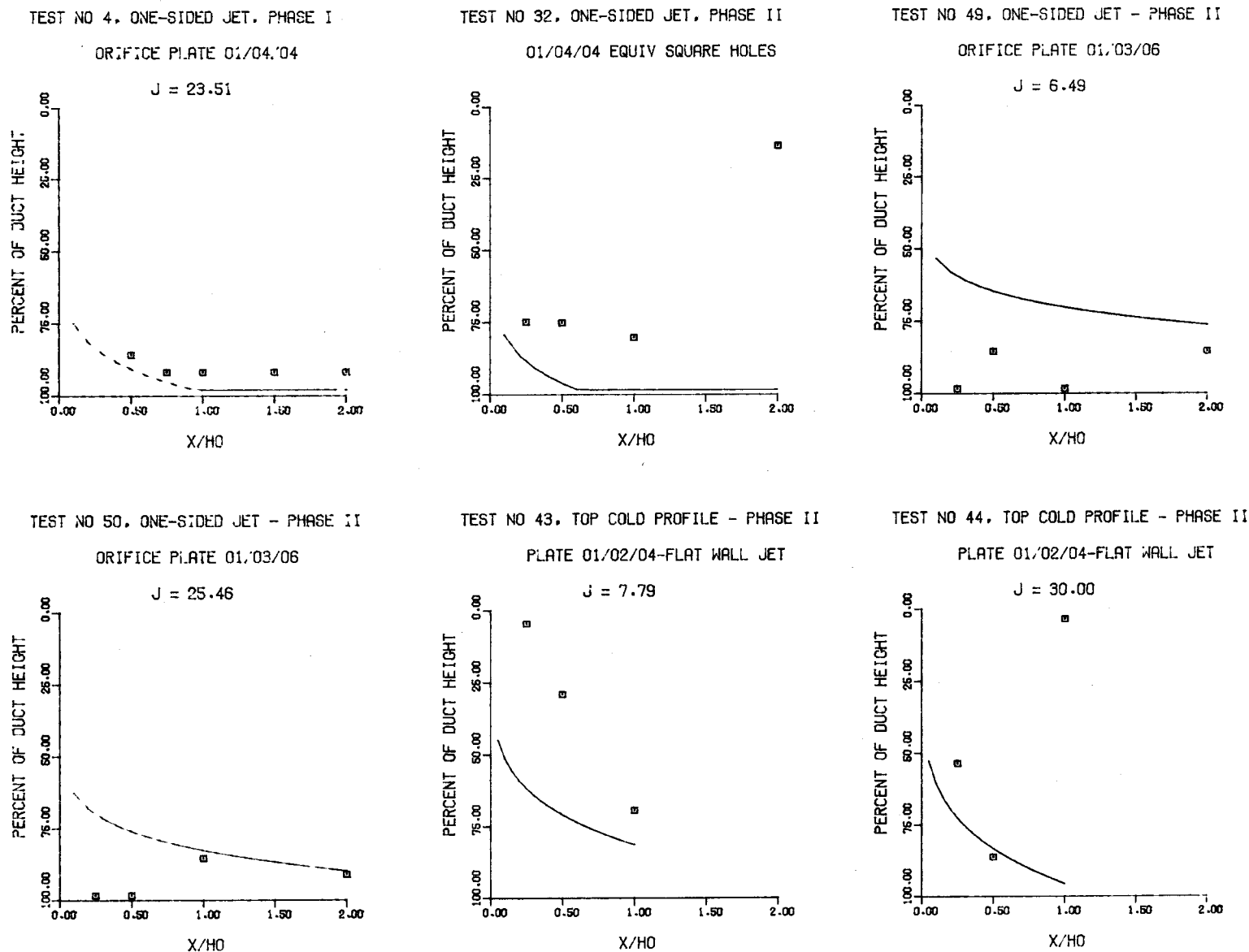
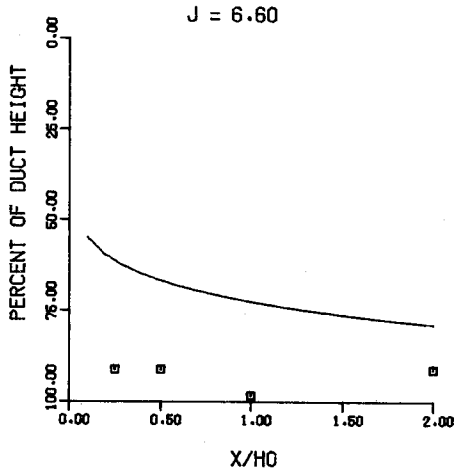


Figure 93. Predicted and Measured Velocity Trajectories for 2-D Slots.

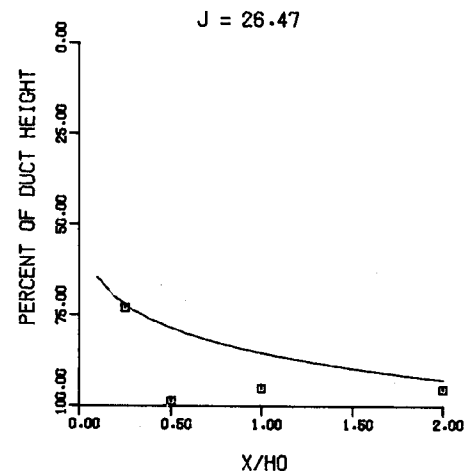


**Figure 94.** Predicted and Measured Velocity Trajectories for the Remaining Test Cases in Phase II.

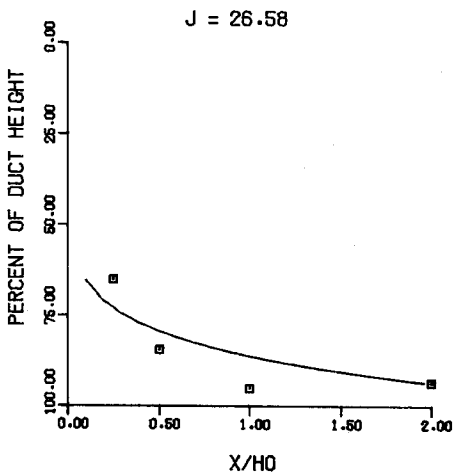
TEST NO 1, ONE-SIDED JET, PHASE III  
STREAMLINED SLOTS, AJ/AM=.098



TEST NO 2, ONE-SIDED JET, PHASE III  
STREAMLINED SLOTS, AJ/AM=.098



TEST NO 3, ONE-SIDED JET - PHASE III  
BLUFF SLOTS , AJ/AM=0.098



TEST NO 4, ONE-SIDED JET - PHASE III  
BLUFF SLOTS , AJ/AM=0.098

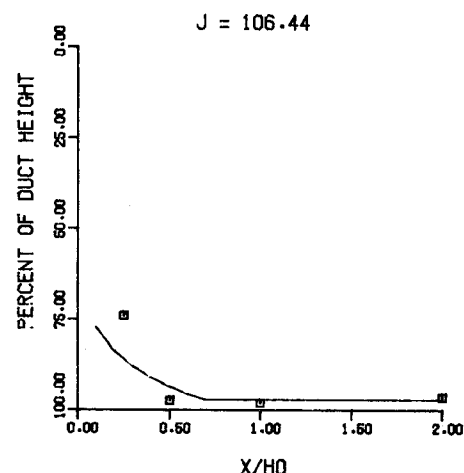


Figure 95. Predicted and Measured Velocity Trajectories for Streamlined and Bluff Slots (Equivalent Site and Spacing to Orifice Plate 01/02/04).

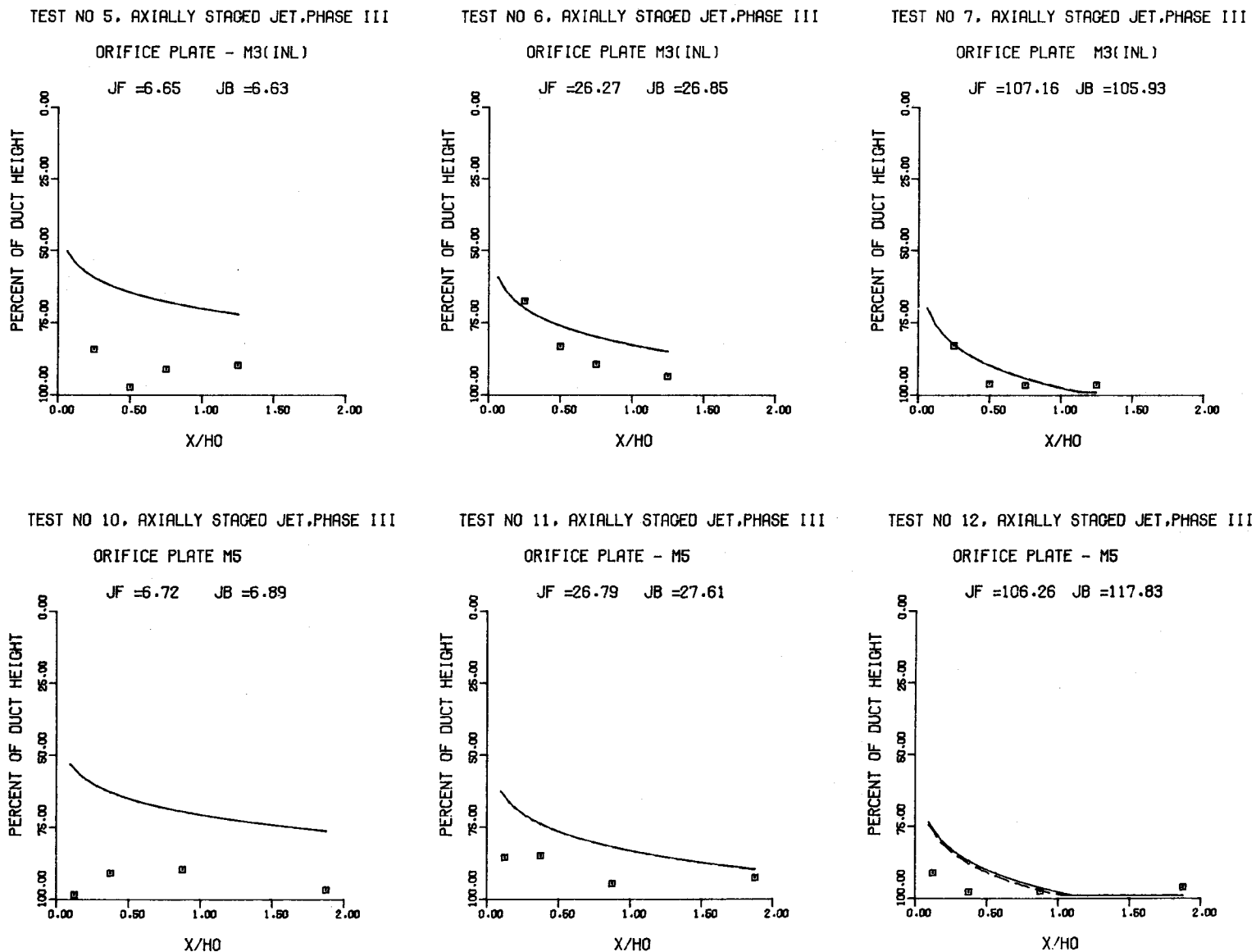
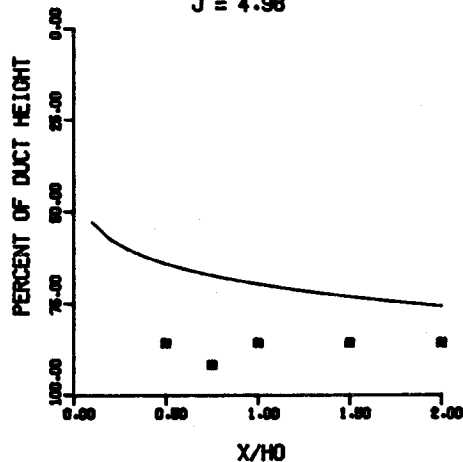


Figure 96. Predicted and Measured Velocity Trajectories for Double Row of Jets (Plate M-3 and M-5).

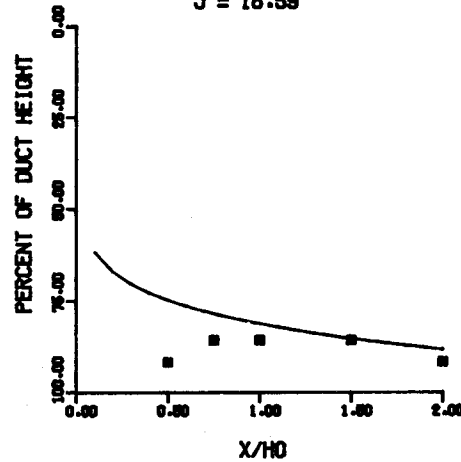
TEST NO 1. SINGLE SIDED ROW OF JETS  
ORIFICE PLATE 01/02/04

$J = 4.98$



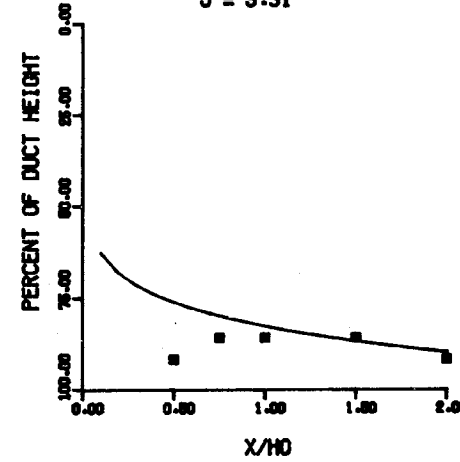
TEST NO 2. SINGLE SIDED ROW OF JETS  
ORIFICE PLATE 01/02/04

$J = 18.59$



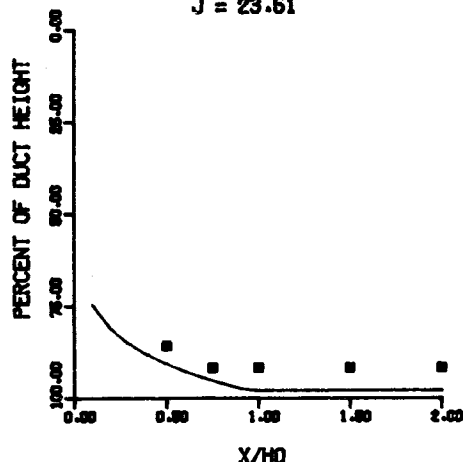
TEST NO 3. SINGLE SIDED ROW OF JETS  
ORIFICE PLATE 01/04/04

$J = 5.31$



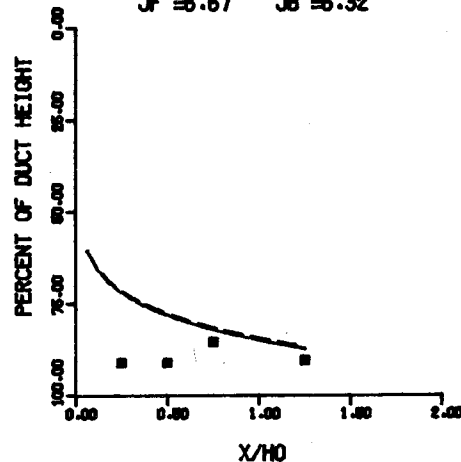
TEST NO 4. SINGLE SIDED ROW OF JETS  
ORIFICE PLATE 01/04/04

$J = 23.51$



TEST NO 5. AXIALLY STAGED STAGGERED JETS  
ORIFICE PLATE - M-4

$J_F = 6.67 \quad J_B = 6.32$



TEST NO 6. AXIALLY STAGED STAGGERED JETS  
ORIFICE PLATE - M-4

$J_F = 26.78 \quad J_B = 26.69$

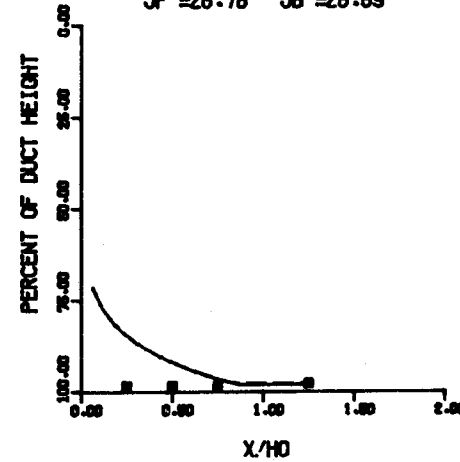


Figure 97. Comparison of Predicted and Measured Velocity Trajectories for Plate 01/02/04, Plate M-4, and Equivalent Single Row of Jet Configurations.

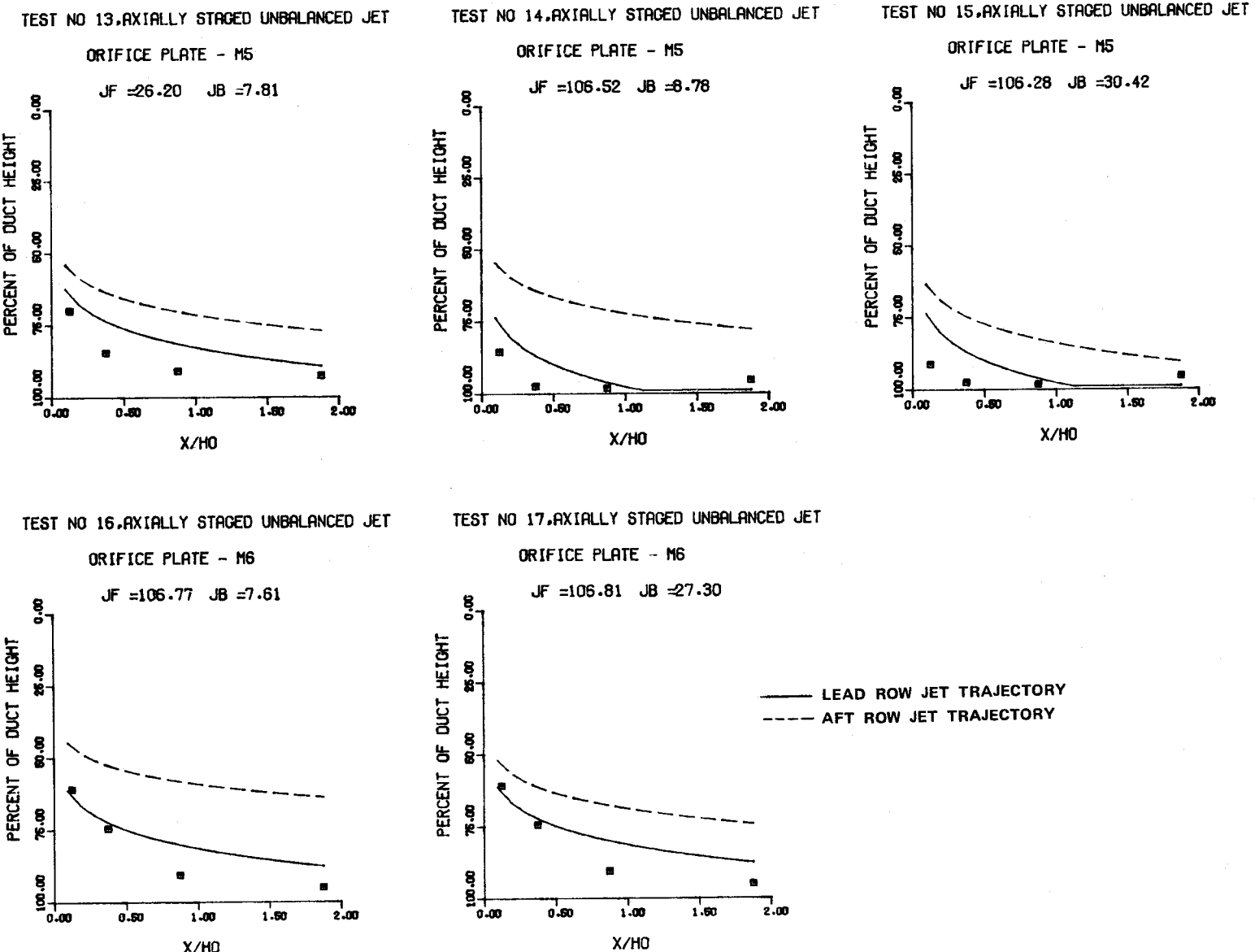
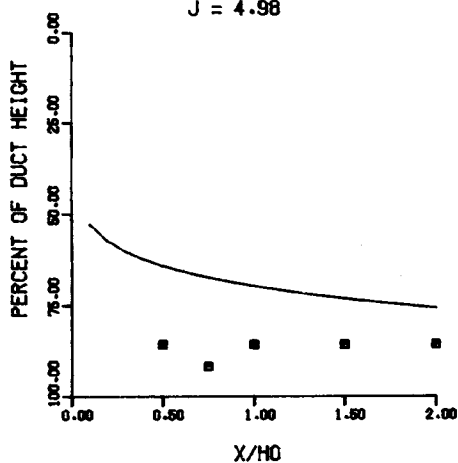
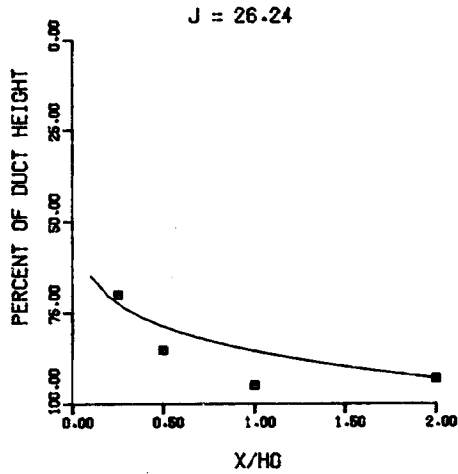


Figure 98. Predicted and Measured Velocity Trajectories for Double Row of Jets with Unequal Momentum Flux Ratios.

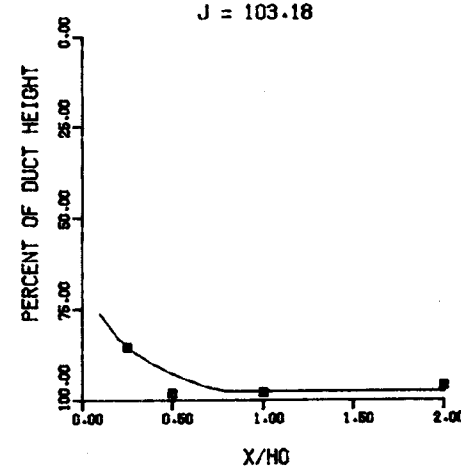
TEST NO 1, ONE-SIDED JET, PHASE I  
ORIFICE PLATE 01/02/04



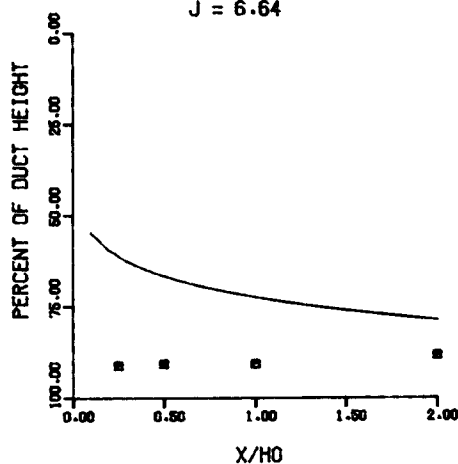
TEST NO 21, ONE-SIDED JET, PHASE III  
ORIFICE PLATE 01/02/04



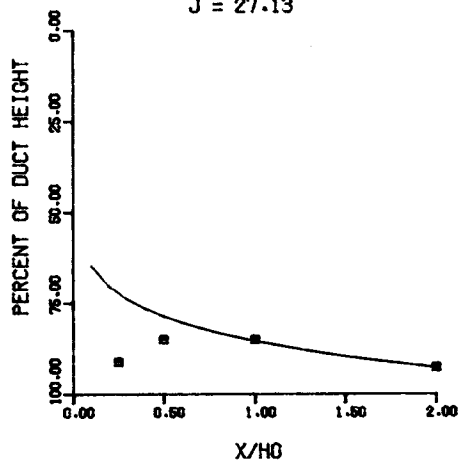
TEST NO 22, ONE-SIDED JET, PHASE III  
ORIFICE PLATE 01/02/04



TEST NO 18, ONE-SIDED JET, PHASE III  
45 DEG SLOTS, RJ/AM=.098



TEST NO 19, ONE-SIDED JET, PHASE III  
45 DEG SLOTS, RJ/AM=.098



TEST NO 20, ONE-SIDED JET - PHASE III  
45 DEG SLOTS , RJ/AM=0.098

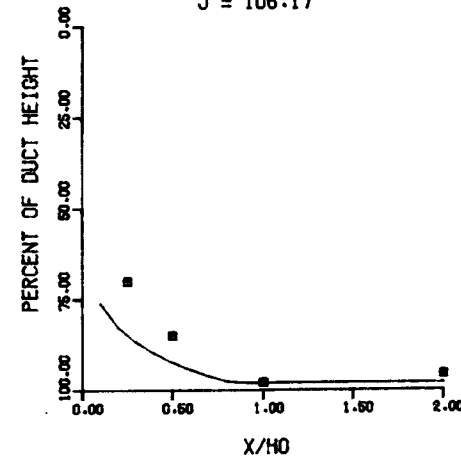


Figure 99. Comparison of Predicted and Measured Velocity Trajectories for 45-degree Slot and Equivalent Circular Holes.



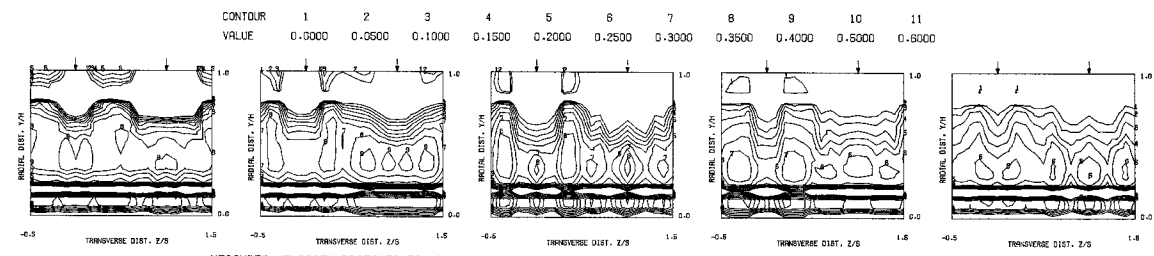
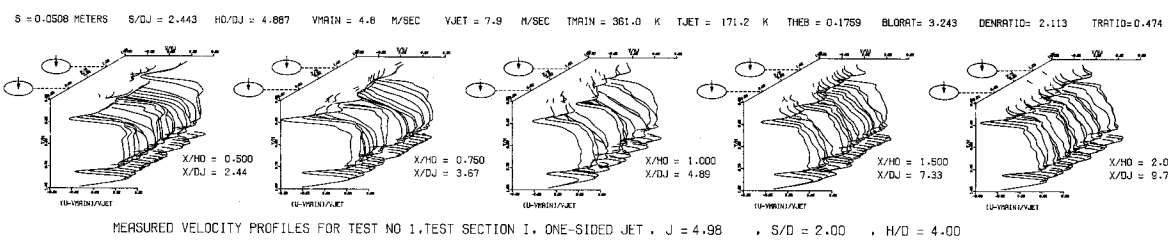


Figure 100. Measured Velocity Distributions for Test No. 1 of DJM Phase I Testing.

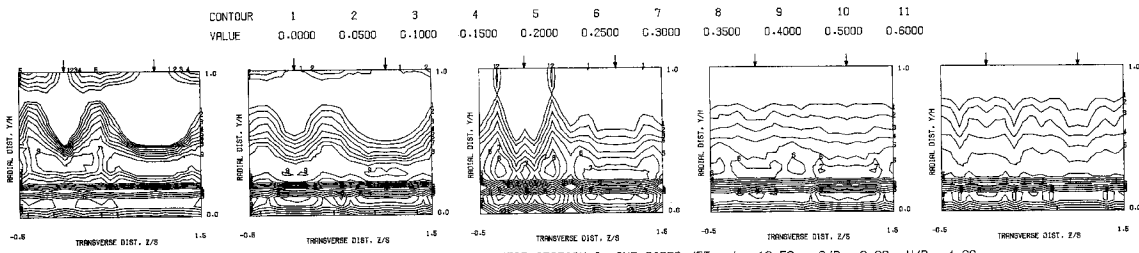
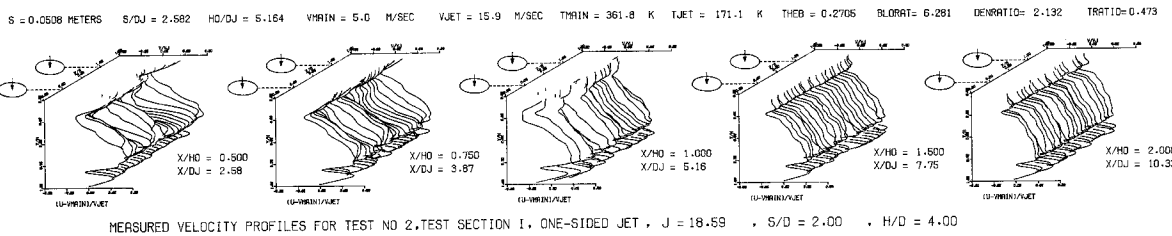
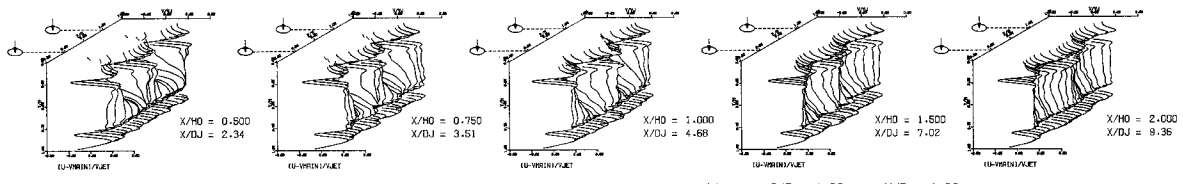
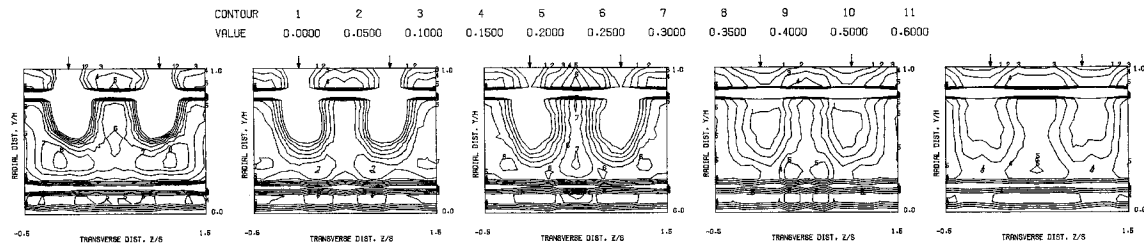


Figure 101. Measured Velocity Distributions for Test No. 2 of DJM Phase I Testing.

$S = 0.1016$  METERS    $S/D_J = 4.682$     $H_0/D_J = 4.682$     $V_{MAIN} = 4.6$  M/SEC    $V_{JET} = 7.9$  M/SEC    $T_{MAIN} = 360.7$  K    $T_{JET} = 170.5$  K    $\theta_{HEB} = 0.1074$     $\theta_{BLURAT} = 3.356$     $\theta_{ENRATIO} = 2.122$     $\theta_{TRATID} = 0.473$



MEASURED VELOCITY PROFILES FOR TEST NO 3, TEST SECTION I, ONE-SIDED JET,  $J = 5.31$     $S/D = 4.00$ ,  $H/D = 4.00$



MEASURED VELOCITY PROFILES FOR TEST NO 3, TEST SECTION I, ONE-SIDED JET,  $J = 5.31$     $S/D = 4.00$ ,  $H/D = 4.00$

Figure 102. Measured Velocity Distributions for Test No. 3 of DJM Phase I Testing.

$S = 0.1016$  METERS    $S/D_J = 4.869$     $H/D_J = 4.869$     $V_{MAIN} = 4.5$  M/SEC    $V_{JET} = 16.9$  M/SEC    $T_{MAIN} = 361.6$  K    $T_{JET} = 168.9$  K    $\Theta_{E8} = 0.1915$     $BLO RAT = 7.148$     $DEN RATIO = 2.174$     $TRATIO = 0.467$

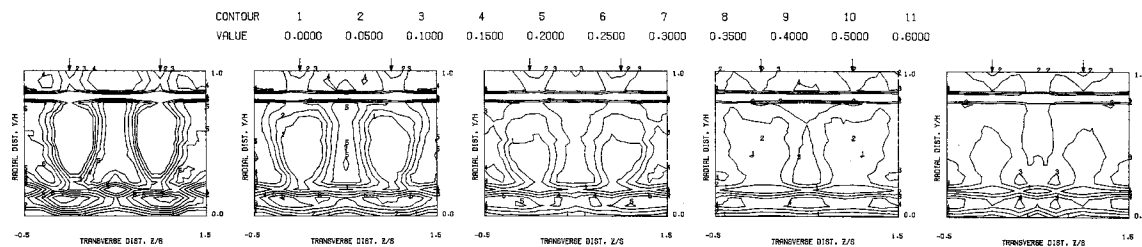
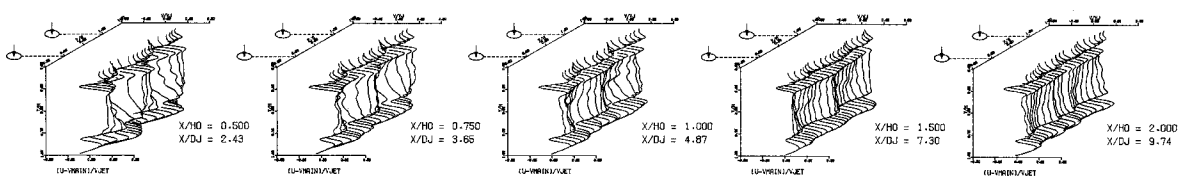
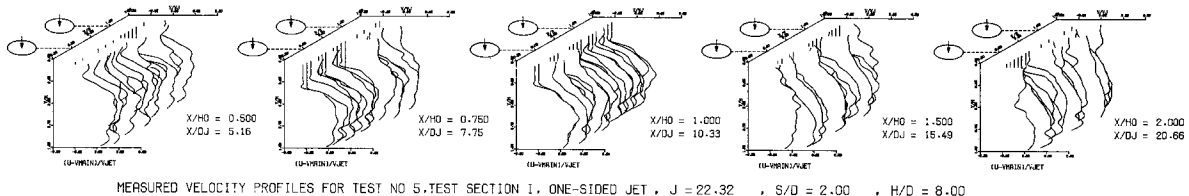


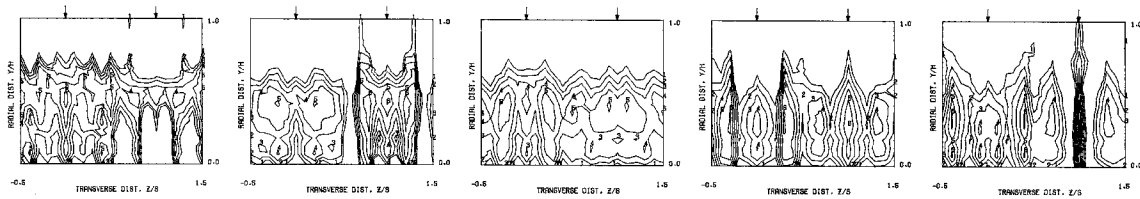
Figure 103. Measured Velocity Distributions for Test No. 4 of DJM Phase I Testing.

$S = 0.0254$  METERS    $S/DJ = 2.582$     $H0/DJ = 10.328$     $VHMIN = 4.6$  M/SEC    $VJET = 16.8$  M/SEC    $THIN = 350.4$  K    $TJET = 171.3$  K    $THEB = 0.1687$     $BLURAT = 6.690$     $DENRATIO = 2.128$     $TRATIO = 0.475$



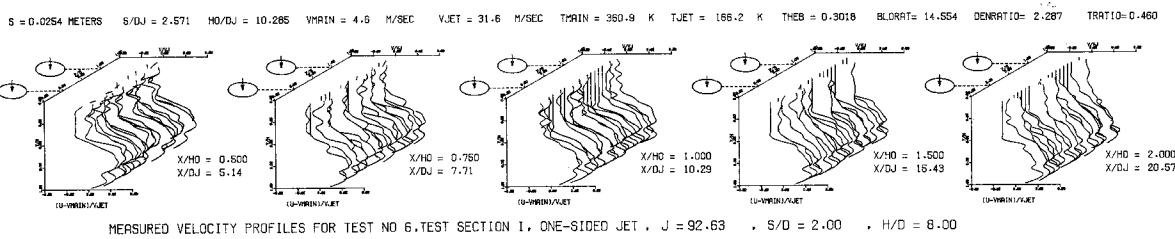
MEASURED VELOCITY PROFILES FOR TEST NO 5, TEST SECTION I, ONE-SIDED JET,  $J = 22.32$ ,  $S/D = 2.00$ ,  $H/D = 8.00$

CONTOUR	1	2	3	4	5	6	7	8	9	10	11
VALUE	0.0000	0.0500	0.1000	0.1500	0.2000	0.2500	0.3000	0.3500	0.4000	0.5000	0.6000

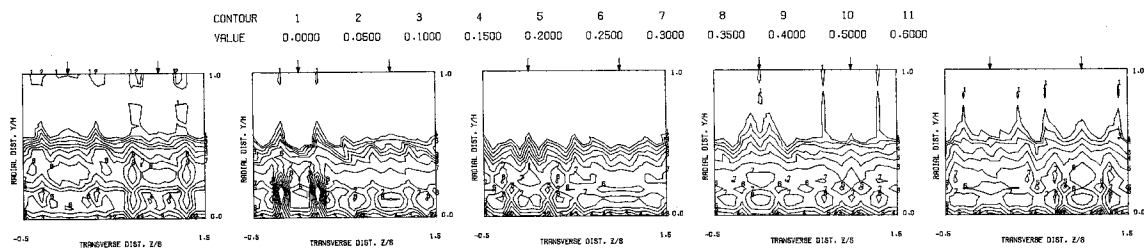


MEASURED VELOCITY PROFILES FOR TEST NO 5, TEST SECTION I, ONE-SIDED JET,  $J = 22.32$ ,  $S/D = 2.00$ ,  $H/D = 8.00$

Figure 104. Measured Velocity  
Distributions for Test No. 5 of DJM Phase I  
Testing.



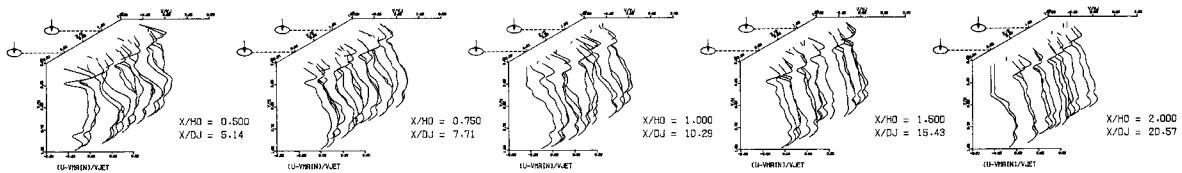
MEASURED VELOCITY PROFILES FOR TEST NO. 6, TEST SECTION I, ONE-SIDED JET,  $J = 92.63$ ,  $S/D = 2.00$ ,  $H/D = 8.00$



MEASURED VELOCITY PROFILES FOR TEST NO. 6, TEST SECTION I, ONE-SIDED JET,  $J = 92.63$ ,  $S/D = 2.00$ ,  $H/D = 8.00$

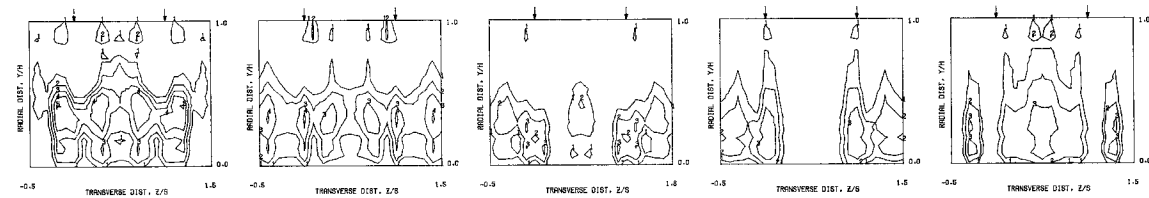
Figure 105. Measured Velocity Distributions for Test No. 6 of DJM Phase I Testing.

S = 0.0508 METERS S/D = 5.143 H/D/J = 10.285 V<sub>MAIN</sub> = 4.6 M/SEC V<sub>JET</sub> = 16.1 M/SEC T<sub>MAIN</sub> = 361.9 K T<sub>JET</sub> = 167.8 K THEB = 0.1048 BLORAT = 7.127 DENRATIO = 2.182 TRATIO = 0.464



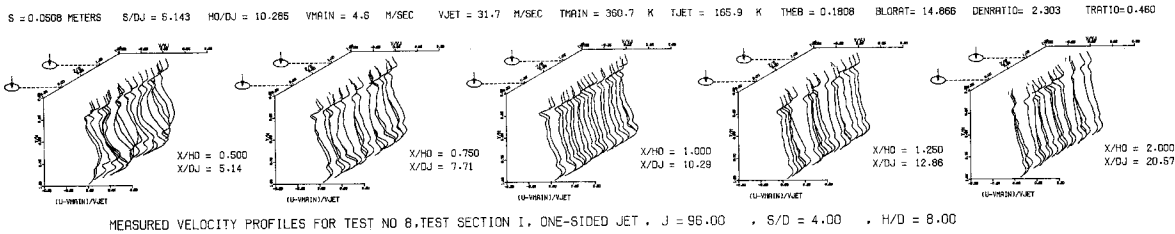
MEASURED VELOCITY PROFILES FOR TEST NO 7, TEST SECTION I, ONE-SIDED JET,  $J = 28.37$ ,  $S/D = 4.00$ ,  $H/D = 8.00$

CONTOUR VALUE	1	2	3	4	5	6	7	8	9	10	11
0.0000	0.0000	0.0500	0.1000	0.1500	0.2000	0.2500	0.3000	0.3500	0.4000	0.5000	0.6000

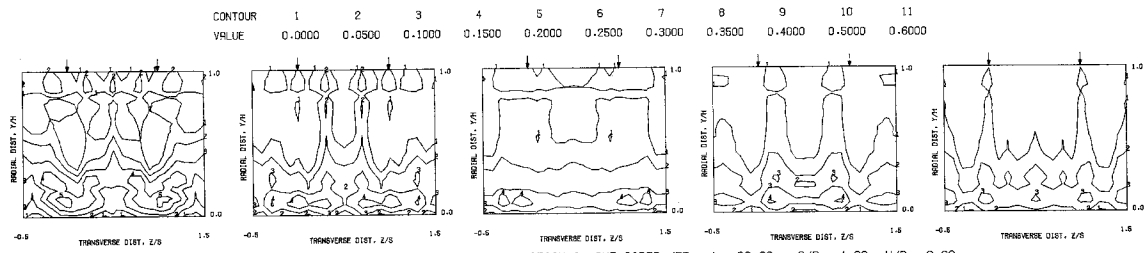


MEASURED VELOCITY PROFILES FOR TEST NO 7, TEST SECTION I, ONE-SIDED JET,  $J = 28.37$ ,  $S/D = 4.00$ ,  $H/D = 8.00$

Figure 106. Measured Velocity Distributions for Test No. 7 of DJM Phase I Testing.



MEASURED VELOCITY PROFILES FOR TEST NO 8, TEST SECTION I, ONE-SIDED JET,  $J = 96.00$ ,  $S/D = 4.00$ ,  $H/D = 8.00$



MEASURED VELOCITY PROFILES FOR TEST NO 8, TEST SECTION I, ONE-SIDED JET,  $J = 96.00$ ,  $S/D = 4.00$ ,  $H/D = 8.00$

Figure 107. Measured Velocity Distributions for Test No. 8 of DJM Phase I Testing.

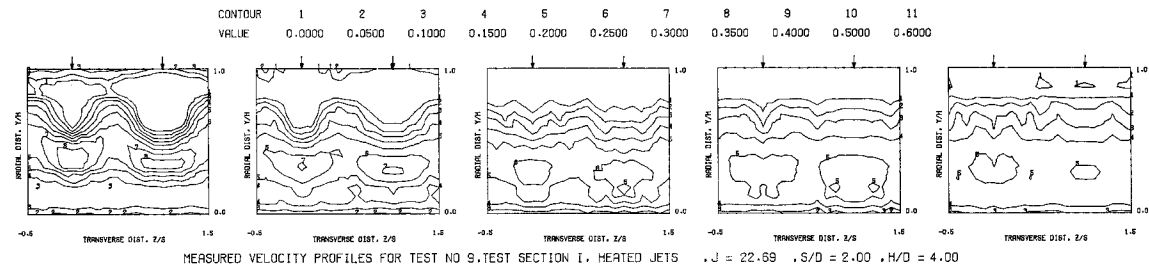
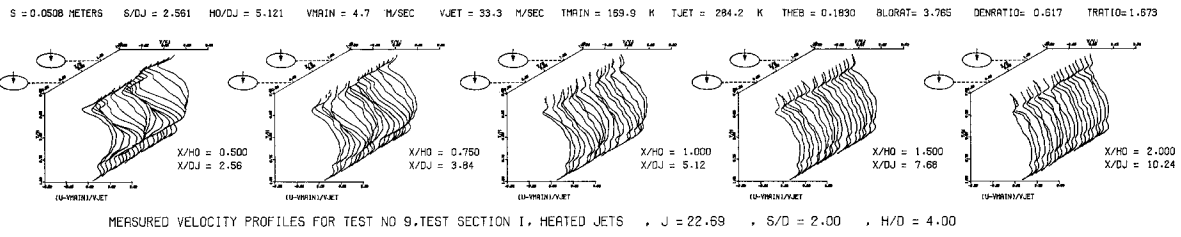
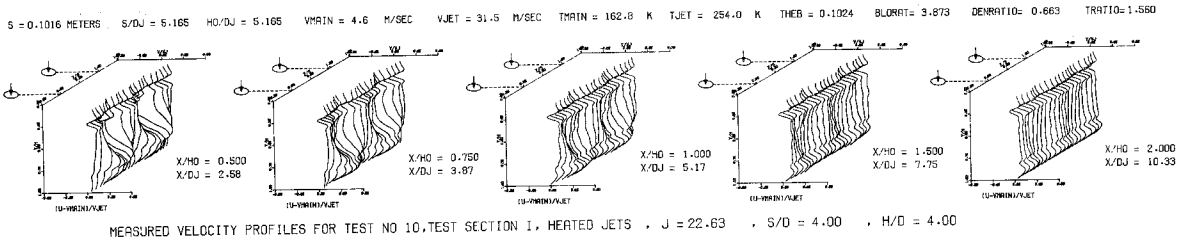


Figure 108. Measured Velocity Distributions for Test No. 9 of DJM Phase I Testing.



MEASURED VELOCITY PROFILES FOR TEST NO 10, TEST SECTION I, HEATED JETS ,  $J = 22.63$  ,  $S/D = 4.00$  ,  $H/D = 4.00$

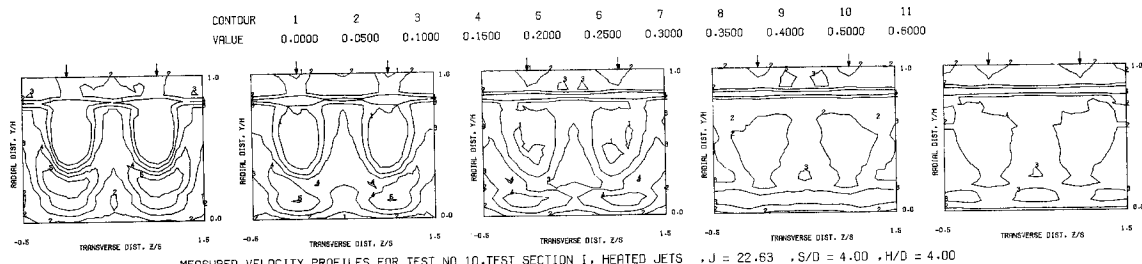


Figure 109. Measured Velocity Distributions for Test No. 10 of DJM Phase I Testing.

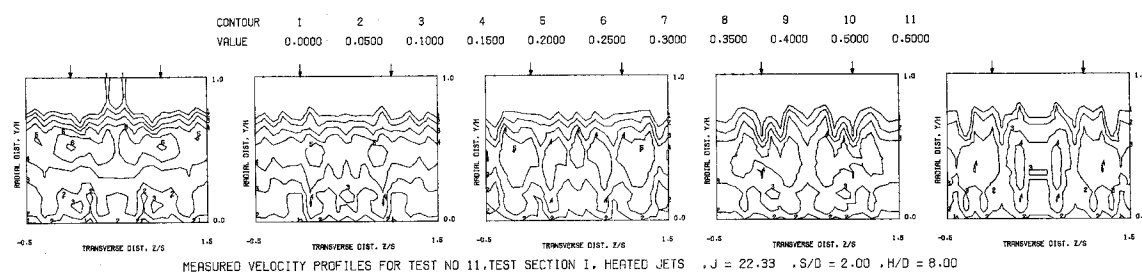
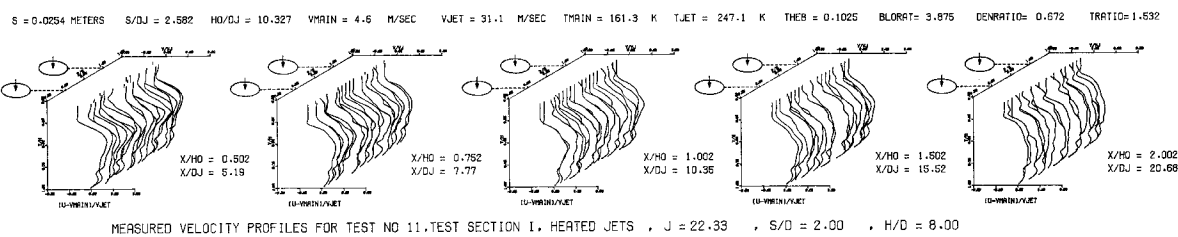


Figure 11c. Measured Velocity Distributions for Test No. 11 of DJM Phase I Testing.

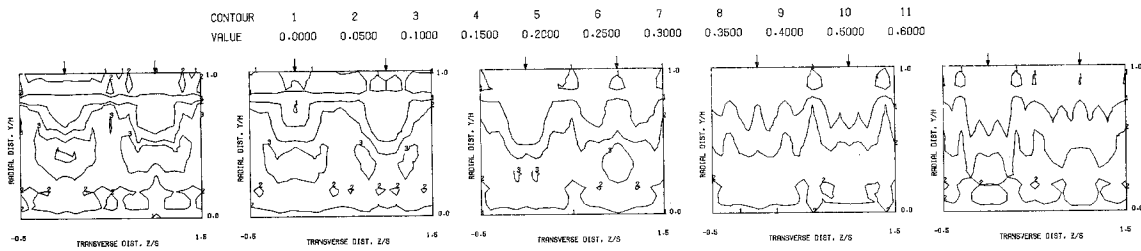
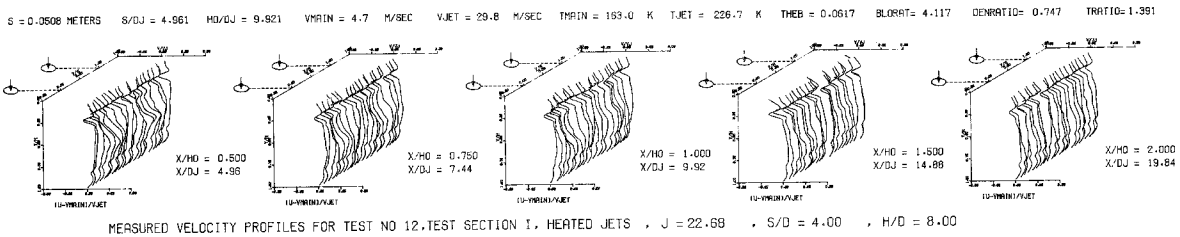
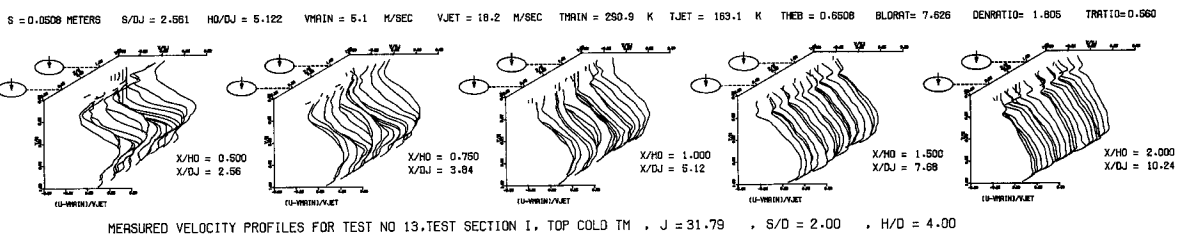


Figure 111. Measured Velocity Distributions for Test No. 12 of DJM Phase I Testing.



MEASURED VELOCITY PROFILES FOR TEST NO 13, TEST SECTION I, TOP COLD TM ,  $J = 31.79$  ,  $S/D = 2.00$  ,  $H/D = 4.00$

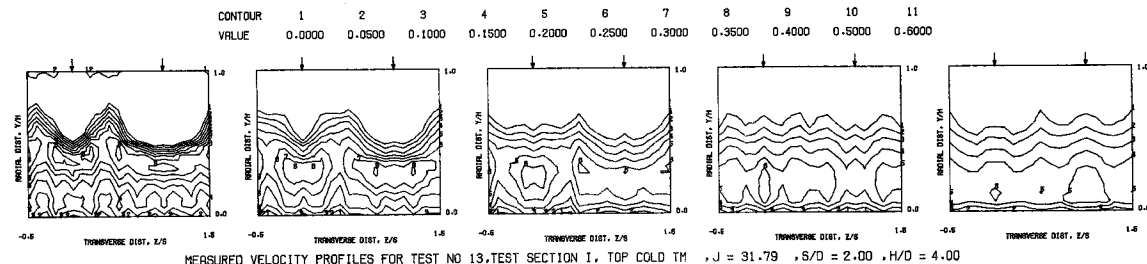


Figure 112. Measured Velocity Distributions for Test No. 13 of DJM Phase I Testing.

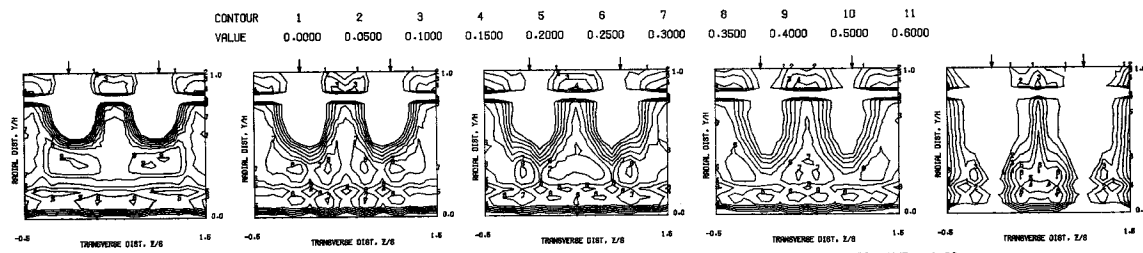
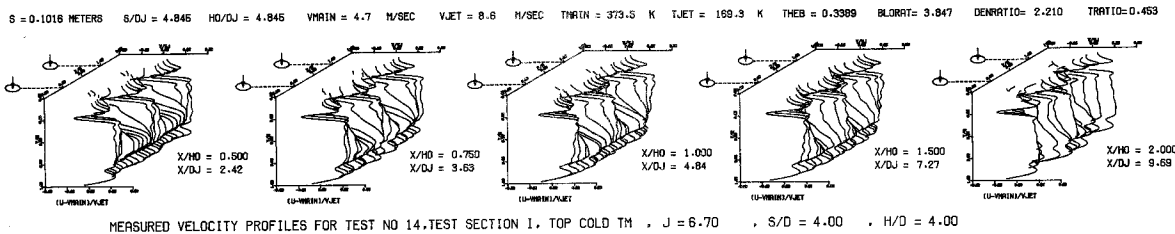
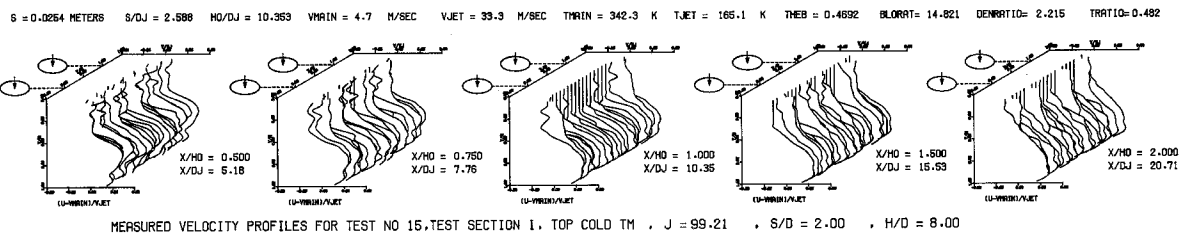
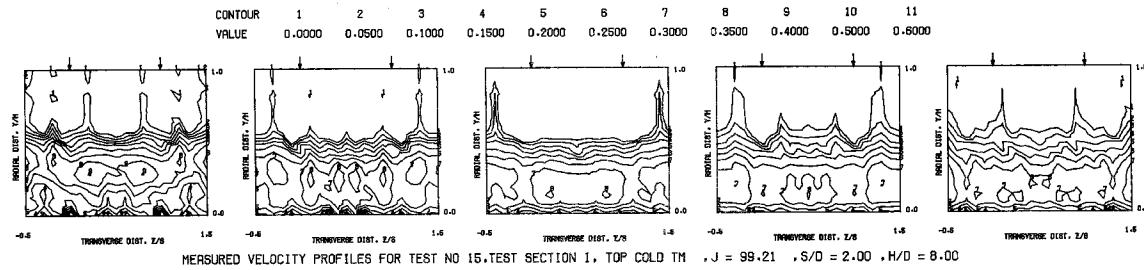


Figure 113. Measured Velocity Distributions for Test No. 14 of DJM Phase I Testing.



MEASURED VELOCITY PROFILES FOR TEST NO 15, TEST SECTION I, TOP COLD TM ,  $J = 99.21$  ,  $S/D = 2.00$  ,  $H/D = 8.00$



MEASURED VELOCITY PROFILES FOR TEST NO 15, TEST SECTION I, TOP COLD TM ,  $J = 99.21$  ,  $S/D = 2.00$  ,  $H/D = 8.00$

Figure 114. Measured Velocity Distributions for Test No. 15 of DJM Phase I Testing.

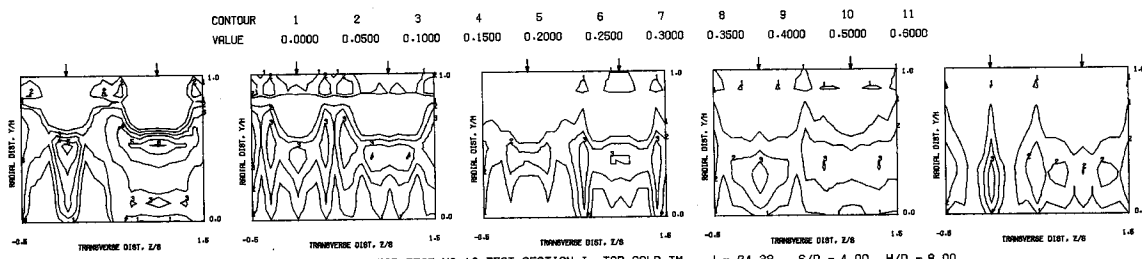
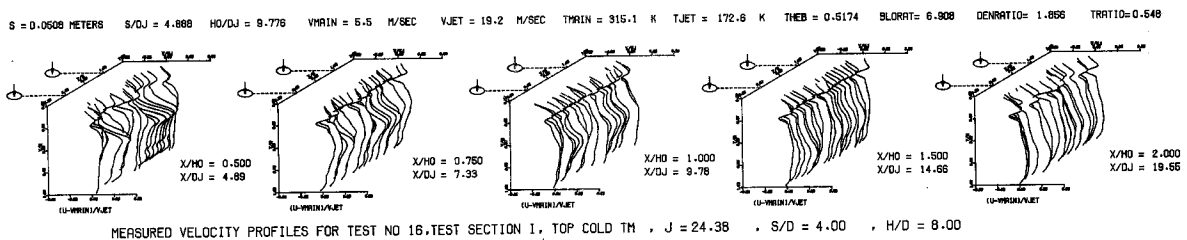
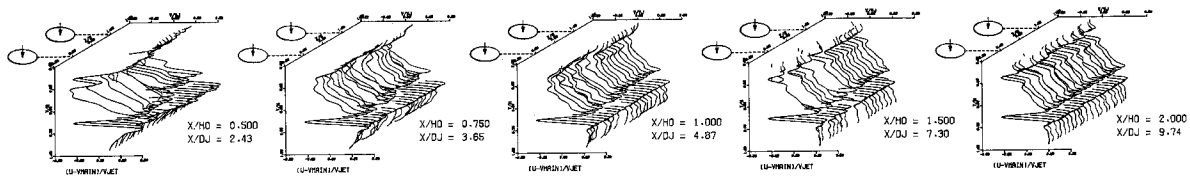


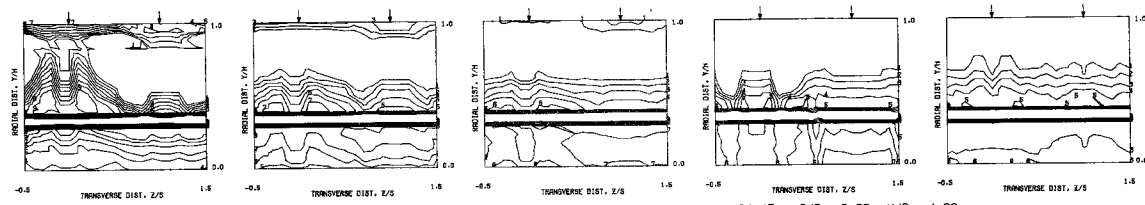
Figure 115. Measured Velocity Distributions for Test No. 16 of DJM Phase I Testing.

$S = 0.0508$  METERS    $S/DJ = 2.434$     $H/DJ = 4.069$     $V_{MIN} = 5.0$  M/SEC    $V_{JET} = 17.7$  M/SEC    $T_{MIN} = 299.0$  K    $T_{JET} = 168.5$  K    $\Theta_{HEB} = 0.6001$     $BLRAT = 5.629$     $DENRATIO = 1.798$     $TRATIO = 0.564$



MESURED VELOCITY PROFILES FOR TEST NO 17-TEST SECTION I, TOP HOT TM , J = 24.45 , S/D = 2.00 , H/D = 4.00

CONTOUR	1	2	3	4	5	6	7	8	9	10	11
VALUE	0.0000	0.0500	0.1000	0.1500	0.2000	0.2500	0.3000	0.3500	0.4000	0.5000	0.6000



MESURED VELOCITY PROFILES FOR TEST NO 17-TEST SECTION I, TOP HOT TM , J = 24.45 , S/D = 2.00 , H/D = 4.00

Figure 116. Measured Velocity Distributions for Test No. 17 of DJM Phase I Testing.

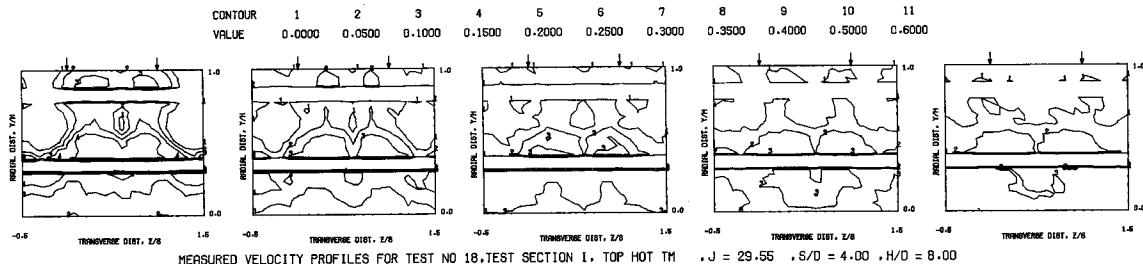
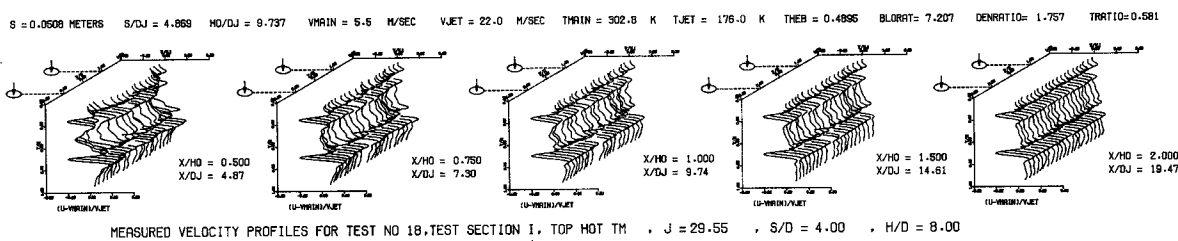
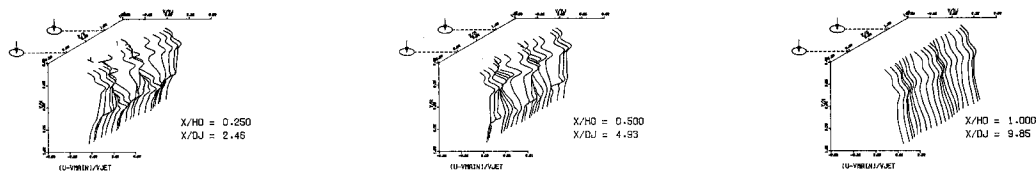


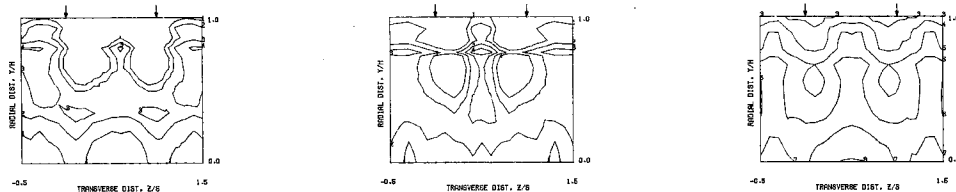
Figure 117. Measured Velocity Distributions for Test No. 18 of DJM Phase I Testing.

$S = 0.0508$  METERS    $S/DJ = 4.925$     $H/DJ = 9.851$     $V_{MAIN} = 5.2$  M/SEC    $V_{JET} = 16.4$  M/SEC    $T_{MAIN} = 358.6$  K    $T_{JET} = 173.5$  K    $\theta_{HEB} = 0.0972$     $BLOOM = 6.653$     $DENRATIO = 2.102$     $TRATIO = 0.484$



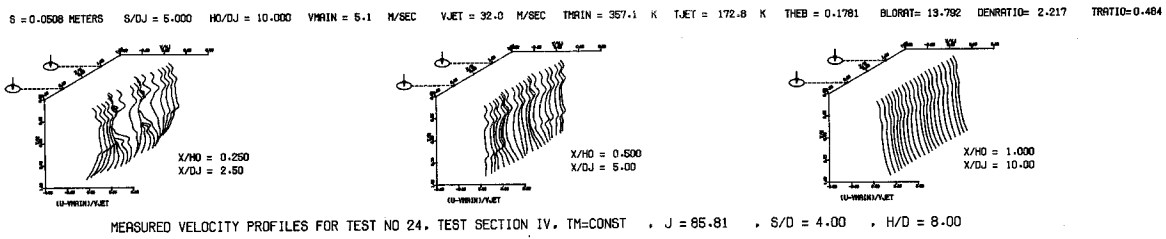
MEASURED VELOCITY PROFILES FOR TEST NO 23, TEST SECTION IV, TM=CONST    $J = 21.05$     $S/D = 4.00$     $H/D = 8.00$

CONTOUR	1	2	3	4	5	6	7	8	9	10	11
VALUE	0.0000	0.0500	0.1000	0.1500	0.2000	0.2500	0.3000	0.3500	0.4000	0.5000	0.6000

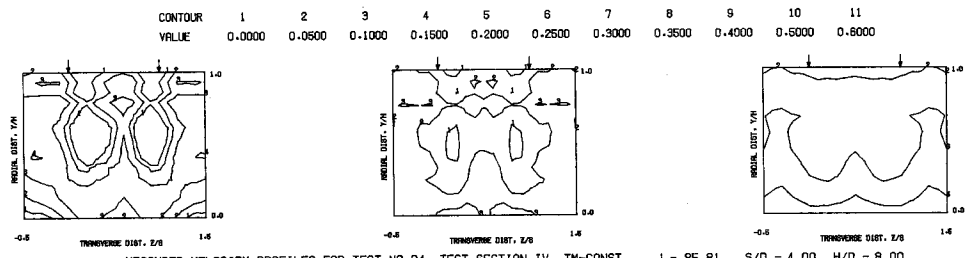


MEASURED VELOCITY PROFILES FOR TEST NO 23, TEST SECTION IV, TM=CONST    $J = 21.05$     $S/D = 4.00$     $H/D = 8.00$

Figure 118. Measured Velocity Distributions for Test No. 23 of DJM Phase I Testing.



MEASURED VELOCITY PROFILES FOR TEST NO 24, TEST SECTION IV, TM=CONST ,  $J = 85.81$  ,  $S/D = 4.00$  ,  $H/D = 8.00$



MEASURED VELOCITY PROFILES FOR TEST NO 24, TEST SECTION IV, TM=CONST ,  $J = 85.81$  ,  $S/D = 4.00$  ,  $H/D = 8.00$

Figure 119. Measured Velocity Distributions for Test No. 24 of DJM Phase I Testing.

$S = 0.0508$  METERS    $S/DJ = 2.538$     $H/DJ = 5.075$     $V_{MAIN} = 4.6$  M/SEC    $V_{JET} = 8.4$  M/SEC    $T_{MAIN} = 367.4$  K    $T_{JET} = 178.7$  K    $\dot{W}_{HEB} = 0.1830$     $B/LRAT = 3.672$     $DENRATIO = 2.003$     $TRATIO = 0.600$

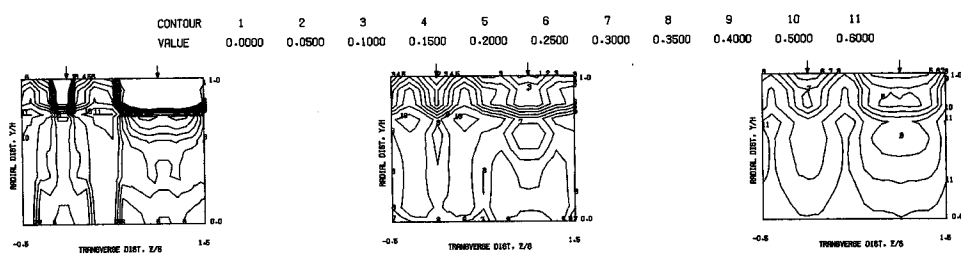
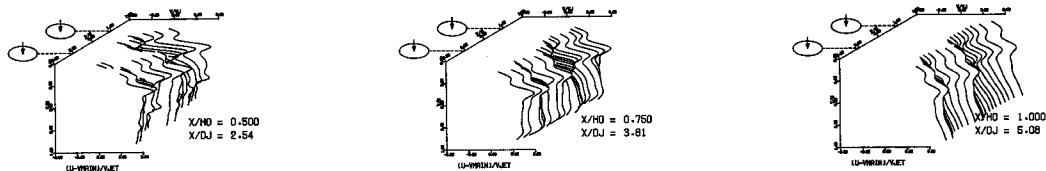
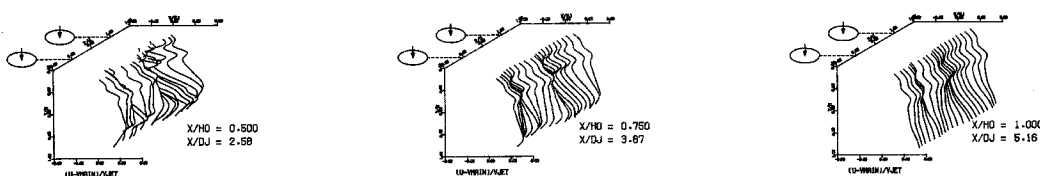


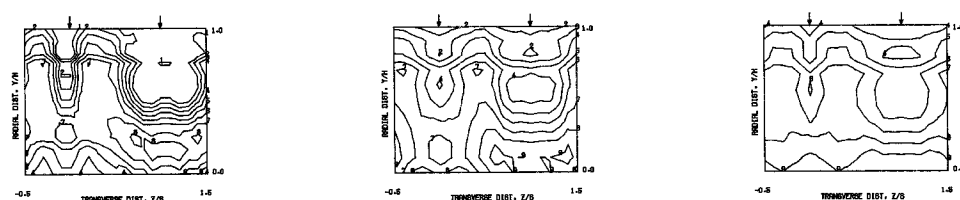
Figure 120. Measured Velocity Distributions for Test No. 25 of DJM Phase I Testing.

S = 0.0508 METERS    S/DJ = 2.592    H0/DJ = 5.164    VMAIN = 4.5 M/SEC    VJET = 16.6 M/SEC    TMIN = 356.9 K    TJET = 189.2 K    THEB = 0.2988    BLURR = 7.233    DENRATIO= 1.956    TRATIO=0.516



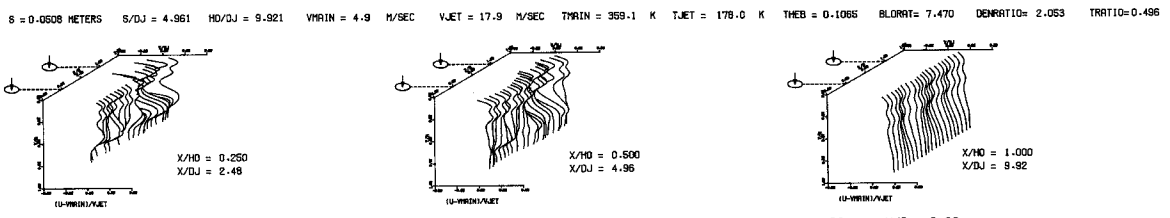
MEASURED VELOCITY PROFILES FOR TEST NO 26, TEST SECTION IV, TM=CONST , J = 26.73 , S/D = 2.00 , H/D = 4.00

CONTOUR	1	2	3	4	5	6	7	8	9	10	11
VALUE	0.0000	0.0500	0.1000	0.1500	0.2000	0.2500	0.3000	0.3500	0.4000	0.5000	0.6000

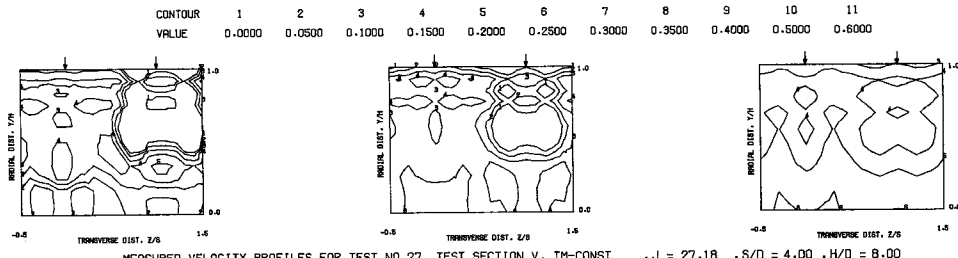


MEASURED VELOCITY PROFILES FOR TEST NO 26, TEST SECTION IV, TM=CONST , J = 26.73 , S/D = 2.00 , H/D = 4.00

Figure 121. Measured Velocity Distributions for Test No. 26 of DJM Phase I Testing.



MEASURED VELOCITY PROFILES FOR TEST NO 27, TEST SECTION V, TM=CONST    $J = 27.18$     $S/D = 4.00$     $H/D = 8.00$



MEASURED VELOCITY PROFILES FOR TEST NO 27, TEST SECTION V, TM=CONST    $J = 27.18$     $S/D = 4.00$     $H/D = 8.00$

Figure 122. Measured Velocity Distributions for Test No. 27 of DJM Phase I Testing.

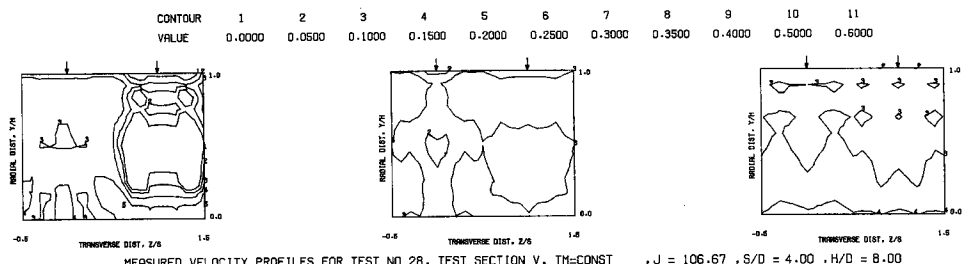
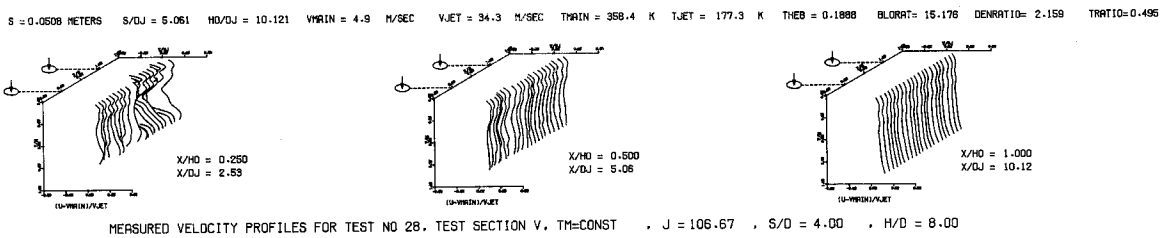
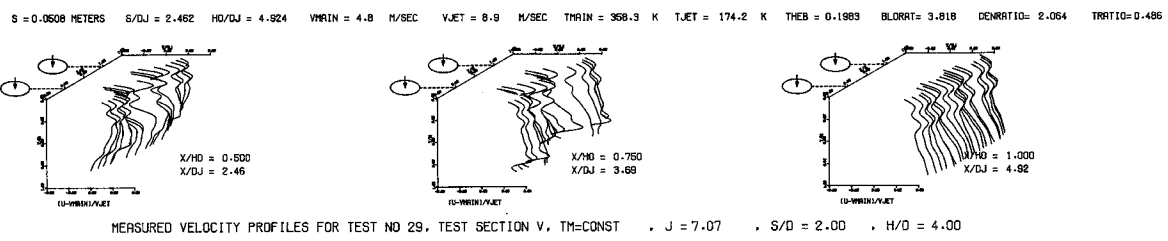
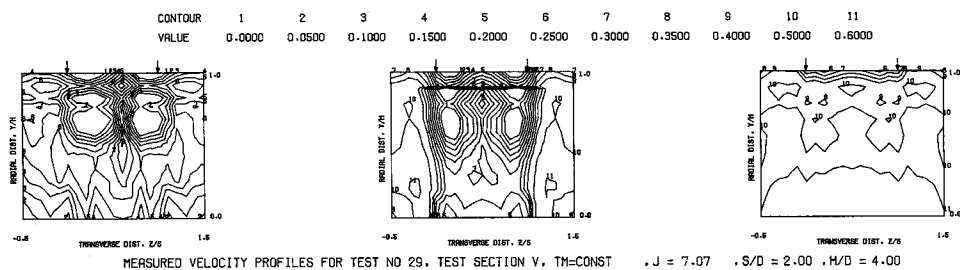


Figure 123. Measured Velocity Distributions for Test No. 28 of DJM Phase I Testing.



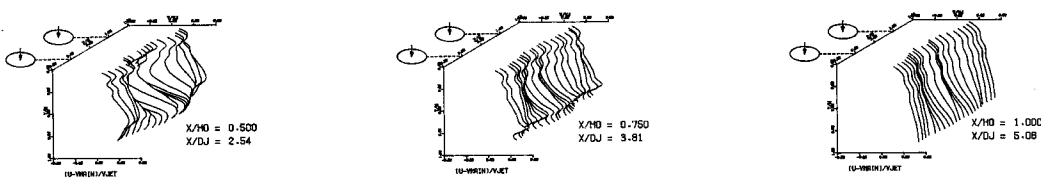
MEASURED VELOCITY PROFILES FOR TEST NO 29, TEST SECTION V, TM=CONST    $J = 7.07$     $S/D = 2.00$ ,  $H/D = 4.00$



MEASURED VELOCITY PROFILES FOR TEST NO 29, TEST SECTION V, TM=CONST    $J = 7.07$     $S/D = 2.00$ ,  $H/D = 4.00$

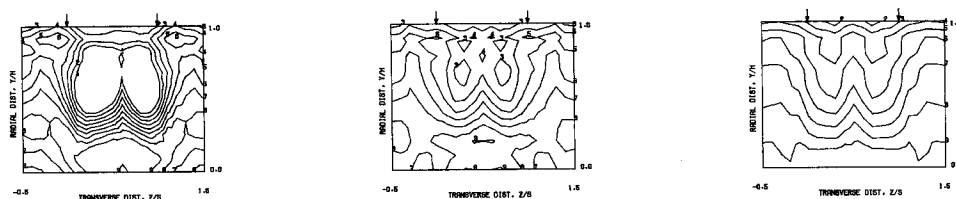
Figure 124. Measured Velocity Distributions for Test No. 29 of DJM Phase I Testing.

$S = 0.0508$  METERS    $S/DJ = 2.540$     $H/DJ = 5.080$     $V_{MIN} = 4.7$  M/SEC    $V_{JET} \approx 17.2$  M/SEC    $T_{MIN} = 358.7$  K    $T_{JET} = 174.3$  K    $\Theta_{EB} = 0.3148$     $B_{LORAT} = 7.549$     $DENRATIO = 2.087$     $TRATIO = 0.486$



MEASURED VELOCITY PROFILES FOR TEST NO 30, TEST SECTION V,  $T_M = \text{CONST}$     $J = 27.31$     $S/D = 2.00$     $H/D = 4.00$

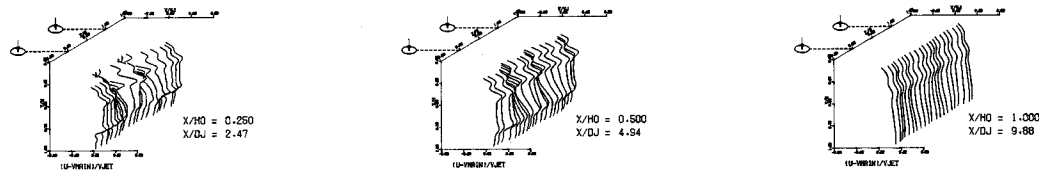
CONTOUR VALUE	1	2	3	4	5	6	7	8	9	10	11
0.0000	0.0000	0.0500	0.1000	0.1500	0.2000	0.2500	0.3000	0.3500	0.4000	0.5000	0.6000



MEASURED VELOCITY PROFILES FOR TEST NO 30, TEST SECTION V,  $T_M = \text{CONST}$     $J = 27.31$     $S/D = 2.00$     $H/D = 4.00$

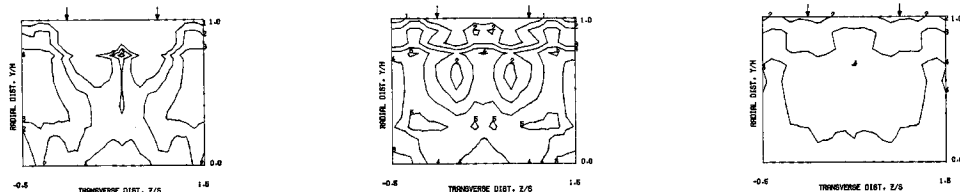
Figure 125. Measured Velocity Distributions for Test No. 30 of DJM Phase I Testing.

$S = 0.0508$  METERS    $S/D_J = 4.941$     $H/D_J = 9.883$     $V_{MAIN} = 5.0$  M/SEC    $V_{JET} = 17.9$  M/SEC    $T_{MAIN} = 360.7$  K    $T_{JET} = 177.5$  K    $\rho_{HEB} = 0.1066$     $\rho_{LORAT} = 7.421$     $\rho_{NRRATIO} = 2.072$     $\rho_{TRATIO} = 0.492$



MEASURED VELOCITY PROFILES FOR TEST NO 31, TEST SECTION VI.  $T_M = \text{CONST}$  ,  $J = 26.58$  ,  $S/D = 4.00$  ,  $H/D = 8.00$

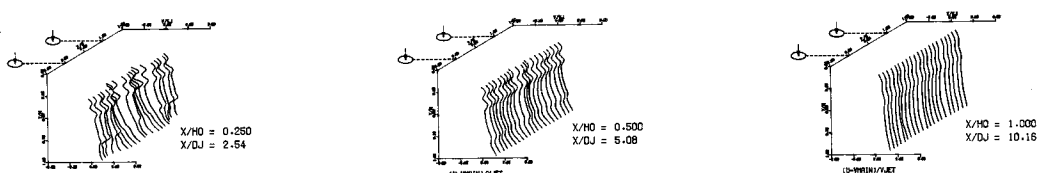
CONTOUR	1	2	3	4	5	6	7	8	9	10	11
VALUE	0.0000	0.0500	0.1000	0.1500	0.2000	0.2500	0.3000	0.3500	0.4000	0.5000	0.6000



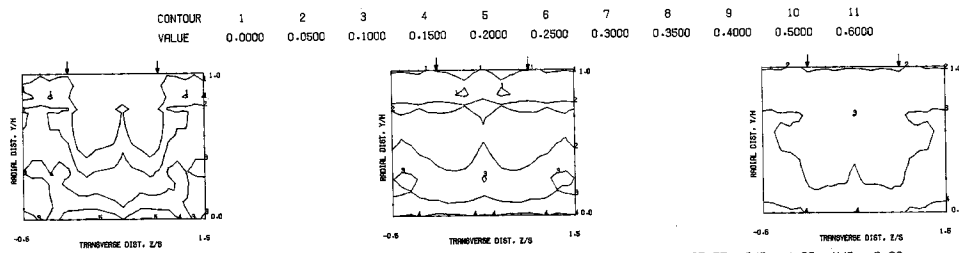
MEASURED VELOCITY PROFILES FOR TEST NO 31, TEST SECTION VI.  $T_M = \text{CONST}$  ,  $J = 26.58$  ,  $S/D = 4.00$  ,  $H/D = 8.00$

Figure 126. Measured Velocity Distributions for Test No. 31 of DJM Phase I Testing.

$S = 0.0508$  METERS    $S/DJ = 5.081$     $H/DJ = 10.163$     $V_{MAIN} = 5.0$  M/SEC    $V_{JET} = 35.4$  M/SEC    $T_{MAIN} = 359.4$  K    $T_{JET} = 176.4$  K    $\rho_{HEB} = 0.1887$     $BLO RAT = 15.297$     $DEN RATIO = 2.176$     $TRATIO = 0.496$

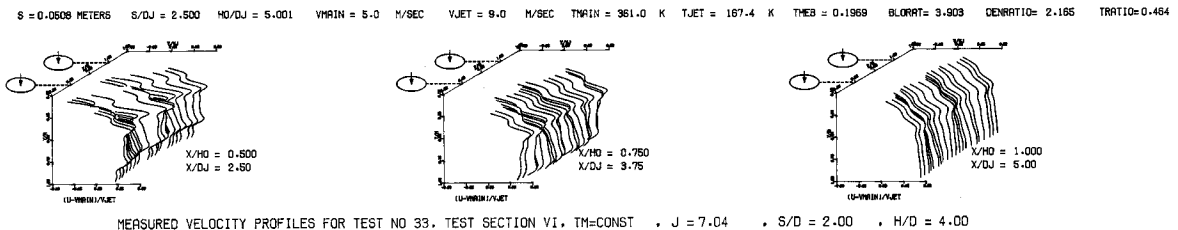


MEASURED VELOCITY PROFILES FOR TEST NO 32, TEST SECTION VI. TM=CONST ,  $J = 107.57$  ,  $S/D = 4.00$  ,  $H/D = 8.00$

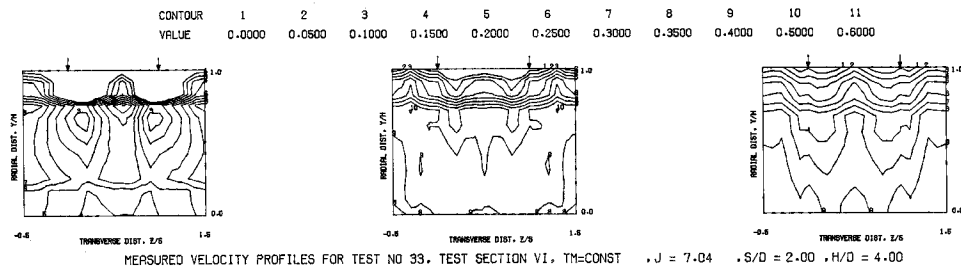


MEASURED VELOCITY PROFILES FOR TEST NO 32, TEST SECTION VI. TM=CONST ,  $J = 107.57$  ,  $S/D = 4.00$  ,  $H/D = 8.00$

Figure 127. Measured Velocity Distributions for Test No. 32 of DJM Phase I Testing.



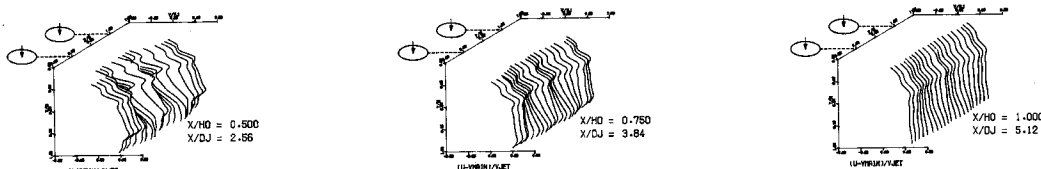
MEASURED VELOCITY PROFILES FOR TEST NO 33, TEST SECTION VI, TM=CONST    $\cdot$   $J = 7.04$     $\cdot$   $S/D = 2.00$     $\cdot$   $H/D = 4.00$



MEASURED VELOCITY PROFILES FOR TEST NO 33, TEST SECTION VI, TM=CONST    $\cdot$   $J = 7.04$     $\cdot$   $S/D = 2.00$     $\cdot$   $H/D = 4.00$

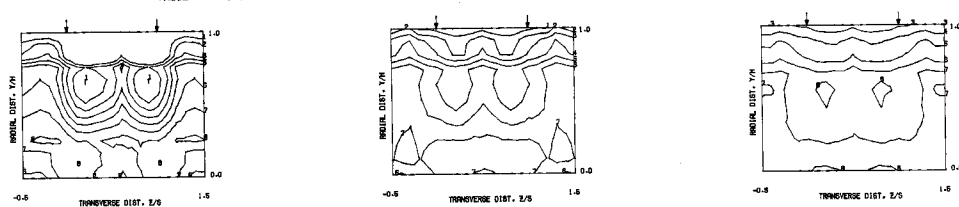
Figure 128. Measured Velocity Distributions for Test No. 33 of DJM Phase I Testing.

$S = 0.0508$  METERS    $S/D_J = 2.561$     $H_0/D_J = 5.122$     $V_{MIN} = 5.0$  M/SEC    $V_{JET} = 17.0$  M/SEC    $T_{MIN} = 361.6$  K    $T_{JET} = 164.9$  K    $\theta_{EB} = 0.3144$     $BLDRAT = 7.657$     $DENRATIO = 2.225$     $TRATIO = 0.456$



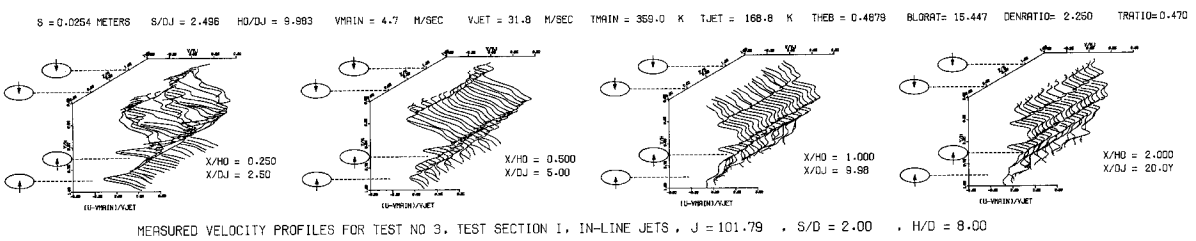
MEASURED VELOCITY PROFILES FOR TEST NO 34. TEST SECTION VI. TM=CONST . J = 26.36 , S/D = 2.00 , H/D = 4.00

CONTOUR VALUE	1	2	3	4	5	6	7	8	9	10	11
0.0000	0.0000	0.0500	0.1000	0.1500	0.2000	0.2500	0.3000	0.3500	0.4000	0.5000	0.6000

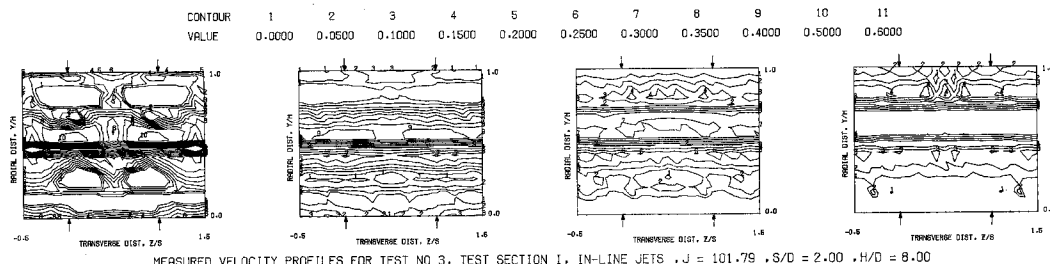


MEASURED VELOCITY PROFILES FOR TEST NO 34. TEST SECTION VI. TM=CONST . J = 26.36 , S/D = 2.00 , H/D = 4.00

Figure 129. Measured Velocity Distributions for Test No. 34 of DUM Phase I Testing.



MEASURED VELOCITY PROFILES FOR TEST NO 3, TEST SECTION I, IN-LINE JETS,  $J = 101.79$ ,  $S/D = 2.00$ ,  $H/D = 8.00$



MEASURED VELOCITY PROFILES FOR TEST NO 3, TEST SECTION I, IN-LINE JETS,  $J = 101.79$ ,  $S/D = 2.00$ ,  $H/D = 8.00$

Figure 130. Measured Velocity Distributions for Test No. 3 of DJM Phase II Testing.

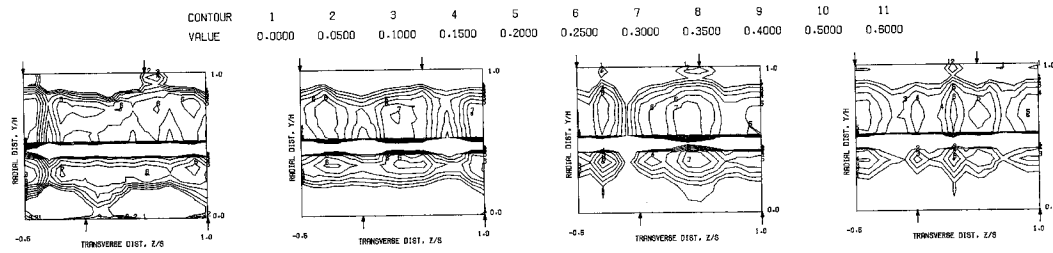
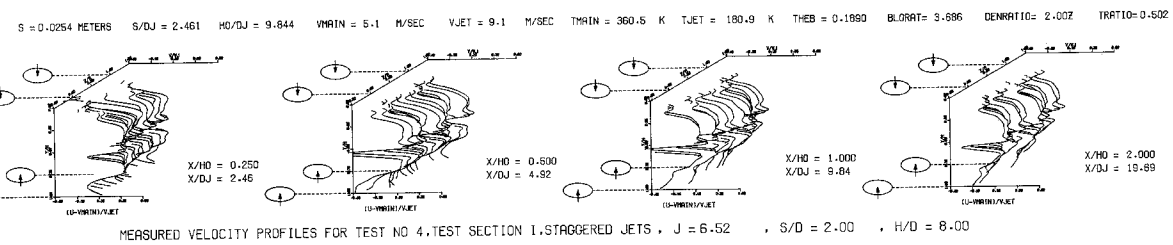


Figure 131. Measured Velocity Distributions for Test No. 4 of DJM Phase II Testing.

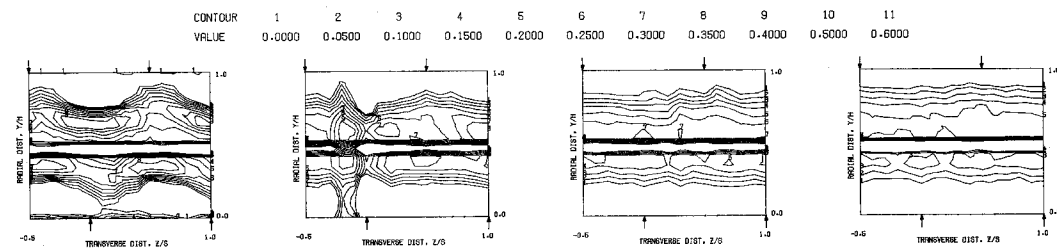
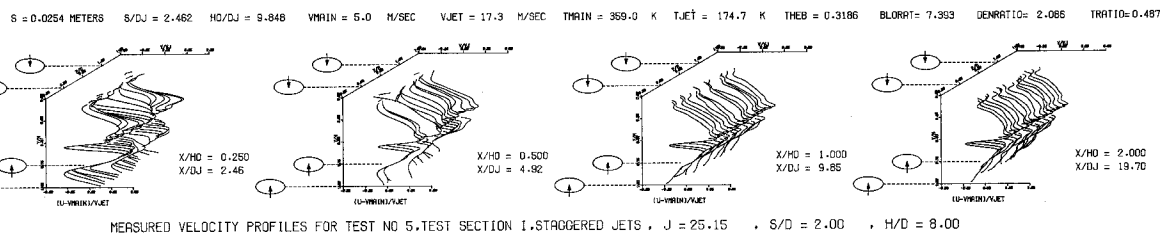


Figure 132. Measured Velocity Distributions for Test No. 5 of DJM Phase II Testing.

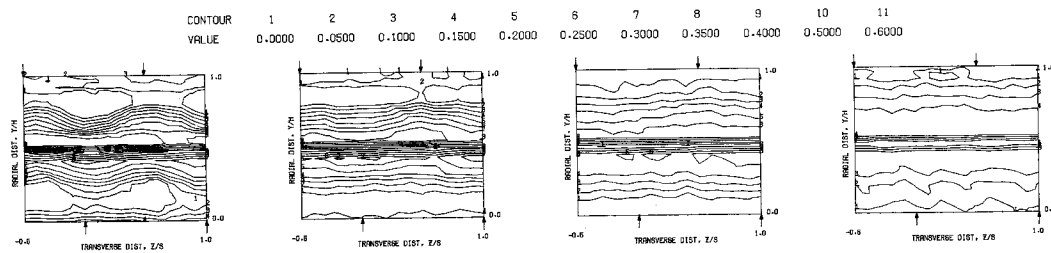
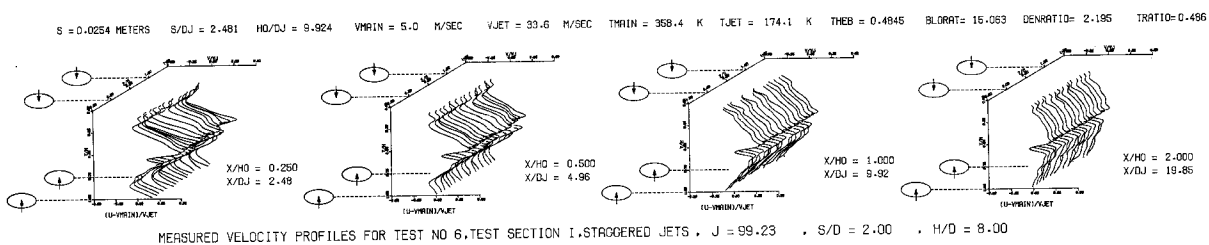
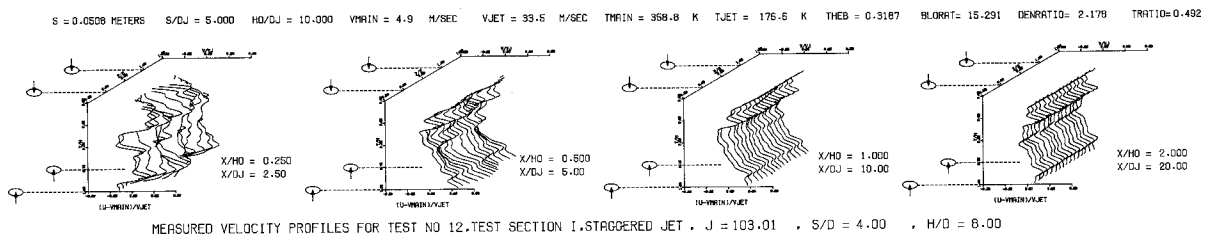
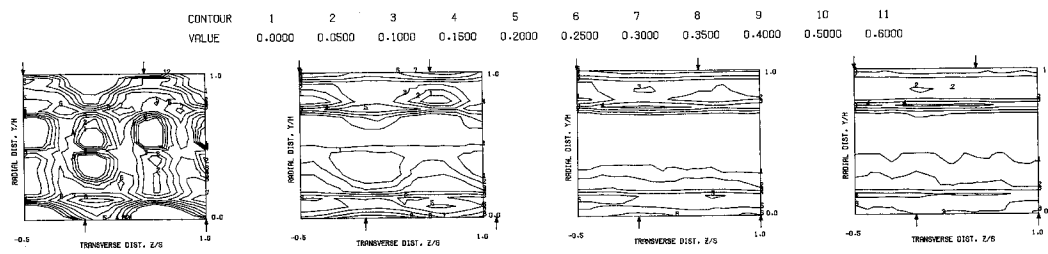


Figure 133. Measured Velocity Distributions for test No. 6 of DJM Phase II Testing.



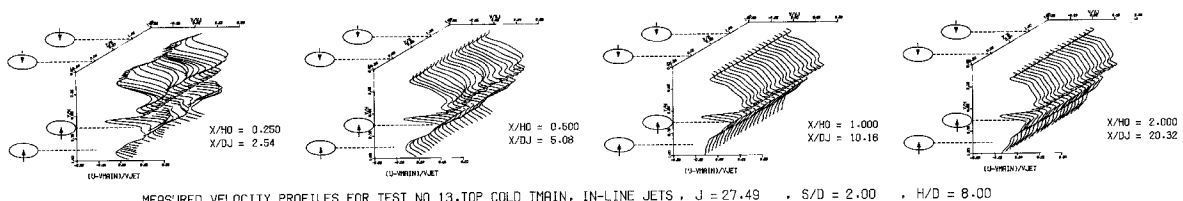
MEASURED VELOCITY PROFILES FOR TEST NO 12, TEST SECTION I, STAGGERED JET,  $J = 103.01$ ,  $S/D = 4.00$ ,  $H/D = 8.00$



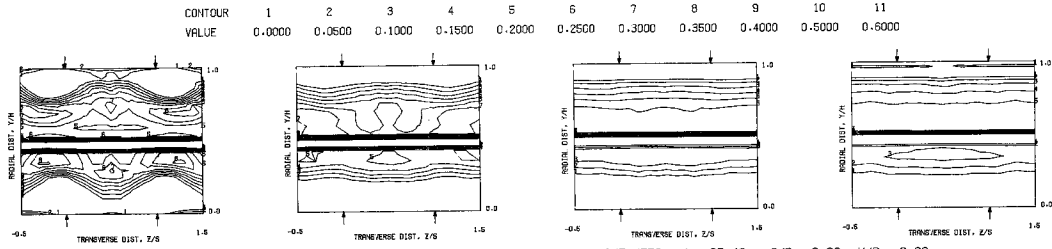
MEASURED VELOCITY PROFILES FOR TEST NO 12, TEST SECTION I, STAGGERED JET,  $J = 103.01$ ,  $S/D = 4.00$ ,  $H/D = 8.00$

Figure 134. Measured Velocity Distributions for Test No. 12 of DJM Phase II Testing.

$S = 0.0254$  METERS  $S/DJ = 2.540$   $H/DJ = 10.159$   $V_{MAIN} = 5.8$  M/SEC  $V_{JET} = 21.1$  M/SEC  $T_{MAIN} = 310.7$  K  $T_{JET} = 172.2$  K  $\rho_{HEB} = 0.6402$   $BLORR = 7.081$   $DENRATIO = 1.825$   $TRATIO = 0.554$

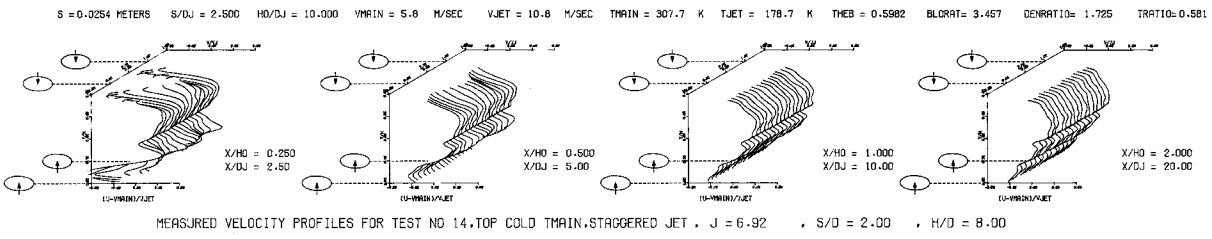


MEASURED VELOCITY PROFILES FOR TEST NO 13, TOP COLD TMAIN, IN-LINE JETS,  $J = 27.49$ ,  $S/D = 2.00$ ,  $H/D = 8.00$

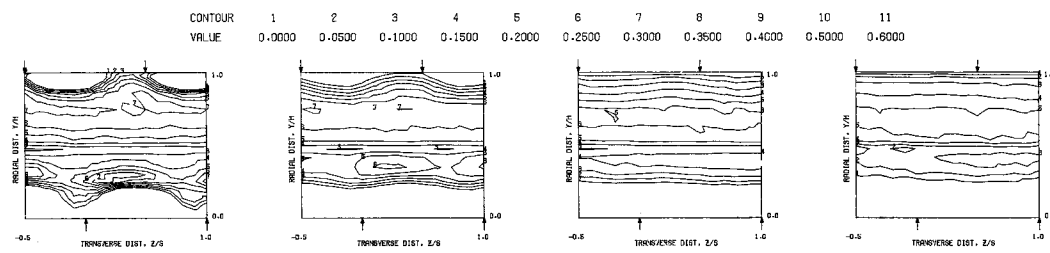


MEASURED VELOCITY PROFILES FOR TEST NO 13, TOP COLD TMAIN, IN-LINE JETS,  $J = 27.49$ ,  $S/D = 2.00$ ,  $H/D = 8.00$

Figure 135. Measured Velocity Distributions for Test No. 13 of DJM Phase II Testing.



MEASURED VELOCITY PROFILES FOR TEST NO 14, TOP COLD TMAIN, STAGGERED JET ,  $J = 6.92$  ,  $S/D = 2.00$  ,  $H/D = 8.00$



MEASURED VELOCITY PROFILES FOR TEST NO 14, TOP COLD TMAIN, STAGGERED JET ,  $J = 6.92$  ,  $S/D = 2.00$  ,  $H/D = 8.00$

Figure 136. Measured Velocity Distributions for Test No. 14 of DJM Phase II Testing.

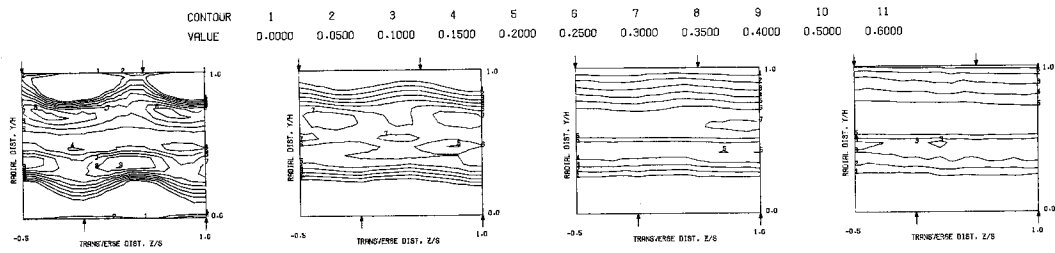
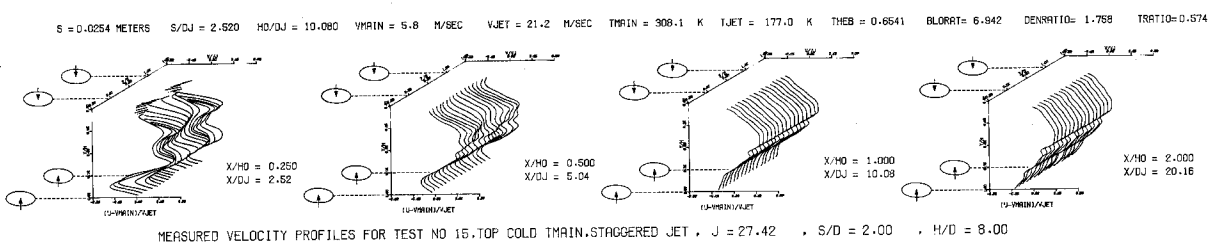
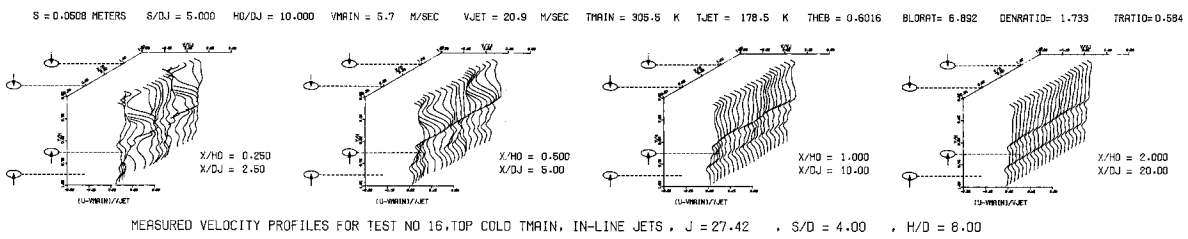
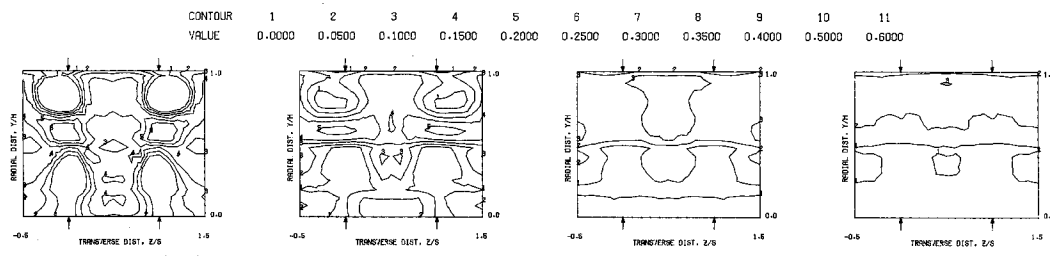


Figure 137. Measured Velocity Distributions for Test No. 15 of DJM Phase II Testing.



MEASURED VELOCITY PROFILES FOR TEST NO 16, TOP COLD TMAIN, IN-LINE JETS,  $J = 27.42$ ,  $S/D = 4.00$ ,  $H/D = 8.00$



MEASURED VELOCITY DISTRIBUTIONS FOR TEST NO 16, TOP COLD TMAIN, IN-LINE JETS,  $J = 27.42$ ,  $S/D = 4.00$ ,  $H/D = 8.00$

Figure 138. Measured Velocity Distributions for Test No. 16 of DJM Phase II Testing.

S = 0.0508 METERS S/DJ = 5.017 H0/DJ = 10.033 VMIN = 5.7 M/SEC VJET = 21.0 M/SEC TMAIN = 304.5 K TJET = 175.2 K THEB = 0.6003 BLORAT = 6.980 DENRATIO = 1.759 TRATIO = 0.575

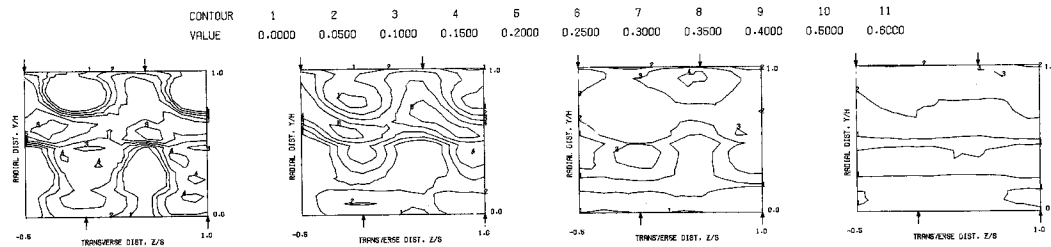
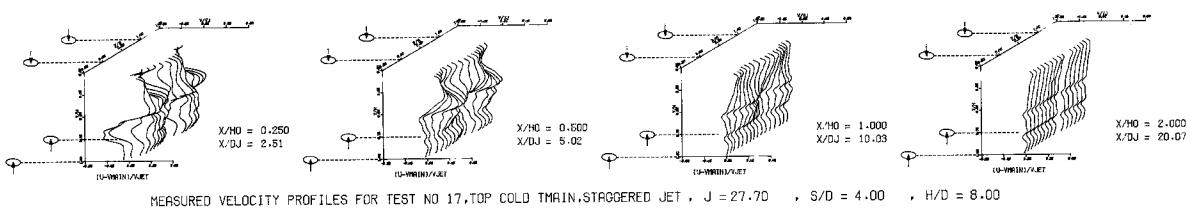
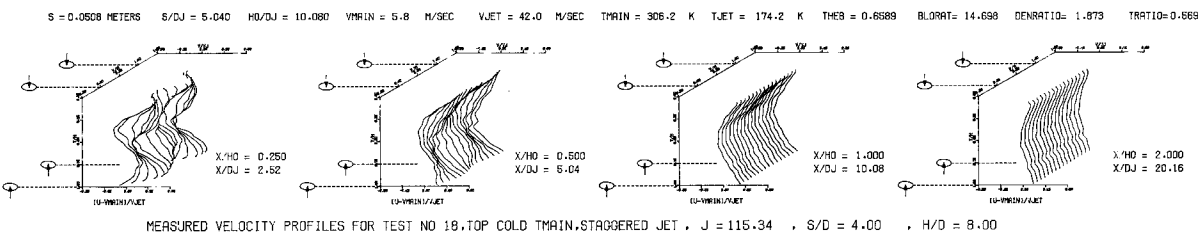


Figure 139. Measured Velocity Distributions for Test No. 17 of DJM Phase II Testing.



MEASURED VELOCITY PROFILES FOR TEST NO 18, TOP COLD TMAIN, STAGGERED JET ,  $J = 115.34$  ,  $S/D = 4.00$  ,  $H/D = 8.00$

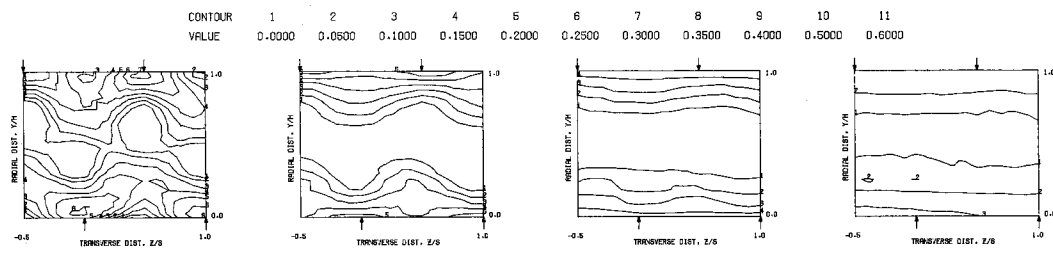
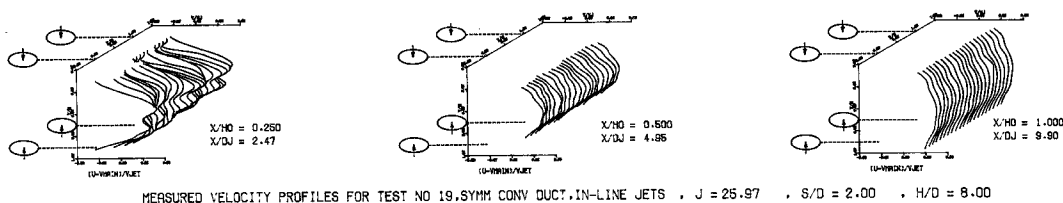


Figure 140. Measured Velocity Distributions for Test No. 18 of DJM Phase II Testing.

$S = 0.0254$  METERS    $S/DJ = 2.475$     $H/DJ = 9.899$     $V_{MAIN} = 5.0$  M/SEC    $V_{JET} = 17.2$  M/SEC    $T_{MAIN} = 368.2$  K    $T_{JET} = 165.7$  K    $\rho_{HEB} = 0.3263$     $BLOBRAT = 7.560$     $DENRATIO = 2.201$     $TRATIO = 0.463$



CONTOUR	1	2	3	4	5	6	7	8	9	10	11
VALUE	0.0000	0.0500	0.1000	0.1500	0.2000	0.2500	0.3000	0.3500	0.4000	0.5000	0.6000

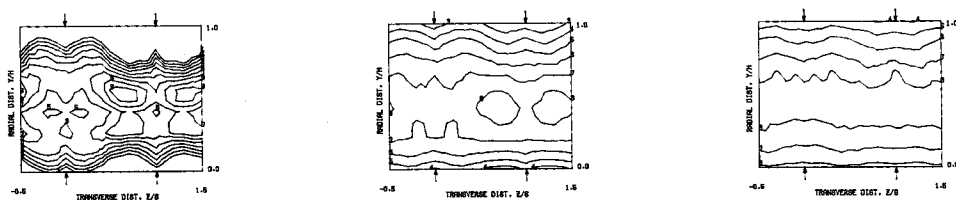
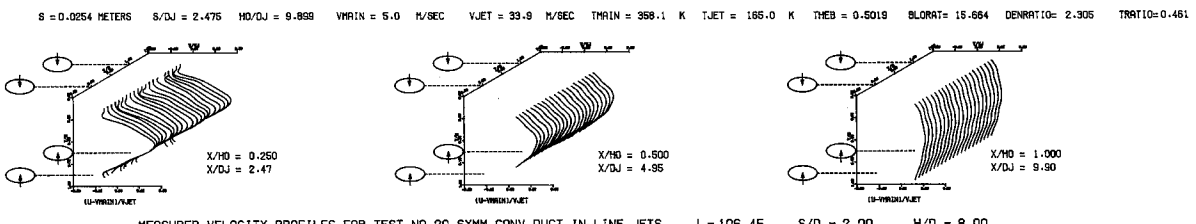
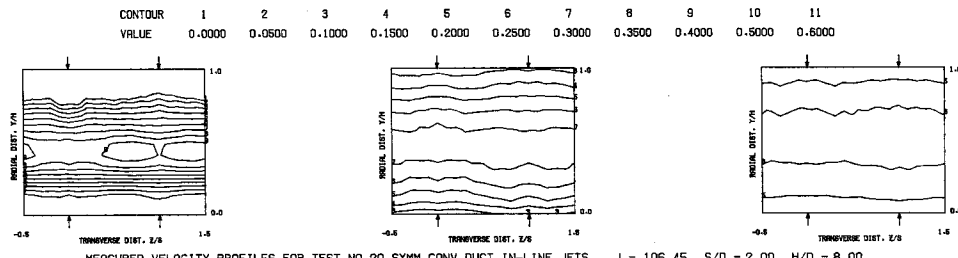


Figure 141. Measured Velocity Distributions for Test No. 19 of DJM Phase II Testing.



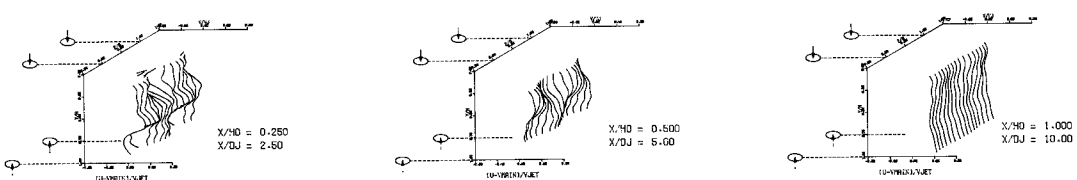
MEASURED VELOCITY PROFILES FOR TEST NO 20, SYMM CONV DUCT, IN-LINE JETS ,  $J = 106.45$  ,  $S/D = 2.00$  ,  $H/D = 8.00$



MEASURED VELOCITY PROFILES FOR TEST NO 20, SYMM CONV DUCT, IN-LINE JETS ,  $J = 106.45$  ,  $S/D = 2.00$  ,  $H/D = 8.00$

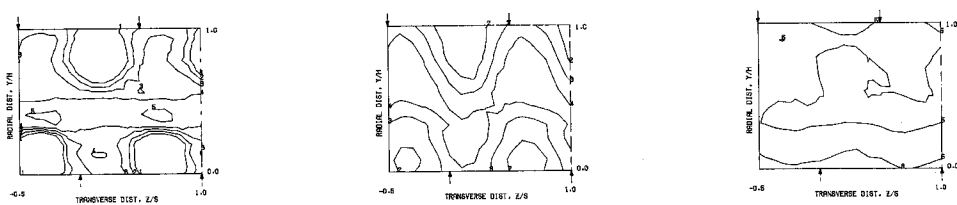
Figure 142. Measured Velocity Distributions for Test No. 20 of DJM Phase II Testing.

S = 0.0508 METERS S/DJ = 5.000 H/DJ = 10.000 VMIN = 5.0 M/SEC VJET = 17.4 M/SEC TMIN = 358.1 K TJET = 168.3 K THB = 0.1929 BLRAT = 7.464 DENRATIO = 2.149 TRATIO = 0.470



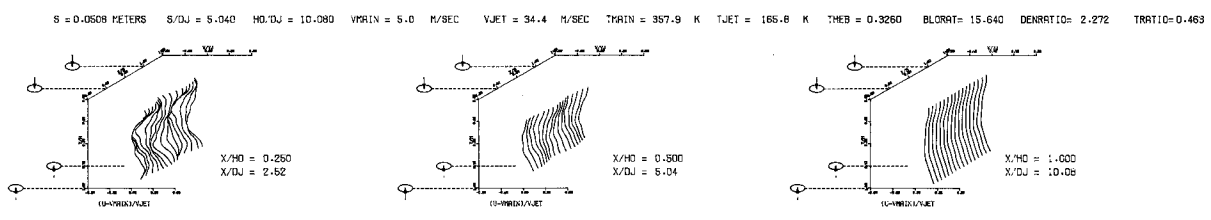
MEASURED VELOCITY PROFILES FOR TEST NO 21, SYMM CONV DUCT, STAGGERED JET,  $J = 25.92$  •  $S/D = 4.00$  •  $H/D = 8.00$

CONTOUR	1	2	3	4	5	6	7	8	9	10	11
VALUE	0.0000	0.0500	0.1000	0.1500	0.2000	0.2500	0.3000	0.3500	0.4000	0.5000	0.6000

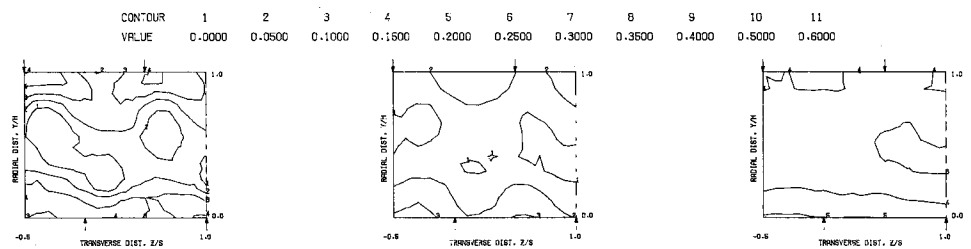


MEASURED VELOCITY PROFILES FOR TEST NO 21, SYMM CONV DUCT, STAGGERED JET,  $J = 25.92$ ,  $S/D = 4.00$ ,  $H/D = 8.00$

Figure 143. Measured Velocity Distributions for Test No. 21 of DJM Phase II Testing.

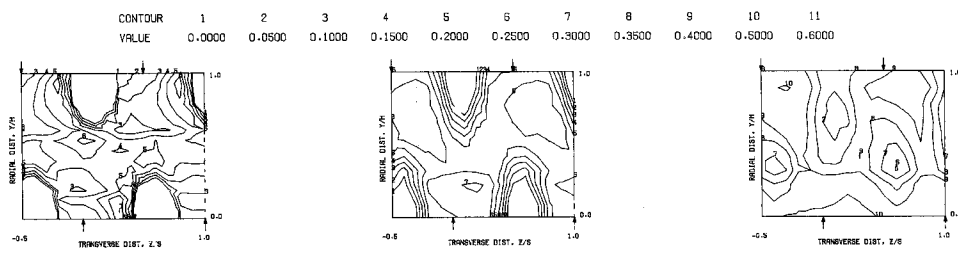
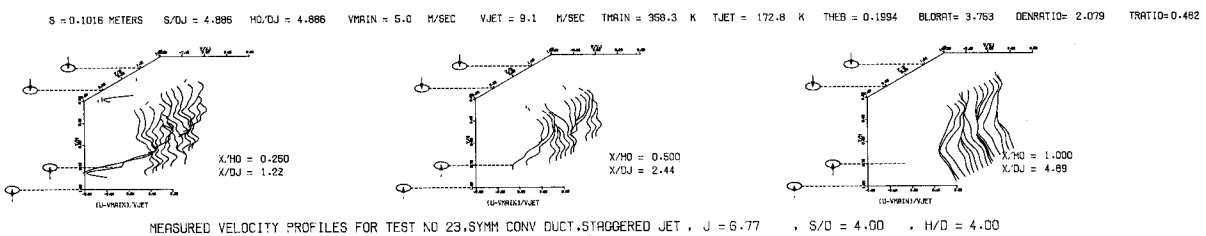


MEASURED VELOCITY PROFILES FOR TEST NO 22, SYMM CONV DUCT, STAGGERED JET ,  $J = 107.66$  ,  $S/D = 4.00$  ,  $H/D = 8.00$



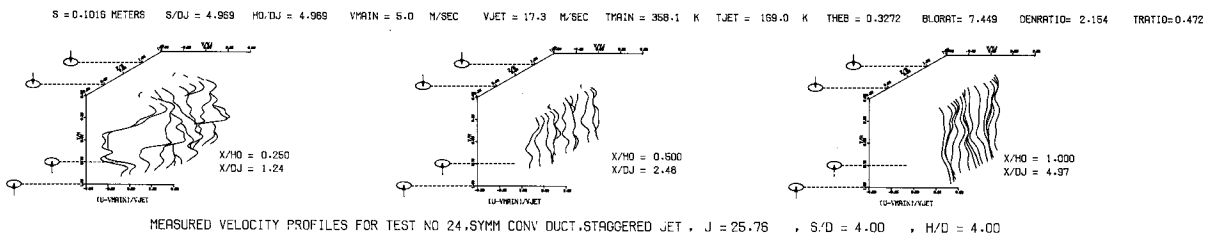
MEASURED VELOCITY PROFILES FOR TEST NO 22, SYMM CONV DUCT, STAGGERED JET ,  $J = 107.66$  ,  $S/D = 4.00$  ,  $H/D = 8.00$

Figure 144. Measured Velocity Distributions for Test No. 22 of DJM Phase II Testing.

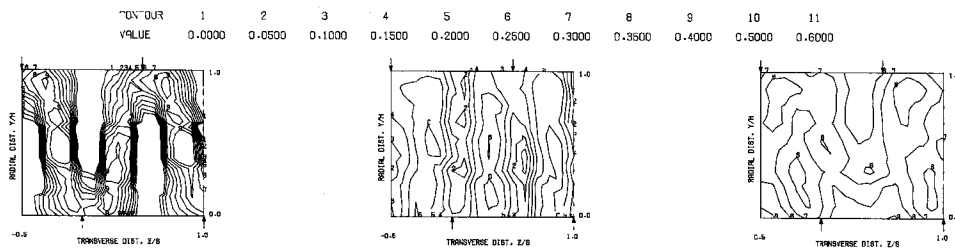


MEASURED VELOCITY PROFILES FOR TEST NO 23, SYMM CONV DUCT, STAGGERED JET,  $J = 6.77$ ,  $S/D = 4.00$ ,  $H/D = 4.00$

Figure 145. Measured Velocity Distributions for Test No. 23 of DJM Phase II Testing.



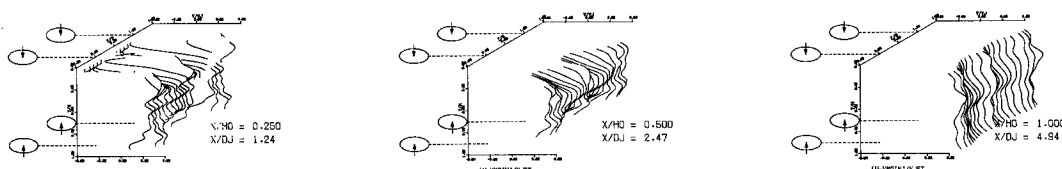
MEASURED VELOCITY PROFILES FOR TEST NO 24, SYMM CONV DUCT, STAGGERED JET ,  $J = 25.76$  ,  $S/D = 4.00$  ,  $H/D = 4.00$



MEASURED VELOCITY PROFILES FOR TEST NO 24, SYMM CONV DUCT, STAGGERED JET ,  $J = 25.76$  ,  $S/D = 4.00$  ,  $H/D = 4.00$

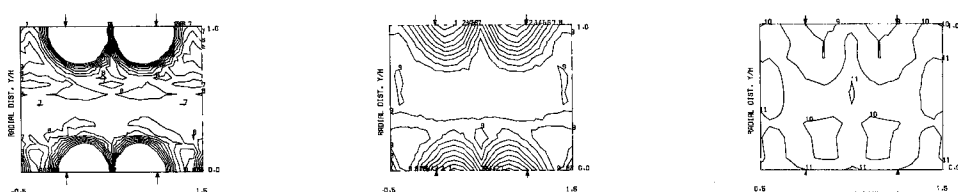
Figure 146. Measured Velocity Distributions for Test No. 24 of DJM Phase II Testing.

$S = 0.0508$  METERS    $S/D_J = 2.471$     $H/D_J = 4.942$     $V_{MAIN} = 5.0$  M/SEC    $V_{JET} = 6.8$  M/SEC    $T_{MAIN} = 358.4$  K    $T_{JET} = 166.9$  K    $\dot{M}_{HEB} = 0.3283$     $BLOWRAT = 3.791$     $DENRATIO = 2.156$     $TRATIO = 0.466$



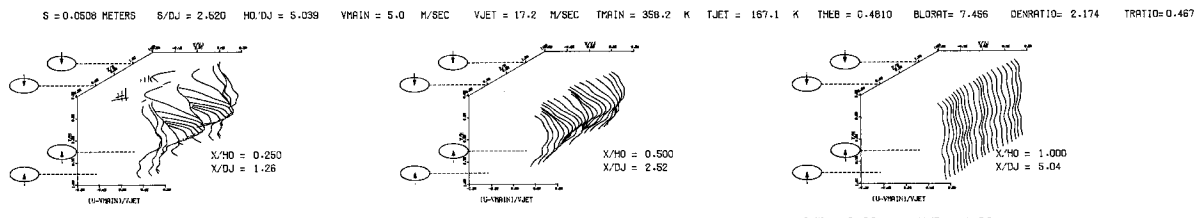
MEASURED VELOCITY PROFILES FOR TEST NO 25, SYMM CONV DUCT, IN-LINE JETS ,  $J = 6.67$  ,  $S/D = 2.00$  ,  $H/D = 4.00$

CONTOUR	1	2	3	4	5	6	7	8	9	10	11
VALUE	0.0000	0.0500	0.1000	0.1500	0.2000	0.2500	0.3000	0.3500	0.4000	0.5000	0.6000

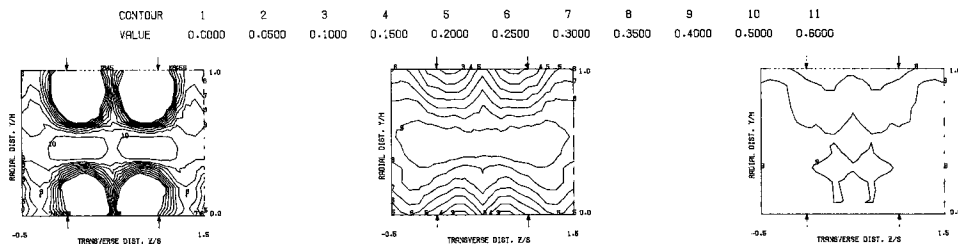


MEASURED VELOCITY PROFILES FOR TEST NO 25, SYMM CONV DUCT, IN-LINE JETS ,  $J = 6.67$  ,  $S/D = 2.00$  ,  $H/D = 4.00$

Figure 147. Measured Velocity Distributions for Test No. 25 of DJM Phase II Testing.



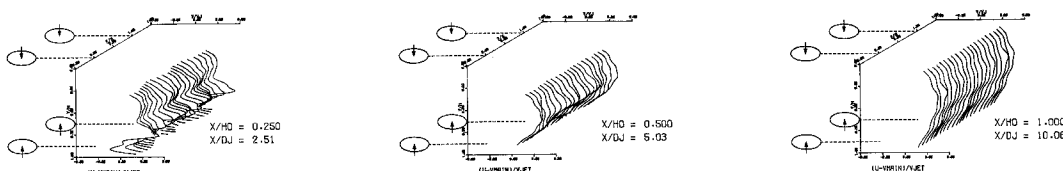
MEASURED VELOCITY PROFILES FOR TEST NO 26,SYMM CONV DUCT,IN-LINE JETS ,  $J = 25.58$  ,  $S/D = 2.00$  ,  $H/D = 4.00$



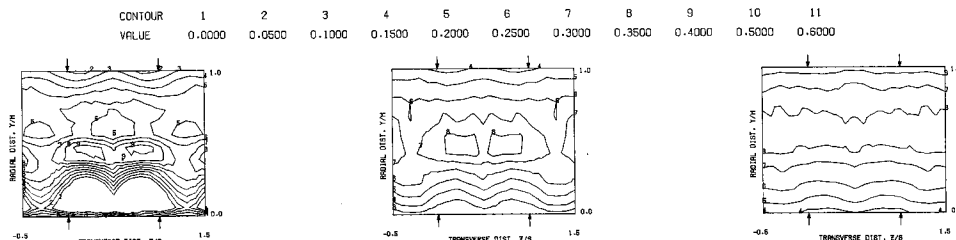
MEASURED VELOCITY PROFILES FOR TEST NO 26,SYMM CONV DUCT,IN-LINE JETS ,  $J = 25.58$  ,  $S/D = 2.00$  ,  $H/D = 4.00$

Figure 148. Measured Velocity Distributions for Test No. 26 of DJM Phase II Testing.

$S = 0.0254$  METERS    $S/DJ = 2.514$     $H/DJ = 10.057$     $V_{MAIN} = 5.0$  M/SEC    $V_{JET} = 17.4$  M/SEC    $T_{MAIN} = 350.3$  K    $T_{JET} = 160.5$  K    $\theta_{HEB} = 0.3195$     $BLRAT = 7.512$     $DENRATIO = 2.155$     $TRATIO = 0.470$

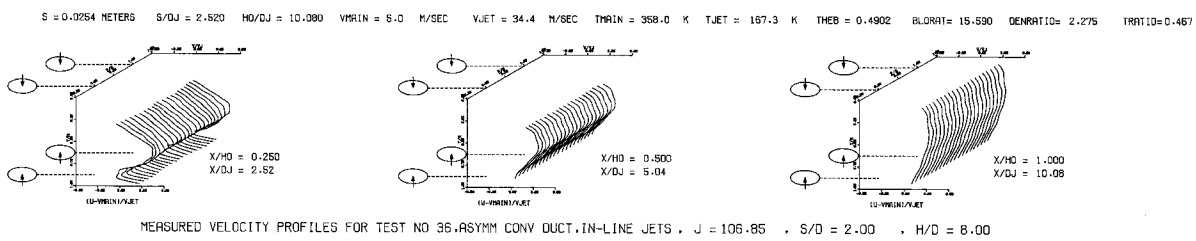


MEASURED VELOCITY PROFILES FOR TEST NO 35, ASYMM CONV DUCT, IN-LINE JETS ,  $J = 26.20$  ,  $S/D = 2.00$  ,  $H/D = 8.00$

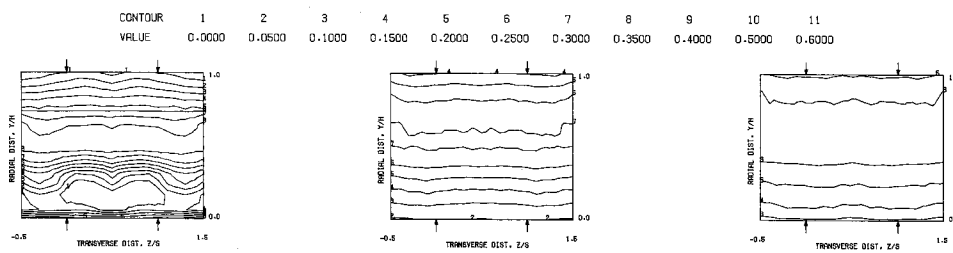


MEASURED VELOCITY PROFILES FOR TEST NO 35, ASYMM CONV DUCT, IN-LINE JETS ,  $J = 26.20$  ,  $S/D = 2.00$  ,  $H/D = 8.00$

Figure 149. Measured Velocity Distributions for Test No. 35 of DJM Phase II Testing.



MEASURED VELOCITY PROFILES FOR TEST NO 36, ASYMM CONV DUCT, IN-LINE JETS ,  $J = 106.85$  ,  $S/D = 2.00$  ,  $H/D = 8.00$



MEASURED VELOCITY PROFILES FOR TEST NO 36, ASYMM CONV DUCT, IN-LINE JETS ,  $J = 106.85$  ,  $S/D = 2.00$  ,  $H/D = 8.00$

Figure 150. Measured Velocity Distributions for Test No. 36 of DJM Phase II Testing.

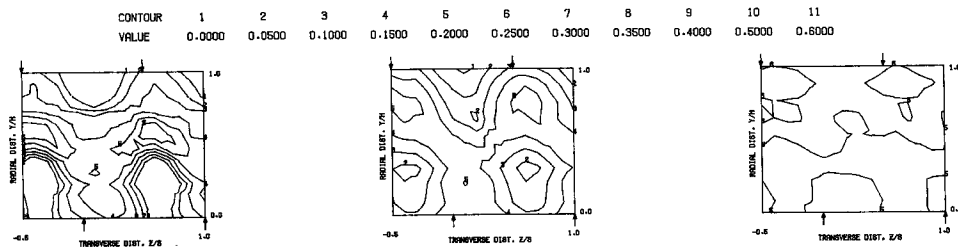
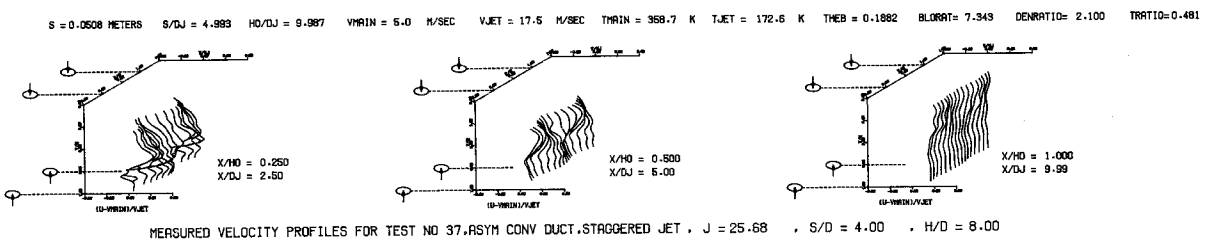


Figure 151. Measured Velocity Distributions for Test No. 37 of DJM Phase II testing.

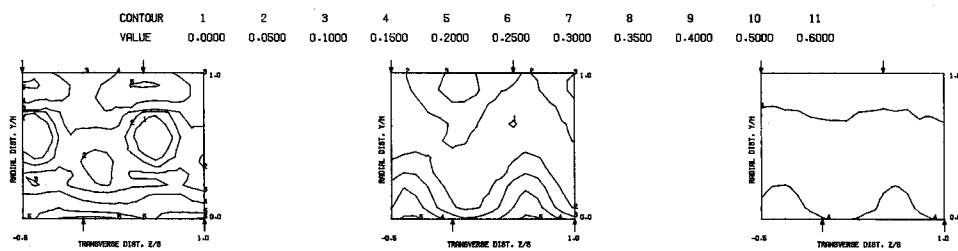
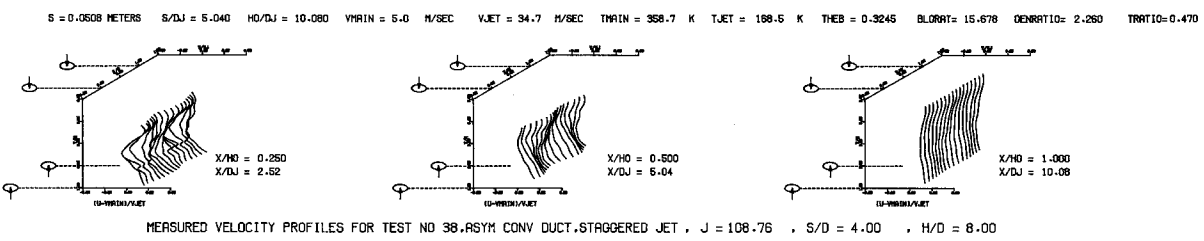


Figure 152. Measured Velocity Distributions for Test No. 38 of DJM Phase II Testing.

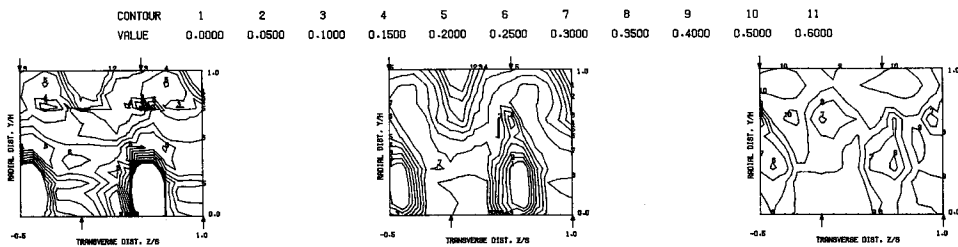
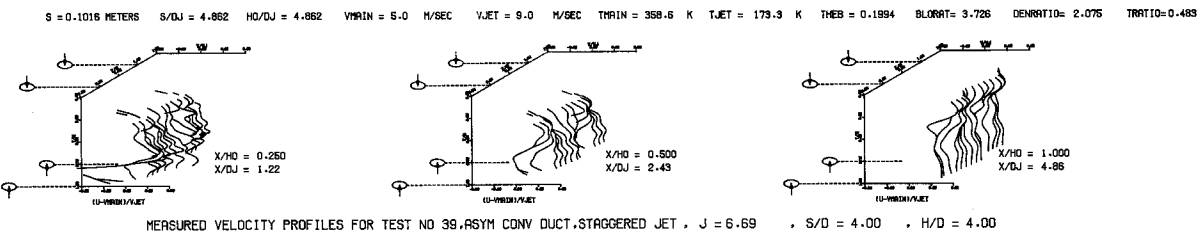


Figure 153. Measured Velocity Distributions for Test No. 39 of DJM Phase II Testing.

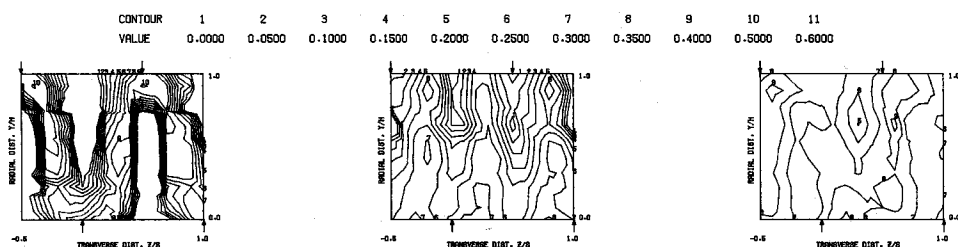
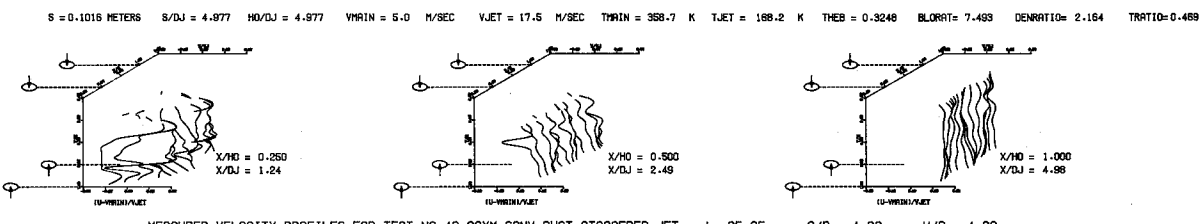


Figure 154. Measured Velocity Distributions for Test No. 40 of DJM Phase II Testing.

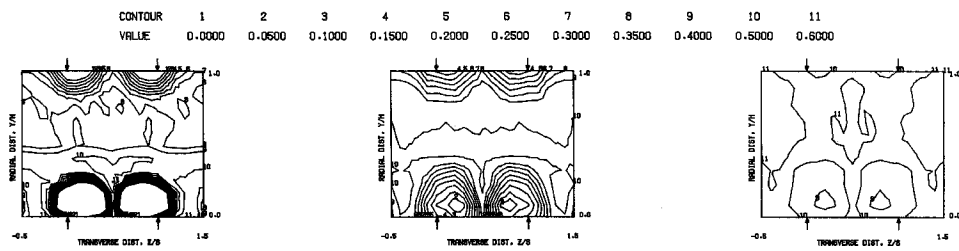
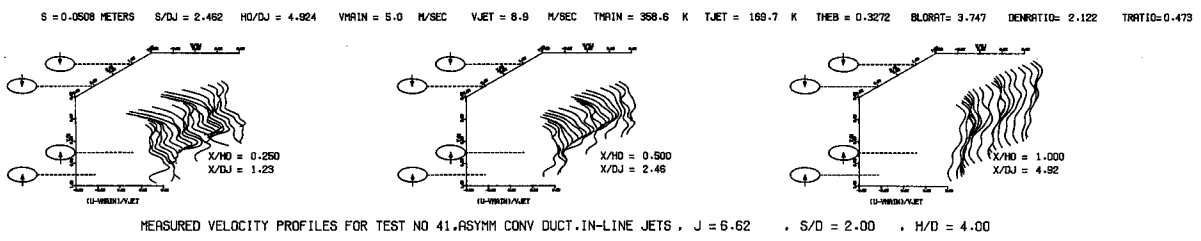
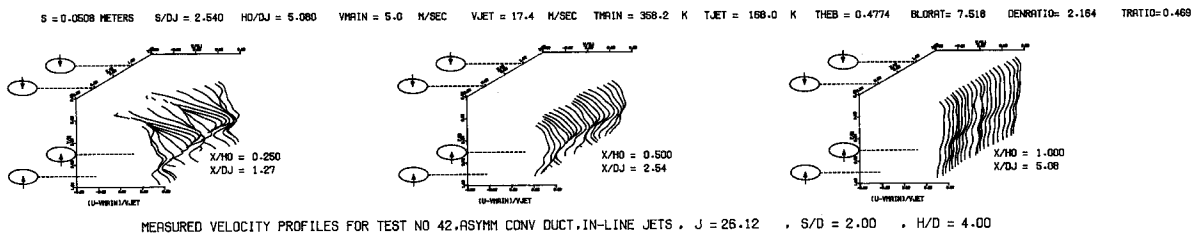
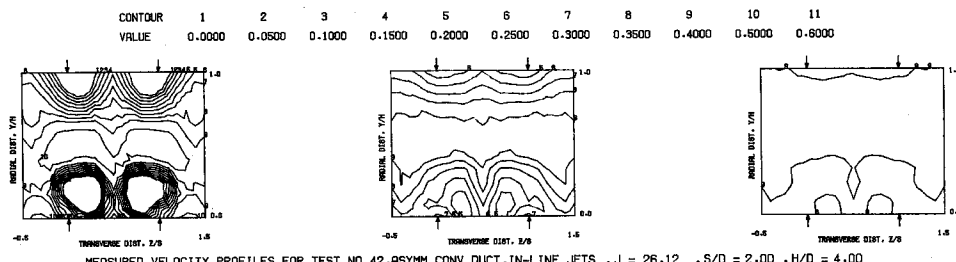


Figure 155. Measured Velocity Distributions for Test No. 41 of DJM Phase II Testing.



MEASURED VELOCITY PROFILES FOR TEST NO 42, ASYMM CONV DUCT, IN-LINE JETS .  $J = 26.12$  .  $S/D = 2.00$  .  $H/D = 4.00$



MEASURED VELOCITY PROFILES FOR TEST NO 42, ASYMM CONV DUCT, IN-LINE JETS .  $J = 26.12$  .  $S/D = 2.00$  .  $H/D = 4.00$

Figure 156. Measured Velocity Distributions for Test No. 42 of DJM Phase II Testing.

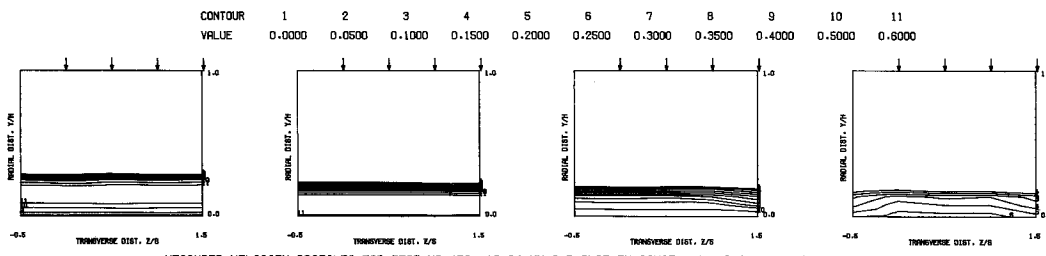
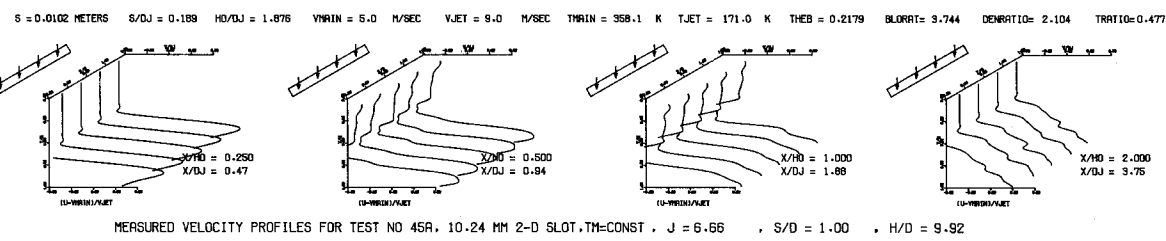


Figure 157. Measured Velocity Distributions for Test No. 45A of DJM Phase II Testing.

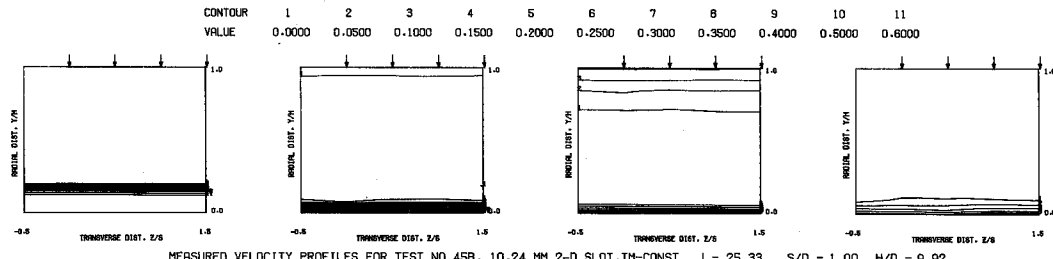
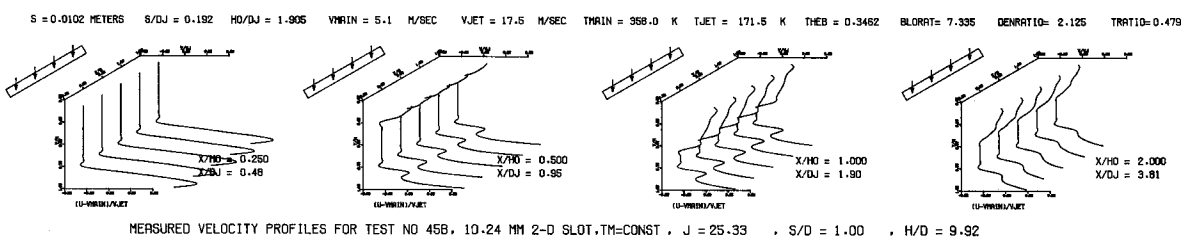
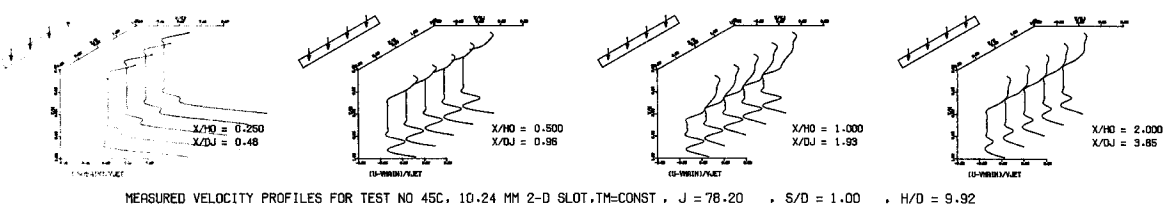
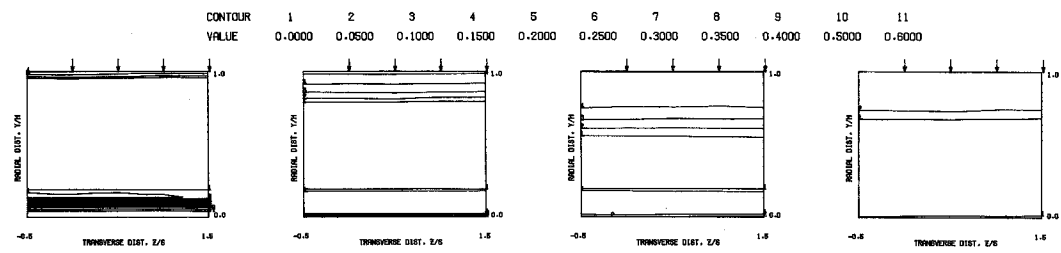


Figure 158. Measured Velocity Distributions for Test No. 45B of DDM Phase II Testing.

S = 0.0102 METERS S/DJ = 0.194 H/DJ = 1.926 V<sub>MAIN</sub> = 5.1 M/SEC V<sub>JET</sub> = 30.2 M/SEC T<sub>MAIN</sub> = 357.7 K T<sub>JET</sub> = 170.8 K THEB = 0.4820 BLORAT = 13.185 DENRATIO = 2.223 TRRATIO = 0.478



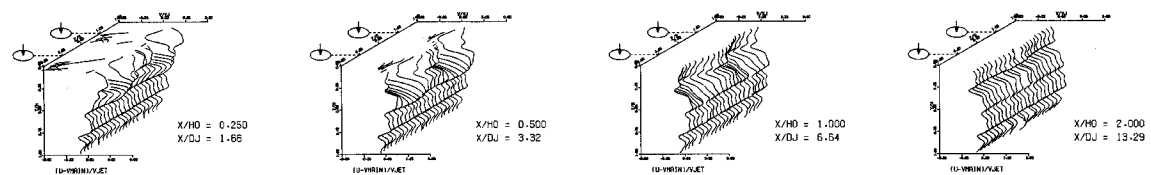
MESURED VELOCITY PROFILES FOR TEST NO 45C, 10.24 MM 2-D SLOT, TM=CONST , J = 78.20 , S/D = 1.00 , H/D = 9.92



MESURED VELOCITY PROFILES FOR TEST NO 45C, 10.24 MM 2-D SLOT, TM=CONST , J = 78.20 , S/D = 1.00 , H/D = 9.92

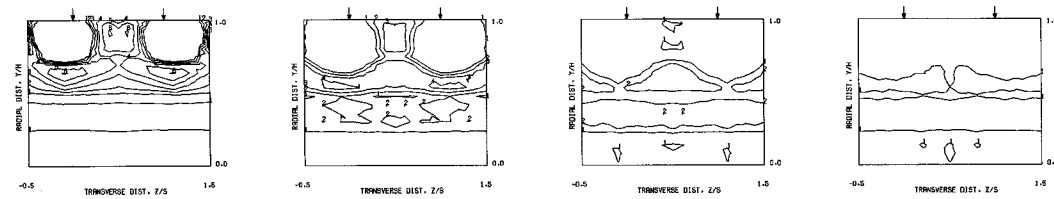
Figure 159. Measured Velocity Distributions for Test No. 45C of DJM Phase II Testing.

$S = 0.0508$  METERS    $S/D_J = 3.322$     $H/D_J = 6.644$     $V_{MIN} = 5.1$  M/SEC    $V_{JET} = 9.0$  M/SEC    $T_{MAIN} = 358.0$  K    $T_{JET} = 171.9$  K    $\theta_{EB} = 0.1159$     $B_{LORR} = 3.682$     $DENRATIO = 2.090$     $TRATIO = 0.480$



MEASURED VELOCITY PROFILES FOR TEST NO 49, SINGLE SIDED JETS,  $T_M = \text{CONST}$ ,  $J = 6.49$ ,  $S/D = 2.83$ ,  $H/D = 5.66$

CONTOUR	1	2	3	4	5	6	7	8	9	10	11
VALUE	0.0000	0.0500	0.1000	0.1500	0.2000	0.2500	0.3000	0.3500	0.4000	0.5000	0.6000



MEASURED VELOCITY PROFILES FOR TEST NO 49, SINGLE SIDED JETS,  $T_M = \text{CONST}$ ,  $J = 6.49$ ,  $S/D = 2.83$ ,  $H/D = 5.66$

Figure 160. Measured Velocity Distributions for Test No. 49 of DJM Phase II Testing.

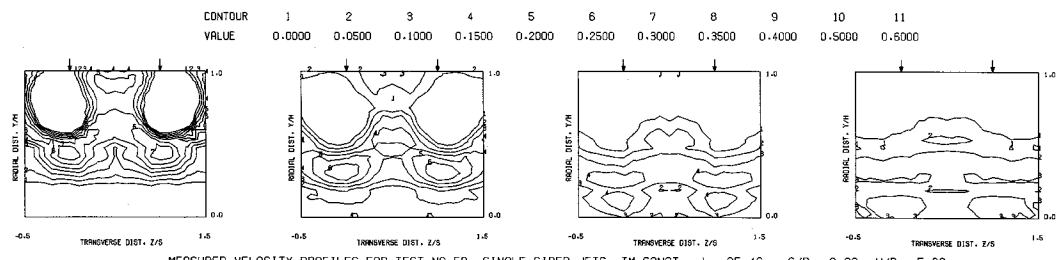
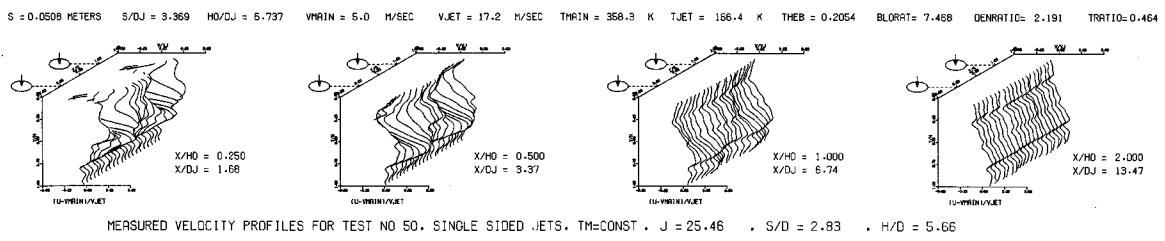


Figure 161. Measured Velocity Distributions for Test No. 50 of DJM Phase II Testing.

$S = 0.0508$  METERS  $S/DJ = 2.286$   $H/DJ = 4.576$   $V_{MAIN} = 17.8$  M/SEC  $V_{JET} = 30.9$  M/SEC  $T_{MAIN} = 690.1$  K  $T_{JET} = 317.1$  K  $\rho_{EB} = 0.2216$   $\rho_{LARAT} = 3.795$  DENSITY = 2.181 TRATIO = 0.460

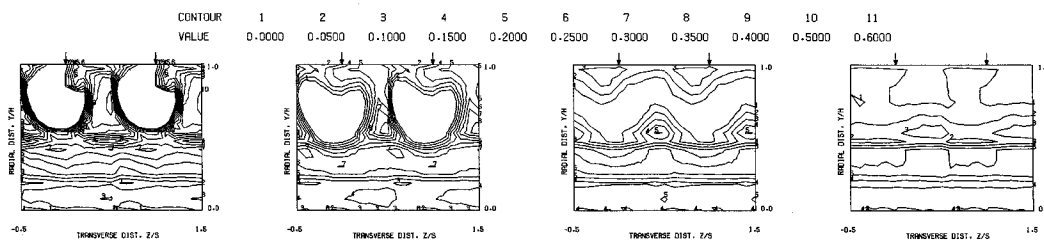
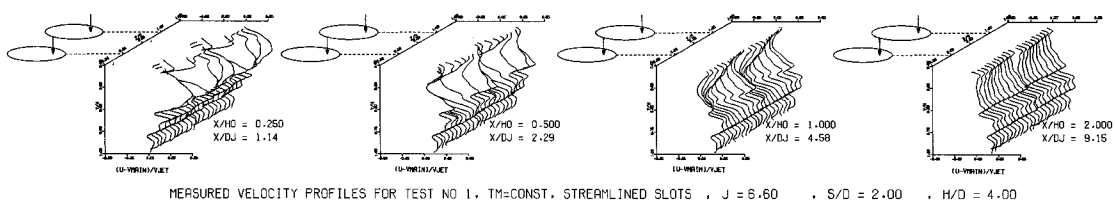
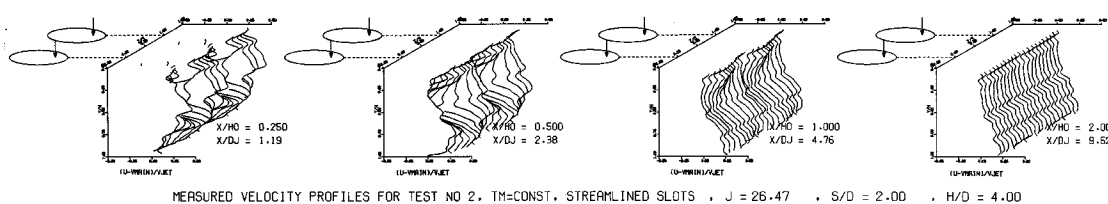
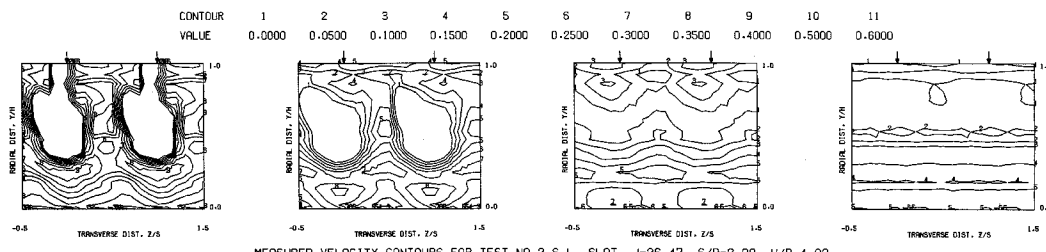


Figure 162. Measured Velocity Distributions for Test No. 1 of DJM Phase III Testing.

$S = 0.0508$  METERS    $S/DJ = 2.379$     $H/DJ = 4.758$     $V_{MAIN} = 16.7$  M/SEC    $V_{JET} = 58.5$  M/SEC    $T_{MAIN} = 661.0$  K    $T_{JET} = 307.3$  K    $\rho_{HEB} = 0.3447$     $\rho_{BLOR} = 7.581$     $\rho_{DENRATIO} = 2.171$     $\rho_{TRATIO} = 0.455$



MEASURED VELOCITY PROFILES FOR TEST NO 2, TM=CONST. STREAMLINED SLOTS , J = 26.47 , S/D = 2.00 , H/D = 4.00



MEASURED VELOCITY CONTOURS FOR TEST NO 2.3-L- SLOT, J=26.47. S/D=2.00, H/D=4.00

Figure 163. Measured Velocity Distributions for Test No. 2 of DJM Phase III Testing.

$S = 0.0508$  METERS    $S/D_J = 2.104$     $H/D_J = 4.207$     $V_{MIN} = 17.2$  M/SEC    $V_{JET} = 60.3$  M/SEC    $T_{MIN} = 675.0$  K    $T_{JET} = 316.5$  K    $\text{THEB} = 0.4026$     $\text{BLFRAT} = 7.592$     $\text{DENRATIO} = 2.168$     $\text{TRATIO} = 0.469$

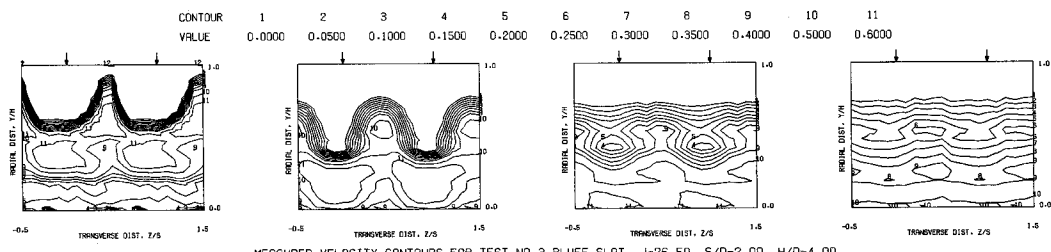
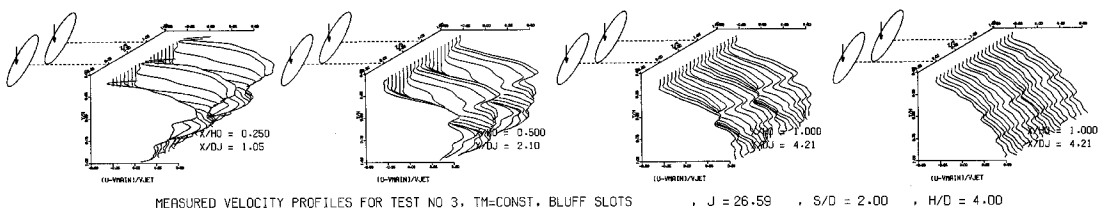
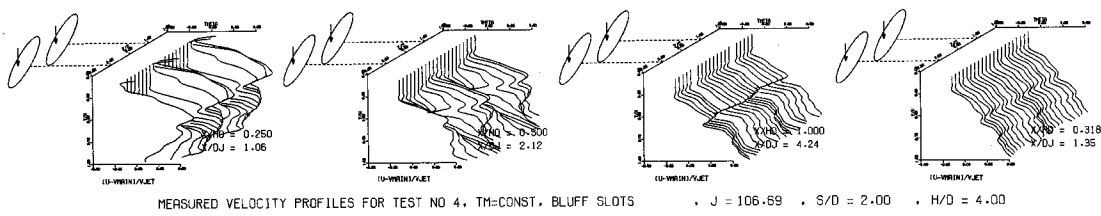
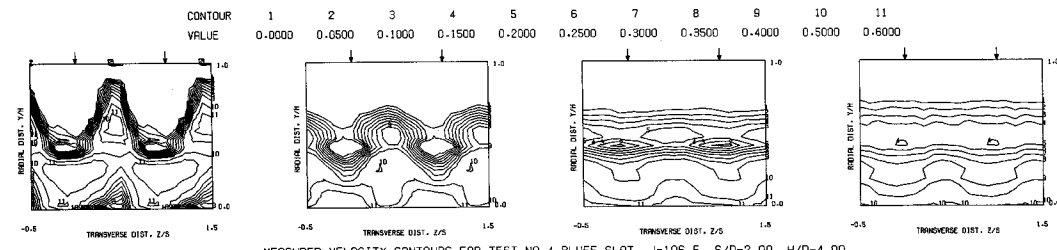


Figure 164. Measured Velocity Distributions for Test No. 3 of DJM Phase III Testing.

$S = 0.0508$  METERS    $S/DJ = 2.118$     $H/DJ = 4.237$     $V_{MAIN} = 12.6$  M/SEC    $V_{JET} = 66.8$  M/SEC    $T_{MAIN} = 655.3$  K    $T_{JET} = 915.0$  K    $\Theta_{EB} = 0.5705$     $BLRAT = 15.183$     $DENRAT = 2.161$     $TRATIO = 0.481$



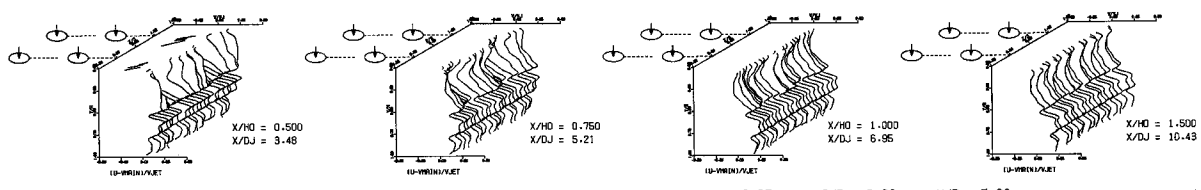
MEASURED VELOCITY PROFILES FOR TEST NO 4, TM=CONST, BLUFF SLOTS    $J = 106.89$     $S/D = 2.00$     $H/D = 4.00$



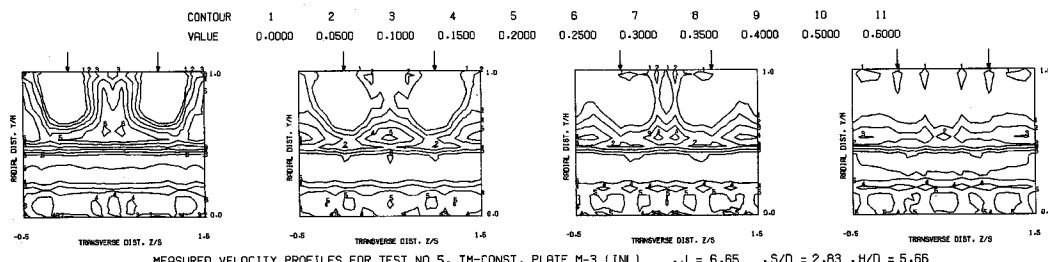
MEASURED VELOCITY CONTOURS FOR TEST NO 4, BLUFF SLOT,  $J=106.5$ ,  $S/D=2.00$ ,  $H/D=4.00$

Figure 165. Measured Velocity Distributions for Test No. 4 of DJM Phase III Testing.

S = 0.0508 METERS S/DJ = 3.476 H/DJ = 6.952 V<sub>MAIN</sub> = 5.4 M/SEC V<sub>JET</sub> = 9.4 M/SEC T<sub>MAIN</sub> = 383.5 K T<sub>JET</sub> = 177.3 K THB = 0.1978 BLORAT = 3.800 DENRATIO = 2.172 TRATIO = 0.462



MEASURED VELOCITY PROFILES FOR TEST NO 5, TM=CONST., PLATE M-3 (INL) J = 6.65 S/D = 2.83 H/D = 5.66



MEASURED VELOCITY PROFILES FOR TEST NO 5, TM=CONST., PLATE M-3 (INL) J = 6.65 S/D = 2.83 H/D = 5.66

Figure 166. Measured Velocity Distributions for Test No. 5 of DJM Phase III Testing.

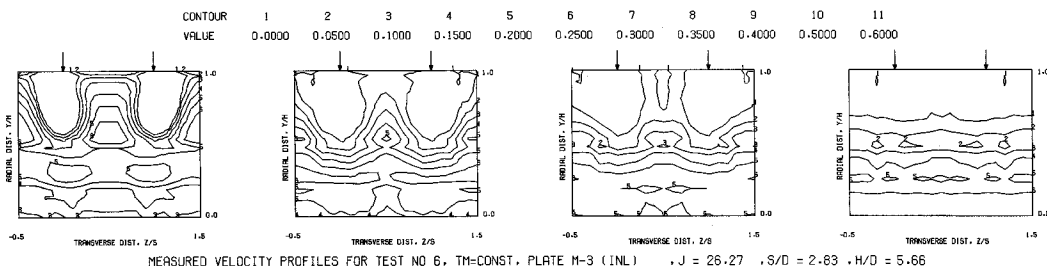
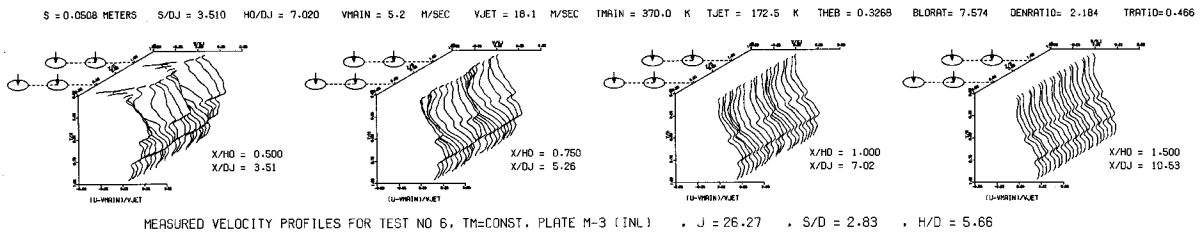


Figure 167. Measured Velocity Distributions for Test No. 6 of DJM Phase III Testing.

194

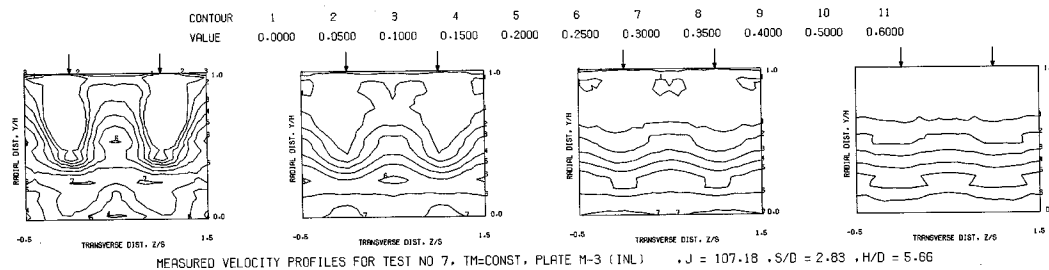
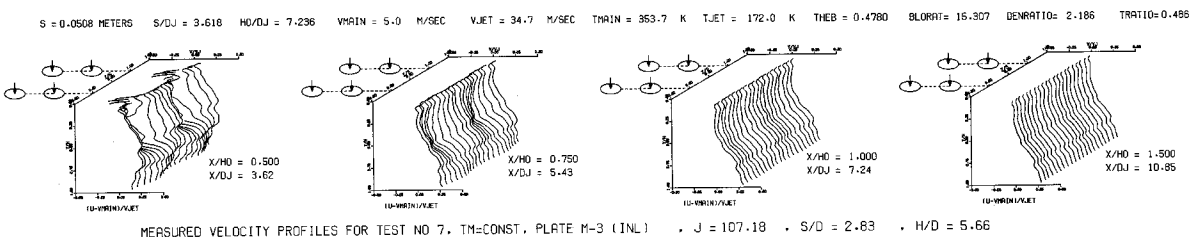


Figure 168. Measured Velocity Distributions for Test No. 7 of DJM Phase III Testing.

S = 0.1016 METERS    S/DJ = 4.716    H/DJ = 4.716    V<sub>MAIN</sub> = 5.3 M/SEC    V<sub>JET</sub> = 9.3 M/SEC    T<sub>MAIN</sub> = 378.9 K    T<sub>JET</sub> = 174.5 K    THB = 0.2151    BLORAT = 3.817    DENRATIO = 2.183    TRATIO = 0.460

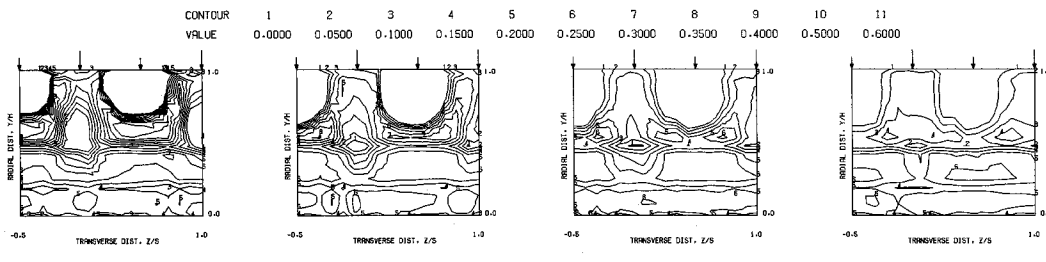
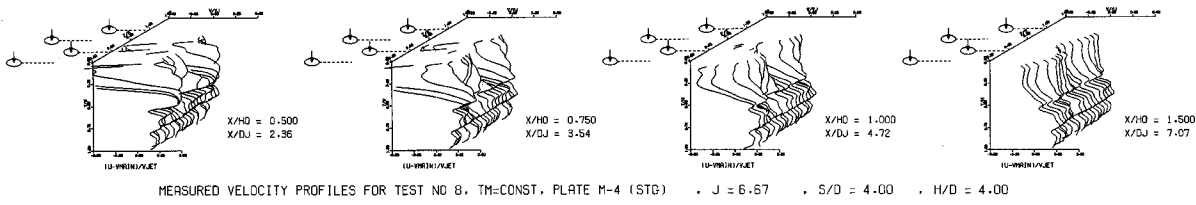


Figure 169. Measured Velocity Distributions for Test No. 8 of DJM Phase III Testing.

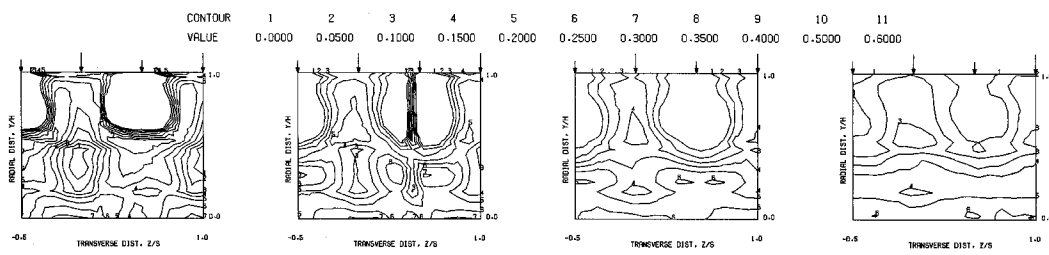
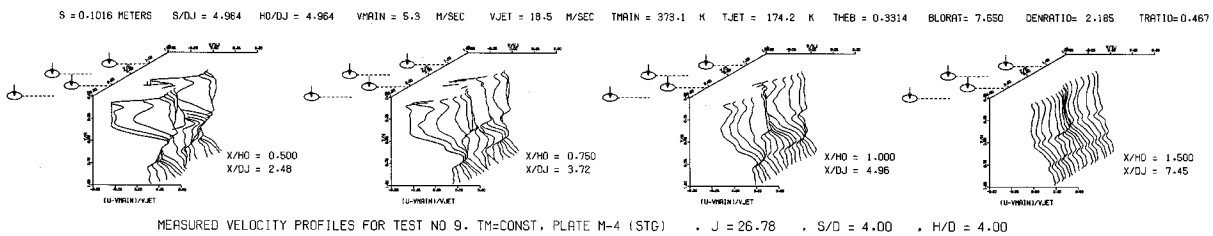
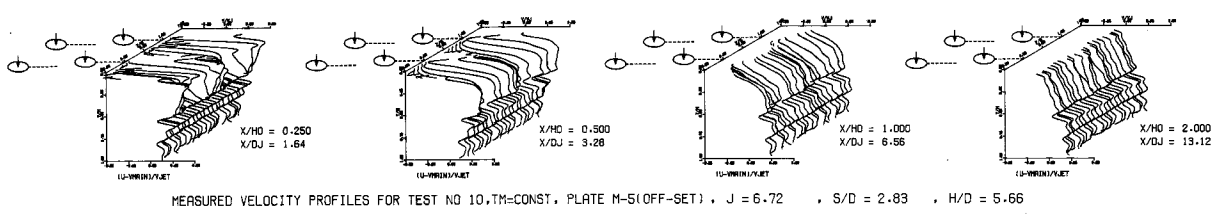
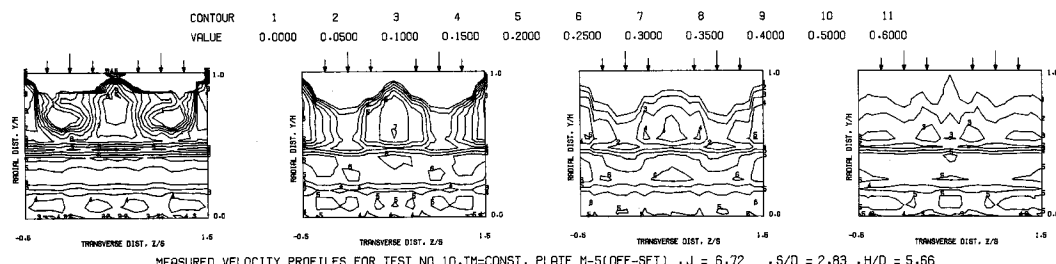


Figure 170. Measured Velocity Distributions for Test No. 9 of DJM Phase III Testing.

S = 0.0508 METERS S/DJ = 9.280 H0/DJ = 6.560 VMAIN = 5.4 M/SEC VJET = 9.5 M/SEC TMRAIN = 386.4 K TJET = 178.4 K TM3 = 0.2194 BLORAT = 3.825 DENRATIO = 2.178 TRATIO = 0.462



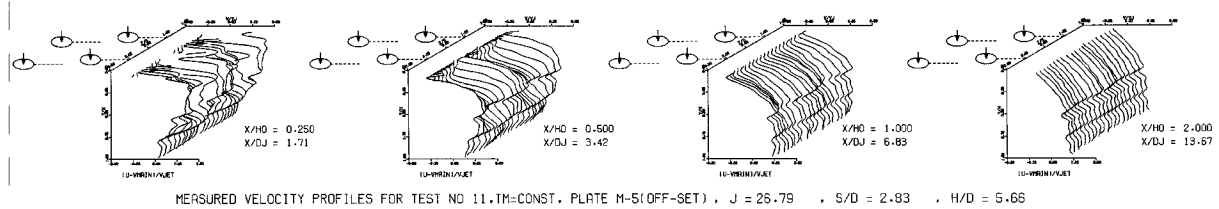
MEASURED VELOCITY PROFILES FOR TEST NO 10, TM=CONST, PLATE M-5(OFF-SET), J = 6.72 , S/D = 2.83 , H/D = 5.66



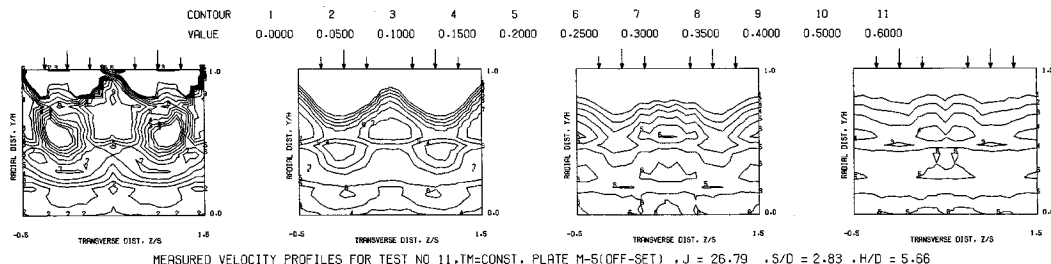
MEASURED VELOCITY PROFILES FOR TEST NO 10, TM=CONST, PLATE M-5(OFF-SET), J = 6.72 , S/D = 2.83 , H/D = 5.66

Figure 171. Measured Velocity Distributions for Test No. 10 of DJM Phase III Testing.

$S = 0.0508$  METERS    $S/DJ = 3.417$     $H/DJ = 6.835$     $V_{MIN} = 5.3$  M/SEC    $V_{JET} = 18.4$  M/SEC    $T_{MIN} = 376.2$  K    $T_{JET} = 174.2$  K    $\Theta_E = 0.3422$     $BLDAT = 7.683$     $DENRATIO = 2.203$     $TRATIO = 0.463$



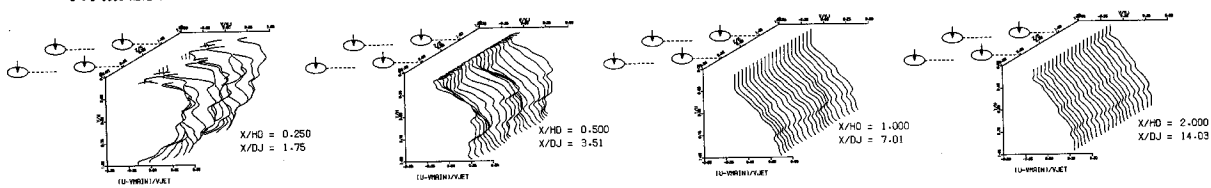
MEASURED VELOCITY PROFILES FOR TEST NO 11. TM=CONST. PLATE M-5(OFF-SET) . J = 26.79 . S/D = 2.83 . H/D = 5.66



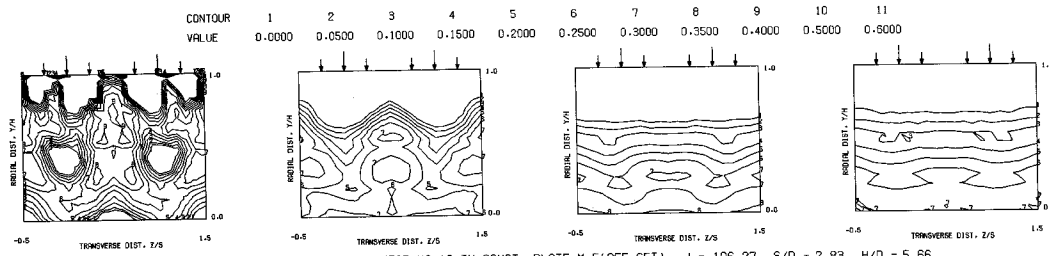
MEASURED VELOCITY PROFILES FOR TEST NO 11. TM=CONST. PLATE M-5(OFF-SET) . J = 26.79 . S/D = 2.83 . H/D = 5.66

Figure 172. Measured Velocity Distributions for Test No. 11 of DJM Phase III Testing.

S = 0.0508 METERS S/DJ = 3.507 H/DJ = 7.013 V<sub>MAIN</sub> = 5.0 M/SEC V<sub>JET</sub> = 34.5 M/SEC T<sub>MAIN</sub> = 358.3 K T<sub>JET</sub> = 174.3 K THEB = 0.5004 BLORET = 15.364 DENS RATIO = 2.221 TRATIO = 0.486



MEASURED VELOCITY PROFILES FOR TEST NO 12. TM=CONST. PLATE M-5(OFF-SET), J = 106.27 , S/D = 2.83 , H/D = 5.66



MEASURED VELOCITY PROFILES FOR TEST NO 12. TM=CONST. PLATE M-5(OFF-SET) . J = 106.27 . S/D = 2.83 . H/D = 5.66

Figure 173. Measured Velocity Distributions for Test No. 12 of DJM Phase III testing.

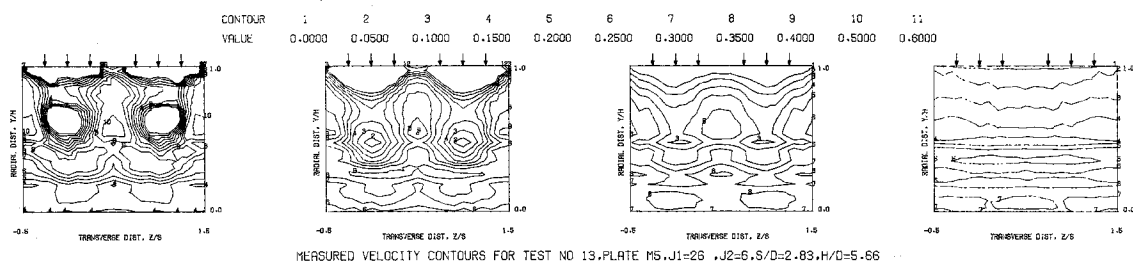
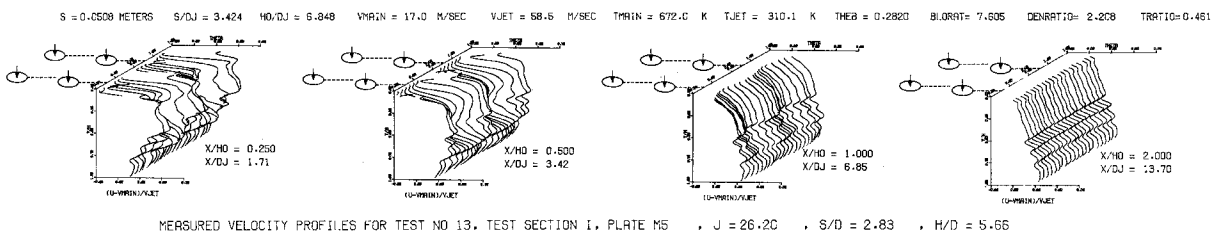
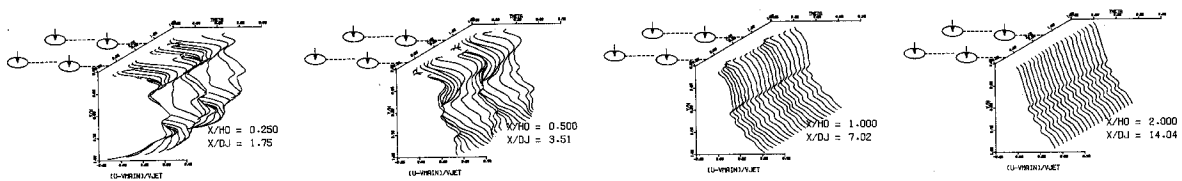
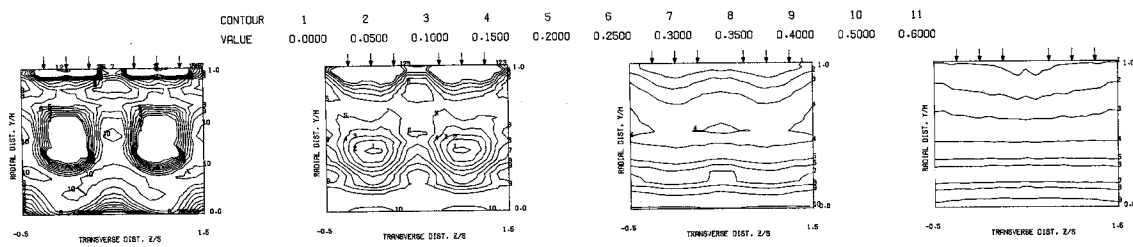


Figure 174. Measured Velocity Distributions for Test No. 13 of DJM Phase III Testing.

$S = 0.0508$  METERS    $S/DJ = 3.510$     $H/DJ = 7.020$     $V_{MAIN} = 16.8$  M/SEC    $V_{JET} = 113.0$  M/SEC    $T_{MAIN} = 566.3$  K    $T_{JET} = 304.5$  K    $\rho_{EB} = 0.3938$     $BLRAT = 15.834$     $DENRATIO = 2.353$     $TRATIO = 0.457$



MEASURED VELOCITY PROFILES FOR TEST NO 14, TEST SECTION I, PLATE M5    $J_1 = 106.54$ ,  $S/D = 2.83$ ,  $H/D = 5.66$



MEASURED VELOCITY CONTOURS FOR TEST NO 14, PLATE M5,  $J_1 = 106.54$ ,  $J_2 = 5.5$ ,  $S/D = 2.83$ ,  $H/D = 5.66$

Figure 175. Measured Velocity Distributions for Test No. 14 of DJM Phase III Testing.

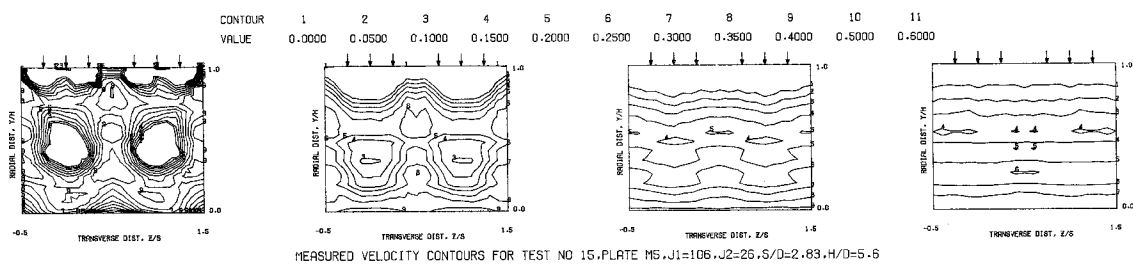
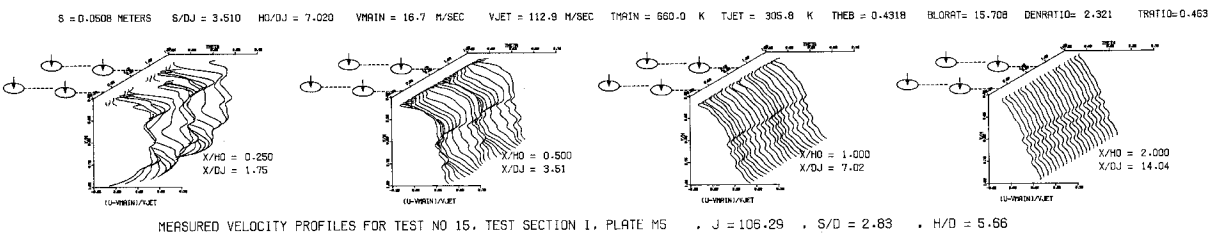
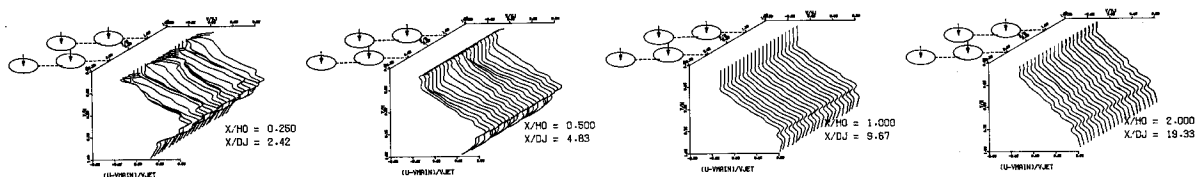
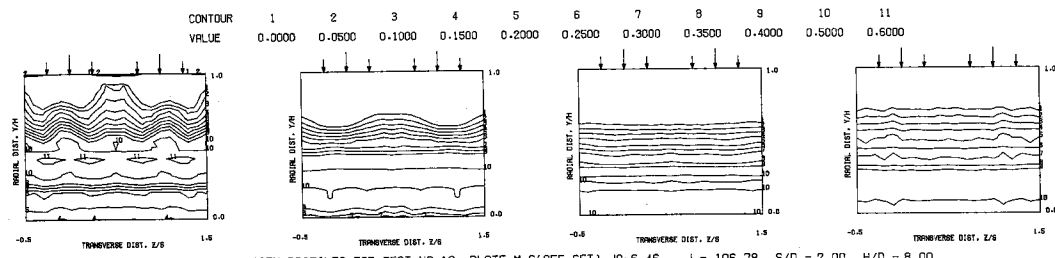


Figure 176. Measured Velocity Distributions for Test No. 15 of DJM Phase III Testing.

$S = 0.0254$  METERS    $S/DJ = 2.416$     $H/DJ = 9.666$     $V_{MAIN} = 5.1$  M/SEC    $V_{JET} = 34.9$  M/SEC    $T_{MAIN} = 364.8$  K    $T_{JET} = 170.4$  K    $\rho_{HEB} = 0.3933$     $B/LORAT = 15.602$     $DENRATIO = 2.280$     $TRATIO = 0.467$



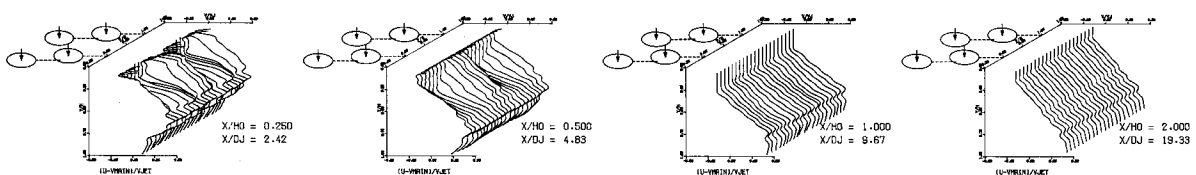
MEASURED VELOCITY PROFILES FOR TEST NO 16, PLATE M-6(OFF-SET), JR=6.46 , J = 106.78 , S/D = 2.00 , H/D = 8.00



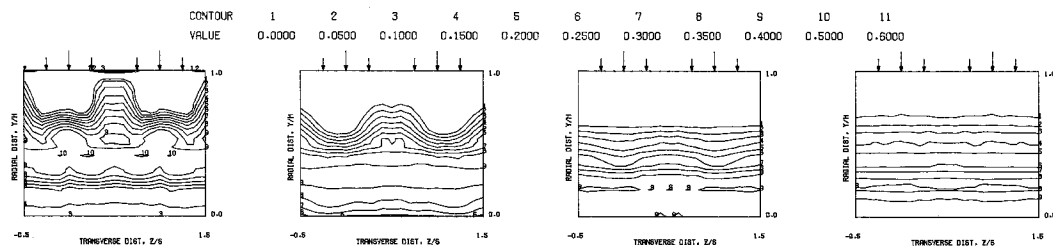
MEASURED VELOCITY PROFILES FOR TEST NO 16, PLATE M-6(OFF-SET), JR=6.46 , J = 106.78 , S/D = 2.00 , H/D = 8.00

Figure 177. Measured Velocity Distributions for Test No. 16 of DJM Phase III Testing.

$S = 0.0254$  METERS    $S/DJ = 2.416$     $H/DJ = 9.666$     $V_{MAIN} = 5.2$  M/SEC    $V_{JET} = 36.0$  M/SEC    $T_{MAIN} = 360.8$  K    $T_{JET} = 169.5$  K    $\Theta_{EB} = 0.4409$     $BLRAT = 15.745$     $DENRATIO = 2.321$     $TRATIO = 0.460$



MEASURED VELOCITY PROFILES FOR TEST NO 17, PLATE M-6(OFF-SET), JR=26.5 , J = 106.82 , S/D = 2.00 , H/D = 8.00



MEASURED VELOCITY PROFILES FOR TEST NO 17, PLATE M-6(OFF-SET), JR=26.5 , J = 106.82 , S/D = 2.00 , H/D = 8.00

Figure 178. Measured Velocity Distributions for Test No. 17 of DJM Phase III Testing.

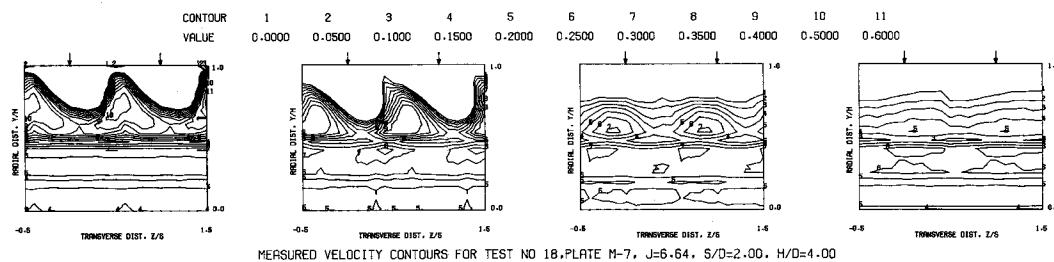
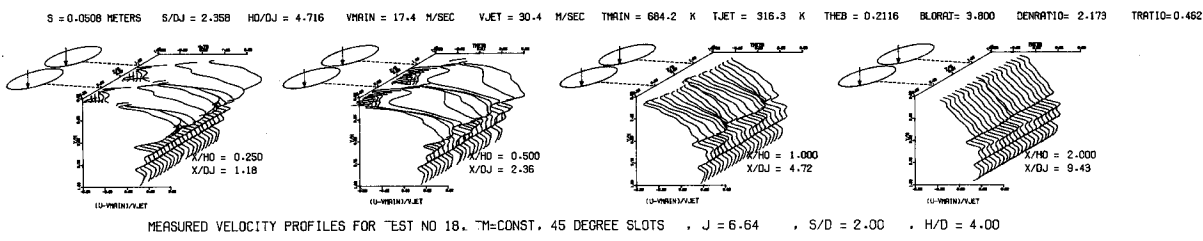


Figure 179. Measured Velocity Distributions for Test No. 18 of DJM Phase III Testing.

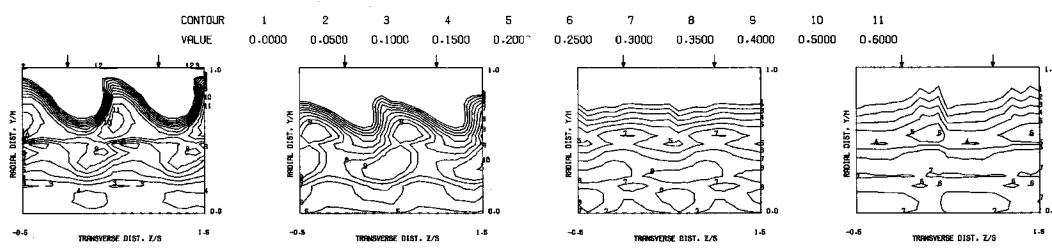
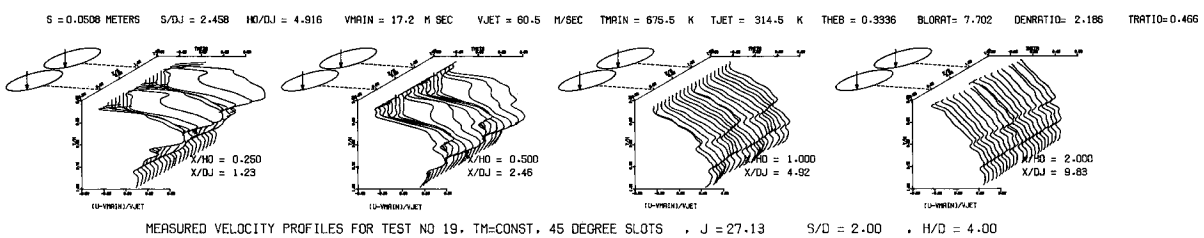


Figure 180. Measured Velocity Distributions for Test No. 19 of DJM Phase III Testing.

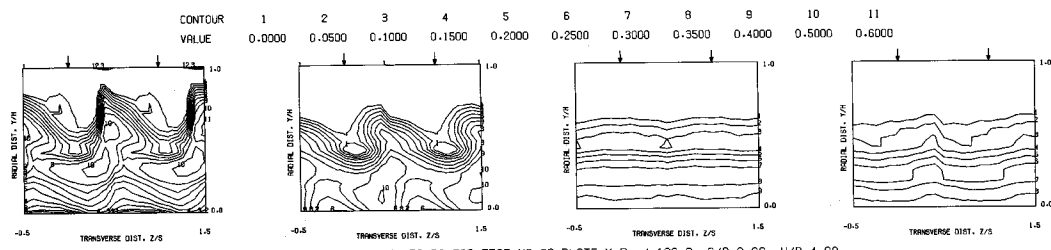
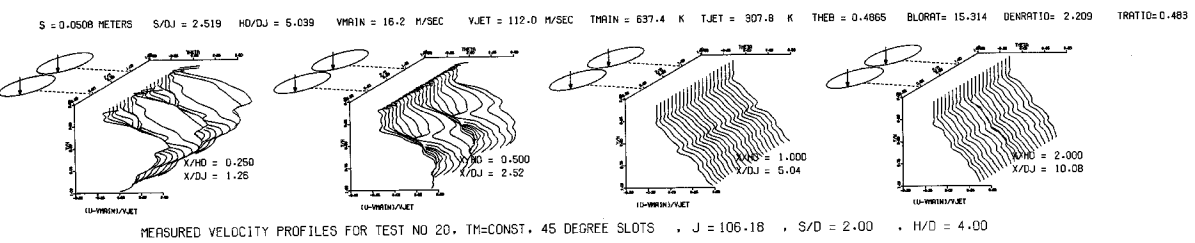
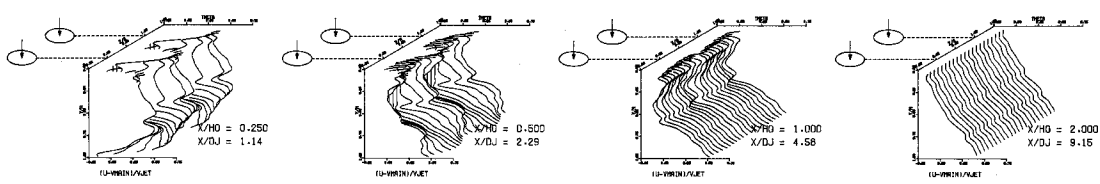
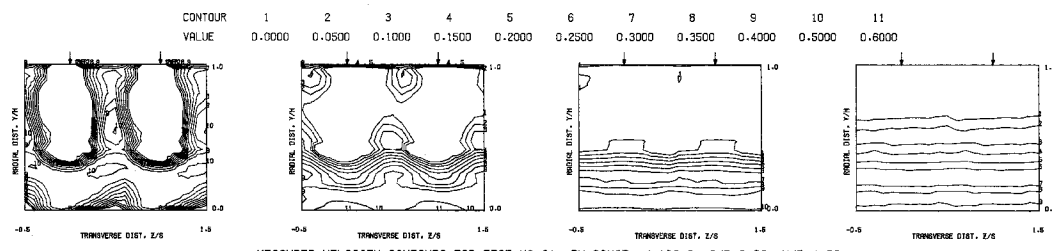


Figure 181. Measured Velocity Distributions for Test No. 20 of DJM Phase III Testing.

$S = 0.0508$  METERS    $S/DJ = 2.288$     $H/DJ = 4.576$     $V_{MAIN} = 16.3$  M/SEC    $V_{JET} = 104.3$  M/SEC    $T_{MAIN} = 629.1$  K    $T_{JET} = 307.0$  K    $\Theta_{EB} = 0.5322$     $BLO RAT = 15.170$     $DEN RATIO = 2.230$     $TRATIO = 0.468$



MEASURED VELOCITY PROFILES FOR TEST NO 21, TEST SECTION I,  $TM=CONST$  ,  $J = 103.19$  ,  $S/D = 2.00$  ,  $H/D = 4.00$



MEASURED VELOCITY CONTOURS FOR TEST NO 21,  $TM=CONST$ ,  $J=103.2$ ,  $S/D=2.00$ ,  $H/D=4.00$

Figure 182. Measured Velocity Distributions for Test No. 21 of DJM Phase III Testing.

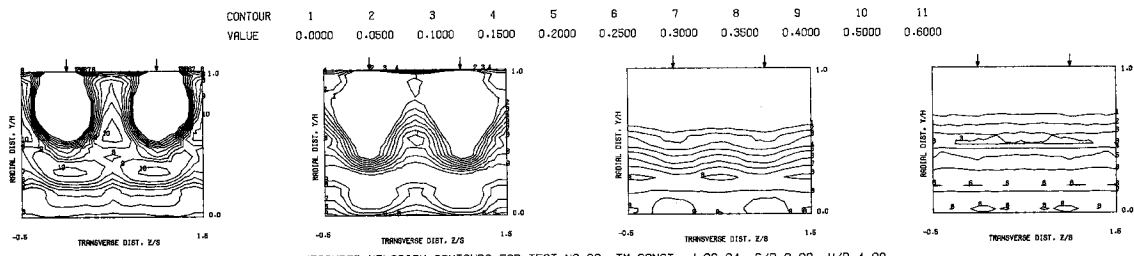
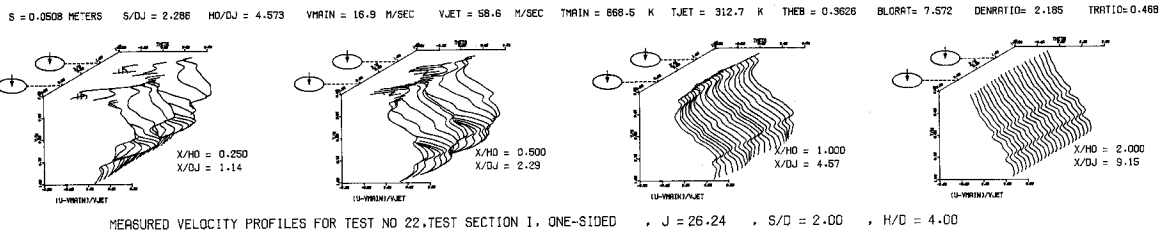


Figure 183. Measured Velocity Distributions for Test No. 22 of DJM Phase III Testing.

TABLE 3. CONFIGURATIONS AND FLOW CONDITIONS FOR PHASE I, SERIES 1 TESTS.

Weld Section	Type	Offices	S No.	Manufacture		Duration Jet		Nominal Thickness (mm)	Penetrating Ability (%)	Emissivity (%)	Absorption (%)	Transmittance (%)	Emissivity (%)	Absorption (%)	Transmittance (%)	Reason of Measurement
				Material ID	Transf. Velocity (mm/s)	Weld Process	Weld Time (sec)									
1	1	2.5	2	4	0.42739	650	15.8	6.08343	100	66.6	6.670	6.39	2.11	6.276	0.5 - > 0	Not to 1.0
2	1	2.54	2	4	0.26855	650	16.3	6.05189	100	62.5	6.600	18.59	2.13	6.279	0.5 - > 0	Not to 1.0
3	1	2.54	4	4	0.26855	650	15.2	6.28136	107	55.9	6.720	18.59	2.13	6.107	0.5 - > 0	Not to 1.0
4	1	2.54	4	4	0.26855	650	14.9	6.06972	104	52.2	6.675	18.59	2.13	6.279	0.5 - > 0	Not to 1.0
5	1	2.57	2	8	0.26854	650	15.0	6.05385	100	51.9	6.600	22.15	2.13	6.169	0.5 - > 0	Not to 1.0
6	1	2.57	2	8	0.28555	650	15.1	6.11484	299	50.5	6.600	22.15	2.13	6.169	0.5 - > 0	Not to 1.0
7	1	2.57	2	8	0.28555	650	15.0	6.03898	100	52.8	6.430	22.15	2.13	6.105	0.5 - > 0	Not to 1.0
8	1	2.57	4	8	0.28553	649	15.1	6.02978	299	104.1	6.605	94.30	2.30	0.181	0.5 - > 0	Not to 1.0
9	1	2.57	4	8	0.28553	649	15.0	6.13990	521	109.4	6.600	22.43	0.62	0.183	0.5 - > 0	Not to 1.0
10	1	2.58	4	8	0.6327	203	15.2	6.17235	400	105.3	6.600	22.43	0.62	0.193	0.5 - > 0	Not to 1.0
11	1	2.57	4	8	0.64931	293	15.3	5.77878	445	97.5	6.600	22.13	0.67	0.192	0.5 - > 0	Not to 1.0
12	1	2.57	4	8	0.64931	293	15.3	5.84342	457	97.5	6.600	22.13	0.67	0.192	0.5 - > 0	Not to 1.0
13	1	2.57	4	8	0.64931	293	15.3	5.84342	457	97.5	6.600	22.13	0.67	0.192	0.5 - > 0	Not to 1.0

TABLE 4. CONFIGURATIONS AND FLOW CONDITIONS FOR PHASE 1, SKRISH 2 TESTS.

Var. No.	Section No.	Geotextile Type	Slope %	Material Type		Orientation		Dimensions		Properties		Properties		Properties of Reinforcement		
				Normal Tensile Strength (kN/m)	Modulus of Elasticity (GPa)	Normal Tensile Strength (kN/m)	Modulus of Elasticity (GPa)	Width (mm)	Thickness (mm)	Modulus of Elasticity (GPa)	Width (mm)	Modulus of Elasticity (GPa)	Width (mm)			
13	1	2.144	2	2.085	534	0.1277	25.5-32	9.630	31.79	1.81	9.132	0.5-2.0	6.6 GPa			
14	1	2.154	4	4	2.085	15.4	0.0311	38.4	6.465	2.21	6.134	0.5-2.0	6.6 GPa			
15	1	1.87	4	6.2777	612	15.4	0.1277	16.9	5.597	59.21	2.07	0.153	0.5-2.0	6.6 GPa		
16	1	1.87	4	6	0.1318	16.1	0.0465	111	6.132	24.36	1.86	0.183	0.5-2.0	6.6 GPa		
17	1	2.154	4	6	0.1318	16.5	0.1343	105	9.713	9.671	24.41	1.86	0.283	0.5-2.0	6.6 GPa	
18	1	1.87	4	6	0.1318	145	0.0872	327	75.2	8.475	29.35	1.76	0.187	0.5-2.0	6.6 GPa	

TABLE 5. CONFIGURATIONS AND FLOW CONDITIONS FOR PHASE 1, SERIES 3 TESTS.

Test No.	Test Section	Orifice Dia. (CM)	B	$R_p/D$	Mainstream				Dilution Jet				Momentum Flux Ratio (J)	Density Ratio (Theta)	Regions of Measurement	
					Mass Flow Rate (KG/S)	Temp (KELVIN) (K)	Velocity (METERS/MIN) (M/S)	Mass Flow Rate (KG/S)	Temp (TEMP) (K)	Velocity (VjET) (M/S)	CpJ	Axial Direction (X/Rp)		Transverse Direction (Z/Rp)		
19	II	1.27	4	8	0.2537	65	15.9	0.02994	330	58.1	0.450	27.07	2.02	0.106	0.25 - 3.0	0.0 to 1.0
20	II	1.27	4	8	0.2543	645	15.5	0.05892	314	106.4	0.439	102.5	2.19	0.186	0.25 - 3.0	0.0 to 1.0
21	II	2.54	2	4	0.2511	654	15.8	0.06222	308	28.1	0.460	6.76	2.13	0.197	0.50 - 3.0	0.0 to 1.0
22	II	2.54	2	4	0.2534	654	15.8	0.11125	304	54.5	0.400	28.07	2.18	0.307	0.50 - 2.0	0.0 to 1.0
23	IV	1.27	1	8	0.2775	646	17.0	0.02988	312	53.8	0.460	21.05	2.10	0.097	0.25 - 1.0	-0.5 to +0.5
24	IV	1.27	4	8	0.2772	643	16.9	0.04006	311	105.1	0.440	55.81	2.07	0.178	0.25 - 1.0	-0.5 to +0.5
25	IV	2.54	2	4	0.2462	643	15.1	0.05513	322	27.7	0.420	6.73	2.00	0.183	0.50 - 1.0	0.0 to 1.0
26	IV	2.54	2	4	0.2452	641	14.9	0.1045	320	55.1	0.460	26.36	1.96	0.299	0.50 - 1.0	0.0 to 1.0
27	V	1.27	4	8	0.2619	646	16.1	0.03122	320	50.7	0.450	27.18	2.05	0.167	0.25 - 1.0	0.0 to 1.0
28	V	1.27	4	8	0.2669	645	16.0	0.04071	319	112.5	0.425	104.7	2.02	0.189	0.25 - 1.0	0.0 to 1.0
29	V	2.54	2	4	0.2560	645	15.7	0.04334	314	29.1	0.480	7.07	2.08	0.190	0.50 - 1.0	-0.5 to +0.5
30	V	2.54	2	4	0.2542	646	15.6	0.1168	314	56.4	0.420	27.31	2.09	0.315	0.50 - 1.0	-0.5 to +0.5
31	VI	1.27	4	8	0.2649	649	14.4	0.03162	320	50.4	0.455	26.58	2.07	0.187	0.25 - 1.0	-0.5 to +0.5
32	VI	1.27	4	8	0.2657	647	15.5	0.04250	321	116.0	0.420	107.4	2.18	0.189	0.25 - 1.0	-0.5 to +0.5
33	VI	2.54	2	4	0.2646	650	15.3	0.06489	301	29.5	0.440	7.04	2.17	0.187	0.50 - 1.0	-0.5 to +0.5
34	VI	2.54	2	4	0.2629	651	16.2	0.1205	297	55.9	0.410	26.36	2.23	0.314	0.50 - 1.0	-0.5 to +0.5

TABLE 6. CONFIGURATIONS AND FLOW CONDITIONS FOR PHASE 1, SERIES 4 TESTS

Test No.	Test section	Orifice Dia. (CM)	B	$R_p/D$	Mainstream				Dilution Jet				Momentum Flux Ratio (J)	Density Ratio (Theta)	Regions of Measurement	
					Mass Flow Rate (KG/S)	Temp (KELVIN) (K)	Velocity (METERS/MIN) (M/S)	Mass Flow Rate (KG/S)	Temp (TEMP) (K)	Velocity (VjET) (M/S)	CpJ	Axial Direction (X/Rp)		Transverse Direction (Z/Rp)		
35	V	1.27	4	8	0.3566	561	18.7	0.03911	308	70.9	0.450	28.13	1.06	0.190	0.25 - 1.0	0.0 to 1.0
36	V	1.27	4	8	0.3579	568	18.8	0.03689	305	139.1	0.460	105.7	2.01	0.177	0.35 - 1.0	0.0 to 1.0
37	V	1.27	4	8	0.3532	417	16.0	0.02619	318	40.7	0.725	21.27	1.37	0.064	0.25 - 1.0	0.0 to 1.0
38	V	1.27	4	8	0.3645	416	16.0	0.04355	315	75.4	0.650	49.18	1.34	0.107	0.25 - 1.0	0.0 to 1.0

TABLE 7. CONFIGURATIONS AND FLUX CONDITIONS FOR PHASE II, SERIES 5 TESTS

TABLE 3. CONFIGURATIONS AND FLUX CONDITIONS FOR PHASE II, SECTION C INVESTIGATIONS

TABLE 9. CONFIGURATIONS AND FLOW CONDITIONS FOR PHASE II, SERIES 7 TESTS WITH SYMMETRICALLY CONVERGENT TEST SECTION.

Test No.	Mach Number (M <sub>1</sub> )	Reynolds Number (R <sub>1</sub> )	H <sub>2</sub> /H <sub>1</sub>	Mainstream			Top Dilation Jet			Bottom Dilation Jet			Regions Of Measurement						
				Mass Flow Rate (lb/sec)	Temperature (°R)	Velocity (ft/sec)	Mass Flow Rate (lb/sec)	Temperature at 2 <sub>0</sub> (°R)	Volume (V <sub>20</sub> ) (ft <sup>3</sup> )	(D) <sub>0</sub>	Mass Flow Rate (lb/sec)	Temperature at 2 <sub>0</sub> (°R)	Volume (V <sub>20</sub> ) (ft <sup>3</sup> )	(D) <sub>0</sub>	Equilibrium Pressure (lb/in. <sup>2</sup> )	Axial Dilution (%)	Transverse Dilution (%)		
													Mean	Deviation	Max				
17	1.27	1183	8	0.2642	444.4	16.5	0.0403	35.97	293.2	54.5	0.410	0.9638	35.57	298.7	58.1	0.450	0.1933	0.25 ± 1.0	-0.5 to +0.5
18	1.27	1183	2	0.2648	444.4	16.4	0.1380	106.5	397.0	111.7	0.430	0.1348	107.7	395.0	111.1	0.450	0.5019	-0.25 ± 1.0	-0.5 to +0.5
21	1.27	1170	8	0.2631	444.4	16.4	0.03155	15.92	372.9	57.1	0.440	0.03275	16.40	290.2	54.7	0.440	0.1929	0.15 ± 1.0	-0.5 to +0.5
22	1.33	1170	8	0.2689	444.2	16.4	0.05934	167.7	296.5	112.8	0.430	0.05920	107.7	299.9	113.1	0.415	0.3240	-0.25 ± 1.0	-0.5 to +0.5
23	1.54	1870	4	0.2641	444.4	16.5	0.01518	5.78	111.0	29.7	0.473	0.03267	6.75	310.4	30.0	0.480	0.1994	0.25 ± 1.0	-0.5 to +0.5
24	2.55	1870	4	0.2645	444.5	16.4	0.05559	21.76	104.2	54.9	0.450	0.05819	24.0	301.1	56.7	0.475	0.3272	0.24 ± 1.0	-0.5 to +0.5
25	2.54	1182	4	0.2675	445.1	16.4	0.05522	6.67	300.4	28.9	0.455	0.05854	6.76	298.9	28.9	0.455	0.3284	0.25 ± 1.0	-0.5 to +0.5
26	2.54	1182	2	0.2698	444.7	16.4	0.1220	25.98	200.8	56.4	0.432	0.1220	25.90	298.9	56.6	0.430	0.4810	0.25 ± 1.0	-0.5 to +0.5

TABLE 10. CONFIGURATIONS AND FLOW CONDITIONS FOR PHASE II, SERIES 8 TESTS

TABLE 10. CONFIGURATIONS AND FLOW CONDITIONS FOR PHASE II, SERIES 8 TESTS (CONTINUED).

Point No.	Total Area Section	Dilution Rate (kg/kg)	S	Mainstream			Top Dilution Jet			Bottom Dilution Jet			Regions of Measurement							
				$\frac{M}{M}$	Mass flow (kg/s)	Velocity (m/s)	Max flow (kg/s)	Nominal Ratio $J_1/J_2$	Top Velocity (m/s)	$[C]_{top}$	Mass flow (kg/s)	Nominal Ratio $J_2/J_1$	Temp (°K)	Velocity (m/s)	$[C]_{bottom}$	Axial Dilation Ratio	Transverse Dilation Ratio			
43	III	2.54	2	4	0.3748	504.5	17.9	0.07832	7.39	310.3	34.9	0.665	--	--	--	--	3.5873	0.25 - 1.0	-0.5 to +0.5	
44	III	2.54	2	4	0.3756	509.4	17.9	0.1526	16.00	167.9	47.9	0.650	--	--	--	--	3.6460	0.25 - 1.0	-0.5 to +0.5	
45a	I	3.024	1	9.92	0.2198	644.7	16.5	0.0749	6.66	307.4	29.4	0.700	--	--	--	--	2.2159	0.25 - 2.0	0.0 to 4.0	
45b	I	3.024	1	9.92	0.3706	644.4	16.6	0.1114	25.33	306.7	57.3	0.722	--	--	--	--	3.3462	0.25 - 2.0	0.0 to 4.0	
45c	I	3.024	1	9.92	0.2735	644.9	16.7	0.2945	78.20	337.9	98.9	0.710	--	--	--	--	3.4820	0.25 - 2.0	0.0 to 4.0	
46	I	2.54	2	1	0.2707	644.3	16.5	0.06667	6.70	304.8	19.4	0.655	0.06554	6.67	304.5	29.4	0.645	3.1299	0.25 - 2.0	-0.5 to +0.5
47	I	2.54	4	4	0.2710	644.3	16.6	0.1276	23.54	302.2	57.0	0.845	0.1271	25.32	303.6	57.3	0.645	3.4016	0.25 - 2.0	-0.5 to +0.5
48	I	2.54	2	4	0.2710	644.1	16.5	0.2324	84.14	302.3	101.4	0.640	0.1334	84.04	302.3	101.7	0.640	3.6327	0.25 - 2.0	-0.5 to +0.5
49	I	2.50	2.83	5.47	0.2104	644.6	14.7	0.23339	8.49	309.5	29.4	0.725	--	--	--	--	3.1159	0.25 - 2.0	-0.5 to +0.5	
50	I	1.80	2.83	5.47	0.1079	644.9	16.5	0.06921	25.46	309.5	56.3	0.705	--	--	--	--	3.2054	0.25 - 2.0	-0.5 to +0.5	
51	I	2.54	8	4	0.2679	644.1	16.5	0.03314	4.67	305.6	29.2	0.673	0.03423	4.60	305.8	28.6	0.675	3.2014	0.25 - 1.0	-0.5 to +0.5

TABLE II. CONFIGURATIONS AND FLOW CONDITIONS FOR PHASE III, SERIES 9 TESTS.

Test No.	Orientation	Distance from Source (m)	Neutron Beam			Fast Dilation Jet			Slow Dilation Jet			Response of Measurement		
			Mean Value (eV)	Velocity (km/s)	Mass View Factor (MVF)	Mean Velocity (m/s)	Mean Momentum (kg m/s)	Temp (K)	Velocity (km/s)	Mass View Factor (MVF)	Mean Velocity (m/s)	Temp (K)	Velocity (km/s)	Equilibrium State
1	H-1	2.50	0.5	0.2345	0.942	0.1234	231.5	10.9	0.9	0.1234	0.942	10.9	0.9	0.1234
2	H-2	2.50	0.5	0.2345	0.941	0.1234	231.5	10.9	0.9	0.1234	0.941	10.9	0.9	0.1234
3	H-3	2.50	0.5	0.2346	0.941	0.1234	231.5	10.9	0.9	0.1234	0.941	10.9	0.9	0.1234
4	M-2	3.00	0.5	0.2345	0.942	0.1234	231.5	10.9	0.9	0.1234	0.942	10.9	0.9	0.1234
5	M-3	3.00	0.5	0.2346	0.942	0.1234	231.5	10.9	0.9	0.1234	0.942	10.9	0.9	0.1234
6	H-1	3.50	0.5	0.2345	0.943	0.1234	231.5	10.9	0.9	0.1234	0.943	10.9	0.9	0.1234
7	H-2	3.50	0.5	0.2346	0.942	0.1234	231.5	10.9	0.9	0.1234	0.942	10.9	0.9	0.1234
8	H-3	3.50	0.5	0.2346	0.943	0.1234	231.5	10.9	0.9	0.1234	0.943	10.9	0.9	0.1234
9	M-2	3.50	0.5	0.2346	0.943	0.1234	231.5	10.9	0.9	0.1234	0.943	10.9	0.9	0.1234
10	M-3	3.50	0.5	0.2346	0.943	0.1234	231.5	10.9	0.9	0.1234	0.943	10.9	0.9	0.1234
11	H-1	4.00	0.5	0.2345	0.944	0.1234	231.5	10.9	0.9	0.1234	0.944	10.9	0.9	0.1234
12	H-2	4.00	0.5	0.2346	0.944	0.1234	231.5	10.9	0.9	0.1234	0.944	10.9	0.9	0.1234
13	H-3	4.00	0.5	0.2346	0.945	0.1234	231.5	10.9	0.9	0.1234	0.945	10.9	0.9	0.1234
14	M-2	4.00	0.5	0.2346	0.945	0.1234	231.5	10.9	0.9	0.1234	0.945	10.9	0.9	0.1234
15	M-3	4.00	0.5	0.2346	0.945	0.1234	231.5	10.9	0.9	0.1234	0.945	10.9	0.9	0.1234

TABLE 12. CONFIGURATIONS AND FLOW CONDITIONS FOR PHASE III, SERIES 10 TESTS.

REFERENCES

1. Srinivasan, R., Berenfeld, A., and Mongia H.C., "Dilution Jet Mixing Program - Phase I Report," NASA CR-168031, 1982.
2. Srinivasan, R., Coleman, E., and Johnson, K., "Dilution Jet Mixing Program - Phase II Report," NASA CR-174624, 1984.
3. Srinivasan, R., Meyers, G., Coleman, E., and White, C., "Dilution Jet Mixing Program - Phase III Report," NASA CR-174884, 1985.
4. Srinivasan, R., et al., "Aerothermal Modeling Program: Phase I Final Report" Garrett Turbine Engine Company, Phoenix, Arizona, Garrett 21-4742, August 1983 (NASA CR-168243).
5. Holdeman, J.D., and Walker, R.E., "Mixing of a Row of Jets with a Confined Crossflow," AIAA Journal, Vol. 15, No. 2, Feb. 1977, pp. 243-249 (also AIAA-76-48 and NASA TM X-71787).
6. Walker, R.E. and Eberhardt, R.G., "Multiple Jet Study Data Correlations," NASA CR-134795, 1975.

<b>REPORT DOCUMENTATION PAGE</b>			<i>Form Approved OMB No. 0704-0188</i>
Public reporting burden for this collection of information is estimated to average 1 hour per response, including the time for reviewing instructions, searching existing data sources, gathering and maintaining the data needed, and completing and reviewing the collection of information. Send comments regarding this burden estimate or any other aspect of this collection of information, including suggestions for reducing this burden, to Washington Headquarters Services, Directorate for Information Operations and Reports, 1215 Jefferson Davis Highway, Suite 1204, Arlington, VA 22202-4302, and to the Office of Management and Budget, Paperwork Reduction Project (0704-0188), Washington, DC 20503.			
1. AGENCY USE ONLY ( <i>Leave blank</i> )	2. REPORT DATE	3. REPORT TYPE AND DATES COVERED	
	March 1986	Final Contractor Report	
4. TITLE AND SUBTITLE		5. FUNDING NUMBERS	
Dilution Jet Mixing Program Supplementary Report		WU-533-04-12-00 NAS3-22110	
6. AUTHOR(S)		7. PERFORMING ORGANIZATION NAME(S) AND ADDRESS(ES)	
R. Srinivasan and C. White		Garrett Turbine Engine Company P.O. Box 5217 Phoenix, Arizona 85010	
8. PERFORMING ORGANIZATION REPORT NUMBER		9. SPONSORING/MONITORING AGENCY NAME(S) AND ADDRESS(ES)	
E-None		National Aeronautics and Space Administration Washington, DC 20546-0001	
10. SPONSORING/MONITORING AGENCY REPORT NUMBER		11. SUPPLEMENTARY NOTES	
NASA CR-175043 Garrett 21-5705		Project Manager, James D. Holdeman, NASA Lewis Research Center, Cleveland, Ohio 44135.	
12a. DISTRIBUTION/AVAILABILITY STATEMENT		12b. DISTRIBUTION CODE	
Unclassified - Unlimited Subject Category: 00  Available electronically at <a href="http://gltrs.grc.nasa.gov">http://gltrs.grc.nasa.gov</a> This publication is available from the NASA Center for AeroSpace Information, 301-621-0390.			
13. ABSTRACT ( <i>Maximum 200 words</i> )			
This report presents a comparison of the velocity and temperature distributions predicted by a 3-D numerical model and experimental measurements. In addition, empirical correlations for the jet velocity trajectory developed in this program are presented. The measured velocity distributions for all test cases of Phase I through Phase III in this program (Contract NAS3-22110) are presented in the form of contour and oblique plots.			
14. SUBJECT TERMS		15. NUMBER OF PAGES 236	
Dilution-zone; Jet-mixing; Combustion		16. PRICE CODE	
17. SECURITY CLASSIFICATION OF REPORT	18. SECURITY CLASSIFICATION OF THIS PAGE	19. SECURITY CLASSIFICATION OF ABSTRACT	20. LIMITATION OF ABSTRACT
Unclassified	Unclassified	Unclassified	